2015 / Volume 53 / Number 4
ISSN 1641-4640

Folia NEUROPATHOLOGICA

www.folianeuro.termedia.pl

Official Journal of Mossakowski Medical Research Centre Polish Academy of Sciences
and
Polish Association of Neuropathologists

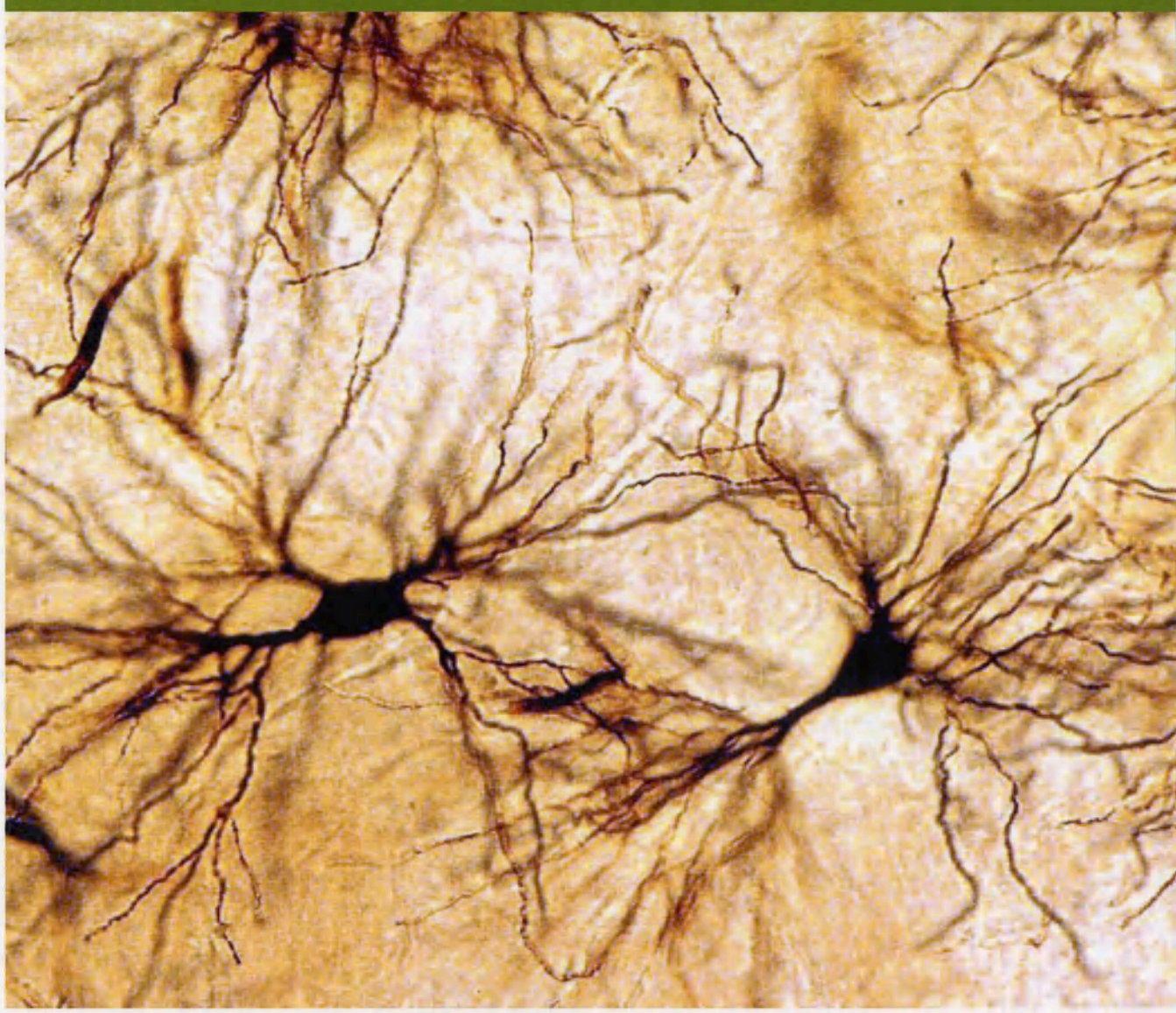

ISSN 1641-4640

Folia Neuropathologica

TERMEDIA Publishing House

Folia
Neuropathologica
former *Neuropatologia Polska*

Official Journal of Mossakowski Medical Research Centre Polish Academy of Sciences and Polish Association of Neuropathologists

The journal is partly financially supported
by the Ministry of Science and Higher Education

termedia

Termedia Publishing House
Kleeberga 2, 61-615 Poznań, Poland
phone/fax: +48 61 822 77 81
e-mail: termedia@termedia.pl
www.termedia.pl
www.folianeuro.termedia.pl

Warsaw office
phone/fax: +48 22 827 75 14
e-mail: biuro.warszawa@termedia.pl

president of the management board
editor-in-chief of the Publishing House, director
Janusz Michalak
e-mail: j.michalak@termedia.pl

director of the Publishing House
Andrzej Kordas
e-mail: a.kordas@termedia.pl

Marketing and Advertising Department
Renata Dolata
phone: +48 61 822 77 81 ext. 508
e-mail: r.dolata@termedia.pl

Distribution Subscription Department
Jolanta Jankowiak
phone: +48 61 656 22 00
e-mail: prenumerata@termedia.pl

Impact Factor for Folia Neuropathologica equals 1.667
MNiSW score for Folia Neuropathologica equals 15.00
Index Copernicus score (2011) for Folia Neuropathologica equals 18.13
Position in Index Copernicus ranking systems available at http://www.indexcopernicus.pl

Abstracted and indexed in Index Medicus/MEDLINE, Neuroscience Citation Index, SciSearch, Research Alert, Chemical Abstracts, EMBASE/Excerpta Medica, Polish Medical Bibiography, Index Copernicus

The journal is financially supported by the Ministry of Sciences and Higher Education.

Print run: 450 copies

Folia
Neuropathologica
2015; 53/4: 281-448

Contents

Toxic effects of silver nanoparticles in mammals – does a risk of neurotoxicity exist? 281
Joanna Skalska, Lidia Strużyńska

Effects of mGluR5 positive and negative allosteric modulators on brain damage evoked by hypoxia-ischemia in neonatal rats 301
Dorota Makarewicz, Marta Słomka, Wojciech Danysz, Jerzy W. Łazarewicz

Protective effect of valproic acid on cultured motor neurons under glutamate excitotoxic conditions. Ultrastructural study 309
Ewa Nagańska, Ewa Matyja, Anna Taraszewska, Janina Rafałowska

The influence of glutamatergic receptor antagonists on biochemical and ultrastructural changes in myelin membranes of rats subjected to experimental autoimmune encephalomyelitis 317
Beata Dąbrowska-Bouta, Lidia Strużyńska, Małgorzata Chalimoniuk, Małgorzata Frontczak-Baniewicz, Grzegorz Sulkowski

Collateral sprouting axons of end-to-side nerve coaptation in the avulsion of ventral branches of the C5-C6 spinal nerves in the brachial plexus 327
Paweł Reichert, Zdzisław Kiełbowicz, Piotr Dzięgiel, Bartosz Puła, Jan Kuryszko, Marcin Wrzosek, Maciej Kiełbowicz, Jerzy Gosk

Polymorphism of the osteopontin gene and clinical course of multiple sclerosis in the Polish population 343
Justyna Biernacka-Lukanty, Grazyna Michalowska-Wender, Sławomir Michalak, Beata Raczak, Wojciech Kozubski, Dariusz Urbanski, Mieczyslaw Wender

Toll-like receptor 2 (TLR2) is a marker of angiogenesis in the necrotic area of human medulloblastoma 347
Danuta Maslinska, Milena Laure-Kamionowska, Sławomir Maslinski, Dariusz Szukiewicz

Sporadic inclusion body myositis: clinical, pathological, and genetic analysis of eight Polish patients 355
Biruta Kierdaszuk, Mariusz Berdynski, Piotr Palczewski, Marek Golebiowski, Cezary Zekanowski, Anna Maria Kaminska

NF-κB deficit in spinal motoneurons in patients with sporadic amyotrophic lateral sclerosis – a pilot study 367
Dorota Sulejczak, Stanisław J. Chrapusta, Dorota Dziewulska, Janina Rafałowska

Effects of supplementation with branched chain amino acids and ornithine aspartate on plasma ammonia and central fatigue during exercise in healthy men 377
Tomasz Mikulski, Jan Dabrowski, Wojciech Hilgier, Andrzej Ziemba, Krzysztof Krzeminski

Holoprosencephaly with agenesia of the prosencephalic ventricle 387
Milena Laure-Kamionowska, Krystyna Szymanska, Teresa Klepacka

Abstracts from the Neurochemical Conference 2015; The Days of Neurochemistry; "Neuropsychoimmunological mechanisms in the pathology of neurodegenerative diseases: From biomarkers to therapeutics" 395

Abstracts from the Conference of Polish Association of Neuropathologists; "Biopsy research-challenge of modern neuropathology" 439

Review paper

Folia Neuropathologica

Toxic effects of silver nanoparticles in mammals – does a risk of neurotoxicity exist?

Joanna Skalska, Lidia Strużyńska

Laboratory of Pathoneurochemistry, Department of Neurochemistry, Mossakowski Medical Research Centre, Polish Academy of Sciences, Warsaw, Poland

Folia Neuropathol 2015; 53 (4): 281-300 DOI: 10.5114/fn.2015.56543

Abstract

Over the last decade, silver nanoparticles have become an important class of nanomaterials utilized in the development of new nanotechnologies. Despite the fact that nanosilver is used in many commercial applications, our knowledge about its associated risks is incomplete. Although a number of studies have been undertaken to better understand the impact of silver nanoparticles on the environment, aquatic organisms and cell lines, little is known about their side effects in mammalian organisms. This review summarizes relevant data and the current state of knowledge regarding toxicity of silver nanoparticles in mammals, as well as the accumulated evidence for potent neurotoxic effects. The influence of nanosilver on the central nervous system is significant because of evidence indicating that it accumulates in mammalian brain tissue.

Key words: *silver nanoparticles, neurotoxicity, mammals, nanotoxicology.*

Introduction

Silver is well known for its many industrial applications such as soldering, electrical conduction and plating applications. Additionally, this metal is used in the production of jewellery, cutlery, coins, medical instruments and photographic materials. In medical applications silver is included in wound dressings, urinary catheters and other medical devices, because of the ability of silver ions to inhibit growth of bacteria and fungi. Known for millennia, the antimicrobial effect of ionic silver arises from its ability to generate reactive oxygen species (ROS) and to inactivate microbial enzymes [19,75,88].

In addition to antibacterial activity, silver (particularly in the form of soluble silver compounds) exerts toxic effects in animals and humans. Acute symptoms of over-exposure to silver ions in humans include damage to the gastrointestinal tract, abdominal pain, diarrhea and convulsions [113]. The most common adverse effects associated with chronic exposure to silver in humans are discoloration of eyes (argyrosis) and pigmentation of the skin and mucous membranes, which turn irreversibly gray or bluish-gray (argyria). Argyria has been reported mainly in workers associated with mining, manufacturing or packing of silver [8,28,96]. Moreover, animal studies have revealed that prolonged administration

Communicating author:

Lidia Strużyńska, PhD, Laboratory of Pathoneurochemistry, Department of Neurochemistry, Mossakowski Medical Research Centre, Polish Academy of Sciences, 5 Pawińskiego St., 02-106 Warsaw, Poland, e-mail: lidkas@imdik.pan.pl

of silver ions in low doses leads to accumulation of silver granules in eyes, heart enlargement, anemia and pathological changes to the liver and kidneys [28,113].

Recently, a resurgence in commercial applications of silver has occurred due to the development of nanotechnologies which make extensive use of silver in the form of nanoparticles (NPs). NPs are defined as materials having at least one dimension below 100 nm. NPs have unique properties useful in many applications. The most important features include a large surface area per unit mass and the potential to generate surface modifications which alter their properties. As a result, NPs have enhanced chemical reactivity, improved cell penetration and specific influences on biological systems. Moreover, the surface of NPs can be modified with various chemical groups which allow them to be conjugated to ligands or drugs [23,90,120]. As a result of their enhanced reactivity, NPs may generate toxic effects which differ from the bulk materials from which they are produced.

The number of NP-based applications is significantly increasing, and many products containing NPs are commercially available. There is great excitement about the potential benefits of NPs in medical applications. NPs have been tested as vehicles for gene therapy and drug delivery and as tools in diagnostic imaging and targeting systems for recognition of cancer cells [90]. Metal NPs in general and silver nanoparticles (AgNPs) in particular are among the most important nanomaterials used in a wide range of industrial applications. According to the Woodrow Wilson inventory, about 30% of all NP-based products in the marketplace contain AgNPs [114]. The list of AgNP-based consumer products includes cleansers for disinfecting hard surfaces, laundry and dishwashing detergents, bath and sports towels, clothing, socks, underwear, water and air filters, personal cleansers, deodorants, cosmetics, cleansing soaps, toothbrushes, toothpastes, health supplements, nursing bottles and associated nipples, children's toys, and nanosilver-coated devices such as mobile phones and laptops. Appliances such as refrigerators and washing machines include interior coatings with AgNPs. Additionally, silver nanoparticles are included in paints used to cover walls in hospital rooms and in food storage containers (a complete listing of AgNP-based products is available at: *http://www.nanotechproject.org/process/assets/files/7039/silver_database_fauss_sept2_final.pdf*). The medical applications of AgNPs are summarized in Table I.

Table I. Selected medical applications of silver nanoparticles

Medical applications	References
Bone prostheses	[17]
Contraceptive devices	[91]
Gloves	[58]
Medical catheters	[117]
Orthopedic implants	[110]
Prosthetic devices	[21]
Endotracheal tubes	[83]
Surgical instruments	[31]
Wound dressings	[142]
Dental restorative materials, endodontic cements, dental implants	[43]

This particular interest in AgNPs relates to their antimicrobial activity. The rapid development of bacterial resistance against conventional antimicrobials and the challenges involved in development of new drugs have led to searches for promising alternatives. The smallest AgNPs, which have sizes within a range of a few nanometers, exhibit particularly strong antibacterial effects [61,82,94]. It has been found that in addition to size, the specific types of surface-coating agents have a significant effect on the biocidal potency of AgNPs [27]. AgNPs are also effective against fungi and viruses [40,42].

Although the commercialization of AgNPs has led to great excitement about potential benefits of their strong antimicrobial activity, it has simultaneously created a risk of hazardous interactions with biological systems [69,76].

There is a potential hazard to the environment and human health when AgNPs present in commercially available products, such as clothing, towels, socks, underwear, and toys, are released to the environment when these items are washed. AgNPs present in personal care products, cleaning supplies, detergents or cosmetics can be directly introduced into the environment during use and/or disposal [10,11]. Applications such as health supplements containing AgNPs, as well as food and drink storage containers, may also be a source of AgNPs [24]. Moreover, increasing

use of silver nanoparticles is expected to raise occupational exposure mainly through inhalation [18].

AgNPs released from consumer products are expected to enter aquatic and terrestrial ecosystems, but their fate after long-term accumulation and their impact on the environment are not fully known. There is significant concern regarding aquatic organisms in locations where AgNPs accumulate [87,115,140]. Unfortunately, our knowledge about the environmental and human risks remains at a very low level. It is therefore challenging to assess the long-term health consequences of environmental contamination. This problem is currently in the center of interest for scientists and various national agencies as well as public and private organizations.

Routes of exposure and biodistribution of AgNPs in mammalian organisms

Since AgNPs are found in a wide variety of products, exposure to them may occur via different routes of entry into the body. AgNPs from consumer products or medical applications may gain access to systemic circulation via oral or intravenous exposure as well as via inhalation or through the skin.

The gastrointestinal tract is the most likely route of entry for silver nanoparticles, directly through intentional ingestion (medical or dietary supplements, toothpastes) or indirectly via dissolution of AgNPs from products (food and drink containers, toothbrushes) [24]. Moreover, increasing environmental contamination may further lead to indirect and unintentional ingestion via consumption of water or fish. Inhalation of dust and fumes containing AgNPs or skin contact occurs mainly in occupational settings. Furthermore, certain products such as cosmetics, clothing, underwear, socks or wound dressings may allow AgNPs to penetrate the skin, primarily under conditions of concomitant presence of skin diseases such as allergic dermatitis, atopic eczema, psoriasis or simply during skin damage [92]. Medical or diagnostic compounds can also cause entry of AgNPs into the circulatory system by intravenous administration.

Information about absorption of AgNPs is incomplete. Park and co-workers observed that the bioavailability of AgNPs (7.9 nm) after oral administration to rats was very low, in the range of 1.2% to 4.2% based on a single dose [101]. Following entry into the systemic circulation, AgNPs can become distributed among a number of mammalian organs, most notably liver and spleen [73,145]. Furthermore, silver nanoparticles have been found in blood, lungs, kidney, brain, heart and genital organs [67,70,73,81,101,131,145]. The results of research on the biodistribution of AgNPs indicate that most organs are able to remove AgNPs over time, with the exception of brain and testes [70,138]. Numerous studies have shown that AgNPs can be distributed within the brain of mammals, regardless of the route of exposure. Selected studies on biodistribution of AgNPs in mammalian brain are listed in Table II.

Lee and co-workers observed that after a single intravenous injection of citrate-coated AgNPs (7.9 nm), they become distributed in serum, liver, kidney, spleen, lungs, brain, testes and thymus of rabbits. Significantly, the presence of silver nanoparticles was observed at time points 1, 7 and 28 days after the injection [73]. Silver was also detected in brain of rats at 24, 96 and 168 h after an intraperitoneal injection of bovine serum albumin-coated 2 nm AgNPs [45].

Studies using the model of oral exposure to nanosilver indicate distribution among many organs of animals, including brain, after 90 days of repeated administration [67]. In organs of rats chronically exposed to AgNPs (10, 25 nm) by the oral route, nano-sized granules were observed in liver, kidney, spleen, brain, testes and ovaries [70]. Moreover, the oral exposure of rats to uncoated AgNPs (< 20 nm) or PVP-coated AgNPs (< 15 nm) showed a very similar pattern of biodistribution. The nano-sized granules were detected in liver, kidney, lungs, heart, spleen, brain, bladder, testes, blood, intestine and stomach [138]. Subchronic inhalation of AgNPs may also cause them to enter systemic circulation. Studies in which rats were exposed to AgNPs (18-19 nm) via inhalation for 13 weeks revealed that the lungs and liver are targeted organs. Additionally, nano-sized granules were identified in kidney, the olfactory bulb, blood and brain tissue [131]. The results of a study on the biodistribution of AgNPs (25 nm) after a single dose via intranasal administration demonstrated that silver accumulates in spleen, lungs, kidney, the nasal cavity and brain tissue [46].

Additionally, the assessment of the level of silver in urine and feces of treated animals suggests that excretion of AgNPs occurs mainly via feces, indicating that AgNPs are secreted in bile [63,73,101].

Table II. Studies on the biodistribution of AgNPs in mammalian organisms

Surface coatings and/or sizes of AgNPs	Animal model	Route of administration and dosage	Time of AgNP level measurement after last administration and time of administration	Organs/tissues examined	References
AgNPs: 20 and 200 nm	Rats	*i.v.*: 5 mg/kg b.w.	1, 7 and 28 days after single injection	Liver, spleen, kidney, lungs and brain	[29]
Citrate-coated AgNPs: 7.9 nm	Rabbits	*i.v.*: 0.5 or 5 mg/kg b.w.	1, 7 and 28 days after single injection	Serum, liver, kidney, spleen, lungs, brain, testes and thymus	[73]
BSA-coated AgNPs: 2 nm	Rats	*i.p.*: 50 mg/kg b.w.	24, 96 and 168 h after single injection	Liver, spleen, kidney, heart, lungs and brain	[45]
AgNPs: 50-100 nm	Rats	*s.c.*: 62.8 mg/kg b.w.	2, 4, 8, 12, 18 and 24 weeks after single injection	Brain	[135]
AgNPs: 25 nm	Mice	Intranasal: 100 or 500 mg/kg b.w.	1 and 7 days after single treatment	Spleen, lungs, kidney, nasal cavity and brain	[46]
AgNPs: 56 nm	Rats	Oral: 30, 125 or 500 mg/kg b.w./day	90 days of repeated exposure	Blood, liver, kidney, lungs, testes and brain	[67]
AgNPs: 10 and 25 nm	Rats	Oral: 100 or 500 mg/kg b.w./day	28 days of repeated exposure with measurement of silver level after a wash-out period of 1, 2 and 4 months	Blood, brain, kidney, spleen, liver, testes and ovaries	[70]
PVP-coated AgNPs: 14 ± 4 nm	Rats	Oral: 9 mg/kg b.w./day	28 days of repeated exposure	Plasma, liver, kidney, stomach, lungs, muscle, brain and small intestine	[81]
AgNPs: 22, 42 and 71 nm	Mice	Oral: 1 mg/kg b.w./day	14 days of repeated exposure	Liver, kidney, brain, lungs and testes	[99]
Uncoated AgNPs: < 20 nm, PVP-coated AgNPs: < 15 nm	Rats	Oral: 90 mg/kg b.w./day	28 days of repeated exposure; the measurement of silver level 1 day, 1 week and 8 weeks after previous administration	Liver, kidney, lungs, heart, spleen, brain, bladder, testes, blood, intestine and stomach	[138]
AgNPs: 18-19 nm	Rats	Inhalation: 49, 133 or 515 µg AgNPs/m(3)	Exposure for 6 h/day, 5 days/week, for 13 weeks in a whole-body inhalation chamber	Liver, kidney, olfactory bulb, brain, lungs, and blood	[131]

AgNPs – silver nanoparticles, BSA – bovine serum albumin, PVP – polyvinylpyrrolidone, i.v. – intravenous, i.p. – intraperitoneal, s.c. – subcutaneous, b.w. – body weight

Toxicity of AgNPs

There has been significant progress in silver-based nanotechnology in recent years. The commercialization of nanoproducts is increasing each year, and studies on the toxicological potential of such products are needed. Currently available information about hazards associated with AgNPs requires further verification.

The existing data suggest that the size of AgNPs is highly correlated with their toxicity. In many studies with mammalian cells, it was found that smaller AgNPs are more toxic than larger ones in equivalent dosages. The role of the size of AgNPs in toxicity was confirmed in *in vitro* experiments comparing cytotoxicity and genotoxicity of 20, 80 and 113 nm AgNPs [102]. Furthermore, cytotoxic effects were exhibited by 10 nm AgNPs, but not 40 and 75 nm citrate-coated silver nanoparticles [48]. Size-dependent toxicity of AgNPs was also confirmed in studies on the influence of 15, 30 and 55 nm AgNPs on viability and oxidative stress induction in alveolar macrophages [15]. Research was also designed to evaluate size-dependent cytotoxic effects of AgNPs of different sizes (5, 20 and 50 nm) on various types of human cells. In all toxicity endpoint studies (cell morphology, viability, cellular membrane integrity and oxidative stress) it was observed that 5 nm AgNPs induce the most severe damage, with larger particles inducing less damage [78].

The surfaces of silver nanoparticles are often coated with various types of compounds to provide stability and prevent agglomeration. For example, polysaccharide-coated AgNPs do not agglomerate, in contrast to uncoated AgNPs [1]. The type of capping agent may also play a crucial role in stabilization of AgNPs. Polyvinylpyrrolidone (PVP)-coated AgNPs were found to be stable over a 1-week period in water, whereas citrate-coated AgNPs are unstable [136].

The most popular types of nanoparticle coatings are citrate, chitosan, PVP, polysaccharides, peptides and carbon. Different types of superficial agents may generate coating-specific behavior of AgNPs in solution [66] or in physiological fluids [13], and consequently may cause different antimicrobial or toxic effects.

Only a few studies have compared the influence of various coating agents on AgNP-induced toxicity; therefore this issue is still not fully understood. Among other effects, it was demonstrated that carbon-coated silver nanoparticles influence cell viability to a lesser extent than uncoated AgNPs of similar size [95], whereas polysaccharide-coated AgNPs cause more severe effects than uncoated AgNPs [1]. Moreover, it was shown that PVP-coated [66] or peptide-coated [51] AgNPs are more toxic than citrate-coated AgNPs with similar particle core sizes.

It is also claimed that all observed AgNP-mediated toxic effects are a consequence of silver ions released from the surface of nanoparticles inside cells through the "Trojan Horse effect" [48,100,126]. Moreover, it is considered that smaller AgNPs are able to release silver ions from their surfaces more efficiently than larger ones, because of the larger surface area per unit mass [48].

Ag^+ ions are released after surface oxidation of AgNPs. Notably, it was shown that the intracellular solubility of AgNPs is 50 times greater than their solubility in pure water [126].

The most effective cellular conditions for dissolving endocytosed AgNPs are found in the acidic environment of lysosomes, which has a pH of about 4.8 [26,122]. However, it has been suggested that the toxic effects are a combined result of both AgNPs and released silver ions [16,44,108,127].

It was observed that PVP-coated AgNPs and Ag^+ ions both affect cellular pathways involved in oxidative stress and homeostasis of Na^+, K^+ and H^+ ions. Toxic effects of AgNPs on fish were found to be mediated by activation of a few nuclear receptors and inhibition of ligand binding to the dopamine receptor. In contrast, in tissues of Ag^+-exposed fish, ligand binding to adrenergic receptors $\alpha 1$ and $\alpha 2$ and cannabinoid receptor CB1 were found to be inhibited [44]. Powers and co-workers showed that ascorbate protects cells against Ag^+-induced oxidative stress, but does not act as an effective antioxidant with respect to stress induced by AgNPs [108].

Other studies indicate that the pattern of expression of stress-related genes in liver of AgNP- or Ag^+-treated fish (Japanese Medaka) is different [16]. Silver ions induce an inflammatory response in the liver of exposed fish, whereas AgNPs increase expression of genes implicated in DNA damage, carcinogenesis and oxidative stress.

Toxic effects of AgNPs in microorganisms

It was observed in a variety of studies that AgNPs exhibit antimicrobial activity against gram-positive (*Staphylococcus aureus*) and gram-negative bacteria (*Pseudomonas aeruginosa* and *Escherichia coli*) [94,129,133]. Thus it was proposed that AgNPs may constitute an attractive alternative to antibiotics. It has been proposed that silver nanoparticles could play a major role in solving the serious public health problem caused by the presence of multidrug-resistant bacteria, which are resistant to most antibiotics [4]. In addition, AgNPs are also useful in disrupting the formation of bacterial biofilms, wherein bacteria aggregate into complex invasive structures. These structures provide the basis for a natural survival strategy used by microorganisms after invasion of a host and provides resistance to a lot of commonly used anti-microbial agents. Strains of *Pseudomonas aeruginosa* and *Staphylococcus epidermidis* have been found to be susceptible to the anti-biofilm properties of AgNPs [65,98].

Even though the antibacterial effects of AgNPs have been extensively examined, their mechanisms of action have been only partially elucidated. Although one hypothesis emphasizes the role of silver ions released from the surfaces of AgNPs inside bacterial cells [53,82], direct action of AgNPs on microorganisms has also been proposed [64].

Many studies indicate that AgNPs or Ag^+ released from their surfaces may directly damage the cell membranes. Silver structures are known to adhere to the microbial cell wall and cause structural changes in the cell membrane proteins, such as cis-trans

isomerization of unsaturated fatty acids. The changes in the membrane components lead to increased membrane fluidity and decreased resistance to environmental factors [53]. Structural changes in membrane proteins cause them to become inactivated and released, causing degradation of membrane structure [129]. These abnormalities lead to a significant increase in permeability, resulting in cell death.

Structural proteins and enzymes with thiol groups are highly sensitive to inactivation by AgNPs or released Ag^+ ions [125]. Interactions of AgNPs with the thiol groups of the L-cysteine residue have been found to disturb the function of several enzymes of *Staphylococcus epidermidis* [50]. Moreover, both forms of silver may interact with bacterial DNA and prevent DNA replication and cell division, leading to cell death [34,125]. Another mechanism of antibacterial action induced by AgNPs is generation of reactive oxygen species, which damage all components of the cell, including cell membranes and DNA [64,72].

The biocidal potency of AgNPs is also effective with respect to fungi and viruses. Antifungal activity against *Cladosporium cladosporioides*, *Aspergillus niger* [109], *Trichophyton rubrum* [104] and *Candida* sp. [93] has been demonstrated. AgNPs have been found to be a potential weapon against a wide range of viruses. Due to the low likelihood of resistance, AgNPs may provide effective antiviral therapies against HIV-1 [68], hepatitis B virus [84], herpes simplex virus types 1 [9] and 2 [97] and influenza virus [143]. The mechanism of antiviral potential of AgNPs is still being investigated. It is thought that AgNPs interact with glycoprotein receptors [68], the viral envelope [143] and double-stranded DNA/RNA [84], thereby preventing the replication of viruses, or block the binding of viruses to the host cell.

Toxic effects of silver nanoparticles in mammals

Following entry of AgNPs into the systemic circulation, they may migrate into many organs and induce toxicity. Table III lists studies demonstrating the negative influence of AgNPs in mammalian organisms. A series of studies has shown that systematically administered AgNPs cause inflammatory and cytotoxic effects including pulmonary toxicity after prolonged inhalation [132] and hepatotoxicity after prolonged oral [30,67,103], intravenous [25] or intraperitoneal [32] administration. Moreover, histopathological changes in kidneys and increasing levels of creatinine have been reported [33,119], indicating that AgNPs may cause nephrotoxic effects. Impairment of spermatogenesis in rats exposed to AgNPs was also observed [128].

Toxic effects of AgNPs in liver of rodents have been intensively investigated. Adverse effects were observed including marked pathological changes in liver morphology [32,67,71], changes in liver enzyme activities [2,56,99], changes in the level of plasma lipids [30,67], generation of ROS [30,103] and inflammatory response [25,99]. Autophagy and apoptosis have been confirmed to play roles in mediating hepatotoxicity [71].

Mechanisms of AgNP-induced toxicity

In recent years, the mechanisms of AgNP-induced toxicity have been intensively investigated. It remains unknown if observed toxic effects are caused only by direct interaction of AgNPs with biological systems, or if silver ions released from the surfaces of the AgNPs inside the cell are also involved. In any case, the contribution of individual forms of silver has been found to induce toxicity, and a number of *in vitro* and *in vivo* studies have provided strong evidence for a connection between AgNP-mediated production of reactive oxygen species, oxidative stress, DNA damage, inflammation and cell death. A schematic representation of mechanisms of toxicity of AgNPs is shown in Figure 1.

It is likely that AgNP-mediated ROS production is related to physical (size, shape, surface charge) and chemical (surface coating, solubility, elemental composition) properties which create chemical conditions to induce an oxidative environment inside the cells. These conditions cause an imbalance in the cellular energy system, which depends on redox potential, leading to initiation of the inflammatory response or cell death. However, there is evidence that the mechanisms of toxicity of AgNPs towards neurons are much more complex [148].

AgNP-induced oxidative stress and disruption of mitochondria

Reactive oxygen species are chemically reactive molecules produced as natural byproducts during the mitochondrial electron transport process in aerobic respiration or by oxidoreductase enzymes and have an important role in cellular processes, such as

Table III. Selected studies demonstrating toxic effects of silver nanoparticles in mammals

Type of AgNPs	Mammalian model	Administration method, dosage, time of exposure	Observed toxic effects	References
AgNPs: 20, 100 nm	Rats	*i.v.*: 28 days of repeated administration, dose 6 mg/kg b.w./day	(Only 20 nm toxic) – Decreased body weight – Enlargement of spleen and liver – Histopathological changes in liver, spleen and lymph nodes – Increased activity of liver enzymes (alkaline phosphatase, alanine transaminase and aspartate transaminase) – Changes in red blood cell parameters – Changes in immune parameters (suppression of natural killer cells; changes in production of cytokines: IL-10, IL-1β, IL-6, TNF-α; decrease in interferon-γ production; increase in IgM and IgE immunoglobulin levels in serum)	[25]
AgNPs: 20 nm	Rats	Oral: 81 days of repeated administration, dose 500 mg/kg b.w./day	– Decreased body weight – Increased level of total cholesterol and LDL-cholesterol and decreased level of triglycerides – Increased plasmatic alanine transaminase activity – Increased liver and cardiac superoxide anion ($O_2^{\cdot-}$) production – Increased level of IL-6 and TNF-α in liver – No changes in liver SOD activity, liver lipid peroxidation and plasma antioxidant capacity	[30]
AgNPs: 56 nm	Rats	Oral: 90 days of repeated administration, dose 30, 125 or 500 mg/kg b.w./day	– Decreased body weight of male rodents – Increased alkaline phosphatase activity (dose 500 mg/kg b.w.) – Increased level of cholesterol (doses: 125 and 500 mg/kg b.w.) – Histopathological changes in liver tissues (bile-duct hyperplasia, fibrosis, pigmentation inflammatory cell infiltration) and intestines (pigmentation) – No changes in hematological parameters, except for a significant increase in the number of monocytes (dose 500 mg/kg b.w.)	[67]
AgNPs: 10-30 nm	Rats	*i.p.*: single injection, dose 500 mg/kg b.w./day	– Low level of ATP content in liver tissue – Induction of autophagy and apoptosis in liver – Histopathological changes in liver tissues (piecemeal necrosis and chronic inflammatory cell infiltration)	[71]
AgNPs: 22, 42 and 71 nm	Mice	Oral: 14 days of repeated administration, dose 1 mg/kg b.w./day or 28 days of repeated administration, dose 1 mg/kg b.w./day (42 nm)	– No changes in body weight of rodents – Increased level of TGF-β in serum after 14 days of administration (other cytokines not investigated) – Increased level of cytokines: IL-1, IL-6, IL-4, IL-10, IL-12 and TGF-β in serum after 28 days of exposure – Increased distribution of NK cells and B cells after 14 and 28 days – Increased activity of liver enzymes (alkaline phosphatase, alanine transaminase and aspartate transaminase) – Increased IgE production after 28 days of administration – No histopathological changes in organs (liver, kidney and small intestine)	[99]

Table III. Cont.

Type of AgNPs	Mammalian model	Administration method, dosage, time of exposure	Observed toxic effects	References
AgNPs: 10 nm	Rats	Oral: 5 days of repeated administration at doses of: 5, 25, 50 and 100 mg/kg b.w./day	(Effects observed for doses of 50 and 100 mg/kg b.w.) – Induction of ROS production in liver – Increased activity of liver enzymes (alkaline phosphatase, alanine transaminase and aspartate transaminase) – Increased lipid peroxidation in liver tissue – Morphological alterations in liver tissue (hepatocyte disruption, hepatocellular vacuolization, degeneration of liver, central vein injury and areas of necrosis) – DNA damage in liver	[103]
AgNPs: size < 100 nm	Rats	*i.p.*: two injections of AgNPs in a dose of 2 mg/kg b.w./day	– Histopathological alterations in liver and renal tissues – Increased number of white blood cells and increased hemoglobin level – Increased serum creatinine, urea, and aspartate and alanine aminotransferases	[119]
AgNPs: 18 nm	Rats	90 days of 6 h/day exposure via inhalation at concentrations of 0.7×10^6, 1.4×10^6 and 2.9×10^6 particles/cm^3	– Significant decrease of tidal volume and minute volume – Histopathological changes in lungs (mixed inflammatory cell infiltration, chronic alveolar inflammation and small granulomatous lesions)	[132]
AgNPs: 8.7 nm	Rats	*i.p.*: 28 days of repeated administration at doses of 1, 2, and 4 mg/kg b.w./day	– No significant changes in the body weight of rodents – Histopathological changes in liver tissue (bile-duct hyperplasia, cholangiofibrosis, hepatocellular necrosis and leukocytosis) – Increased lipid peroxidation in liver tissue after dose of 2 and 4 mg/kg b.w. – No change in GSH level in liver tissue – Chromosomal aberrations after 4 mg/kg b.w.	[32]
AgNPs: 35-45 nm	Mice	Oral: 14 days of repeated administration at a dose of 50 µl of AgNP solution at concentration of 20 or 50 ppm	– Increased activity of liver enzymes (alanine transaminase and aspartate transaminase) – No change in blood parameters (values of red blood cells, hemoglobin and hematocrit) – Histopathological changes in liver (cytoplasmic vacuolization of hepatocytes with necrosis, inflammation and degeneration of hepatic cells)	[56]
AgNPs: 21 ± 8 nm	Rats	*i.v.*: single injection, dose 10 mg/kg b.w.; intratympanic injection: 40 µl of 0.4 % of AgNP was injected into the middle ear cavity	– Glycosaminoglycan accumulation in the basement membrane associated with up-regulation of production of hyaluronic acid in kidney and cochlea (after *i.v.* injection) leading to renal failure and hearing loss (a significant hearing loss over a broad range of frequencies after intratympanic injection) – Increased concentration of urea and creatinine in the serum (after *i.v.* injection) – Presence of proteins in the urine (after *i.v.* injection)	[33]

Table III. Cont.

Type of AgNPs	Mammalian model	Administration method, dosage, time of exposure	Observed toxic effects	References
AgNPs: 43.6 ± 6.4 nm	Mice	*i.p.*: single injection in doses of 26, 52 and 78 mg/kg b.w.; animals were sacrificed 24 and 72 h after injection	– Increased activity of liver enzymes (alkaline phosphatase, alanine transaminase and aspartate transaminase) – 24 and 72 h after injection in all doses – Oxidative DNA damage in lymphocytes – 24 and 72 h after injection in all doses – Induction of apoptosis in liver tissue – mainly after 78 mg AgNPs/kg b.w.) – Histopathological changes in liver (lymphocyte infiltration in the hepatic portal space, necrosis, vacuolization of hepatocytes and edema around the blood vessels)	[2]
AgNPs: 20 nm	Rats	*i.v.*: 28 days of repeated administration at doses of 0.0082, 0.025, 0.074, 0.22, 0.67, 2, and 6 mg/kg b.w.	– Decreased body weight – Reduced thymus weight and increased spleen weight, no effect on liver and kidney weights – Decrease of NK cell activity – Changes in red blood cell, hemoglobin and white blood cell parameters – Decreased IgG and increased IgM levels – Changes in the level of cytokines	[139]
AgNPs: 20 nm	Rats	*i.v.*: single injection, dose: 238-263 µg/kg b.w.	– No changes in GSH level in liver – Increased mRNA expression of IL-8, macrophage inflammatory protein 2, IL-1 receptor and TNF-α; and no changes in mRNA level of IL-1β, IL-10	[39]

b.w. – body weight, GSH – reduced glutathione, IgE – immunoglobulin E, IgG – immunoglobulin G, IgM – immunoglobulin M, IL – interleukin, i.p. – intraperitoneal, i.v. – intravenous, SOD – superoxide dismutase, TGF-β – transforming growth factor β, TNF-α – tumor necrosis factor α

growth, proliferation, apoptosis, differentiation and activation of cell signaling cascades [55]. Moreover, phagocytic cells are able to produce ROS while participating in induction of host cell defense mechanisms [111,121].

ROS are generated mainly in mitochondria during oxidative phosphorylation. Physiologically, cells defend themselves against ROS damage with antioxidant enzymes such as superoxide dismutase (SOD), catalase, glutathione peroxidase (GPx) and glutathione S-transferase, as well as using non-enzymatic factors such as glutathione to reduce ROS. An imbalance between the level of destructive ROS and the availability of biological systems for detoxification of the reactive species leads to oxidative stress [12]. Pathologically increased free radicals cause oxidative damage to all cell components, including oxidation of polyunsaturated fatty acids in lipids, oxidation of amino acids in proteins and DNA damage. Significant damage to cell structures leads to apoptotic cell death if cellular repair mechanisms are ineffective [37]. Brain tissues are highly sensitive to abnormal levels of ROS, because their defensive mechanisms are limited. Moreover, reactive oxygen species are involved in the development of the inflammatory response, which is an important element of the pathogenesis of neurodegenerative diseases such as Alzheimer's disease [107] or Parkinson's disease [41].

Presumably, AgNP-mediated ROS production is associated with intracellular oxidation of AgNPs to Ag^+ ions. This chemical process creates a pro-oxidant environment which interferes with mitochondrial functions and may lead to overproduction of ROS and mitochondrial damage [126]. A deleterious influence of silver on mitochondrial functions has been observed *in vitro* in rat liver cells [60], human liver cells [106,130] and human colon cancer cells [118]. Moreover, AgNPs were shown to decrease the activity of mitochondrial respiratory chain complexes I, II, III and IV, leading to a drop in ATP levels and increased rates of ROS production [7,22].

Furthermore, it has also been proposed that AgNPs may interact, directly or via released Ag^+ ions, with amino acid thiol groups, disrupting the function of structural proteins in mitochondrial membranes

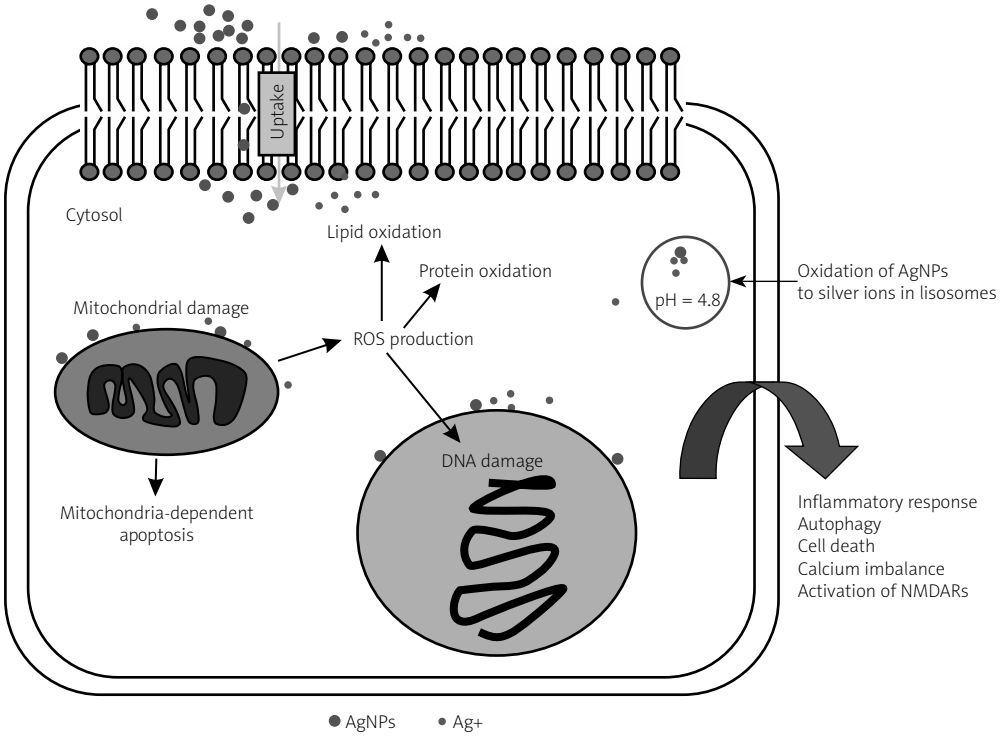

Fig. 1. Schematic representation of the mechanisms of AgNPs toxicity.

and/or mitochondrial enzymes [62]. For example, Ag^+ ions were observed to interfere with thiol groups in the mitochondrial inner membrane, increasing its permeability [5]. This mechanism of AgNPs toxicity may be confirmed by the fact that weak antioxidants with –SH groups such as 2,3-dithiopropanol [26], N-acetylcysteine (NAC) [62], methionine and cysteine are more effective against AgNP-induced cytotoxicity than the most potent antioxidants without thiol groups such as Trolox (water soluble vitamin E analog) or Tempol [126].

Overproduction of ROS during exposure to AgNPs has been proven directly in several *in vitro* investigations [15,26,78,141] and also *in vivo* [30,103]. Among the oxidative stress-related changes caused by AgNPs, depletion of reduced glutathione (GSH) has been observed in human skin carcinoma cells [6], rat liver cells [60], mouse macrophage cells [100], human liver cells [106,141] and mouse embryonic fibroblasts [74]. Results of studies on aquatic organisms strongly support these *in vitro* observations [3,38,86], whereas limited *in vivo* studies demonstrate a lack of changes in GSH levels in liver of exposed rodents [32,39].

Furthermore, oxidative stress-related lipid peroxidation was demonstrated *in vitro* [6,106] and *in vivo* in liver of exposed rats [32,103]. DNA damage induced by ROS has been detected *in vitro* as increased DNA fragmentation in human alveolar cells [35], human liver cells [106], human epithelial embryonic cells [116], and *in vivo* in rodents [2,32,103] and aquatic organisms exposed to AgNPs [3,38].

Moreover, changes in the activity of antioxidant enzymes have been suggested to occur under the influence of AgNPs. Both decreased [6,130] and increased [141] SOD activity has been observed. It was also found that exposure to AgNPs leads to a decrease in the activity levels of glutathione peroxidases in a human liver cell line [130].

AgNP-induced inflammation and cell death

Several *in vitro* studies provide evidence of an inflammatory response in cells exposed to AgNPs. The connection between increased ROS levels and the release of inflammatory mediators such as interleukin-6, tumor necrosis factor-alpha [95], interleukin-1β and macrophage inhibitory protein (MIP-2) in macro-

phages [15] has been observed. The AgNP-mediated inflammatory response was also observed in rodent liver [30,56,67,71] and lungs [132], and increased expression of cytokines was observed in serum [25,39,99].

As described above, AgNP-induced changes in the mitochondrial membrane potential disrupt mitochondria and lead to reduction of ATP content. This may activate the protective process of autophagy. This conservative intracellular protein degradation system promotes cell survival by allowing the use of misfolded proteins as well as injured and unnecessary cellular components as alternative energy sources. However, it has been shown that prolonged autophagy may induce cell death through excessive autolysis or apoptosis [47,89].

There have been limited studies demonstrating that AgNPs may induce autophagy. Correlations between decreasing ATP content, autophagy and apoptosis have been observed in liver of rats exposed to AgNPs [71]. Additionally, relationships between oxidative stress, autophagy and apoptosis have been demonstrated in mouse embryonic fibroblast cells [74]. Induction of apoptosis by AgNPs has been demonstrated *in vitro* in many types of mammalian cells, for example in THP-1 monocytes [36], human lung cancer cells [35], human liver cells [106], human colon cancer cells [118], fibroblast cells [57], mouse embryonic fibroblasts [74], HeLa cells (human cervical carcinoma), A549 cells (human lung carcinoma) [26], baby hamster kidney (BHK21) and human colon adenocarcinoma cells (HT29) [49]. It was suggested that exposure of cells to AgNPs promotes ROS- and JNK-dependent apoptotic pathways [57]. Activation of p53 [49], down-regulation of the anti-apoptotic protein Bcl-2, up-regulation of pro-apoptotic protein Bax [49,106], activation of caspase-3 [49,74,106,118], release of cytochrome c from mitochondria into the cytosol, translocation of Bax to mitochondria [57,106], formation of DNA adducts and DNA fragmentation [26,35,36,118] have also been reported.

Current evidence of AgNP-induced neurotoxicity

The available data introduced in the section entitled "Routes of exposure and biodistribution of AgNPs in mammalian organisms" suggest that after entering bodily fluids, AgNPs can penetrate the brain tissues and be deposited there for long periods of time. There is a lack of information on the long-lasting effects of accumulation of AgNPs in brain parenchyma, and thorough studies on this subject are required. In this chapter we concentrate on the analysis of the side effects of AgNPs in cultured cells of cerebral origin and in brain tissue of exposed mammals.

Certain data demonstrate that AgNPs may enter the brain along the olfactory nerve when administered via inhalation or intranasally [46]. AgNPs may also penetrate the brain through the blood-brain barrier (BBB) during systemic or oral administration, as indicated in Table II. The evidence that AgNPs cause neurotoxic effects is demonstrated in Table IV.

The influence of AgNPs on blood-brain barrier function

The blood-brain barrier is a highly specialized brain endothelial structure which separates components of the circulating blood from brain parenchyma. The BBB is composed of a basement membrane and microvascular endothelial cells (BMVECs) which interact with pericytes, perivascular astrocytes and neurons. Transport of substances across the BBB is strictly regulated by both physical and metabolic barriers. The physical barrier is created by tight junctions between the BMVECs, whereas the metabolic barrier is provided by specialized enzymes and diverse transport systems [105]. It is quite likely that AgNPs influence the function of endothelial cells and increase the permeability of the BBB by direct toxic effects or by induction of a cascade of events leading to disruption of tight junctions. Since the tight junctions maintaining the integrity of the BBB have a gap of 4-6 nm, it is very likely that nanoparticles pass through the endothelial cell membrane rather than through the inter-endothelial junctions. This is supported by the observation that endothelial cell membranes are undamaged [135].

It was demonstrated using an *in vitro* BBB model that AgNPs can pass the BBB mainly by transcytosis and accumulate inside endothelial cells of microvessels [134]. Moreover, there is evidence that AgNPs induce the release of IL-1β and TNF-α in rat brain microvessels and that this leads to inflammation and a subsequent increase in the permeability of the BBB [137].

The influence of silver nanoparticles on the BBB was also demonstrated *in vivo*. Tang and co-workers observed that subcutaneous injections of AgNPs (50-100 nm) to rats in a dose of 62.8 mg/kg b.w. induce astrocyte swelling outside the blood-brain

Table IV. Studies demonstrating neurotoxic effects of AgNPs in mammalian cells and mammals

Type of AgNPs	Mammals/ Cell lines	Time of exposure, dose	Observed neurotoxic effects	References
***In vitro* studies**				
AgNPs: 32.74-380.25 nm	Rat hippocampal slices	Final concentrations: 10^{-6}, 5×10^{-6}, 10^{-5} g/ml	– Decreased amplitude of voltage-gated sodium current (I_{Na}) of hippocampal CA1 neurons (observed within 2 min after AgNP treatment, 10^{-5} g/ml) – Extension of the recovery time of I_{Na} from inactivity (10^{-5} g/ml)	[80]
AgNPs: 25, 40 and 80 nm	Primary rat brain microvessel endothelial cells (rBMECs)	Time of incubation: 8 or 24 h Final concentration: up to 50 µg/cm^3	(Toxic effects observed for 25 nm AgNPs) – Induction of release of IL-1β, TNF-α and PGE_2 in rBMECs – Increased BBB permeability – Cellular damage with the appearance of large perforations in the monolayers – Decreased cell viability (mainly for 25 and 40 nm AgNPs)	[137]
Peptide- coated AgNPs: 20 and 40 nm, AuNPs: 20 nm	Mixed primary cortical neural cell culture	Time of incubation: up to 24 h Final concentrations: 5, 10, 20, 30, 50 and 100 µg/ml	(Toxic effects observed for 20 nm AgNPs) – Increased ROS production, reduced by antioxidants (NAC) – Formation of protein carbonyls – Induction of heme oxygenase-1 expression – Acute calcium response – Dose-dependent decrease of cell viability	[52]
PVP-coated AgNPs: 75 ± 20 nm	Astroglia-rich primary cultures	Time of incubation: 4 h and further cultured in AgNP-free medium for up to 7 days Final concentrations: 10, 30 and 100 µM silver	– Upregulation of metallothioneins in cells – Unchanged total glutathione level and the GSSG/GSH ratio – No changes in cell viability – No changes in ROS generation – No changes in glucose consumption and lactate production – No changes in extracellular concentration of glucose and lactate	[85]
polyethylene glycol-coated AgNPs: 5 ± 2 nm	Neuroendocrine cells (chromaffin cells)	Final concentrations: 13, 16, 43, 130 µM and 1.3 mM	– Dose-dependent reduction of the amplitude of sodium currents – Induction of local changes in network activity	[14]
AgNPs: 20 nm	Rat cortical cells	Time of incubation: 2 or 3 days Final concentrations: 1, 5, 10 and 50 µg/ml	– Degeneration of cytoskeletal components (β-tubulin, F-actin) – Inhibition of axonal outgrowth, reduction of the intensity of neuronal branches and overlaps, and reduction of cell viability of premature neurons and glial cells – Decreased cell viability of neurons and glia at mature stages of development – Mitochondrial dysfunction leading to mitochondria-dependent cell death – Synaptic degeneration in cortical neurons (reduction of the level of synaptic proteins: synaptophysin and PSD-95)	[144]
PVP-coated AgNPs: from 21.7 ± 1.1 nm to 24.4 ± 0.6 nm	Rat cerebellar granule cells *In vivo*: neonatal rats	Time of incubation: 4 or 24 h Final concentration: up to 50 µg/ml *In vivo*: intranasally, 21 days of repeated exposure; dose: 0.2 or 1 mg/kg b.w.	– Decreased cell viability (after 24 h incubation with AgNPs at a concentration of 0.05 µg/ml) – Increased ROS production after 4 h exposure – Depletion of reduced glutathione after 4 h incubation – Induction of apoptosis after 24 h of incubation – Increased intracellular calcium concentration <u>*In vivo* observations:</u> – Histopathological changes in cerebellum (alterations in the morphology of the granular layer: granule cells with abnormal shape and shrinking nucleus, degeneration granular layer with loss and separation of structure, edema and necrotic areas) – Activation of caspase-3	[146]

Table IV. Cont.

Type of AgNPs	Mammals/ Cell lines	Time of exposure, dose	Observed neurotoxic effects	References
AgNPs: 20 nm	Human cerebral cells: neuroblastoma (SH-SY5Y), astrocytoma (D384); human lung epithelial cells (A549)	Short-term exposure: 4, 24 and 48 h; final concentration: 1-100 µg/ml; prolonged exposure: 7 and 10 days; final concentrations: 0.5-50 µg/ml	– Dose- and time-dependent changes in mitochondrial metabolism and cell membrane damage leading to decreased cell viability – observed for cerebral cell lines after short-term exposure – No significant changes in cell viability of A549 cells after short-term exposure – Dose-dependent reduction of proliferation ability and capacity to form colonies after long-term exposure of human cerebral cells and A549 cells to AgNPs	[20]
PVP-coated AgNPs: < 100 nm	Rat cerebellar granule cells	incubation times: 10, 30 and 60 min, final concentrations: 2.5-75 µg/ml	– Decreased cell viability after 24h incubation (50 µg/ml) – Dose-dependent increase in the uptake of radioactive calcium after 10 min of incubation with the effect abolished by an antagonist of NMDAR (MK-801) – Dose-dependent increase in the intracellular calcium concentration – Activation of glutamatergic N-methyl-D-aspartate receptors – Increased ROS production after 30 min of incubation with 75 µg/ml – Decreased mitochondrial potential after 60 min of incubation	[148]
AgNPs: 3-5 nm	Mouse brain neural cells: murine brain ALT astrocytes, murine microglial BV-2 cells, mouse neuroblastoma Neuro-2a cells	time of incubation: 24 h, final concentration: 5, 10, 12.5 µg/ml	– Increased IL-1β secretion in microglial cells exposed to AgNPs (dose: 12.5 µg/mL) – Increased gene expression of C-X-C motif chemokine 13 and macrophage receptor with collagenous structure in all types of neural cells – Increased expression of glutathione synthetase in microglial cells and decreased in astrocytes – Generation and deposition of amyloid-β (Aβ) protein in neuroblastoma cells (dose: 12.5 µg/ml) – Increased gene expression of amyloid precursor protein (APP) in all neural cells and APP protein level in Neuro-2a cells – Decreased gene expression of LDLR (all types of neural cells) and neprilysin (for neuroblastoma cells), decreased LDLR protein level for Aβ uptake in Neuro-2a cells exposed to AgNPs – Decreased cell proliferation of astrocytes and Neuro-2a cells with no change in microglial cells	[59]
***In vivo* studies**				
AgNPs: 14 nm	Rats, neuronal-like PC12 cells	Oral: 28 days of repeated exposure; doses: 4.5 and 9 mg/kg b.w., *in vitro*: 4-48 h of incubation; final concentrations: 0.5, 5 and 10 µg/ml	*In vivo*: – Increased dopamine concentration in the brain (dose: 4.5 and 9 mg/kg b.w.) – Increased 5-hydroxytryptamine (5-HT) concentration in the brain (dose: 9 mg/kg b.w.) – Unchanged noradrenaline concentration in brain *In vitro*: – Decreased viability of PC12 cells – Induction of necrosis in PC12 not observed – Induction of the mitochondrial and the death receptor pathways	[54]
AgNPs: 50-100 nm	Rats	*s.c.*: single injection; dose: 62.8 mg/kg b.w.	– Histological changes (astrocyte swelling outside the blood–brain barrier, presence of pyknotic and necrotic neurons)	[135]

Table IV. Cont.

Type of AgNPs	Mammals/ Cell lines	Time of exposure, dose	Observed neurotoxic effects	References
AgNPs: 29.3 ± 12.5 nm	Mice	*i.p.*: single injection, dose: 100, 500, 1000 mg/kg b.w.	– Alterations in expression of oxidative stress-related genes in various regions of the brain (caudate nucleus, frontal cortex and hippocampus)	[112]
AlNPs, AgNPs, CuNPs: 50-60 nm	Rats, mice	*i.v.*: single injection, dose: 30 mg/kg b.w.; *i.p.*: single injection, dose: 50 mg/kg b.w.; intracarotid: single injection, dose: 2.5 mg/kg b.w.; and intracerebroventricular: 20 µg/10 µl	Effects observed after administration of AgNPs or CuNPs: – Increased BBB permeability leading to brain edema formation and decrease of local cerebral blood flow – Glial cell activation – Increased level of heat shock protein (HSP) – Loss of myelinated fibers	[123]
AlNPs, AgNPs, CuNPs: 50-60 nm	Rats	*i.v.*: single injection, dose: 30 mg/kg b.w.; *i.p.*: single injection, dose: 50 mg/kg b.w.; and intracerebroventricular: 20 µg/10 µl	– Increased BBB permeability leading to brain edema formation caused by AgNPs, CuNPs	[124]
AgNPs: 32.68-380.21 nm	Rats	Nasal administration: once every two days for 14 days; dose: 3 and 30 mg/kg b.w.	– Deterioration of space learning and memory ability, mainly in the group of animals exposed to 30 mg AgNPs/kg b.w. – Increased ROS production in hippocampal homogenate (3 and 30 mg/kg b.w.) – Histological changes of pyramidal neurons in the PP and DG regions of hippocampus (edema and nuclear shrink phenomenon as well as neurobiosis among the neurons)	[79]
AgNPs: 36.3 ± 1.2 nm	Mice	*i.p.*: 7 days of repeated exposure; dose: 10, 25 and 50 mg/kg b.w.	– No influence on spatial learning and memory – Unmodified adult hippocampal neurogenesis (no changes in hippocampal progenitor proliferation, new born cell survival and differentiation)	[77]
citrate-coated AgNPs: 10 ± 4 nm	Rats	Oral: 14 days of repeated exposure; dose: 0.2 mg/kg b.w.	– Ultrastructural changes in synapses, mainly in hippocampus (e.g. swelling of nerve endings, blurred structure of synaptic cleft, enhanced density of synaptic vesicles, disturbed synaptic membrane with free synaptic vesicles located in neuropil, myelin–like bodies and multi-vesicular bodies) – Decreased level of synaptic proteins: synaptophysin, synapsin I and PSD- 95	[127]
citrate-coated AgNPs: 20-25 nm	Neonatal rats	Intranasal instillation: 14 weeks of repeated exposure; dose: 0.1, 0.2, 0.5 or 1 mg/kg b.w.	– Significant body weight loss – Histological changes (neuroglial cell activation with destruction of the granular layer of the cerebellum) – Increased level of glial fibrillary acidic protein (a marker of astrocyte activation) – Activation of caspase-3	[147]

BBB – blood-brain barrier, b.w. – body weight, GSH – reduced glutathione, GSSG – oxidized glutathione, IL – interleukin, i.p. – intraperitoneal, i.v. – intravenous, LDLR – low-density lipoprotein receptor, NAC – N-acetylcysteine, NMDAR – N-methyl-D-aspartate receptor, PGE_2 – prostaglandin E_2, PSD-95 – postsynaptic receptor density protein, PVP – poly(N-vinylpyrrolidone), ROS – free radicals, TNF-α – tumor necrosis factor-alpha

barrier, and produce pyknotic and necrotic neurons [135]. The influence of nanoparticles on the integrity of the BBB after single intravenous (30 mg/kg b.w.), intraperitoneal (50 mg/kg b.w.) and intracerebroventricular (20 µg/10 µl) administration to rodents was investigated. Increased BBB permeability and brain edema formation [123,124], a marked decrease in local cerebral blood flow, glial cell activation and loss of myelinated fibers [123] were identified.

These limited studies have shown that AgNPs can induce BBB dysfunction and cause neuronal degeneration.

AgNP toxicity towards neuronal cells

The influence of AgNPs on neurons and glial cells has been predominately investigated using *in vitro* models. Many of the results show that exposure to AgNPs causes decreased cell viability, mainly of neurons [20,52,54,59,137,144,146,148]. In the case of astroglia-rich primary cultures, the results are generally inconsistent with either no changes in viability observed after incubation with AgNPs [85] or observations of high sensitivity [52]. Such differences are likely related to both the incubation time and the size of the AgNPs. Moreover, it was observed that AgNPs may negatively influence proliferation of human cerebral cells [20] and axonal outgrowth of premature neurons and glial cells [144].

Additionally, histopathological analysis of the cerebellum of neonatal rats exposed intranasally to AgNPs for 21 days showed many abnormalities including degeneration of the granular layer with loss of structure, edema and necrotic areas [146,147]. Similar changes were also identified in regions of rat hippocampus [79].

AgNPs can also cause changes in action potential, because they may lead to the reduction of the amplitude of voltage-gated sodium currents [14,80]. Xu and co-workers identified degeneration of cytoskeletal components (β-tubulin and F-actin) and synaptic degeneration in cortical neurons [144]. Additionally, ultrastructural changes in synapses were observed in hippocampus of exposed rats together with decreased levels of two presynaptic proteins (synaptophysin and synapsin I) and one postsynaptic protein (PSD-95) [127].

The contribution of oxidative stress to the mechanisms of AgNP-mediated neurotoxicity has been considered. In *in vitro* studies of activation of ROS generation [52,146,148], protein carbonylation [52], induction of heme oxygenase-1 expression [52], and depletion of reduced glutathione concentration [146] were observed. However, loading of primary astrocytes with AgNPs did not cause significant alterations in total and reduced glutathione or ROS production [85]. Mitochondrial dysfunction caused by AgNPs [144,148] and activation of caspase-3 [54,146], which may result in mitochondria-dependent neuronal cell death [54,144,146], have been reported. Limited *in vivo* studies also confirm the connection between AgNPs, oxidative stress and apoptosis in the central nervous system. It was demonstrated that AgNPs may cause up-regulation of oxidative stress-related genes in the brain tissues of mice after a single intraperitoneal injection [112], increased ROS production in rat hippocampus after 7 days of intranasal administration [79] and activation of caspase-3 [147]. However, the mechanisms of neurotoxicity of AgNPs may be more complex in the brain than in other tissues. Recently, new lines of research have indicated an influence of AgNPs on intracellular calcium homeostasis [52,146,148]. Moreover, it was suggested that calcium imbalance, resulting in neuronal cell death, may be connected to activation of glutamatergic receptors (NMDARs) [148]. This observation is in line with data showing impairment of cognitive functions of rats after prolonged intranasal exposure [79]. In contrast to the effect on neurons, protective mechanisms are induced in astrocytic cells. During exposure of primary astrocytes to AgNPs, metallothioneins (metal-binding proteins involved in cell protection against metal-induced toxicity) were shown to be upregulated [85].

Based on these findings, it is apparent that exposure to AgNPs exerts neurotoxic effects in mammals. However, the more subtle or permanent effects should be further investigated. Because our knowledge of the neurotoxic effects of AgNPs is based mainly on *in vitro* studies, future investigations should focus on animal studies. With increasing recognition of the dangers related to extensive usage of AgNPs and potential environmental hazards, we will be able to limit human health risks.

Acknowledgments

The study was supported partially by a statutory grant for Mossakowski Medical Research Centre, Polish Academy of Sciences, and by grant no. NN 401619938 from the Polish Ministry of Science and Higher Education.

References

1. Ahamed M, Karns M, Goodson M, Rowe J, Hussain SM, Schlager JJ, Hong Y. DNA damage response to different surface chemistry of silver nanoparticles in mammalian cells. Toxicol Appl Pharmacol 2008; 233: 404-410.
2. Al Gurabi MA, Ali D, Alkahtani S, Alarifi S. In vivo DNA damaging and apoptotic potential of silver nanoparticles in Swiss albino mice. Onco Targets Ther 2015; 8: 295-302.
3. Ali D. Oxidative stress-mediated apoptosis and genotoxicity induced by silver nanoparticles in freshwater snail Lymnea luteola L. Biol Trace Elem Res 2014; 162: 333-341.
4. Allahverdiyev AM, Abamor ES, Bagirova M, Rafailovich M. Antimicrobial effects of TiO(2) and Ag(2)O nanoparticles against drug-resistant bacteria and leishmania parasites. Future Microbiol 2011; 6: 933-940.
5. Almofti MR, Ichikawa T, Yamashita K, Terada H, Shinohara Y. Silver ion induces a cyclosporine a-insensitive permeability transition in rat liver mitochondria and release of apoptogenic cytochrome C. J Biochem 2003; 134: 43-49.
6. Arora S, Jain J, Rajwade JM, Paknikar KM. Cellular responses induced by silver nanoparticles: in vitro studies. Toxicol Lett 2008; 179: 93-100.
7. Asharani PV, Low Kah Mun G, Hande MP, Valiyaveettil S. Cytotoxicity and genotoxicity of silver nanoparticles in human cells. ACS Nano 2009; 3: 279-290.
8. ATSDR (Agency for Toxic Substances and Disease Registry). Toxicological Profile for Silver. Prepared by Clement International Corporation, under Contract 205-88-0608. U.S. Public Health Service 1990 ATSDR/TP-90-24.
9. Baram-Pinto D, Shukla S, Perkas N, Gedanken A, Sarid R. Inhibition of herpes simplex virus type 1 infection by silver nanoparticles capped with mercaptoethane sulfonate. Bioconjug Chem 2009; 20: 1497-1502.
10. Benn T, Cavanagh B, Hristovski K, Posner JD, Westerhoff P. The release of nanosilver from consumer products used in the home. J Environ Qual 2010; 39: 1875-1882.
11. Benn TM, Westerhoff P. Nanoparticle silver released into water from commercially available sock fabrics. Environ Sci Technol 2008; 42: 4133-4139.
12. Betteridge DJ. What is oxidative stress? Metabolism 2000; 49: 3-8.
13. Braydich-Stolle LK, Breitner EK, Comfort KK, Schlager JJ, Hussain SM. Dynamic characteristics of silver nanoparticles in physiological fluids: toxicological implications. Langmuir 2014; 30: 15309-15316.
14. Busse M, Stevens D, Kraegeloh A, Cavelius C, Vukelic M, Arzt E, Strauss DJ. Estimating the modulatory effects of nanoparticles on neuronal circuits using computational upscaling. Int J Nanomedicine 2013; 8: 3559-3572.
15. Carlson C, Hussain SM, Schrand AM, Braydich-Stolle LK, Hess KL, Jones RL, Schlager JJ. Unique cellular interaction of silver nanoparticles: size-dependent generation of reactive oxygen species. J Phys Chem B 2008; 112: 13608-13619.
16. Chae YJ, Pham CH, Lee J, Bae E, Yi J, Gu MB. Evaluation of the toxic impact of silver nanoparticles on Japanese medaka (Oryzias latipes). Aquat Toxicol 2009; 94: 320-327.
17. Chen X, Schluesener HJ. Nanosilver: a nanoproduct in medical application. Toxicol Lett 2008; 176: 1-12.
18. Christensen FM, Johnston HJ, Stone V, Aitken RJ, Hankin S, Peters S, Aschberger K. Nano-silver - feasibility and challenges for human health risk assessment based on open literature. Nanotoxicology 2010; 4: 284-295.
19. Clement JL, Jarrett PS. Antibacterial silver. Met Based Drugs 1994; 1: 467-482.
20. Coccini T, Manzo L, Bellotti V, De Simone U. Assessment of cellular responses after short- and long-term exposure to silver nanoparticles in human neuroblastoma (SH-SY5Y) and astrocytoma (D384) cells. ScientificWorldJournal 2014; 2014: 259765.
21. Cohen MS, Stern JM, Vanni AJ, Kelley RS, Baumgart E, Field D, Libertino JA, Summerhayes IC. In vitro analysis of a nanocrystalline silver-coated surgical mesh. Surg Infect (Larchmt) 2007; 8: 397-403.
22. Costa CS, Ronconi JV, Daufenbach JF, Goncalves CL, Rezin GT, Streck EL, Paula MM. In vitro effects of silver nanoparticles on the mitochondrial respiratory chain. Mol Cell Biochem 2010; 342: 51-56.
23. Cronholm P, Karlsson HL, Hedberg J, Lowe TA, Winnberg L, Elihn K, Wallinder IO, Moller L. Intracellular uptake and toxicity of Ag and CuO nanoparticles: a comparison between nanoparticles and their corresponding metal ions. Small 2013; 9: 970-982.
24. Cushen M, Kerry J, Morris M, Cruz-Romero M, Cummins E. Evaluation and simulation of silver and copper nanoparticle migration from polyethylene nanocomposites to food and an associated exposure assessment. J Agric Food Chem 2014; 62: 1403-1411.
25. De Jong WH, Van Der Ven LT, Sleijffers A, Park MV, Jansen EH, Van Loveren H, Vandebriel RJ. Systemic and immunotoxicity of silver nanoparticles in an intravenous 28 days repeated dose toxicity study in rats. Biomaterials 2013; 34: 8333-8343.
26. De Matteis V, Malvindi MA, Galeone A, Brunetti V, De Luca E, Kote S, Kshirsagar P, Sabella S, Bardi G, Pompa PP. Negligible particle-specific toxicity mechanism of silver nanoparticles: the role of Ag+ ion release in the cytosol. Nanomedicine 2015; 11: 731-739.
27. Dos Santos CA, Seckler MM, Ingle AP, Gupta I, Galdiero S, Galdiero M, Gade A, Rai M. Silver nanoparticles: therapeutical uses, toxicity, and safety issues. J Pharm Sci 2014; 103: 1931-1944.
28. Drake PL, Hazelwood KJ. Exposure-related health effects of silver and silver compounds: a review. Ann Occup Hyg 2005; 49: 575-585.
29. Dziendzikowska K, Gromadzka-Ostrowska J, Lankoff A, Oczkowski M, Krawczynska A, Chwastowska J, Sadowska-Bratek M, Chajduk E, Wojewodzka M, Dusinska M, Kruszewski M. Time-dependent biodistribution and excretion of silver nanoparticles in male Wistar rats. J Appl Toxicol 2012; 32: 920-928.
30. Ebabe Elle R, Gaillet S, Vide J, Romain C, Lauret C, Rugani N, Cristol JP, Rouanet JM. Dietary exposure to silver nanoparticles in Sprague-Dawley rats: effects on oxidative stress and inflammation. Food Chem Toxicol 2013; 60: 297-301.
31. Eby DM, Luckarift HR, Johnson GR. Hybrid antimicrobial enzyme and silver nanoparticle coatings for medical instruments. ACS Appl Mater Interfaces 2009; 1: 1553-1560.

32. El Mahdy MM, Eldin TA, Aly HS, Mohammed FF, Shaalan MI. Evaluation of hepatotoxic and genotoxic potential of silver nanoparticles in albino rats. Exp Toxicol Pathol 2015; 67: 21-29.
33. Feng H, Pyykko I, Zou J. Hyaluronan up-regulation is linked to renal dysfunction and hearing loss induced by silver nanoparticles. Eur Arch Otorhinolaryngol 2015; 272: 2629-2642.
34. Feng QL, Wu J, Chen GQ, Cui FZ, Kim TN, Kim JO. A mechanistic study of the antibacterial effect of silver ions on Escherichia coli and Staphylococcus aureus. J Biomed Mater Res 2000; 52: 662-668.
35. Foldbjerg R, Dang DA, Autrup H. Cytotoxicity and genotoxicity of silver nanoparticles in the human lung cancer cell line, A549. Arch Toxicol 2011; 85: 743-750.
36. Foldbjerg R, Olesen P, Hougaard M, Dang DA, Hoffmann HJ, Autrup H. PVP-coated silver nanoparticles and silver ions induce reactive oxygen species, apoptosis and necrosis in THP-1 monocytes. Toxicol Lett 2009; 190: 156-162.
37. Franco R, Sanchez-Olea R, Reyes-Reyes EM, Panayiotidis MI. Environmental toxicity, oxidative stress and apoptosis: menage a trois. Mutat Res 2009; 674: 3-22.
38. Gagne F, Auclair J, Turcotte P, Gagnon C. Sublethal effects of silver nanoparticles and dissolved silver in freshwater mussels. J Toxicol Environ Health A 2013; 76: 479-490.
39. Gaiser BK, Hirn S, Kermanizadeh A, Kanase N, Fytianos K, Wenk A, Haberl N, Brunelli A, Kreyling WG, Stone V. Effects of silver nanoparticles on the liver and hepatocytes in vitro. Toxicol Sci 2013; 131: 537-547.
40. Gajbhiye M, Kesharwani J, Ingle A, Gade A, Rai M. Fungus-mediated synthesis of silver nanoparticles and their activity against pathogenic fungi in combination with fluconazole. Nanomedicine 2009; 5: 382-386.
41. Gaki GS, Papavassiliou AG. Oxidative stress-induced signaling pathways implicated in the pathogenesis of Parkinson's disease. Neuromolecular Med 2014; 16: 217-230.
42. Galdiero S, Falanga A, Vitiello M, Cantisani M, Marra V, Galdiero M. Silver nanoparticles as potential antiviral agents. Molecules 2011; 16: 8894-8918.
43. Garcia-Contreras R, Argueta-Figueroa L, Mejia-Rubalcava C, Jimenez-Martinez R, Cuevas-Guajardo S, Sanchez-Reyna PA, Mendieta-Zeron H. Perspectives for the use of silver nanoparticles in dental practice. Int Dent J 2011; 61: 297-301.
44. Garcia-Reyero N, Kennedy AJ, Escalon BL, Habib T, Laird JG, Rawat A, Wiseman S, Hecker M, Denslow N, Steevens JA, Perkins EJ. Differential effects and potential adverse outcomes of ionic silver and silver nanoparticles in vivo and in vitro. Environ Sci Technol 2014; 48: 4546-4555.
45. Garza-Ocanas L, Ferrer DA, Burt J, Diaz-Torres LA, Ramirez Cabrera M, Rodriguez VT, Lujan Rangel R, Romanovicz D, Jose-Yacaman M. Biodistribution and long-term fate of silver nanoparticles functionalized with bovine serum albumin in rats. Metallomics 2010; 2: 204-210.
46. Genter MB, Newman NC, Shertzer HG, Ali SF, Bolon B. Distribution and systemic effects of intranasally administered 25 nm silver nanoparticles in adult mice. Toxicol Pathol 2012; 40: 1004-1013.
47. Glick D, Barth S, Macleod KF. Autophagy: cellular and molecular mechanisms. J Pathol 2010; 221: 3-12.
48. Gliga AR, Skoglund S, Wallinder IO, Fadeel B, Karlsson HL. Size-dependent cytotoxicity of silver nanoparticles in human lung cells: the role of cellular uptake, agglomeration and Ag release. Part Fibre Toxicol 2014; 11: 11.
49. Gopinath P, Gogoi SK, Sanpui P, Paul A, Chattopadhyay A, Ghosh SS. Signaling gene cascade in silver nanoparticle induced apoptosis. Colloids Surf B Biointerfaces 2010; 77: 240-245.
50. Gordon O, Vig Slenters T, Brunetto PS, Villaruz AE, Sturdevant DE, Otto M, Landmann R, Fromm KM. Silver coordination polymers for prevention of implant infection: thiol interaction, impact on respiratory chain enzymes, and hydroxyl radical induction. Antimicrob Agents Chemother 2010; 54: 4208-4218.
51. Haase A, Arlinghaus HF, Tentschert J, Jungnickel H, Graf P, Mantion A, Draude F, Galla S, Plendl J, Goetz ME, Masic A, Meier W, Thunemann AF, Taubert A, Luch A. Application of laser postionization secondary neutral mass spectrometry/time-of-flight secondary ion mass spectrometry in nanotoxicology: visualization of nanosilver in human macrophages and cellular responses. ACS Nano 2011; 5: 3059-3068.
52. Haase A, Rott S, Mantion A, Graf P, Plendl J, Thunemann AF, Meier WP, Taubert A, Luch A, Reiser G. Effects of silver nanoparticles on primary mixed neural cell cultures: uptake, oxidative stress and acute calcium responses. Toxicol Sci 2012; 126: 457-468.
53. Hachicho N, Hoffmann P, Ahlert K, Heipieper HJ. Effect of silver nanoparticles and silver ions on growth and adaptive response mechanisms of Pseudomonas putida mt-2. FEMS Microbiol Lett 2014; 355: 71-77.
54. Hadrup N, Loeschner K, Mortensen A, Sharma AK, Qvortrup K, Larsen EH, Lam HR. The similar neurotoxic effects of nanoparticulate and ionic silver in vivo and in vitro. Neurotoxicology 2012; 33: 416-423.
55. Hancock JT, Desikan R, Neill SJ. Role of reactive oxygen species in cell signalling pathways. Biochem Soc Trans 2001; 29: 345-350.
56. Heydrnejad MS, Samani RJ, Aghaeivanda S. Toxic Effects of Silver Nanoparticles on Liver and Some Hematological Parameters in Male and Female Mice (Mus musculus). Biol Trace Elem Res 2015; 165: 153-158.
57. Hsin YH, Chen CF, Huang S, Shih TS, Lai PS, Chueh PJ. The apoptotic effect of nanosilver is mediated by a ROS- and JNK-dependent mechanism involving the mitochondrial pathway in NIH3T3 cells. Toxicol Lett 2008; 179: 130-139.
58. http://www.nanosilver.com.my/images/silversol/SilverlSol-Coated-Glove.jpg.
59. Huang CL, Hsiao IL, Lin HC, Wang CF, Huang YJ, Chuang CY. Silver nanoparticles affect on gene expression of inflammatory and neurodegenerative responses in mouse brain neural cells. Environ Res 2015; 136: 253-263.
60. Hussain SM, Hess KL, Gearhart JM, Geiss KT, Schlager JJ. In vitro toxicity of nanoparticles in BRL 3A rat liver cells. Toxicol In Vitro 2005; 19: 975-983.
61. Ivask A, Kurvet I, Kasemets K, Blinova I, Aruoja V, Suppi S, Vija H, Kakinen A, Titma T, Heinlaan M, Visnapuu M, Koller D, Kisand V, Kahru A. Size-dependent toxicity of silver nanoparticles to bacteria, yeast, algae, crustaceans and mammalian cells in vitro. PLoS One 2014; 9: e102108.
62. Jiang X, Miclaus T, Wang L, Foldbjerg R, Sutherland DS, Autrup H, Chen C, Beer C. Fast intracellular dissolution and per-

sistent cellular uptake of silver nanoparticles in CHO-K1 cells: implication for cytotoxicity. Nanotoxicology 2015; 9: 181-189.
63. Jimenez-Lamana J, Laborda F, Bolea E, Abad-Alvaro I, Castillo JR, Bianga J, He M, Bierla K, Mounicou S, Ouerdane L, Gaillet S, Rouanet JM, Szpunar J. An insight into silver nanoparticles bioavailability in rats. Metallomics 2014; 6: 2242-2249.
64. Joshi N, Ngwenya BT, Butler IB, French CE. Use of bioreporters and deletion mutants reveals ionic silver and ROS to be equally important in silver nanotoxicity. J Hazard Mater 2015; 287: 51-58.
65. Kalishwaralal K, Barathmanikanth S, Pandian SR, Deepak V, Gurunathan S. Silver nanoparticles impede the biofilm formation by Pseudomonas aeruginosa and Staphylococcus epidermidis. Colloids Surf B Biointerfaces 2010; 79: 340-344.
66. Kim KT, Truong L, Wehmas L, Tanguay RL. Silver nanoparticle toxicity in the embryonic zebrafish is governed by particle dispersion and ionic environment. Nanotechnology 2013; 24: 115101.
67. Kim YS, Song MY, Park JD, Song KS, Ryu HR, Chung YH, Chang HK, Lee JH, Oh KH, Kelman BJ, Hwang IK, Yu IJ. Subchronic oral toxicity of silver nanoparticles. Part Fibre Toxicol 2010; 7: 20.
68. Lara HH, Ayala-Nunez NV, Ixtepan-Turrent L, Rodriguez-Padilla C. Mode of antiviral action of silver nanoparticles against HIV-1. J Nanobiotechnology 2010; 8: 1.
69. Lee J, Mahendra S, Alvarez PJ. Nanomaterials in the construction industry: a review of their applications and environmental health and safety considerations. ACS Nano 2010; 4: 3580-3590.
70. Lee JH, Kim YS, Song KS, Ryu HR, Sung JH, Park JD, Park HM, Song NW, Shin BS, Marshak D, Ahn K, Lee JE, Yu IJ. Biopersistence of silver nanoparticles in tissues from Sprague-Dawley rats. Part Fibre Toxicol 2013; 10: 36.
71. Lee TY, Liu MS, Huang LJ, Lue SI, Lin LC, Kwan AL, Yang RC. Bioenergetic failure correlates with autophagy and apoptosis in rat liver following silver nanoparticle intraperitoneal administration. Part Fibre Toxicol 2013; 10: 40.
72. Lee W, Kim KJ, Lee DG. A novel mechanism for the antibacterial effect of silver nanoparticles on Escherichia coli. Biometals 2014; 27: 1191-1201.
73. Lee Y, Kim P, Yoon J, Lee B, Choi K, Kil KH, Park K. Serum kinetics, distribution and excretion of silver in rabbits following 28 days after a single intravenous injection of silver nanoparticles. Nanotoxicology 2013; 7: 1120-1130.
74. Lee YH, Cheng FY, Chiu HW, Tsai JC, Fang CY, Chen CW, Wang YJ. Cytotoxicity, oxidative stress, apoptosis and the autophagic effects of silver nanoparticles in mouse embryonic fibroblasts. Biomaterials 2014; 35: 4706-4715.
75. Liau SY, Read DC, Pugh WJ, Furr JR, Russell AD. Interaction of silver nitrate with readily identifiable groups: relationship to the antibacterial action of silver ions. Lett Appl Microbiol 1997; 25: 279-283.
76. Likus W, Bajor G, Siemianowicz K. Nanosilver – does it have only one face? Acta Biochim Pol 2013; 60: 495-501.
77. Liu P, Huang Z, Gu N. Exposure to silver nanoparticles does not affect cognitive outcome or hippocampal neurogenesis in adult mice. Ecotoxicol Environ Saf 2013; 87: 124-130.
78. Liu W, Wu Y, Wang C, Li HC, Wang T, Liao CY, Cui L, Zhou QF, Yan B, Jiang GB. Impact of silver nanoparticles on human cells: effect of particle size. Nanotoxicology 2010; 4: 319-330.
79. Liu Y, Guan W, Ren G, Yang Z. The possible mechanism of silver nanoparticle impact on hippocampal synaptic plasticity and spatial cognition in rats. Toxicol Lett 2012; 209: 227-231.
80. Liu Z, Ren G, Zhang T, Yang Z. Action potential changes associated with the inhibitory effects on voltage-gated sodium current of hippocampal CA1 neurons by silver nanoparticles. Toxicology 2009; 264: 179-184.
81. Loeschner K, Hadrup N, Qvortrup K, Larsen A, Gao X, Vogel U, Mortensen A, Lam HR, Larsen EH. Distribution of silver in rats following 28 days of repeated oral exposure to silver nanoparticles or silver acetate. Part Fibre Toxicol 2011; 8: 18.
82. Lok CN, Ho CM, Chen R, He QY, Yu WY, Sun H, Tam PK, Chiu JF, Che CM. Silver nanoparticles: partial oxidation and antibacterial activities. J Biol Inorg Chem 2007; 12: 527-534.
83. Loo CY, Young PM, Lee WH, Cavaliere R, Whitchurch CB, Rohanizadeh R. Non-cytotoxic silver nanoparticle-polyvinyl alcohol hydrogels with anti-biofilm activity: designed as coatings for endotracheal tube materials. Biofouling 2014; 30: 773-788.
84. Lu L, Sun RW, Chen R, Hui CK, Ho CM, Luk JM, Lau GK, Che CM. Silver nanoparticles inhibit hepatitis B virus replication. Antivir Ther 2008; 13: 253-262.
85. Luther EM, Schmidt MM, Diendorf J, Epple M, Dringen R. Upregulation of metallothioneins after exposure of cultured primary astrocytes to silver nanoparticles. Neurochem Res 2012; 37: 1639-1648.
86. Massarsky A, Abraham R, Nguyen KC, Rippstein P, Tayabali AF, Trudeau VL, Moon TW. Nanosilver cytotoxicity in rainbow trout (Oncorhynchus mykiss) erythrocytes and hepatocytes. Comp Biochem Physiol C Toxicol Pharmacol 2014; 159: 10-21.
87. Massarsky A, Trudeau VL, Moon TW. Predicting the environmental impact of nanosilver. Environ Toxicol Pharmacol 2014; 38: 861-873.
88. Matsumura Y, Yoshikata K, Kunisaki S, Tsuchido T. Mode of bactericidal action of silver zeolite and its comparison with that of silver nitrate. Appl Environ Microbiol 2003; 69: 4278-4281.
89. Mizushima N. Autophagy: process and function. Genes Dev 2007; 21: 2861-2873.
90. Mody VV, Siwale R, Singh A, Mody HR. Introduction to metallic nanoparticles. J Pharm Bioallied Sci 2010; 2: 282-289.
91. Mohammed Fayaz A, Ao Z, Girilal M, Chen L, Xiao X, Kalaichelvan P, Yao X. Inactivation of microbial infectiousness by silver nanoparticles-coated condom: a new approach to inhibit HIV- and HSV-transmitted infection. Int J Nanomedicine 2012; 7: 5007-5018.
92. Monteiro-Riviere NA, Tran L. Safety implications of nanomaterial exposure to skin. In Nanotoxicology: Progress toward Nanomedicine. CRC Press, Boca Raton 2014; pp. 247–272.
93. Monteiro DR, Takamiya AS, Feresin LP, Gorup LF, De Camargo ER, Delbem AC, Henriques M, Barbosa DB. Susceptibility of Candida albicans and Candida glabrata biofilms to silver nanoparticles in intermediate and mature development phases. J Prosthodont Res 2015; 59: 42-48.
94. Morones JR, Elechiguerra JL, Camacho A, Holt K, Kouri JB, Ramirez JT, Yacaman MJ. The bactericidal effect of silver nanoparticles. Nanotechnology 2005; 16: 2346-2353.
95. Nishanth RP, Jyotsna RG, Schlager JJ, Hussain SM, Reddanna P. Inflammatory responses of RAW 264.7 macrophages upon expo-

sure to nanoparticles: role of ROS-NFkappaB signaling pathway. Nanotoxicology 2011; 5: 502-516.
96. Nordberg GF, Gerhardsson L. Silver. In: Handbook on Toxicity of Inorganic Compounds. Seiler HG, Sigel H (eds.). Marcel Dekker, New York 1988; pp. 619-623.
97. Orlowski P, Tomaszewska E, Gniadek M, Baska P, Nowakowska J, Sokolowska J, Nowak Z, Donten M, Celichowski G, Grobelny J, Krzyzowska M. Tannic acid modified silver nanoparticles show antiviral activity in herpes simplex virus type 2 infection. PLoS One 2014; 9: e104113.
98. Palanisamy NK, Ferina N, Amirulhusni AN, Mohd-Zain Z, Hussaini J, Ping LJ, Durairaj R. Antibiofilm properties of chemically synthesized silver nanoparticles found against Pseudomonas aeruginosa. J Nanobiotechnology 2014; 12: 2.
99. Park EJ, Bae E, Yi J, Kim Y, Choi K, Lee SH, Yoon J, Lee BC, Park K. Repeated-dose toxicity and inflammatory responses in mice by oral administration of silver nanoparticles. Environ Toxicol Pharmacol 2010; 30: 162-168.
100. Park EJ, Yi J, Kim Y, Choi K, Park K. Silver nanoparticles induce cytotoxicity by a Trojan-horse type mechanism. Toxicol In Vitro 2010; 24: 872-878.
101. Park K, Park EJ, Chun IK, Choi K, Lee SH, Yoon J, Lee BC. Bioavailability and toxicokinetics of citrate-coated silver nanoparticles in rats. Arch Pharm Res 2011; 34: 153-158.
102. Park MV, Neigh AM, Vermeulen JP, De La Fonteyne LJ, Verharen HW, Briede JJ, Van Loveren H, De Jong WH. The effect of particle size on the cytotoxicity, inflammation, developmental toxicity and genotoxicity of silver nanoparticles. Biomaterials 2011; 32: 9810-9817.
103. Patlolla AK, Hackett D, Tchounwou PB. Silver nanoparticle-induced oxidative stress-dependent toxicity in Sprague-Dawley rats. Mol Cell Biochem 2015; 399: 257-268.
104. Pereira L, Dias N, Carvalho J, Fernandes S, Santos C, Lima N. Synthesis, characterization and antifungal activity of chemically and fungal-produced silver nanoparticles against Trichophyton rubrum. J Appl Microbiol 2014; 117: 1601-1613.
105. Persidsky Y, Ramirez SH, Haorah J, Kanmogne GD. Blood-brain barrier: structural components and function under physiologic and pathologic conditions. J Neuroimmune Pharmacol 2006; 1: 223-236.
106. Piao MJ, Kang KA, Lee IK, Kim HS, Kim S, Choi JY, Choi J, Hyun JW. Silver nanoparticles induce oxidative cell damage in human liver cells through inhibition of reduced glutathione and induction of mitochondria-involved apoptosis. Toxicol Lett 2011; 201: 92-100.
107. Pohanka M. Alzheimer's disease and oxidative stress: a review. Curr Med Chem 2014; 21: 356-364.
108. Powers CM, Badireddy AR, Ryde IT, Seidler FJ, Slotkin TA. Silver nanoparticles compromise neurodevelopment in PC12 cells: critical contributions of silver ion, particle size, coating, and composition. Environ Health Perspect 2011; 119: 37-44.
109. Pulit J, Banach M, Szczyglowska R, Bryk M. Nanosilver against fungi. Silver nanoparticles as an effective biocidal factor. Acta Biochim Pol 2013; 60: 795-798.
110. Qureshi AT, Terrell L, Monroe WT, Dasa V, Janes ME, Gimble JM, Hayes DJ. Antimicrobial biocompatible bioscaffolds for orthopaedic implants. J Tissue Eng Regen Med 2014; 8: 386-395.
111. Rada B, Leto TL. Oxidative innate immune defenses by Nox/Duox family NADPH oxidases. Contrib Microbiol 2008; 15: 164-187.
112. Rahman MF, Wang J, Patterson TA, Saini UT, Robinson BL, Newport GD, Murdock RC, Schlager JJ, Hussain SM, Ali SF. Expression of genes related to oxidative stress in the mouse brain after exposure to silver-25 nanoparticles. Toxicol Lett 2009; 187: 15-21.
113. RAIS (The Risk Assessment Information System). Formal Toxicity Summary for silver. Prepared by: Rosmarie A. Faust, Ph.D., Chemical Hazard Evaluation and Communication Group, Biomedical and Environmental Information Analysis Section, Health and Safety Research Division, Oak Ridge, Tennessee, for the U.S. Department of Energy under Contract No. DE-AC05-84OR21400 1992.
114. Rejeski D. Project on emerging Emerging Nanotechnologies. Woodrow Wilson International Center for Scholars, Washington 2011.
115. Ribeiro F, Gallego-Urrea JA, Jurkschat K, Crossley A, Hassellov M, Taylor C, Soares AM, Loureiro S. Silver nanoparticles and silver nitrate induce high toxicity to Pseudokirchneriella subcapitata, Daphnia magna and Danio rerio. Sci Total Environ 2014; 466-467: 232-241.
116. Rinna A, Magdolenova Z, Hudecova A, Kruszewski M, Refsnes M, Dusinska M. Effect of silver nanoparticles on mitogen-activated protein kinases activation: role of reactive oxygen species and implication in DNA damage. Mutagenesis 2015; 30: 59-66.
117. Samuel U, Guggenbichler JP. Prevention of catheter-related infections: the potential of a new nano-silver impregnated catheter. Int J Antimicrob Agents 2004; 23 Suppl 1: S75-78.
118. Sanpui P, Chattopadhyay A, Ghosh SS. Induction of apoptosis in cancer cells at low silver nanoparticle concentrations using chitosan nanocarrier. ACS Appl Mater Interfaces 2011; 3: 218-228.
119. Sarhan OM, Hussein RM. Effects of intraperitoneally injected silver nanoparticles on histological structures and blood parameters in the albino rat. Int J Nanomedicine 2014; 9: 1505-1517.
120. SCENIHR (Scientific Committee on Emerging and Newly Identified Health Risks): Risk assessment of products of nanotechnologies, 2009.
121. Segal AW. How neutrophils kill microbes. Annu Rev Immunol 2005; 23: 197-223.
122. Setyawati MI, Yuan X, Xie J, Leong DT. The influence of lysosomal stability of silver nanomaterials on their toxicity to human cells. Biomaterials 2014; 35: 6707-6715.
123. Sharma HS, Ali SF, Hussain SM, Schlager JJ, Sharma A. Influence of engineered nanoparticles from metals on the blood-brain barrier permeability, cerebral blood flow, brain edema and neurotoxicity. An experimental study in the rat and mice using biochemical and morphological approaches. J Nanosci Nanotechnol 2009; 9: 5055-5072.
124. Sharma HS, Hussain S, Schlager J, Ali SF, Sharma A. Influence of nanoparticles on blood-brain barrier permeability and brain edema formation in rats. Acta Neurochir Suppl 2010; 106: 359-364.

125. Shrivastava S, Bera T, Roy A, Singh G, Ramachandrarao P, Dash D. Characterization of enhanced antibacterial effects of novel silver nanoparticles. Nanotechnology 2007; 18: 103-225.
126. Singh RP, Ramarao P. Cellular uptake, intracellular trafficking and cytotoxicity of silver nanoparticles. Toxicol Lett 2012; 213: 249-259.
127. Skalska J, Frontczak-Baniewicz M, Struzynska L. Synaptic degeneration in rat brain after prolonged oral exposure to silver nanoparticles. Neurotoxicology 2015; 46: 145-154.
128. Sleiman HK, Romano RM, Oliveira CA, Romano MA. Effects of prepubertal exposure to silver nanoparticles on reproductive parameters in adult male Wistar rats. J Toxicol Environ Health A 2013; 76: 1023-1032.
129. Sondi I, Salopek-Sondi B. Silver nanoparticles as antimicrobial agent: a case study on E. coli as a model for Gram-negative bacteria. J Colloid Interface Sci 2004; 275: 177-182.
130. Song XL, Li B, Xu K, Liu J, Ju W, Wang J, Liu XD, Li J, Qi YF. Cytotoxicity of water-soluble mPEG-SH-coated silver nanoparticles in HL-7702 cells. Cell Biol Toxicol 2012; 28: 225-237.
131. Sung JH, Ji JH, Park JD, Yoon JU, Kim DS, Jeon KS, Song MY, Jeong J, Han BS, Han JH, Chung YH, Chang HK, Lee JH, Cho MH, Kelman BJ, Yu IJ. Subchronic inhalation toxicity of silver nanoparticles. Toxicol Sci 2009; 108: 452-461.
132. Sung JH, Ji JH, Yoon JU, Kim DS, Song MY, Jeong J, Han BS, Han JH, Chung YH, Kim J, Kim TS, Chang HK, Lee EJ, Lee JH, Yu IJ. Lung function changes in Sprague-Dawley rats after prolonged inhalation exposure to silver nanoparticles. Inhal Toxicol 2008; 20: 567-574.
133. Tamboli DP, Lee DS. Mechanistic antimicrobial approach of extracellularly synthesized silver nanoparticles against gram positive and gram negative bacteria. J Hazard Mater 2013; 260: 878-884.
134. Tang J, Xiong L, Zhou G, Wang S, Wang J, Liu L, Li J, Yuan F, Lu S, Wan Z, Chou L, Xi T. Silver nanoparticles crossing through and distribution in the blood-brain barrier in vitro. J Nanosci Nanotechnol 2010; 10: 6313-6317.
135. Tang J, Xiong L, Wang S, Wang J, Liu L, Li J, Wan Z, Xi T. Influence of silver nanoparticles on neurons and blood-brain barrier via subcutaneous injection in rats. Appl Surf Sci 2008; 255: 502-504.
136. Topuz E, Sigg L, Talinli I. A systematic evaluation of agglomeration of Ag and TiO2 nanoparticles under freshwater relevant conditions. Environ Pollut 2014; 193: 37-44.
137. Trickler WJ, Lantz SM, Murdock RC, Schrand AM, Robinson BL, Newport GD, Schlager JJ, Oldenburg SJ, Paule MG, Slikker W, Jr., Hussain SM, Ali SF. Silver nanoparticle induced blood-brain barrier inflammation and increased permeability in primary rat brain microvessel endothelial cells. Toxicol Sci 2010; 118: 160-170.
138. Van Der Zande M, Vandebriel RJ, Van Doren E, Kramer E, Herrera Rivera Z, Serrano-Rojero CS, Gremmer ER, Mast J, Peters RJ, Hollman PC, Hendriksen PJ, Marvin HJ, Peijnenburg AA, Bouwmeester H. Distribution, elimination, and toxicity of silver nanoparticles and silver ions in rats after 28-day oral exposure. ACS Nano 2012; 6: 7427-7442.
139. Vandebriel RJ, Tonk EC, De La Fonteyne-Blankestijn LJ, Gremmer ER, Verharen HW, Van Der Ven LT, Van Loveren H, De Jong WH. Immunotoxicity of silver nanoparticles in an intravenous 28-day repeated-dose toxicity study in rats. Part Fibre Toxicol 2014; 11: 21.
140. Volker C, Boedicker C, Daubenthaler J, Oetken M, Oehlmann J. Comparative toxicity assessment of nanosilver on three Daphnia species in acute, chronic and multi-generation experiments. PLoS One 2013; 8: e75026.
141. Vrcek IV, Zuntar I, Petlevski R, Pavicic I, Dutour Sikiric M, Curlin M, Goessler W. Comparison of in vitro toxicity of silver ions and silver nanoparticles on human hepatoma cells. Environ Toxicol 2014.
142. Wu J, Zheng Y, Song W, Luan J, Wen X, Wu Z, Chen X, Wang Q, Guo S. In situ synthesis of silver-nanoparticles/bacterial cellulose composites for slow-released antimicrobial wound dressing. Carbohydr Polym 2014; 102: 762-771.
143. Xiang D, Zheng Y, Duan W, Li X, Yin J, Shigdar S, O'Connor ML, Marappan M, Zhao X, Miao Y, Xiang B, Zheng C. Inhibition of A/Human/Hubei/3/2005 (H3N2) influenza virus infection by silver nanoparticles in vitro and in vivo. Int J Nanomedicine 2013; 8: 4103-4113.
144. Xu F, Piett C, Farkas S, Qazzaz M, Syed NI. Silver nanoparticles (AgNPs) cause degeneration of cytoskeleton and disrupt synaptic machinery of cultured cortical neurons. Mol Brain 2013; 6: 29.
145. Xue Y, Zhang S, Huang Y, Zhang T, Liu X, Hu Y, Zhang Z, Tang M. Acute toxic effects and gender-related biokinetics of silver nanoparticles following an intravenous injection in mice. J Appl Toxicol 2012; 32: 890-899.
146. Yin N, Liu Q, Liu J, He B, Cui L, Li Z, Yun Z, Qu G, Liu S, Zhou Q, Jiang G. Silver nanoparticle exposure attenuates the viability of rat cerebellum granule cells through apoptosis coupled to oxidative stress. Small 2013; 9: 1831-1841.
147. Yin N, Yao X, Zhou Q, Faiola F, Jiang G. Vitamin E attenuates silver nanoparticle-induced effects on body weight and neurotoxicity in rats. Biochem Biophys Res Commun 2015; 458: 405-410.
148. Zieminska E, Stafiej A, Struzynska L. The role of the glutamatergic NMDA receptor in nanosilver-evoked neurotoxicity in primary cultures of cerebellar granule cells. Toxicology 2014; 315: 38-48.

Original article

Folia Neuropathologica

Effects of mGluR5 positive and negative allosteric modulators on brain damage evoked by hypoxia-ischemia in neonatal rats

Dorota Makarewicz[1], Marta Słomka[1], Wojciech Danysz[2], Jerzy W. Łazarewicz[1]

[1]Department of Neurochemistry, Mossakowski Medical Research Centre, Polish Academy of Sciences, Warsaw, Poland,
[2]Merz Pharmaceuticals GmbH, Frankfurt am Main, Germany

Folia Neuropathol 2015; 53 (4): 301-308 DOI: 10.5114/fn.2015.56544

Abstract

In the present study, we examined the effects of negative and positive allosteric modulators of metabotropic glutamate receptor 5 (mGluR5), fenobam and ADX47273, respectively, on brain damage induced by hypoxia-ischemia (H-I) in 7-day-old rats. The test drugs were administered intraperitoneally 10 min after H-I. Rectal body temperature was measured for 2.5 h after the insult. The number of apoptotic neurons in the immature rat brain was evaluated after 24 h. The wet weight of both hemispheres was determined 14 days after H-I, and its loss was used as an indicator of brain damage. In the vehicle-treated groups, H-I reduced the weight of the ipsilateral (ischemic) hemisphere by approximately 33% and sixfold increased the number of apoptotic cells in the cortex. Fenobam (10 mg/kg) and ADX47273 (5, 10, and 30 mg/kg) had no significant effect on brain damage, although application of fenobam at this dose significantly reduced the number of apoptotic cells. In contrast, fenobam (20 mg/kg) potentiated ischemic brain damage to 57.4% and had no effect on H-I-induced apoptosis. In all of the experimental groups, we detected no significant changes in the weight of the contralateral (control) hemisphere or the rectal temperature. In conclusion, in 7-day-old rats, the bidirectional modulation of mGluR5 by fenobam (10 mg/kg) and ADX47273 (all doses tested) did not result in significant changes in H-I-evoked brain damage, supporting our previous data indicating that also the antagonists of mGluR5 MPEP and MTEP, which reduce neuronal lesions in adult animals submitted to brain ischemia, were ineffective in 7-day-old rat pups.

Key words: *ischemia, neuroprotection, perinatal asphyxia, rat, metabotropic glutamate receptors, NMDA receptors.*

Introduction

Excitotoxicity mediated by ionotropic glutamate receptors, particularly *N*-methyl-*D*-aspartate receptors (NMDARs), is known to play a key role in brain damage caused by different forms of brain ischemia, including perinatal asphyxia [for review, see 11,14,38]. Preclinical studies have used various animal models of cerebral ischemia, demonstrating that NMDAR antagonists are neuroprotective [39]. However, because of the serious adverse effects of high-affinity NMDAR antagonists [34], their beneficial neuroprotective effects have not been directly confirmed in clinical tests [11]. Of particular concern is the developing brain, in which the pro-apoptotic

Communicating author
Dorota Makarewicz, Department of Neurochemistry, Mossakowski Medical Research Centre, Polish Academy of Sciences, 5 Pawińskiego St., 02-106 Warsaw, Poland, e-mail: dorota.makarewicz@gmail.com

effects of these compounds have been reported [12, 22,24].

Group I metabotropic glutamate receptors (mGluRs) comprising mGlu1 and mGlu5 subtypes, which potentiate the induction of calcium signals, may be an attractive therapeutic target because mGluR antagonism is relatively free of undesirable side effects, in which they only interfere with the modulatory control of excitatory neurotransmission instead of harming the tonic inhibition of excitation [3]. In addition it has been shown that mGlu5 receptors are positively coupled to NMDA receptors [6,29], and therefore they might also be involved in the NMDAR-mediated mechanisms associated with ischemic brain damage, and mGluR5 inhibition might be neuroprotective.

Many preclinical studies have demonstrated that mGluR1 antagonists were neuroprotective in brain ischemia in adult and developing animals [4,15, 19,23,35]. However, contradictory data have been reported concerning the neuroprotective effects of mGluR5 antagonists. Potent neuroprotection induced by the mGluR5 antagonists MPEP and MTEP in global brain ischemia in adult Mongolian gerbils [19,26] was not observed in another study [23]. Szydlowska *et al*. [35] reported that MTEP was highly neuroprotective in focal brain ischemia in adult rats, while in our previous study, this compound failed to provide neuroprotection against hypoxia-ischemia (H-I) in 7-day-old rats [19]. We tentatively attributed this difference in the effectiveness of mGluR5 antagonist in adult and developing rats to the distinctly specific properties of the developing brain, but this explanation requires verification by testing other pharmacological tools, including mGluR5 antagonists and mGluR5 positive allosteric modulators (PAMs), to determine how negative and positive mGluR5 modulation affects ischemic brain damage in immature rats.

Fenobam is a selective negative allosteric modulator of mGluR5, with anxiolytic and analgesic properties [13,25]. Recently mGluR5 PAMs emerged as a new group of drugs that may potentiate NMDAR-mediated currents by utilizing the functional coupling between mGluR5 and NMDARs [6]. Behavioral studies demonstrated that ADX47273, which is an mGluR5 PAM, enhances NMDA-dependent functions *in vitro* and *in vivo* in adult rodents and exerts antipsychotic-like and pro-cognitive effects [7,17,29,32,33]. To our knowledge, neither fenobam nor ADX47273 has been tested in studies of neuroprotection in brain ischemia, particularly in a rat model of perinatal asphyxia.

The aim of the present study was to assess the effects of mGluR5 modulation by fenobam and ADX47273 on ischemic brain damage in developing animals using a rat model of perinatal asphyxia. Weight deficit of the ipsilateral (ischemic) hemispheres served as an indicator of ischemic brain damage.

Material and methods

ADX47273 [*S*-(4-fluoro-phenyl)-{3-[3-(4-fluoro-phenyl)-[1,2,4]oxadiazol-5-yl]-piperidin-1-yl}-methanone], fenobam [*N*-(3-chlorophenyl)-*N'*-(4,5-dihydro-1-methyl-4-oxo-1*H*-imidazole-2-yl)urea], and the vehicles dimethyl sulfoxide (DMSO) and Cremophor were obtained from Sigma-Aldrich (Poznan, Poland). ADX47273 was suspended in a mixture of DMSO and Cremophor (1 : 1, v/v), and the vehicle for fenobam was a mixture of DMSO and Cremophor (1 : 9, v/v).

Rat pups of both genders were obtained from the breeding animal house of the Mossakowski Medical Research Centre PAS in Warsaw. The animal experiments were approved by the Third Local Ethical Committee in Warsaw and performed in accordance with the European Community Council Directive of 24 November 1986 (86/609/EEC) and corresponding Polish government regulations concerning animal experimentation. All efforts were made to minimize animal suffering and the number of animals required.

A model of H-I in 7-day-old Wistar rat pups was used as previously described [27], with slight modifications [19,20]. Briefly, halothane-anesthetized rats were subjected to occlusion of the left common carotid artery. After 1 h, they were exposed to a gas mixture that contained 7.3% oxygen in nitrogen for 75 min at 36°C. The test drugs were administered intraperitoneally (i.p.) 10 min after the termination of hypoxia. The solutions were administered in a volume of 3.3 ml/kg (approximately 50 µl per animal, each weighing approximately 15 g). The concentration of the drugs in stock solutions was adjusted according to the final doses required (5, 10, and 30 mg/kg ADX47273 and 10 and 20 mg/kg fenobam). Control animals received corresponding volumes of the vehicles. The pups were then returned to their dams, kept for 2.5 h at 27°C, with control

of their rectal body temperature [19,20]. Then the dams were housed at an environmental temperature of 20°C under a 12 h/12 h light/dark cycle.

On postnatal day 21 (i.e., 14 days after the insult), the rats were anesthetized with halothane and decapitated. Both cerebral hemispheres were weighed. Brain damage was reflected by a deficit in the wet weight of the ipsilateral (left) ischemic hemisphere and is expressed as a percentage of the wet weight of the contralateral (right) control hemisphere [19,20]. This method of assessing the developing brain damage in a rat model of HI has recently been used by a number of other research groups [8,17,30]. Our previous control experiments demonstrated equal weight of the left and right hemisphere in naive and sham-operated animals and that H-I induction in 7-day-old rats does not interfere with the mass of the contralateral (reference) hemisphere. The obtained data are expressed as means ± SEM, with the number of repetitions (*n*) provided in parentheses. Statistical significance was tested using analysis of variance (ANOVA) followed by Tukey's multiple-comparison test. Values of $p < 0.05$ were considered statistically significant.

In order to evaluate the effects of fenobam in dosage of 10 or 20 mg/kg applied 10 min after hypoxia-ischemia on ischemia-induced apoptosis, the animals treated as described above were sacrificed 24 hours after hypoxia-ischemia. The animals were deeply anesthetized using Nembutal (80 mg/kg w. m. *i.p.*) and perfused through the ascending aorta with 0.9% NaCl in 0.01 M sodium-potassium phosphate buffer pH 7.4 (PBS), followed by *in situ* perfusion-fixation with ice-cold fixatives applied under gravity. Afterwards, the brains were saturated with sucrose through immersing in 10, 20 and 30% (w/v) sucrose solutions in PBS and cut into 40 µm-thick free-floating coronal sections using a cryostat. Morphology of cell nuclei was examined on brain sections mounted on microscope slides. Sections were washed in PBS and incubated in a 1 µg/ml solution of Hoechst stain (bisbenzimide dye in PBS) for 2 minutes, at room temperature. The stain was then drained off and cover slipped with PBS for visualization. The number of apoptotic cells at the last stage of apoptosis (formation of apoptotic bodies) was measured using a Zeiss fluorescent microscope with a 40× (NA 1.0) objective with additional 10× ocular zoom. Three to four animals from each experimental group were investigated. For each animal we analyzed 6-8 sections. The dying cells were counted within 10 microscopic fields of observation located randomly within the somatosensory region of the cerebral cortex.

Results

The evaluation of brain damage 14 days after H-I in untreated animals revealed a 33.4% loss of weight of the ipsilateral brain hemisphere, indicating the same degree of brain damage induced by H-I (results not shown). The same level of brain damage was found in the vehicle-treated groups (Figs. 1 and 3). Compared to the corresponding vehicle control animals with a reduction of weight of the ischemic hemisphere at the level of 34.3 ± 2.19% ($n = 27$), brain damage of 24.6 ± 2.45% ($n = 35$) found in animals treated with the mGluR5 negative allosteric modulator fenobam (10 mg/kg) did not differ significantly ($p > 0.05$). In contrast, 20 mg/kg fenobam significantly ($p < 0.05$) potentiated brain damage to 57.4 ± 3.2% ($n = 18$) (Fig. 1).

In order to investigate the influence of fenobam on apoptosis in the rat brain, evoked by hypoxia-isch-

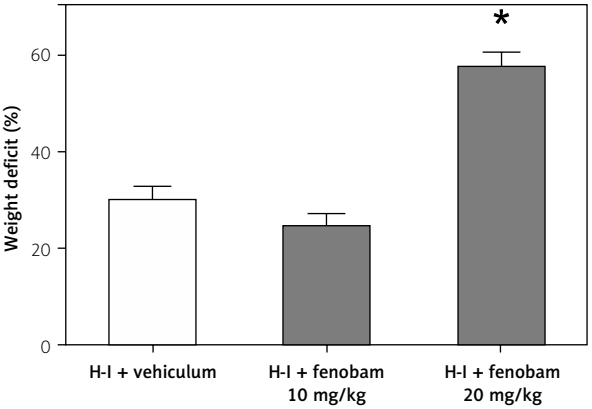

Fig. 1. Effects of fenobam on brain damage induced by hypoxia-ischemia in 7-day-old rats. Indicated doses of fenobam (Fen) or vehicle were administered *i.p.* 10 min after hypoxia-ischemia (H-I). Brain damage was evaluated by weighing the brain hemispheres 14 days after hypoxia-ischemia and is expressed as the weight deficit of the ipsilateral hemisphere as a percentage of the weight of the contralateral hemisphere. The bars represent mean ± SEM (group size: $n \geq 19$ rats per time point in each group). *$p < 0.05$, significant difference from vehicle-treated controls (H-I+veh; ANOVA followed by Tukey's multiple-comparison test).

emia, the animals were treated with fenobam in dosage of 10 or 20 mg/kg. Then, the number of apoptotic neurons was assessed 24 hours after the insult. The results presented in Figure 2A and B demonstrate that in the group of rats treated with fenobam in the dose of 20 mg/kg the mean number of apoptotic cells per field of observation was at the same level as observed in the H-I group (about 60 cells per field). Treatment with fenobam in the dose of 10 mg/kg significantly reduced the number of apoptotic cells by 36.7%.

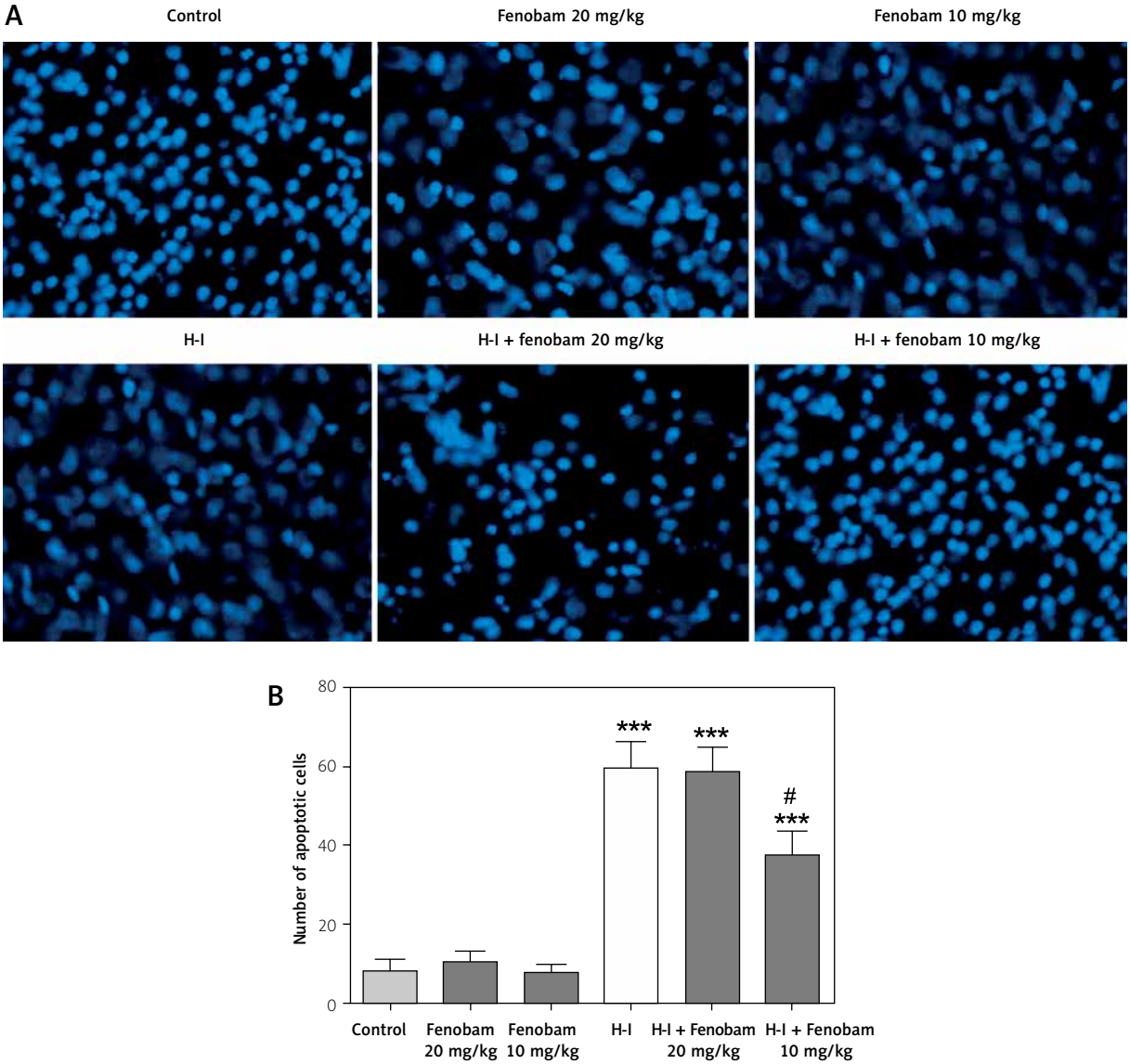

Fig. 2. The effect of fenobam on hypoxia-ischemia evoked induction of apoptosis in the cortex of immature rat brain assessed 24 hours after the insult. Morphology of cell nuclei in cerebral cortex visualized by Hoechst staining **(A)**. Note many apoptotic cells within the section subjected to H-I and H-I Fenobam + 20 mg/kg as well. Note the reduction of apoptotic cell number within the material of animals pretreated with fenobam 10 mg/kg. Quantitative evaluation of the number of apoptotic cells. Fluorescent images were taken using a Zeiss microscope equipped with a 40x (NA 1.0) objective with additional 10x ocular zoom. **B)** Bars represent means ± SEM (n = 4 animals for each experimental group). For each animal we analyzed 8-10 sections. Significant differences from the appropriate ischemic control (H-I) were tested by ANOVA followed by Tukey's multiple comparison test. *$p < 0.001$ vs. number of apoptotic cells assessed in the 24 h control group.

Application of the mGluR5 PAM ADX47273 tended to increase brain damage (Fig. 3), but this effect did not reach statistical significance. To illustrate this, statistical analysis of data for ADX47273 10 mg/kg, which are also representative for other ADX47273 doses, demonstrated that the level of reduction of weight of the ischemic hemisphere in the ADX47273 treated group by 42.3 ± 3.25% (n = 24) did not differ significantly ($p > 0.05$) from the corresponding vehicle control data (34 ± 2.2%) (n = 27) (Fig. 3).

To evaluate the possible negative effects of fenobam and ADX47273 on brain development, and effects of the test substances on post-ischemic body temperature, the mass of the contralateral hemispheres and rectal body temperature were also measured. The vehicles for fenobam and ADX47273 as well as these test substances regardless of the drug dose administered had no effect on the mass of the contralateral hemispheres and did not interfere with rectal body temperature during the 2.5-h period after H-I (results not shown).

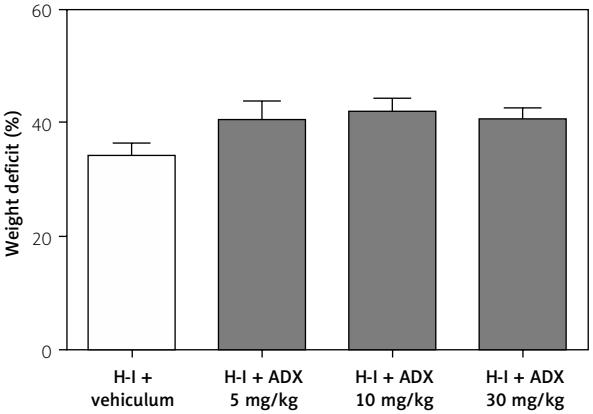

Fig. 3. Effects of ADX47273 on brain damage induced by hypoxia-ischemia in 7-day-old rats. Indicated doses of ADX47273 (ADX) or vehicle administered *i.p.* 10 min after hypoxia-ischemia (H-I). For other explanations see legends to Fig. 1.

Discussion

Based on the well-established role of NMDARs in ischemic brain damage and the functional coupling of mGluR5 and NMDARs, one might expect that the negative modulation of mGluR5 provides neuroprotection, whereas the enhancement of mGluR5 activity exacerbates brain damage in animal models of brain ischemia. However, the results of the present study using a rat model of perinatal asphyxia and evaluating brain damage based on the ipsilateral hemisphere's mass deficit 14 days after the insult indicate that the mGluR5 negative and positive modulators fenobam and ADX47273 at typically used doses failed to influence brain damage in 7-day-old rats subjected to H-I, but fenobam at a high dose (20 mg/kg) enhanced it. Examination of the number of apoptotic cells in the brain 24 h after H-I showed a significant reduction in the number of apoptotic cells in the animals treated with the lower dose of fenobam, and no effect at its higher dose.

Our negative data are consistent with previously published results indicating that the other mGluR5 antagonist MTEP provided neuroprotection in brain ischemia in adult but not in developing rats [19,35]. Collectively these data appear to support the hypothesis that mGluR5 activity and consequently its functional coupling to NMDARs, which may determine the effects of mGluR5 modulators on H-I-evoked brain damage, depend on the level of brain development, and that mGluR5 may not be fully operational in 7-day-old rats. We propose that the mechanism of unexpected potentiation of the ischemic brain damage evoked by fenobam 20 mg/kg may result from unspecific interactions of its metabolites.

In the present study, we used H-I in 7-day-old rats, which is an established model of perinatal asphyxia [27, for review see 37]. We used this model previously to test the neuroprotective potential of other mGluR ligands [19,20]. The involvement of NMDARs in the mechanisms of ischemic brain damage in this experimental model is clear [9,10,11,14,38,39], but less clear is the role of particular group ImGluRs subtypes. mGluR1 and mGluR5 have significantly different developmental profiles in various brain regions and in the subcellular localization [5,18]. Immunocytochemical studies have shown that mGluR5 predominates in the immature rat brain [28], whereas mGluR1 appears in the rat brain only in limited amounts at the end of the first postnatal week [18]. However, the results of functional studies demonstrated that mGluR1 rather than mGluR5 mediates transient calcium currents in rat brain neurons during early postnatal days [36]. Thus, a model of H-I in 7-day-old rats appears to be suitable for studies that address developmental aspects of the effects of mGluR5 modulation on ischemic brain damage. As pharmacological tools we used fenobam and ADX47273, which are selective

mGluR5 negative and positive allosteric modulators, respectively [16,25]. Oral fenobam administration in adult rats (10-30 mg/kg) exerted analgesic and anxiolytic-like effects and impaired learning [13], whereas the behavioral effects of ADX47273 were observed in rats treated with 10 and 30 mg/kg *i.p*. [16]. The doses of the test substances used in our study were based on the above data from the literature.

As mentioned above, based on theoretical assumptions, the negative modulation of mGluR5 should lead to a decrease in the activity of NMDARs and consequently neuroprotection in brain ischemia. However, the present study failed to demonstrate such effects of fenobam in the H-I model in 7-day-old rats. These results fit in with the divergent literature data on the neuroprotective effects of mGluR5 antagonists in different models of brain ischemia. Although Meli *et al*. [23] did not find a neuroprotective effect of the mGluR5 antagonist MPEP on global brain ischemia in adult Mongolian gerbils, other authors reported potent neuroprotection induced by the mGluR5 antagonists MPEP and MTEP in the same gerbil model and a model of focal brain ischemia in adult rats [2,19,26,35]. In contrast to the results of studies in adult animals, our previous study demonstrated a lack of neuroprotection provided by MTEP in 7-day-old rats subjected to H-I [19]. The present data are consistent with these earlier findings.

The aforementioned differences in the subcellular localization of mGluR1 and mGluR5 and minimal functional role of mGluR5 in calcium signaling during the first postnatal week [18,36] may suggest that mGluR5 may not be functional during this early developmental period with corresponding consequences for the operation of coupling between mGluR5 and NMDARs. It has been demonstrated that the antagonism of NMDARs in the developing brain increases constitutive apoptosis [12,24] and decreases brain weight 2 weeks after a single MK-801 injection [21]. Moreover, NMDAR antagonists interfere with thermoregulation and induce hypothermia in neonatal rats [9]. Our present data showed the absence of a decrease in the weight of the contralateral brain and of hypothermia in rats treated with fenobam, which is consistent with lack of interference with NMDAR activity.

To our knowledge the impact that fenobam has on induction of apoptosis in brain neurons by ischemia, hypoxia and similar pathological situations has not previously been investigated extensively. Ahn *et al*. [1] demonstrated in *in vitro* that fenobam given alone only marginally reduced activation by H_2O_2 of Akt and p38 in C6 cells or protected them against DNA damage. These authors revealed that fenobam significantly potentiated cytoprotective effects of the exogenous peptide construct PEP-1-FK506BP both in C6 cells submitted to oxidative stress and in the hippocampus of Mongolian gerbils after global forebrain ischemia. Our present results showed that application of fenobam at a dose of 10 mg/kg significantly reduced the number of apoptotic neurons in H-I challenged immature rat brains, which is a new and interesting finding. This finding may indicate that although mGluR5 participates in the H-I-evoked triggering of apoptosis in the rat pups, its role may still be rather weak. Indeed, this significant fenobam-evoked protection against neuronal apoptosis observed 24 hours after HI (Fig. 2) contrasts with only an insignificant tendency to neuroprotection as assessed after 14 days on the basis of the brain mass deficit (Fig. 1).

The justification for the use of ADX47273 was the same as for fenobam (i.e., NMDARs play an instrumental role in ischemic brain damage, and mGlu5 receptors are functionally coupled to NMDARs and potentiate glutamate-induced Ca^{2+} signaling). Although based on these assumptions the expected result for ADX47273 was exacerbation of damage, previously published results did not demonstrate an increase of ischemic brain injury by activation of mGluR5 in different experimental models. On the contrary, Bao *et al*. [2] used an adult rat model of focal brain ischemia and reported neuroprotection provided by the selective mGluR5 agonist CHPG. Meli *et al*. [23] reported that CHPG failed to exacerbate neuronal damage in an *in vitro* model of rat organotypic hippocampal slices challenged with oxygen-glucose deprivation (OGD), while the activation of group I mGluRs by DHPG was shown to induce tolerance of OGD in the same model [31,40]. Consistent with these data, in our present study we observed only a non-significant trend toward an exacerbation of ischemia-evoked brain damage induced by ADX47273.

Our results unexpectedly revealed that fenobam 20 mg/kg significantly increased damage in the ipsilateral hemisphere which was assessed based on brain mass deficit 14 days after H-I, and had no protective effect on the number of apoptotic cells evaluated one day after the insult. Considering the mechanisms of this phenomenon, one should take into account selectivity. The brain concentration of

30 mg/kg fenobam 40 min after oral administration in adult rats reaches 600 nM, whereas its IC_{50} for mGluR5 is only 58 nM [25]. Fenobam is also very rapidly metabolized in rats *in vivo* [41]. Therefore, the exacerbation of brain injury by i.p. administration of fenobam (20 mg/kg) may result from fenobam and/or its metabolite interactions with as-yet unidentified receptors other than mGluR5.

In summary, the present study evaluated the effects of negative and positive allosteric modulators of mGluR5, fenobam and ADX47273, respectively, on brain damage evoked by H-I in 7-day-old rats. We found no significant effects of such treatment. Only a weak tendency toward a neuroprotective effect of 10 mg/kg fenobam and equally nonsignificant potentiation of brain damage by the mGluR5 PAM ADX47273 were observed in this animal model. Moreover, aggravation of brain damage by fenobam at a dose of 20 mg/kg was noted. Our results are inconsistent with the theoretically predicted pattern of changes in ischemic brain damage evoked by the modulation of mGluR5 activity, based on the hypothesis that mGluR5 and its positive coupling to NMDARs may participate in these phenomena. Most likely functions of mGluR5 depend on brain development and may be inadequate in 7-day-old rat pups. Further studies using models of brain ischemia in adult animals are needed to verify whether the present findings are specific to juvenile animals and result from developmental changes in mGluR5 functions.

Acknowledgments

This study was supported by statutory funds from the Mossakowski Medical Research Centre, Warsaw, Poland. The authors would like to thank Marcin Gamdzyk, M.S., for aid in the induction of hypoxia-ischemia and temperature measurements in some of the experimental groups. Expert technical assistance from Mrs. Apolonia Ziembowicz is gratefully acknowledged.

Disclosure

Authors report no conflict of interest.

References

1. Ahn EH, Kim DW, Shin MJ, Jo HS, Eom SA, Kim DS, Park EY, Park JH, Cho SW, Park J, Eum WS, Son O, Hwang HS, Choi SY. Fenobam promoted the neuroprotective effect of PEP-1-FK506BP following oxidative stress by increasing its transduction efficiency. BMB Rep 2013; 46: 561-566.
2. Bao WL, Williams AJ, FadenAI, Tortella FC. Selective mGluR5 receptor antagonist or agonist provides neuroprotection in a rat model of focal cerebral ischemia. Brain Res 2001; 922: 173-179.
3. Bruno V, Battaglia G, Copani A, D'Onofrio M, Di Iorio P, De Blasi A, Melchiorri D, Flor PJ, Nicoletti F. Metabotropic glutamate receptor subtypes as targets for neuroprotective drugs. J Cereb Blood Flow Metab 2001; 21: 1013-1033.
4. Bruno V, Battaglia G, Kingston A, O'Neill MJ, Catania MV, Di Grezia R, Nicoletti F. Neuroprotective activity of the potent and selective mGlu1a metabotropic glutamate receptor antagonist, (+)-2-methyl-4 carboxyphenylglycine (LY367385): comparison with LY357366, a broader spectrum antagonist with equal affinity for mGlu1a and mGlu5 receptors. Neuropharmacology 1999; 38: 199-207.
5. Catania MV, Landwehrmeyer GB, Testa CM, Standaert DG, Penney JB Jr, Young AB. Metabotropic glutamate receptors are differentially regulated during development. Neuroscience 1994; 61: 481-495.
6. Doherty AJ, Palmer MJ, Henley JM, Collingridge GL, Jane DE. (RS)-2-chloro-5-hydroxyphenylglycine (CHPG) activates mGlu5, but notmGlu1, receptors expressed in CHO cells and potentiates NMDA responses in the hippocampus. Neuropharmacology 1997; 36: 265-267.
7. Engers DW, Rodriguez AL, Williams R, Hammond AS, Venable D, Oluwatola O, Sulikowski GA, Conn PJ, Lindsley CW. Synthesis, SAR and unanticipated pharmacological profiles of analogues of the mGluR5 ago-potentiator ADX-47273. Chem Med Chem 2009; 4: 505-511.
8. Feng Y, Liu YM, Leblanc MH, Bhatt AJ, Rhodes PG. Grape seed extract given three hours after injury suppresses lipid peroxidation and reduces hypoxic-ischemic brain injury in neonatal rats. Pediatr Res 2007; 61: 295-300.
9. Gilland E, Hagberg H. Is MK-801 neuroprotection mediated by systemic hypothermia in the immature rat? Neuroreport 1997; 8: 1603-1605.
10. Hagberg H, Gilland E, Diemer NH, Andine P. Hypoxia-ischemia in the neonatal rat brain: histopathology after post-treatment with NMDA and non-NMDA receptor antagonists. Biol Neonate 1994; 66: 205-213.
11. Hardingham GE. Coupling of the NMDA receptor to neuroprotective and neurodestructive events. Biochem Soc Trans 2009; 37: 1147-1160.
12. Ikonomidou C. Triggers of apoptosis in the immature brain. Brain Dev 2009; 31: 488-492.
13. Jacob W, Gravius A, Pietraszek M, Nagel J, Belozertseva I, Shekunova E, Malyshkin A, Greco S, Barberi C, Danysz W. The anxiolytic and analgesic properties of fenobam, a potent mGlu5 receptor antagonist, in relation to the impairment of learning. Neuropharmacology 2009; 57: 97-108.
14. Johnston MV. Excitotoxicity in perinatal brain injury. Brain Pathol 2005; 15: 234-240.
15. Kohara A, Takahashi M, Yatsugi S, Tamura S, Shitaka Y, Hayashibe S, Kawabata S, Okada M. Neuroprotective effects of the selective type 1 metabotropic glutamate receptor antagonist YM-202074 in rat stroke models. Brain Res 2008; 1191: 168-179.
16. Liu F, Grauer S, Kelley C, Navarra R, Graf R, Zhang G, Atkinson PJ, Popiolek M, Wantuch C, Khawaja X, Smith D, Olsen M, Kourano-

va E, Lai M, Pruthi F, Pulicicchio C, Day M, Gilbert A, Pausch MH, Brandon NJ, Beyer CE, Comery TA, Logue S, Rosenzweig-Lipson S, Marquis KL. ADX47273 [S-(4-fluoro-phenyl)-{3-[3-(4-fluoro-phenyl)-[1,2,4]-oxadiazol-5- yl]-piperidin-1-yl}-methanone]: a novel metabotropic glutamate receptor 5-selective positive allosteric modulator with preclinical antipsychotic-like and precognitive activities. J Pharmacol Exp Ther 2008; 327: 827-839.
17. Liu C, Lin N, Wu B, Qiu Y. Neuroprotective effect of memantine combined with topiramate in hypoxic-ischemic brain injury. Brain Res 2009; 1282: 173-182.
18. Lopez-Bendito G, Shigemoto R, Fairen A, Lujan R. Differential distribution of group I metabotropic glutamate receptors during rat cortical development. Cereb Cortex 2002; 12: 625-638.
19. Makarewicz D, Duszczyk M, Gadamski R, Danysz W, Łazarewicz JW. Neuroprotective potential of group I metabotropic glutamate receptor antagonists in two ischemic models. Neurochem Int 2006; 48: 485-490.
20. Makarewicz D, Gadamski R, Ziembowicz A, Kozikowski AP, Wroblewski JT, Lazarewicz JW. Neuroprotective effects of the agonist of metabotropic glutamate receptors ABHxD-I in two animal models of cerebral ischaemia. Resuscitation 2006; 68: 119-126.
21. Makarewicz D, Sulejczak D, Duszczyk M, Małek M, Łazarewicz JW. Delayed preconditioning with NMDA receptor antagonists in the rat model of perinatal asphyxia. Folia Neuropathol 2014; 52: 270-284.
22. Manning SM, Boll G, Fitzgerald E, Selip DB, Volpe JJ, Jensen FE. The clinically available NMDA receptor antagonist, memantine, exhibits relative safety in the developing rat brain. Int J Dev Neurosci 2011; 29: 767-773.
23. Meli E, Picca R, Attucci S, Cozzi A, Peruginelli F, Moroni F, Pellegrini-Giampietro DE. Activation of mGlu1 but not mGlu5 metabotropic glutamate receptors contributes to postischemic neuronal injury in vitro and in vivo. Pharmacol Biochem Behav 2002; 73: 439-446.
24. Olney JW, Wozniak DF, Jevtovic-Todorovic V, Farber NB, Bittigau P, Ikonomidou C. Drug-induced apoptotic neurodegeneration in the developing brain. Brain Pathol 2002; 12: 488-498.
25. Porter RH, Jaeschke G, Spooren W, Ballard TM, Büttelmann B, Kolczewski S, Peters JU, Prinssen E, Wichmann J, Vieira E, Mühlemann A, Gatti S, Mutel V, Malherbe P. Fenobam: a clinically validated nonbenzodiazepine anxiolytic is a potent, selective, and noncompetitive mGlu5 receptor antagonist with inverse agonist activity. J Pharmacol Exp Ther 2005; 315: 711-721.
26. Rao AM, Hatcher JF, Dempsey RJ. Neuroprotection by group I metabotropic glutamate receptor antagonists in forebrain ischemia of gerbil. Neurosci Lett 2000; 293: 1-4.
27. Rice JE, Vannucci RC, Brierley JB. The influence of immaturity on hypoxic-ischemic brain damage in the rat. Ann Neurol 1981; 9: 131-141.
28. Romano C, van den Pol AN, O'Malley KL. Enhanced early developmental expression of the metabotropic glutamate receptor mGluR5 in rat brain: protein, mRNA splice variants, and regional distribution. J Comp Neurol 1996; 367: 403-412.
29. Rosenbrock H, Kramer G, Hobson S, Koros E, Grundl M, Grauert M, Reymann KG, Schröder UH. Functional interaction of metabotropic glutamate receptor 5 and NMDA-receptor by a metabotropic glutamate receptor 5 positive allosteric modulator. Eur J Pharmacol 2010; 639: 40-46.
30. Sanches EF, Arteni NS, Spindler C, Moysés F, Siqueira IR, Perry ML, Netto CA. Effects of pre- and postnatal protein malnutrition in hypoxic-ischemic rats. Brain Res 2012; 1438: 85-92.
31. Scartabelli T, Gerace E, Landucci E, Moroni F, Pellegrini-Giampietro DE. Neuroprotection by group I mGlu receptors in a rat hippocampal slice model of cerebral ischemia is associated with the PI3K-Akt signaling pathway: a novel postconditioning strategy? Neuropharmacology 2008; 55: 509-516.
32. Schlumberger C, Pietraszek M, Gravius A, Danysz W. Effects of a positive allosteric modulator of mGluR5 ADX47273 on conditioned avoidance response and PCP-induced hyperlocomotion in the rat as models for schizophrenia. Pharmacol Biochem Behav 2010; 95: 23-30.
33. Schlumberger C, Pietraszek M, Gravius A, Klein KU, Greco S, Morè L, Danysz W. Comparison of the mGlu5 receptor positive allosteric modulator ADX47273 and the mGlu2/3 receptor agonist LY354740 in tests for antipsychotic-like activity. Eur J Pharmacol 2009; 623: 73-83.
34. Smith PF. Therapeutic N-methyl-D-aspartate receptor antagonists: will reality meet expectation? Curr Opin Investig Drugs 2003; 4: 826-832.
35. Szydlowska K, Kaminska B, Baude A, Parsons CG, Danysz W. Neuroprotective activity of selective mGlu1 and mGlu5 antagonists in vitro and in vivo. Eur J Pharmacol 2007; 554: 18-29.
36. Taketo M, Matsuda H. Modulation of intracellular calcium mobilization and GABAergic currents through subtype-specific metabotropic glutamate receptors in neonatal rat hippocampus. Brain Res Bull 2010; 81: 73-80.
37. Vannucci RC, Vannucci SJ. Perinatal hypoxic-ischemic brain damage: evolution of an animal model. Dev Neurosci 2005; 27: 81-86.
38. Villmann C, Becker CM. On the hypes and falls in neuroprotection: targeting the NMDA receptor. Neuroscientist 2007; 13: 594-615.
39. Weigl M, Tenze G, Steinlechner B, Skhirtladze K, Reining G, Bernardo M, Pedicelli E, Dworschak M. A systematic review of currently available pharmacological neuroprotective agents as a sole intervention before anticipated or induced cardiac arrest. Resuscitation 2005; 65: 21-39.
40. Werner CG, Scartabelli T, Pancani T, Landucci E, Moroni F, Pellegrini-Giampietro DE. Differential role of mGlu1 and mGlu5 receptors in rat hippocampal slice models of ischemic tolerance. Eur J Neurosci 2007; 25: 3597-3604.
41. Wu WN, McKown LA, O'Neill PJ. In vitro and in vivo metabolism of the antianxiolytic agent fenobam in the rat. J Pharm Sci 1995; 84: 185-189.

Original article

Folia Neuropathologica

Protective effect of valproic acid on cultured motor neurons under glutamate excitotoxic conditions. Ultrastructural study

Ewa Nagańska, Ewa Matyja, Anna Taraszewska, Janina Rafałowska

Department of Experimental and Clinical Neuropathology, M. Mossakowski Medical Research Centre, Polish Academy of Sciences, Warsaw, Poland

Folia Neuropathol 2015; 53 (4): 309-316 DOI: 10.5114/fn.2015.56545

Abstract

Amyotrophic lateral sclerosis (ALS) is a fatal neurodegenerative disorder that involves the upper and lower motor neurons and leads to the patient's death within 5 years after diagnosis. Approximately 2 per 100,000 people worldwide are affected every year. The only FDA-approved drug available for medical treatment is riluzole. It slows the disease progression and improves limb function and muscle strength for 3-4 months. Thus, looking for new therapeutic agents is a pressing challenge.

Valproic acid (VPA) is a short-chain fatty acid, widely used for the treatment of seizures and bipolar mood disorder. The beneficial effect of VPA has been documented in different neurodegenerative experimental models, including amyotrophic lateral sclerosis (ALS). The real mechanisms underlying numerous beneficial effects of VPA are complex, but recently it has been postulated that the neuroprotective properties might be related to direct inhibition of histone deacetylase (HDAC).

The aim of this ultrastructural study was to evaluate the beneficial effect of VPA on the spinal cord motor neurons (MNs) in a glutamate (GLU)-induced excitotoxic ALS model in vitro. It had been previously documented that chronic GLU excitotoxicity resulted in various MN injuries, including necrotic, apoptotic and autophagic modes of cell death. The present results demonstrated the neuroprotective properties of VPA associated with inhibition of apoptotic and autophagic changes of spinal MNs in a model of neurodegeneration in vitro.

Key words: *amyotrophic lateral sclerosis, valproic acid, neuroprotection, ultrastructural study.*

Introduction

Amyotrophic lateral sclerosis (ALS), known as Charcot's or Lou Gehrig's disease, is a fatal neurodegenerative disease, one of the heterogeneous group referred to as motor neuron diseases (MNDs). It primarily affects upper and lower motoneurons (MNs) of the cerebral cortex, brainstem and spinal cord, but surrounding glial cells, muscle cells, interneurons, and Renshaw inhibitory neurons might also be involved [5]. The generalized weakness and progressive muscle atrophy usually lead to death by respiratory muscle failure within five years after the disease onset [42]. Most ALS cases occur sporadically, while about 5-10% of them are inherited and classified as familial form of the disease [1]. So far more than 16 causative

Communicating author:

Prof. Ewa Matyja, Department of Experimental and Clinical Neuropathology, M. Mossakowski Medical Research Centre, Polish Academy of Sciences, Warsaw, Poland, phone: +48 22 608 65 43, e-mail: ematyja@imdik.pan.pl

genes responsible for ALS/MNDs have been identified. Among them, 10-20% are probably caused by mutations in the gene encoding Cu/Zn superoxide dismutase-1 (SOD1), one of the main free-radical scavenging enzymes that protect cells against oxidative stress [2,37].

Until now, there is no effective therapeutic intervention for ALS, but different potential therapeutic targets are widely discussed [48]. It has been recently suggested that acetylation and/or deacetylation play an important role in the pathogenesis of different neurological diseases, including ALS [26]. Thus, histone deacetylase (HDAC) inhibitors have proved to be promising treatment in the broadly defined neurodegeneration.

Valproic acid (VPA; 2-n-propylpentanoic acid) is widely used as an anticonvulsant and mood stabilizing drug. Although different results suggest that this agent may exhibit a neuroprotective effect, the mechanism of such protection is not yet clear. VPA may exert its beneficial effect on neuronal survival and synaptic plasticity by acting directly on neurons and indirectly through glial cells [27]. Being a simple fatty acid, VPA is a substrate for the fatty acid β-oxidation (FAO) pathway, which takes place primarily in mitochondria. Recently, it has been also demonstrated that VPA effectively inhibits HDAC [15], making it valuable for investigations into the therapeutic role of chromatin remodeling in various pathological states of the central nervous system.

The purpose of this study was to determine whether valproate exhibits efficient neuroprotection against neuronal damage caused by glutamate toxicity in the organotypic culture of rat's lumbar spinal cord.

Material and methods

The study was performed on organotypic cultures of lumbar spinal cord obtained from 8-day-old rat pups. The cultures were kept at 36.6°C in a medium consisting of 25% inactivated fetal bovine serum and 75% DMEM (Dulbecco Modified Eagle's Medium) supplemented with glucose to a final concentration of 600 mg% and with antibiotics. The medium was changed twice a week. On the 10-14th day *in vitro* (DIV), the well-differentiated cultures were subjected to 1) glutamate (GLU) alone in a concentration of 100 μM; 2) 100 μM GLU with 10 μM VPA; 3) 10 μM VPA alone. The control cultures were grown in standard conditions.

After 3, 6 and 11 days, the cultures were processed for electron microscopic study. They were rinsed in a cacodylate buffer (pH 7.2), fixed in a mixture containing 0.8% formaldehyde and 2.5% glutaraldehyde for 1 hour, postfixed in 1% osmium tetroxide, dehydrated in alcohols in graded concentrations and embedded in Epon 812. Ultrathin sections were counterstained with uranyl acetate and lead citrate and examined in a JEOL 1200EX electron microscope.

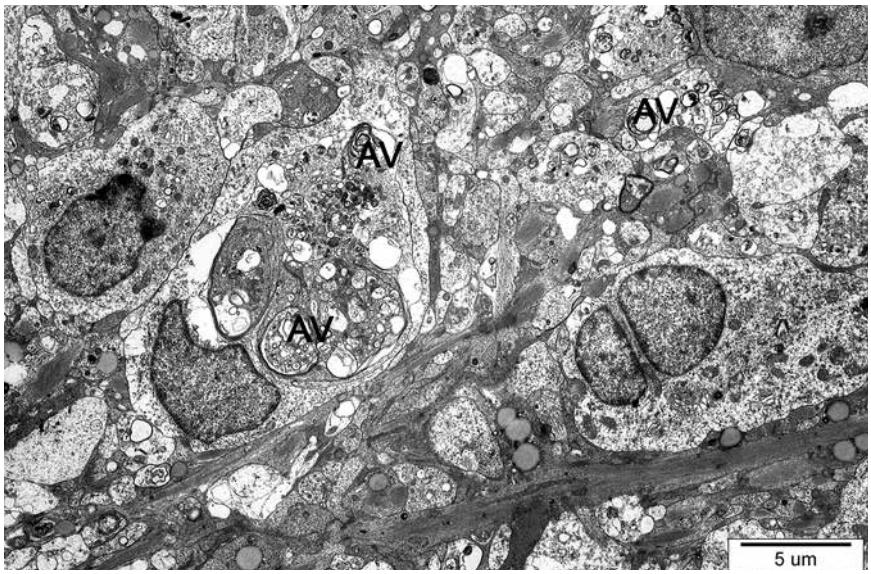

Fig. 1. Profiles of cellular processes and some neuronal cells with features of various degenerative changes, including numerous autophagic vacuoles (AV). Six days after 100 μM GLU.

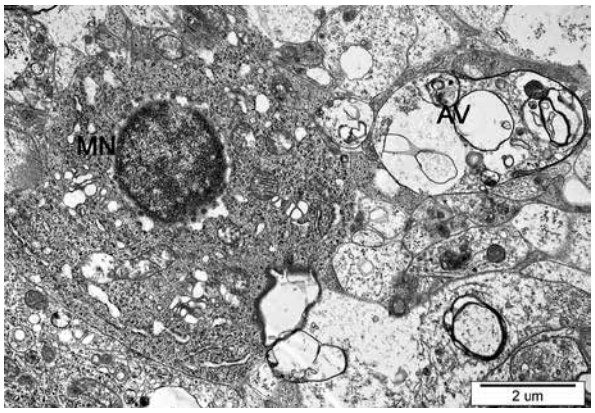

Fig. 2. Signs of apoptotic changes in motor neuron (MN), exhibiting condensed nuclear chromatin, increased electron density of cytoplasm and shrinkage of the whole cell body. Vesicular-autophagic changes (AV) seen in the vicinity of MN. Numerous damaged neuronal processes with signs of autophagy and destruction of organelles in surrounding neuropil. Eleven days after 100 µM GLU.

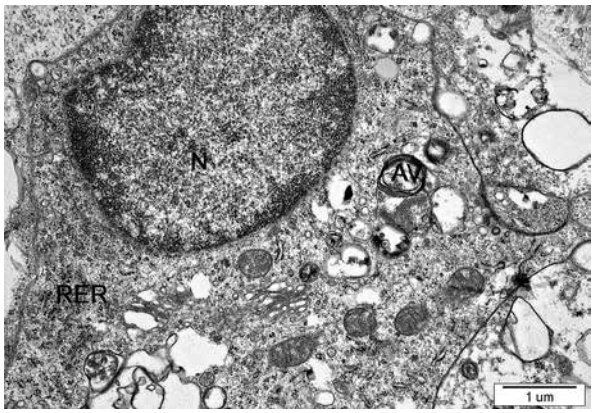

Fig. 3. Motor neuron with cytoplasm containing numerous autophagic vacuoles (AV) and dispersion of rough endoplasmic reticulum (RER). Nucleus (N) with condensed chromatin. Eleven days after 100 µM GLU.

Results

The spinal cord cultures exposed to GLU exhibited a range of advanced degenerative changes of MNs and destruction of neuronal processes in the surrounding neuropil. After 6 days of GLU exposure, the signs of various modes of cell death, including necrotic, apoptotic and autophagic changes, could be seen. Necrotic changes of MNs and their processes were characterized by extensive swelling and total destruction of organelles. The apoptotic bodies within large autophagic vacuoles were seen (Fig. 1). After 11 days of exposure to GLU, many MNs displayed signs of apoptotic changes in the form of a shrinkage of the cell body and condensation of nuclear chromatin (Fig. 2). Moreover, numerous autophagic vacuoles in the cytoplasm of MNs and neuronal processes were observed (Figs. 2 and 3). Less severe damage of MNs includes disaggregation and loss of rough endoplasmic reticulum and the Golgi complex, increase of cytoplasmic microvesicles and swelling of mitochondria (Fig. 4).

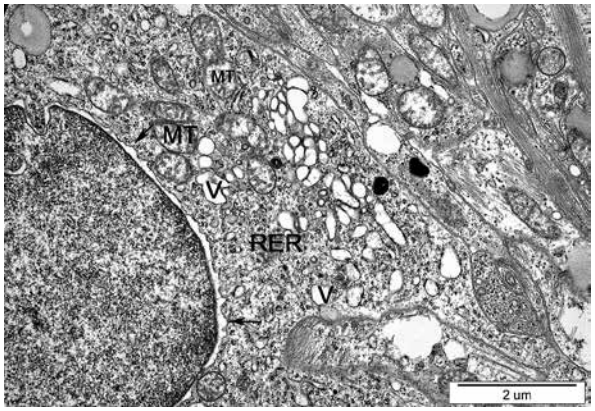

Fig. 4. Fragment of motor neuron exhibiting dispersed rough endoplasmic reticulum (RER), increased number of intracytoplasmic vesicles (V), distended perinuclear space (arrows) and slightly swollen mitochondria (MT). Eleven days after 100 µM GLU.

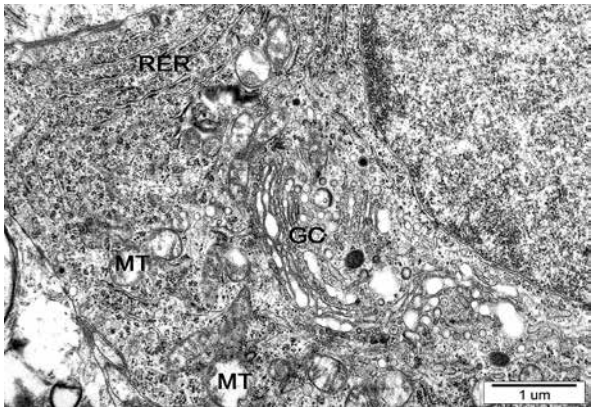

Fig. 5. Motor neuron with well-preserved nucleus and cytoplasm containing long, regularly arranged profiles of rough endoplasmic reticulum (RER), Golgi complex (GC), rich ribosomes and swollen mitochondria (MT). Three days after 100 µM GLU + 10 µM VPA.

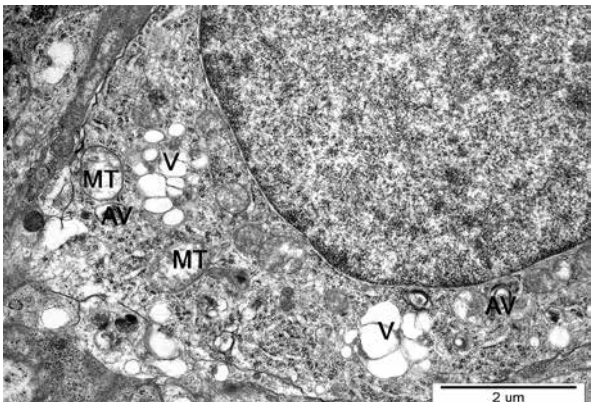

Fig. 6. Fragment of motor neuron with well-preserved nucleus and slight cytoplasmic abnormalities including presence of cytoplasmic vacuoles (V) with a few autophagic vacuoles (AV) and swollen mitochondria (MT). Three days after 100 µMGLU + 10 µM VPA.

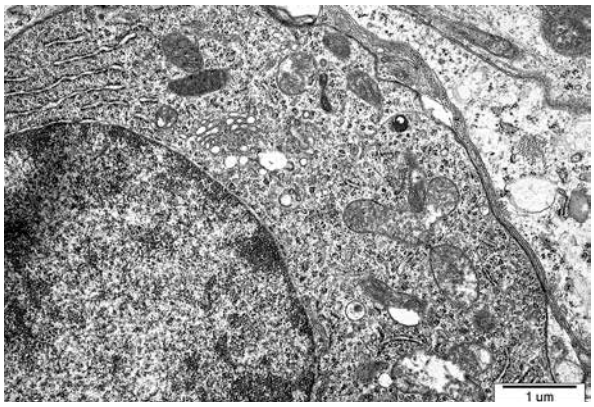

Fig. 7. Fragment of well-preserved motor neuron with normal organelles. Six days after 100 µM GLU + 10 µM VPA.

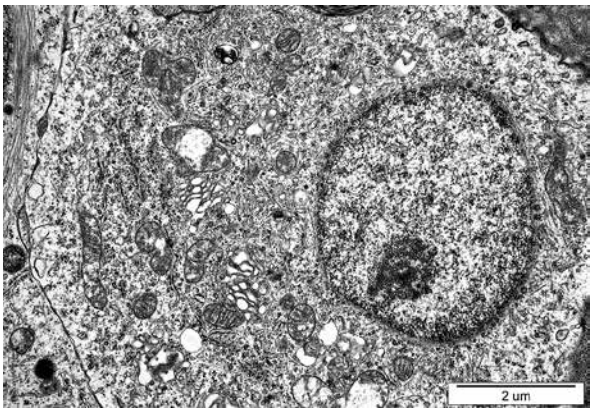

Fig. 8. Fragment of neuron, containing quite well-preserved organelles and nucleus with distinct nucleolus and dispersed heterochromatin. Six days after 100 µM GLU + 10 µM VPA.

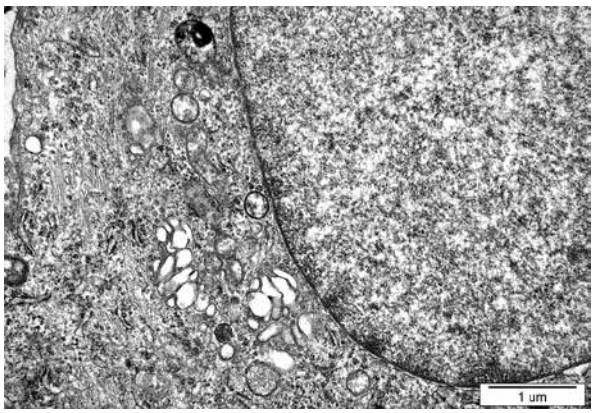

Fig. 9. Fragment of well-preserved motor neuron with large nucleus and cytoplasm containing normal organelles, microtubules and neurofilaments. Eleven days after 100 µM GLU + 10 µM VPA.

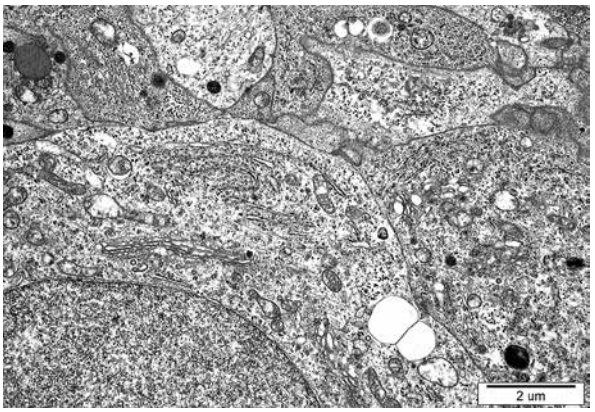

Fig. 10. Fragments of quite well-preserved neurons surrounded by neuropil with normal appearing neuronal and glial processes. Eleven days after 100 µM GLU + 10 µM VPA.

The treatment with VPA effectively prevents GLU-induced MN degenerative changes. Numerous well-preserved large motor neurons could be identified after 3, 6 and 11 days of co-treatment of VPA and GLU. After 3 days of VPA + GLU exposure the neurons exhibited perikaryal cytoplasm containing long profiles of rough endoplasmic reticulum, a well-developed Golgi complex (Fig. 5), and sometimes slightly swollen mitochondria and small autophagic vacuoles (Fig. 6). Quite well-preserved MNs, exhibiting a large nucleus with dispersed chromatin, distinct nucleolus and cytoplasm, containing well-organized rough endoplasmic reticulum and Golgi complex, were still recognizable after 6 days (Figs. 7 and 8) and 11 days (Figs. 9 and 10) of VPA + Glu exposure. Numerous microtubules and

neurofilaments in perikaryal cytoplasm were noticed (Fig. 9). The neuropil contained unchanged neuronal and glial processes (Fig. 10). Some large MNs exhibited only subtle ultrastructural abnormalities, such as slightly damaged mitochondria, focal cytoplasmic vacuolization and a few autophagic vacuoles. MNs with signs of apoptotic changes or autophagic degeneration could be seen only occasionally. Totally destroyed cells appeared sporadically.

Discussion

The mechanism underlying the pathogenesis of ALS remains unknown [28]. Genetic, molecular and environmental factors are believed to participate in the development of this progressive neurodegenerative process. Among various pathogenic factors, oxidative stress, mitochondrial dysfunction, apoptosis, glutamate excitotoxicity and proteasomal dysfunction are considered. However, the real cause of the disease, its natural history, classification, mechanism of progression and potential therapeutic targets are still under debate [13,29-31,35,36,41].

The cumulative evidence suggests that a mutation in Cu/Zn-superoxide dismutase (SOD1) protein contributes to the pathogenesis of familial ALS [38,44]. Dysfunction of neuronal mitochondria has been suggested to play an important role in MN degeneration [20]. The oxidative and endoplasmic reticulum (ER) stress [16,17] and deregulation of the ER mitochondrial calcium cycle [22] are described as the most likely causes of motor neuronal death, but it is believed that a complex mechanism of multiple toxic pathways is implicated in the ALS onset and progression [32]. Glutamate-induced excitotoxicity is also considered as one of the possible pathophysiological factors of motor neuron death [4,12].

Recently, a decreased histone acetylation level has been reported in the degenerating MNs in ALS experimental models [18]. Low histone deacetylase 6 (HDAC6) expression was reported at the onset and at the late stages of ALS in a mouse model [6]. Thus, it could be suggested that histone deacetylase inhibition may be a promising new therapeutic strategy for various neurodegenerative disorders, including motor neuron diseases (MNDs) [8,10]. As valproic acid (VPA), a short-chain fatty acid, effectively inhibits histone deacetylase [14,25] and delays apoptosis in degenerating neurons, it may be a good candidate for studies on its therapeutic role in different neurodegenerative conditions [3,19]. Its therapeutic potential has been documented in various cellular and animal models of neurologic, neurodegenerative, and neuropsychiatric disorders [7]. Combined treatment with lithium and VPA delays onset of clinical symptoms, reduces neurological deficits and prolongs survival in the SOD1 mouse model of amyotrophic lateral sclerosis [11]. Co-treatment of cerebellar granular cell cultures with lithium and VPA induced synergistic neuroprotective effects against glutamate excitotoxicity in a time-dependent manner [24].

Histone proteins organize DNA into nucleosomes, which are regular repeating structures of chromatin. This organization is required for the efficient packaging of large amounts of eukaryotic genomic DNA [45]. Acetylation and deacetylation of histone proteins play an important role in various cellular events, including epigenetic regulation of transcription. Histone acetyltransferases (HATs) catalyze acetylation, whereas histone deacetylases (HDACs) enhance deacetylation. Therefore VPA, via HDAC inhibition, might potentiate gene expression and promote a more transcriptionally active chromatin conformation. Thus, VPA protects neurons from excitotoxicity through inhibition of HDAC activity and suppression of apoptotic neuronal death associated with nuclear accumulation of glyceraldehyde-3-phosphate dehydrogenase (GAPDH) [21]. It was also suggested that VPA exerts neuroprotective effects through changes in a variety of intracellular signaling pathways, including upregulation of Bcl-2 protein with an antiapoptotic property [40]. Some results suggest that chronic treatment with valproate produce neuroprotection of cultured neuronal cells from damage caused by endoplasmic reticulum stress-mediated apoptosis [47] and oxidative stress [46]. It has been shown that combined treatment with histone deacetylase inhibitor and catalytic oxidant exerts additive neuroprotective effect in a transgenic mouse model of ALS [33]. Rouaux *et al*. [40] demonstrated that chronic VPA treatment *in vivo* prevented histone deacetylation in the spinal cord of symptomatic ALS mice. It delayed MN death and disease onset but did not significantly increase the mean lifespan of SOD1 (G86R) transgenic ALS mice and did not prevent distal pathology, i.e. neuromuscular denervation. However, despite the beneficial effect on MNs, VPA-treated animals died with

the neuropathological features typical for ALS. These results indicate that beneficial effects of VPA might be related to other factors than only a strict neuroprotection. On the other hand, neuroprotection of lower MNs is not sufficient for clinical therapy of ALS, because it does not prevent neuromuscular denervation.

In the mouse ALS model, CREB-binding protein, a transcriptional coactivator with histone acetyltransferase activity, was specifically reduced in motor neurons of the lumbar spinal cord. Consistently, decreased histone acetylation levels were observed in degenerating motor neurons [39]. Numerous studies have reported the beneficial effects of HDAC inhibitors on different aspects of neurodegeneration. Although treatment with VPA was found to protect motor neurons against glutamate toxicity in an organotypic culture of spinal cord and the ALS mouse model [43], another study using the same G93A mouse model found that long-term dietary VPA administration protected motor neurons but did not significantly affect the animal lifespan [9]. Overall, these data indicate poor efficiency of HDAC in treatment for ALS therapy despite the neuroprotective efficiency of HDAC. The randomized sequential clinical trial evidenced that VPA, at one dosage corresponding to the therapeutic dose used in epilepsy, did not show a beneficial effect on survival and disease progression in patients with ALS [34]. It has implications for future trials in neurodegenerative diseases with various histone deacetylase inhibitors.

Our ultrastructural study documented the neuroprotective efficacy of VPA in an experimental model of neurodegeneration related to GLU excitotoxicity in vitro. GLU-induced excitotoxicity has been implicated in the pathophysiology of various neurodegenerative diseases, including ALS. It was shown that valproic acid protected cultured cerebellar granule cells against GLU-induced excitotoxicity with concomitant transcriptional activation and induction of α-synuclein. This presynaptic protein was induced by valproic acid through histone deacetylase inhibition and participates in neuroprotection [23].

Our ultrastructural study evidenced that prevention of neuronal excitotoxic changes in vitro was related to inhibition of apoptosis and autophagy. The cultures subjected to GLU with VPA treatment exhibited well-retained parallel profiles of rough endoplasmic reticulum in the majority of motoneurons at 3 to 11 days after exposure. These results might support previous data indicating that neuroprotective effects of VPA might act via suppressing ER stress-mediated apoptosis. It could suggest that this mechanism may cause the VPA-induced therapeutic effects in neurodegenerative processes. Additional studies are necessary to clarify this issue.

Acknowledgments

This study was supported by grant no. NN 401 014 640 from the Ministry of Science and Higher Education of Poland and by statutory funds from the Mossakowski Research Institute, Polish Academy of Science.

Disclosure

Authors report no conflict of interest.

References

1. Ajroud-Driss S, Siddique T. Sporadic and hereditary amyotrophic lateral sclerosis (ALS). Biochim Biophys Acta 2015; 1852: 679-684.
2. Andersen PM, Sims KB, Xin WW, Kiely R, O'Neill G, Ravits J, Pioro E, Harati Y, Brower RD, Levine JS, Heinicke HU, Seltzer W, Boss M, Brown RH, Jr. Sixteen novel mutations in the Cu/Zn superoxide dismutase gene in amyotrophic lateral sclerosis: a decade of discoveries, defects and disputes. Amyotroph Lateral Scler Other Motor Neuron Disord 2003; 4: 62-73.
3. Biermann J, Grieshaber P, Goebel U, Martin G, Thanos S, Di Giovanni S, Lagreze WA. Valproic acid-mediated neuroprotection and regeneration in injured retinal ganglion cells. Invest Ophthalmol Vis Sci 2010; 51: 526-534.
4. Blasco H, Mavel S, Corcia P, Gordon PH. The glutamate hypothesis in ALS: pathophysiology and drug development. Curr Med Chem 2014; 21: 3551-3575.
5. Boillee S, Vande Velde C, Cleveland DW. ALS: a disease of motor neurons and their nonneuronal neighbors. Neuron 2006; 52: 39-59.
6. Chen S, Zhang XJ, Li LX, Wang Y, Zhong RJ, Le W. Histone deacetylase 6 delays motor neuron degeneration by ameliorating the autophagic flux defect in a transgenic mouse model of amyotrophic lateral sclerosis. Neurosci Bull 2015; 31: 459-468.
7. Chiu CT, Wang Z, Hunsberger JG, Chuang DM. Therapeutic potential of mood stabilizers lithium and valproic acid: beyond bipolar disorder. Pharmacol Rev 2013; 65: 105-142.
8. Chuang DM, Leng Y, Marinova Z, Kim HJ, Chiu CT. Multiple roles of HDAC inhibition in neurodegenerative conditions. Trends Neurosci 2009; 32: 591-601.
9. Crochemore C, Virgili M, Bonamassa B, Canistro D, Pena-Altamira E, Paolini M, Contestabile A. Long-term dietary administration of valproic acid does not affect, while retinoic acid decreases, the lifespan of G93A mice, a model for amyotrophic lateral sclerosis. Muscle Nerve 2009; 39: 548-552.

10. Echaniz-Laguna A, Bousiges O, Loeffler JP, Boutillier AL. Histone deacetylase inhibitors: therapeutic agents and research tools for deciphering motor neuron diseases. Curr Med Chem 2008; 15: 1263-1273.
11. Feng HL, Leng Y, Ma CH, Zhang J, Ren M, Chuang DM. Combined lithium and valproate treatment delays disease onset, reduces neurological deficits and prolongs survival in an amyotrophic lateral sclerosis mouse model. Neuroscience 2008; 155: 567-572.
12. Fulceri F, Ferrucci M, Lazzeri G, Paparelli S, Bartalucci A, Tamburini I, Paparelli A, Fornai F. Autophagy activation in glutamate-induced motor neuron loss. Arch Ital Biol 2011; 149: 101-111.
13. Gonzalez de Aguilar JL, Echaniz-Laguna A, Fergani A, Rene F, Meininger V, Loeffler JP, Dupuis L. Amyotrophic lateral sclerosis: all roads lead to Rome. J Neurochem 2007; 101: 1153-1160.
14. Gottlicher M. Valproic acid: an old drug newly discovered as inhibitor of histone deacetylases. Ann Hematol 2004; 83 Suppl 1: S91-92.
15. Gottlicher M, Minucci S, Zhu P, Kramer OH, Schimpf A, Giavara S, Sleeman JP, Lo Coco F, Nervi C, Pelicci PG, Heinzel T. Valproic acid defines a novel class of HDAC inhibitors inducing differentiation of transformed cells. EMBO J 2001; 20: 6969-6978.
16. Ikawa M, Okazawa H, Tsujikawa T, Matsunaga A, Yamamura O, Mori T, Hamano T, Kiyono Y, Nakamoto Y, Yoneda M. Increased oxidative stress is related to disease severity in the ALS motor cortex: a PET study. Neurology 2015; 84: 2033-2039.
17. Ilieva EV, Ayala V, Jove M, Dalfo E, Cacabelos D, Povedano M, Bellmunt MJ, Ferrer I, Pamplona R, Portero-Otin M. Oxidative and endoplasmic reticulum stress interplay in sporadic amyotrophic lateral sclerosis. Brain 2007; 130: 3111-3123.
18. Janssen C, Schmalbach S, Boeselt S, Sarlette A, Dengler R, Petri S. Differential histone deacetylase mRNA expression patterns in amyotrophic lateral sclerosis. J Neuropathol Exp Neurol 2010; 69: 573-581.
19. Jeong MR, Hashimoto R, Senatorov VV, Fujimaki K, Ren M, Lee MS, Chuang DM. Valproic acid, a mood stabilizer and anticonvulsant, protects rat cerebral cortical neurons from spontaneous cell death: a role of histone deacetylase inhibition. FEBS Lett 2003; 542: 74-78.
20. Jiang Z, Wang W, Perry G, Zhu X, Wang X. Mitochondrial dynamic abnormalities in amyotrophic lateral sclerosis. Transl Neurodegener 2015; 4: 14.
21. Kanai H, Sawa A, Chen RW, Leeds P, Chuang DM. Valproic acid inhibits histone deacetylase activity and suppresses excitotoxicity-induced GAPDH nuclear accumulation and apoptotic death in neurons. Pharmacogenomics J 2004; 4: 336-344.
22. Lautenschlaeger J, Prell T, Grosskreutz J. Endoplasmic reticulum stress and the ER mitochondrial calcium cycle in amyotrophic lateral sclerosis. Amyotroph Lateral Scler 2012; 13: 166-177.
23. Leng Y, Chuang DM. Endogenous alpha-synuclein is induced by valproic acid through histone deacetylase inhibition and participates in neuroprotection against glutamate-induced excitotoxicity. J Neurosci 2006; 26: 7502-7512.
24. Leng Y, Liang MH, Ren M, Marinova Z, Leeds P, Chuang DM. Synergistic neuroprotective effects of lithium and valproic acid or other histone deacetylase inhibitors in neurons: roles of glycogen synthase kinase-3 inhibition. J Neurosci 2008; 28: 2576-2588.
25. Leng Y, Marinova Z, Reis-Fernandes MA, Nau H, Chuang DM. Potent neuroprotective effects of novel structural derivatives of valproic acid: potential roles of HDAC inhibition and HSP70 induction. Neurosci Lett 2010; 476: 127-132.
26. Liu D, Liu C, Li J, Azadzoi K, Yang Y, Fei Z, Dou K, Kowall NW, Choi HP, Vieira F, Yang JH. Proteomic analysis reveals differentially regulated protein acetylation in human amyotrophic lateral sclerosis spinal cord. PLoS One 2013; 8: e80779.
27. Monti B, Polazzi E, Contestabile A. Biochemical, molecular and epigenetic mechanisms of valproic acid neuroprotection. Curr Mol Pharmacol 2009; 2: 95-109.
28. Musaro A. Understanding ALS: new therapeutic approaches. FEBS J 2013; 280: 4315-4322.
29. Orsini M, Oliveira AB, Nascimento OJ, Reis CH, Leite MA, de Souza JA, Pupe C, de Souza OG, Bastos VH, de Freitas MR, Teixeira S, Bruno C, Davidovich E, Smidt B. Amyotrophic Lateral Sclerosis: New Perpectives and Update. Neurol Int 2015; 7: 5885.
30. Paez-Colasante X, Figueroa-Romero C, Sakowski SA, Goutman SA, Feldman EL. Amyotrophic lateral sclerosis: mechanisms and therapeutics in the epigenomic era. Nat Rev Neurol 2015; 11: 266-279.
31. Palomo GM, Manfredi G. Exploring new pathways of neurodegeneration in ALS: the role of mitochondria quality control. Brain Res 2015; 1607: 36-46.
32. Pasinelli P, Brown RH. Molecular biology of amyotrophic lateral sclerosis: insights from genetics. Nat Rev Neurosci 2006; 7: 710-723.
33. Petri S, Kiaei M, Kipiani K, Chen J, Calingasan NY, Crow JP, Beal MF. Additive neuroprotective effects of a histone deacetylase inhibitor and a catalytic antioxidant in a transgenic mouse model of amyotrophic lateral sclerosis. Neurobiol Dis 2006; 22: 40-49.
34. Piepers S, Veldink JH, de Jong SW, van der Tweel I, van der Pol WL, Uijtendaal EV, Schelhaas HJ, Scheffer H, de Visser M, de Jong JM, Wokke JH, Groeneveld GJ, van den Berg LH. Randomized sequential trial of valproic acid in amyotrophic lateral sclerosis. Ann Neurol 2009; 66: 227-234.
35. Przedborski S, Mitsumoto H, Rowland LP. Recent advances in amyotrophic lateral sclerosis research. Curr Neurol Neurosci Rep 2003; 3: 70-77.
36. Ravits J. Focality, stochasticity and neuroanatomic propagation in ALS pathogenesis. Exp Neurol 2014; 262 Pt B: 121-126.
37. Rosen DR, Sapp P, O'Regan J, McKenna-Yasek D, Schlumpf KS, Haines JL, Gusella JF, Horvitz HR, Brown RH, Jr. Genetic linkage analysis of familial amyotrophic lateral sclerosis using human chromosome 21 microsatellite DNA markers. Am J Med Genet 1994; 51: 61-69.
38. Rotunno MS, Bosco DA. An emerging role for misfolded wild-type SOD1 in sporadic ALS pathogenesis. Front Cell Neurosci 2013; 7: 253.
39. Rouaux C, Jokic N, Mbebi C, Boutillier S, Loeffler JP, Boutillier AL. Critical loss of CBP/p300 histone acetylase activity by caspase-6 during neurodegeneration. EMBO J 2003; 22: 6537-6549.
40. Rouaux C, Panteleeva I, Rene F, Gonzalez de Aguilar JL, Echaniz-Laguna A, Dupuis L, Menger Y, Boutillier AL, Loeffler JP. Sodium valproate exerts neuroprotective effects in vivo through

CREB-binding protein-dependent mechanisms but does not improve survival in an amyotrophic lateral sclerosis mouse model. J Neurosci 2007; 27: 5535-5545.
41. Rowland LP. Controversies about amyotrophic lateral sclerosis. Neurologia 1996; 11 Suppl 5: 72-74.
42. Rowland LP. Diagnosis of amyotrophic lateral sclerosis. J Neurol Sci 1998; 160 Suppl 1: S6-24.
43. Sugai F, Yamamoto Y, Miyaguchi K, Zhou Z, Sumi H, Hamasaki T, Goto M, Sakoda S. Benefit of valproic acid in suppressing disease progression of ALS model mice. Eur J Neurosci 2004; 20: 3179-3183.
44. Tafuri F, Ronchi D, Magri F, Comi GP, Corti S. SOD1 misplacing and mitochondrial dysfunction in amyotrophic lateral sclerosis pathogenesis. Front Cell Neurosci 2015; 9: 336.
45. Verdone L, Caserta M, Di Mauro E. Role of histone acetylation in the control of gene expression. Biochem Cell Biol 2005; 83: 344-353.
46. Wang JF, Azzam JE, Young LT. Valproate inhibits oxidative damage to lipid and protein in primary cultured rat cerebrocortical cells. Neuroscience 2003; 116: 485-489.
47. Wang X, Ma M, Teng J, Che X, Zhang W, Feng S, Zhou S, Zhang Y, Wu E, Ding X. Valproate Attenuates 25-kDa C-Terminal Fragment of TDP-43-Induced Neuronal Toxicity via Suppressing Endoplasmic Reticulum Stress and Activating Autophagy. Int J Biol Sci 2015; 11: 752-761.
48. Zhu Y, Fotinos A, Mao LL, Atassi N, Zhou EW, Ahmad S, Guan Y, Berry JD, Cudkowicz ME, Wang X. Neuroprotective agents target molecular mechanisms of disease in ALS. Drug Discov Today 2015; 20: 65-75.

Original article

Folia Neuropathologica

The influence of glutamatergic receptor antagonists on biochemical and ultrastructural changes in myelin membranes of rats subjected to experimental autoimmune encephalomyelitis

Beata Dąbrowska-Bouta[1], Lidia Strużyńska[1], Małgorzata Chalimoniuk[2], Małgorzata Frontczak-Baniewicz[3], Grzegorz Sulkowski[1]

[1]Laboratory of Pathoneurochemistry, Department of Neurochemistry, [2]Department of Cellular Signaling, [3]Electron Microscopy Platform, Mossakowski Medical Research Centre Polish Academy of Sciences, Warsaw, Poland

Folia Neuropathol 2015; 53 (4): 317-326 DOI: 10.5114/fn.2015.56546

Abstract

Elevated extracellular glutamate in the synaptic cleft causes overactivation of glutamate receptors and kills neurons by an excitotoxic mechanism. Recent studies have shown that glutamate can also lead to toxic injury of white matter oligodendrocytes in myelin sheaths and consequently to axon demyelination. The present study was performed using the rodent model of multiple sclerosis known as experimental autoimmune encephalomyelitis (EAE). The aim of the study was to test the effects of the glutamatergic receptor antagonists amantadine and memantine (antagonists of NMDA receptors), LY 367384 (an antagonist of mGluR1), and MPEP (an mGluR5 antagonist) on the development of neurological symptoms in immunized animals, morphological changes in cerebral myelin, and expression of mRNA of the principal myelin proteins PLP, MBP, MOG, MAG, and CNPase. Pharmacological inhibition of NMDA receptors by amantadine and memantine was found to suppress neurological symptoms in EAE rats, whereas antagonists of the group I metabotropic glutamate receptors (mGluRs G I) did not function positively. In the symptomatic phase of the disease we observed destruction of myelin sheaths via electron microscopy and decreased levels of mRNA for all of the principal myelin proteins. The results reveal that glutamate receptor antagonists have a positive effect on the expression of mRNA MBP and glycoproteins MAG and MOG but not on myelin ultrastructure.

Key words: *EAE, glutamate receptors antagonists, myelin proteins, excitotoxicity.*

Introduction

Glutamate is the primary excitatory amino acid neurotransmitter in the mammalian brain. It plays an important role in both physiological and pathological mechanisms operating in the central nervous system (CNS). Glutamate released from nerve endings participates in signaling processes prior to being taken up from the synaptic cleft via a mechanism mediated mainly by glial transporters and to a lesser extent neuronal, excitatory amino acid transporters (EAATs) [10,27]. The extracellular levels of glutamate must be tightly controlled because excessive accumulation of glutamate leads to overstimulation of

Communicating author:
Grzegorz Sulkowski, Laboratory of Pathoneurochemistry, Department of Neurochemistry, Mossakowski Medical Research Centre Polish Academy of Sciences, 5 Pawińskiego St., 02-106 Warsaw, Poland, phone: +48 22 608 65 30, fax: + 48 22 608 54 23, e-mail: gsulkowski@imdik.pan.pl

glutamate receptors (GluRs) and subsequent cell damage by an excitotoxic mechanism [6,8,29].

Excitotoxicity is implicated in the pathomechanism of a number of chronic neurodegenerative diseases such as Alzheimer's disease, Parkinson's disease, Huntington's disease, and amyotrophic lateral sclerosis (ALS) [2,7,8,28]. Although the pathology of each of these diseases is different, each involves overstimulation of GluRs (especially the N-methyl-D-aspartate receptor [NMDAR] subtype). Such overstimulation ultimately leads to injury of neurons by necrotic or apoptotic cell death [13,32]. The pathomechanism of excitotoxicity also operates in multiple sclerosis (MS), wherein the immune system attacks the CNS. MS is characterized by infiltration of immune cells from peripheral circulation, loss of oligodendrocytes and the appearance of demyelinating areas (plaques) in the white matter of the spinal cord and brain. These disorders lead to axonal damage and disrupted neurotransmission [13,17,23]. The etiology of MS has not yet been established. Many pathological factors participate in the pathogenesis of MS, including proinflammatory cytokines, reactive oxygen species (ROS), matrix metalloproteinases, autoantibodies and cell-mediated cytotoxicity [13,19].

Enhancement of glutamate levels in cerebrospinal fluid and changes in the expression of metabotropic (mGluRs) and ionotropic (iGluRs) glutamate receptors have been observed in the inflammatory demyelination plaques in the brains of MS patients [12,13]. Elevation of glutamate in brain was also observed in experimental autoimmune encephalomyelitis (EAE, the animal model of MS) pathology in rats [6]. The hypothesis concerning the involvement of excitotoxicity in pathogenesis of MS and EAE has been confirmed by the observation that anti-glutamatergic agents provide neuroprotection [28]. Our previous studies using EAE rats revealed that administration of amantadine or memantine (iGluR antagonists) reduces the severity of symptoms, inflammation and axonal damage in immunized animals [33-35]. This is a strong indication that glutamate, operating through its ionotropic receptors, plays a key role in the pathology of the disease. If we can gain an understanding of how myelin and oligodendrocytes are damaged by excitotoxicity, we will be able to develop therapeutic strategies to protect nerve axons against demyelination.

The myelin sheath is the predominant element of the white matter of the CNS, its function being to facilitate signal conduction in axons. Myelin is a highly specialized structure with a unique molecular composition and architecture. It is characterized by a high proportion of lipids (70-85%) and a low proportion of proteins (15-30%) [25]. It contains distinctive proteins such as proteolipid protein (PLP), myelin basic protein (MBP), 2′,3′-cyclic nucleotide 3′-phosphodiesterase (CNPase), myelin-associated glycoprotein (MAG) and myelin oligodendrocyte glycoprotein (MOG). PLP and MBP constitute the majority of the total myelin proteins (about 70%) [4,25]. CNPase is a specific enzyme localized in the cytoplasm of non-compacted myelin. MOG is a transmembrane protein representing one of the main autoantigens in MS. MAG is a glycoprotein involved in the myelin-related inhibition of axonal regeneration. Each of these myelin-specific proteins plays an important role in the formation and maintenance of myelin membranes [4,5,31].

The present study was undertaken to investigate whether the glutamate receptor antagonists amantadine and memantine (antagonists of NMDA receptors), LY 367384 (an antagonist of mGluR1) and MPEP (an mGluR5 antagonist) improve the condition of animals subjected to EAE and exert protective effects on mRNA expression of selected myelin proteins (PLP, MBP, MOG, MAG, and CNPase). Ultrastructural observations of myelin membranes in the acute phase of EAE and after treatment with GluR antagonists were also made using transmission electron microscopy (TEM).

Material and methods

Animal model

The study was carried out in strict accordance with the regulations of the Experiments on Animals Act (Act of 21 January 2005 on experiments on live animals, the Parliament of the Republic of Poland, Dz. U. Nr 33, pos. 289). All experiments using animals were approved by the Fourth Warsaw Local Ethics Committee for Animal Experimentation; permit number 61/2009. All procedures using animals were performed under sodium pentobarbital anesthesia to minimize suffering.

Female Lewis rats weighing approximately 200 g were used. To induce EAE, we immunized rats subcutaneously in both hind feet with 100 µl of inoculum containing guinea pig spinal cord homogenate emulsified in Freund's complete adjuvant (CFA) containing

5.5 mg/ml *Mycobacterium tuberculosis* H37Ra (Difco, Detroit, Mi, USA). The control group received inoculum containing CFA without spinal cord homogenate.

After immunization, the rats were provided with unrestricted access to food and water and were housed under environmentally controlled conditions. Body weight and neurological deficits were measured daily according to the following scale: 0 = no signs, 1 = flaccid tail, 2 = impairment of fighting reflex and/or loss of muscle tone in hind limbs, 3 = complete paralysis of hind limbs, 4 = paraplegia, and 5 = moribund state/death [15,26].

Experimental groups and tissue processing

All experiments were performed during the acute phase of the disease at day 12 post immunization (d.p.i.). Six experimental groups of animals were defined: group I (control), group II (EAE), group III (EAE + amantadine), group IV (EAE + memantine), group V (EAE + LY 367385), and group VI (EAE + MPEP). During the experiments the part of rats in each experimental group (n = 12) were monitored until day 25 after the initial injection inducing EAE or after drug administration.

Glutamate receptor antagonists were dissolved in PBS and administered via intraperitoneal injection to the EAE rats once daily for 7 consecutive days, from 5 d.p.i. to 11 d.p.i., according to the previously described procedure [33-35]. Amantadine (Sigma-Aldrich, Steinheim, Germany) was administered at a dose of 100 mg/kg b.w./day, memantine (Sigma-Aldrich, Steinheim, Germany) was administered at a dose of 60 mg/kg b.w./day, and LY 367385 (Tocris, Bristol, UK) and MPEP (Tocris, Bristol, UK) were both administered at a dose of 10 mg/kg b.w./day.

At 12 d.p.i. (in the acute, symptomatic phase of the disease, when the neurological deficits were maximal), eight rats were sacrificed in each experimental group for real-time PCR analysis. The brains were rapidly removed, frozen in liquid nitrogen and stored at –70°C for further analysis (extraction of RNA).

Determination of mRNA levels of myelin proteins by real time-PCR

Total RNA was extracted from the brain cortex of all six groups of rats according to the method of Chomczyński [9] using TRI Reagent (Sigma, St. Louis, MO, USA). Reverse transcription of 2 µg of total RNA was performed in a final volume of 20 µl using random primers and avian myeloblastosis virus (AMV) reverse transcriptase (Life Technologies, Forest City, CA, USA). The RT-PCR conditions were as follows: reverse transcription at 42°C for 45 min and denaturation at 94°C for 30 s. For quantitative real-time PCR analysis, TaqMan technology was applied. Rat myelin protein-specific primers for MOG Rn 00575354_m1, PLP Rn00456892_m1, MBP Rn01399619_m1, MAG Rn02586362, CNPase Rn01399463_m1 and the corresponding probes were obtained from Life Technologies (Forest City, CA, USA). The mRNA expression levels of myelin proteins and actin were determined using the pre-validated TaqMan assay reagents (Applied Biosystems, Forest City, CA, USA). Real-time PCR was conducted on an ABI Prism 7500 system using 5 µl of RT product, TaqMan PCR Master Mix, primers, and a TaqMan probe in a total volume of 20 µl. The PCR cycle conditions were as follows: initial denaturation at 95°C for 10 min, 50 cycles of 95°C for 15 s, and 60°C for 1 min. Each sample was analyzed in triplicate. The relative expression levels of the myelin protein mRNAs were calculated using a standard curve and normalized to actin.

Electron microscopic studies (TEM)

The analysis of ultrastructural changes in brain myelin was performed at 12 d.p.i. using five animals from each experimental group (control, EAE, EAE + amantadine, EAE + memantine, EAE + LY 368573, and EAE + MPEP). The animals were anaesthetized and perfused through the heart with fixative solution (2% paraformaldehyde, 2.5% glutaraldehyde, and 0.1 M cacodylate buffer, pH 7.4). After perfusion, small specimens from the forebrain were fixed overnight in the same solution and then post-fixed in 1.5% OsO_4 and 0.8% $K_4(FeCN)_6$ for 2 h. Then the material, after dehydration in ethanol and propylene oxide, was embedded in Spurr resin. Ultrathin sections were examined using a JEM 1200 Ex electron microscope.

Statistical analysis

The results are expressed as means ± SD from 3-8 experiments as identified in the legends of respective figures. Statistical significance was assessed by one-way ANOVA. Dunnett's multiple comparison test was used to identify the changes deemed to be significantly different from the control values.

Results

The influence of glutamate receptor antagonists on the course of EAE

The modulatory effects of glutamate receptor antagonists (amantadine, memantine, LY 367385, and MPEP) on the course of EAE, changes in body mass, duration of the disease, and inductive phase of EAE (characteristic parameters of the disease) were investigated. All studies were performed during the acute phase of EAE at 12 d.p.i., while the neurological deficits were maximal. We observed a 30% loss of body mass in EAE rats compared to the control animals. In groups treated with amantadine or memantine the loss of body mass was lower. We observed about a 20% decrease relative to the control, and about a 10% increase compared to EAE rats in body weight (Fig. 1A). Neurological deficits during the course of EAE were classified daily according to a scale from 1+ to 5+ as described in the Materials and Methods section. After administration of either memantine or amantadine, we observed a reduction in duration of neurological deficits (Fig. 1B) and in the severity of the disease (lowering of the score) (Fig. 1C) compared with EAE rats. Paralysis of the tail and hind limbs, reduction of muscle tone and physical activity in experimental rats were exclusively observed. The maximal cumulative index (maxCI) value reached 4.5+ in EAE rats, whereas in the amantadine- and memantine-treated groups it was 2.5+ (Fig. 1C). All rats in both of these groups exhibited improved physiological conditions relative

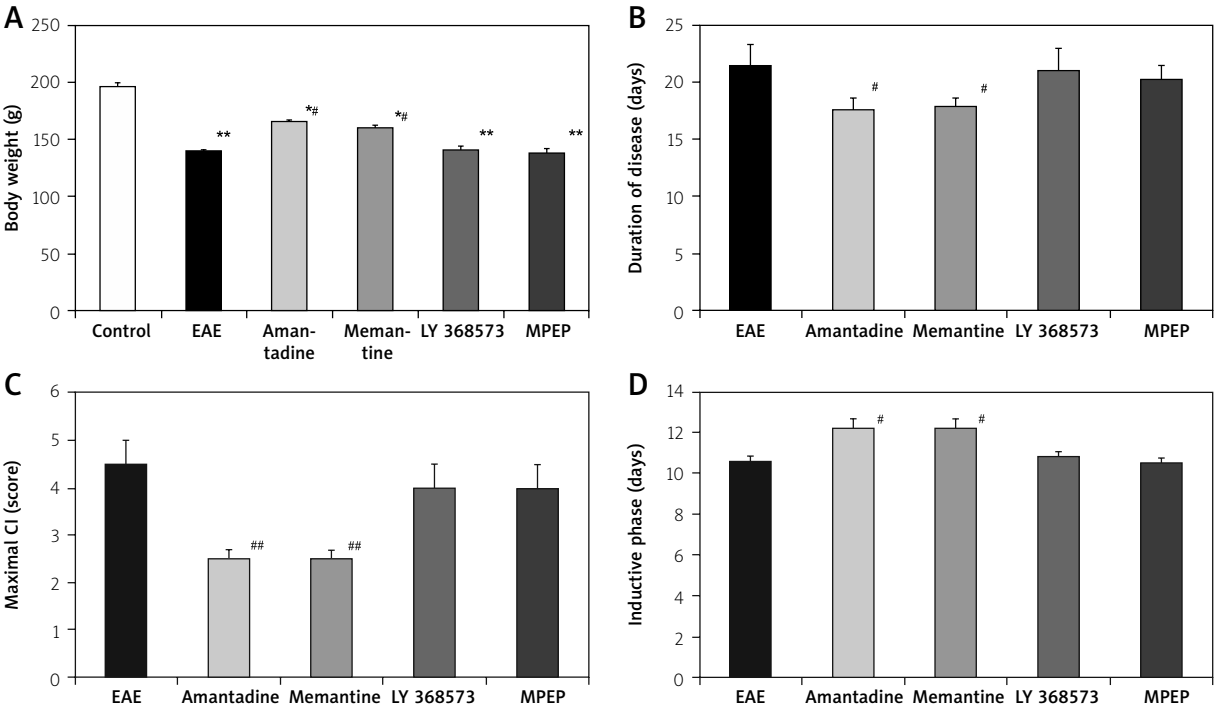

Fig. 1. Scores of the neurological symptoms and characteristic disease parameters observed in the acute phase of EAE (at 12 d.p.i.) and after treatment with antagonists of glutamate receptors. Neurological signs were monitored in the part of rats in each experimental group (n = 12) until recovery of the control EAE group (at 25 d.p.i.). Doses of antagonist were as follows: amantadine 100 mg/kg b.w./day, memantine 60 mg/kg b.w./day, LY 367385 10 mg/kg b.w./day and MPEP 10 mg/kg b.w./day. The antagonists were administered once daily for 7 consecutive days, starting from 5 d.p.i. to 11 d.p.i. The graphs indicate: **A)** body weight of animals; **B)** duration of the disease; **C)** maximal cumulative index (score); **D)** duration of inductive phase of the disease. Results were obtained from five to eight animals in each group and represent means ± SD. $^{*}p < 0.05$, $^{**}p < 0.01$ significantly different vs. control (healthy untreated rats). $^{\#}p < 0.05$ significantly different vs. EAE rats not subjected to therapy at 12 d.p.i. (one-way ANOVA followed by Dunnett's multiple comparison post test).

to the untreated EAE animals. The duration of the inductive phase of the disease (Fig. 1D) was lengthened by 1-2 days, whereas the total disease duration (Fig. 1B) was reduced by 2-4 days, relative to the untreated EAE rats. We did not observe any neuroprotective effects of LY 367385 or MPEP with respect to body mass, neurological deficits or duration of the disease. In these groups, all examined parameters were found to be statistically insignificant compared with the untreated EAE rats (Fig. 1A-D).

Analysis of the clinical parameters of the disease, as well as the effects of GluR antagonist administration on neurological deficits and the condition of the EAE rats during longer experiments (until 25 d.p.i.), are described and illustrated in detail in our previous papers [33-35].

Influence of drug administration on expression of mRNA of myelin proteins in EAE rats

We investigated the mRNA levels of myelin-specific proteins: PLP and MBP (structural proteins); MOG and MAG (myelin glycoproteins); and the enzyme CNPase (a myelin marker). The analysis of mRNA was conducted in the forebrains of rats obtained from all experimental groups (control, EAE, and EAE treated with antagonists of glutamate receptors) by real-time PCR.

In the EAE rats, at the peak of the disease, we observed significantly lower levels of PLP and MBP mRNA, which reached about 70% and 60% of control values, respectively (Fig. 2A-B). In the groups treated with amantadine or memantine, the PLP mRNA level was found to be similar to that observed in the untreated EAE rats. Administration of LY 367385 (the mGluR1 antagonist) and MPEP (the mGluR5 antagonist) resulted in a further decrease of PLP mRNA, to 90% of the control value, and to 50% of the value observed in the untreated EAE rats (Fig. 2A). The level of MBP mRNA was about 40% lower than that of the control but about 40% higher than that of the EAE rats in all groups treated with GluR antagonists (amantadine, memantine, LY 367385, and MPEP) (Fig. 2B).

The analysis of expression of MOG and MAG mRNAs in EAE animals indicated a 60% and a 70% decrease, respectively, relative to the control value (Fig. 2C, 2D). In groups treated with amantadine or memantine, the mRNA level of MOG was found to be similar to that of the untreated EAE rats, but in the LY 367385- or MPEP-treated rats the mRNA level increased to about 50% of that of the untreated EAE animals (Fig. 2C). An increased level of MAG mRNA was also observed in all treated groups (Fig. 2D). After administration of amantadine or memantine the level of MAG mRNA was found to be 20% higher, whereas in LY 367385- and MPEP-treated groups the MAG mRNA level was found to decrease by about 50-60% of the MAG mRNA level of the untreated EAE rats (Fig. 2D). Our studies also revealed changes in the level of CNPase mRNA in all experimental groups compared with control animals. We observed a statistically significant decrease in the CNPase mRNA level, which reached 60-70% of the control value. Administration of all tested GluR antagonists resulted in a decrease in CNPase mRNA expression by 30% relative to the level of CNPase mRNA expression in untreated EAE rats (Fig. 2E).

Electron microscopic analysis

TEM analysis was performed in forebrain specimens obtained from rat brains during the acute phase of EAE at 12 d.p.i. In control rats, the myelin exhibited normal lamellar ultrastructure characterized by ordered layers closely adhering to each other (Fig. 3A). In large areas of untreated EAE rat brains (Fig. 3B), as in brains of rats from all experimental groups treated with the GluR antagonists amantadine (Fig. 3C), memantine (Fig. 3D), LY 367385 (Fig. 3E), and MPEP (Fig. 3F), we observed visible changes in the myelin membranes. The characteristic compact myelin structure was essentially completely destroyed. Multilayered membranes of myelin sheaths were irregular and loosely arranged. Administration of GluR antagonists did not provide protective effects on the ultrastructure of myelin relative to the untreated EAE rats (Fig. 3B-F).

Discussion

Recent studies have demonstrated that glutamate excitotoxicity is an important mechanism which is related to tissue injury in MS lesions [3,6,22,38]. Any imbalance in glutamate homeostasis in MS, either by increased production, reduced transport or impaired metabolism, is likely to affect oligodendrocytes [38] and cells producing myelin sheaths that support electrical conduction in the CNS [25].

The present study investigates whether administration of glutamate receptor antagonists to EAE

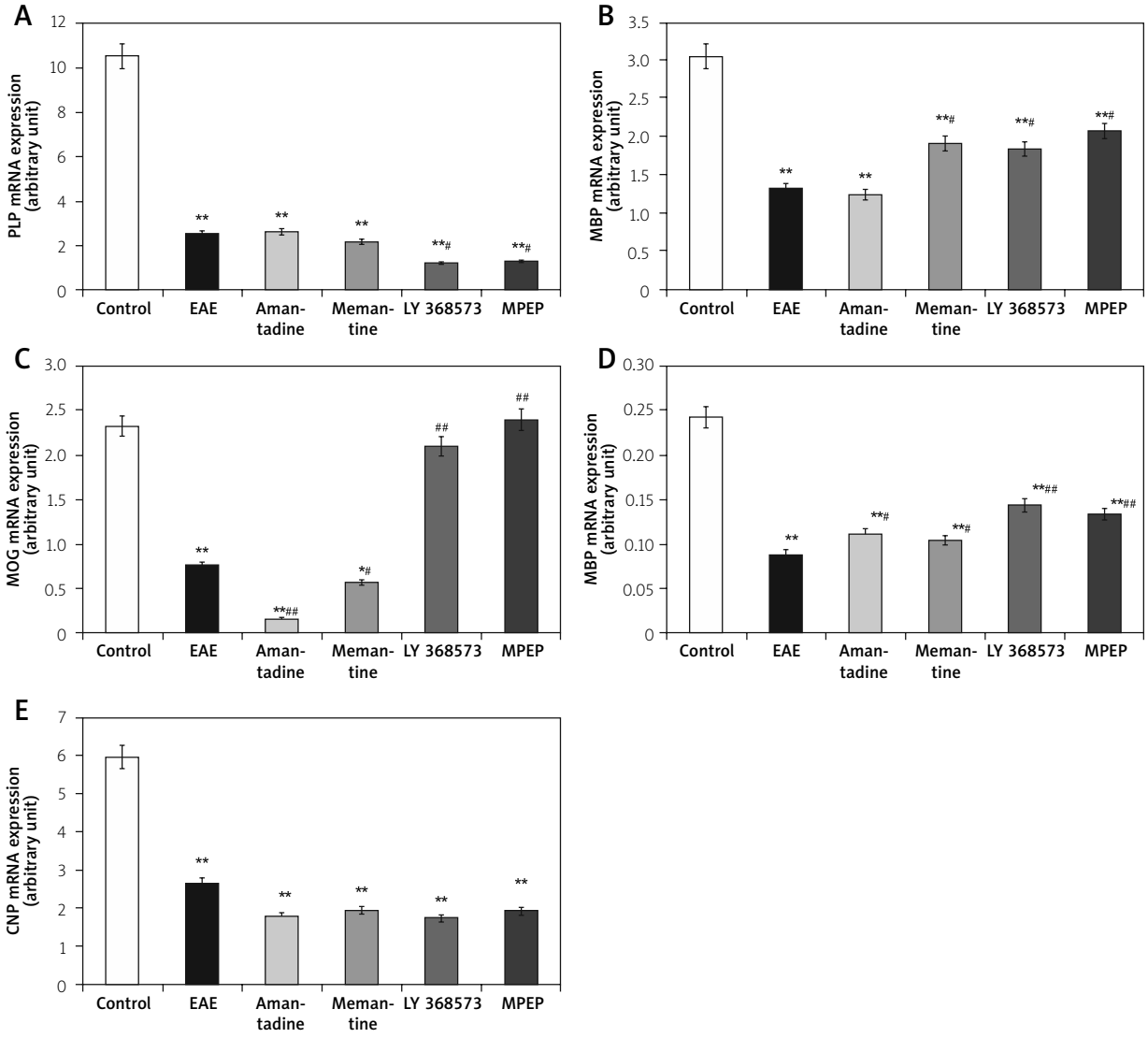

Fig. 2. Expression of mRNA of myelin proteins in the forebrains of control, EAE rats, and EAE rats after treatment with antagonists of glutamatergic receptors: amantadine, memantine, LY 367385, and MPEP) in the acute phase of the disease (at 12 d.p.i.). The mRNA levels of **A)** PLP, **B)** MBP, **C)** MOG, **D)** MAG, and **E)** CNPase were determined by quantitative real time-PCR (see Material and methods) and normalized against actin. Graphs indicate the results expressed as arbitrary units from four independent experiments, each performed using distinct brain samples. The values represent the means ± SD, $^{*}p < 0.05$, $^{**}p < 0.01$, significantly different vs. control rats. $^{\#}p < 0.05$, $^{\#\#}p < 0.01$, significantly different vs. EAE rats not subjected to therapy (one-way ANOVA followed by Dunnett's multiple comparison post-test).

rats may exert an effect on the development of neurological symptoms during EAE or improve the quality of myelin membranes at the biochemical level and the ultrastructural level. We tested two antagonists of NMDA receptors (amantadine and memantine), an antagonist of mGluR1 (LY 367384) and an antagonist of mGluR5 (MPEP) during the acute phase of EAE.

Reduction in the strength of neurological symptoms of EAE was observed only in animals treated with the NMDAR antagonists. Administration of either amantadine or memantine resulted in a reduction of both severity and duration of the neurological deficits. The duration of the inductive phase of the disease and the length of the disease were reduced by 2 and 4 days, respectively, relative

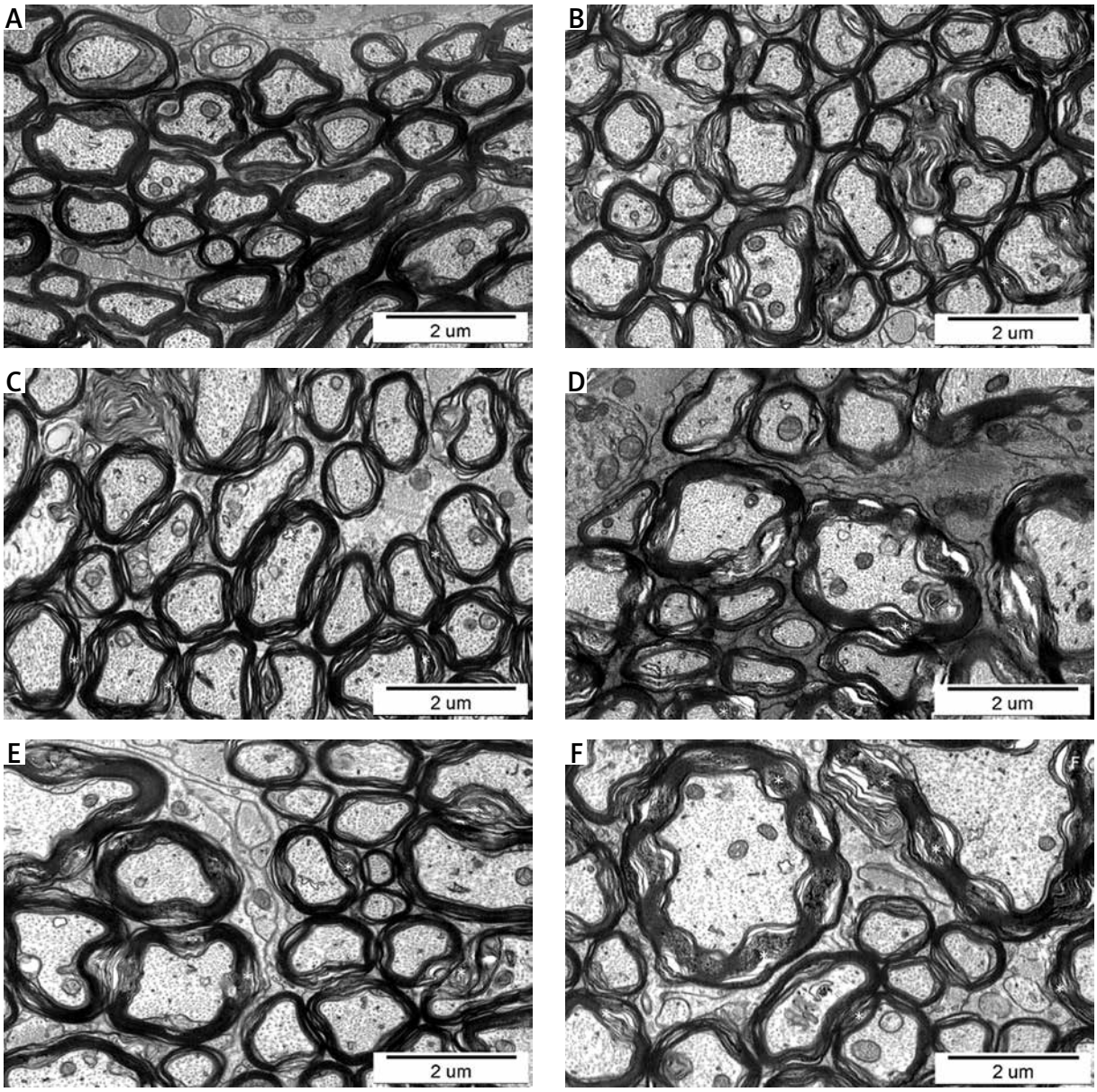

Fig. 3. Representative electron micrographs of myelin in forebrain specimens obtained from control and EAE rats untreated or treated with antagonists of the glutamatergic receptors amantadine, memantine, LY 367385, and MPEP) in the acute phase of EAE (at 12 d.p.i.). **A)** Control rats, **B)** EAE rats, **C)** EAE + amantadine, **D)** EAE + memantine, **E)** EAE + LY 367385 and **F)** EAE + MPEP. Asterisks mark disintegrated lamellar structure of myelin membranes.

to the untreated EAE rats. Rats treated with amantadine and memantine also generally retained better physiological conditions relative to the untreated EAE animals. Administration of LY 367385 or MPEP did not result in any improvement of the neurological parameters of EAE animals.

Glutamatergic NMDA receptors play a vital role in maintaining normal synaptic transmission [6,21]. Specific prevention of the pathological activation of NMDA receptors with drugs such as memantine or amantadine reduces undesirable activity and thereby improves the neurological conditions of EAE rats. Amantadine and memantine have been previously found to be effective in different models of excitotoxic damage in both *in vivo* and *in vitro* experiments [1,28,36,37].

It was also of interest to determine whether administration of GluR antagonists to EAE rats would simultaneously improve animals' condition and have a positive effect on the destroyed brain myelin. Myelin is a multilayered stack of thick membranes with alternating electron-dense and electron-light layers (the major dense line and the intraperiod line, respectively). These layers can be seen by electron microscopy [14]. We observed these layers in electron micrographs of control rat brain tissue (Fig. 3A). This membrane is formed as an extension of the plasma membrane of oligodendrocytes in the CNS and provides the insulation required to facilitate rapid signal transmission between neurons [4]. Numerous electron microscopy studies have demonstrated degeneration of myelin sheaths in MS and EAE models [18,20,22]. Our observations of disturbed myelin ultrastructure are consistent with observations in these previous studies. In contrast to our expectations, none of the applied glutamate receptor antagonists were found to exert a protective effect on the myelin ultrastructure. Characteristics of myelin damage were similar in all of the treatment groups. We also observed focal detachment of the myelin lamellae and increased volumes of cytoplasm in the regions of mature compacted myelin.

Subsequently we investigated whether the antagonists of glutamate receptors (NMDA and mGluRs) may exert an effect on biochemical parameters of myelin during the acute phase of EAE. We analyzed the expression of all primary proteins, which include proteolipid protein, myelin basic protein, 2′,3′-cyclic nucleotide-3′-phosphohydrolase, myelin-associated glycoprotein, and myelin/oligodendrocyte glycoprotein. The results indicate that the expression of myelin proteins in all experimental groups is altered. The level of mRNA of each of the tested proteins was found to be reduced in EAE rats compared to the controls. However, treatment with the glutamate receptor antagonists was found to alter expression levels of the mRNAs. We observed an increase in the level of MBP mRNA in all of the therapeutic groups. These increases were in the range of 30%-50% relative to the untreated EAE rats. MBP is a major protein of CNS myelin, constituting as much as 30% of total protein and playing a pivotal role in myelin compaction. It also stabilizes the major dense line to facilitate the adhesion of the membrane layers [4,31]. Conversely, we did not observe increased levels of PLP mRNA after administration of glutamate receptor antagonists. PLP is another major myelin constituent (about 50% of myelin proteins) whose role is to maintain separation between the layers of myelin membranes. Possibly as a result of its key role in maintaining myelin structure, the improvement was not visible in TEM, although the expression of MBP was found to increase simultaneously. Furthermore, we analyzed expression of 2′,3′-cyclic nucleotide-3′-phosphohydrolase (CNPase), an enzyme specifically expressed in myelin and located in oligodendrocytes, mainly around the nucleus and in the paranodal loops [31]. CNPase may have an additional enzymatic function unrelated to its hydrolase activity, for which no physiological substrate has been found. The protein exists in two splice variants and constitutes 3-4% of total myelin protein. In the case of CNPase mRNA level we did not observe protective efficacy of tested GluR antagonists. Administration of both NMDARs and mGluR antagonists caused a decrease in CNPase mRNA expression by about 30% relative to EAE rats.

Interestingly, mRNA expression levels of the glycoproteins MAG and MOG were found to be altered. MAG is a large (approximately 100 kDa) protein and is quantitatively a minor constituent, representing only 1% of the total myelin protein. This protein is located at the inner surface of the myelin sheath opposing the axon surface [16]. MOG is a transmembrane glycoprotein which constitutes 0.01-0.05% of total myelin proteins [4] and is located on the outer surface of the membrane of oligodendrocytes. This protein is widely used to induce EAE [30]. We observed that glutamate receptor antagonists modify the expression of both of these myelin glycoproteins. After treatment with amantadine or memantine, MOG mRNA levels were found to be similar to the levels expressed in EAE rats, whereas LY 367385 and MPEP resulted in increased expression of MOG mRNA relative to EAE rats. The levels of MAG mRNA were found to increase in all groups of animals treated with GluR antagonists. Although oligodendrocytes possess both NMDAR and mGluR classes of glutamatergic receptors [11,24], exclusively group I (mGluR G I) was shown to play an important role in regulation of MOG mRNA expression.

The results of our experiments confirm the involvement of glutamate in the pathology of EAE. Not all neurological symptoms and biochemical changes in the expression of basic myelin proteins were abolished, but some of the tested parameters

showed statistically significant improvements after administration of glutamate receptor antagonists. Our previous studies demonstrated that glutamate excitotoxicity is one of the pathomechanisms implicated in the acute phase of EAE. Treatment of EAE rats with antagonists of both group I mGluRs (LY 367385 and MPEP) and NMDARs (amantadine and memantine) was found to modulate the expression of mRNA and proteins for both types of glutamate receptors, to decrease the expression of proinflammatory cytokines, to modulate glutamate transport (uptake and release) in nerve endings, and to reduce the levels of mRNA of glutamate transporters (EAATs) [34,35]. The present study indicates that glutamate excitotoxicity is a crucial factor involved in the process of myelin destruction during EAE. This effect is a separate and distinct effect from neuroinflammation.

Conclusions

Antagonists of NMDARs exert a neuroprotective effect and inhibit neurological deficits in EAE rats. Both amantadine and memantine reduce the severity of neurological deficits, maximal score, and duration of disease. A neuroprotective effect was not observed after administration of group I mGluR antagonists (LY 367385 and MPEP). Neither the general condition of EAE rats nor the neurological deficits were improved.

Ultrastructural studies showed that in EAE rats the characteristic multilamellar structure of myelin is destroyed. We did not observe protective effects on the morphology of myelin membranes after administration of GluR antagonists. At the peak of the disease we observed a significant decrease in mRNA levels for each of the investigated myelin proteins (PLP, MBP, MOG, MAG, and CNPase) in EAE rats relative to the controls. The mRNA expression was found to be modified in EAE rats treated with the GluR antagonists. After treatment with each of the GluR antagonists, the expression levels of MBP mRNA and MAG mRNA were found to increase significantly, whereas the expression levels of CNPase mRNA were found to decrease relative to untreated EAE animals. After amantadine or memantine administration PLP mRNA and MAG mRNA expression levels were unchanged compared with untreated EAE rats. Administration of mGluR G I antagonists (LY 367385 and MPEP) was found to increase the mRNA expression levels of MAG glycoprotein, whereas the expression levels of PLP mRNA were found to decrease relative to the untreated EAE rats. Changes in mRNA expression of myelin proteins which are subsequently altered by administration of GluR antagonists may indicate participation of glutamate-mediated excitotoxicity in myelin degradation during the acute phase of EAE.

Acknowledgments

This study was partially supported by grant no. NN401 620038 from the Polish Ministry of Science and Higher Education.

Disclosure

Authors report no conflict of interest.

References

1. Abdurasulova IN, Serdyuk SE, Gmiro VE. Combined blockade of GLUR1 AMPA and NMDA receptors effectively eliminates neurological disorders in rats with experimental allergic encephalomyelitis. Eksperimentalnaya i Klinicheskaya Farmakologiya 2007; 70: 15-19.
2. Anneser JMH, Barasio GD, Berthele A, Zieglgansberger W, Tolle TR. Differential expression of group I metabotropic glutamate receptors in rat spinal cord somatic and autonomic motoneurons: possible implications for the pathogenesis of amyotrophic lateral sclerosis. Neurobiol Dis 1999; 6: 140-147.
3. Basso AS, Frenkel D, Quintana FJ, Costa-Pinto FA, Petrovic-Stojkovic S, Puckett L, Monsonego A, Bar-Shir A, Engel Y, Gozin M, Weiner HL. Reversal of axonal loss and disability in a mouse model of progressive multiple sclerosis. J Clin Invest 2008; 118: 1532-1543.
4. Baumann N, Pham-Dinh D. Biology of oligodendrocyte and myelin in the mammalian central nervous system. Physiol Rev 2001; 81: 871-927.
5. Berger T, Rubner P, Schautzer F, Egg R, Ulmer H, Mayringer I, Dilitz E, Deisenhammer F, Reindl M. Antimyelin antibodies as a predictor of clinically definite multiple sclerosis after a first demyelinating event. N Engl J Med 2003; 349: 139-145.
6. Bolton C, Paul C. Glutamate receptors in neuroinflammatory demyelinating disease. Mediators Inflamm 2006; 2: 93684.
7. Bradley SR, Marino MJ, Wittmann M, Rouse ST, Awad H, Levey AE, Conn PJ. Activation of group II metabotropic glutamate receptors inhibits synaptic excitation of the substantia nigra pars reticulate. J Neurosci 2000; 20: 3085-3094.
8. Choi DW. Calcium and excitotoxic neuronal injury. Ann N Y Acad Sci 1994; 747: 162-171.
9. Chomczyński P, Sacchi N. Single-step method of RNA isolation by acid guanidinium thiocyanate-phenol-chloroform extraction. Anal Biochem 1987; 162: 156-159.
10. Danbolt N. Glutamate uptake. Prog Neurobiol 2001; 65: 1-105.
11. Deng W, Wang H, Rosenberg PA, Volpe JJ, Jensen FE. Role of metabotropic glutamate receptors in oligodendrocyte excito-

toxicity and oxidative stress. Proc Natl Acad Sci U S A 2004; 101: 7751-7756.
12. Geurts JJ, Wolswijk G, Bö L, van der Valk P, Polman CH, Troost D, Aronica E. Altered expression patterns of group I and II metabotropic glutamate receptors in multiple sclerosis. Brain 2003; 126: 1755-1766.
13. Groom AJ, Smith T, Turski L. Multiple sclerosis and glutamate. Ann N Y Acad Sci 2003; 993: 229-275.
14. Hartline DK. What is myelin? Neuron Glia Biol 2008; 4: 153-163.
15. Kerschensteiner M, Stadelmann C, Buddeberg BS, Merkler D, Bareyre FM, Anthony DC, Linington C, Brück W, Schwab ME. Targeting experimental autoimmune encephalomyelitis lesions to a predetermined axonal tract system allows for refined behavioral testing in an animal model of multiple sclerosis. Am J Pathol 2004; 164: 1455-1469.
16. Kursula P. Structural properties of proteins specific to the myelin sheath. Amino Acids 2008; 34: 175-185.
17. Lassmann H. Mechanisms of demyelination and tissue destruction in multiple sclerosis. Clin Neurol Neurosurg 2002; 104: 168-171.
18. Lassmann H. Mechanisms of white matter damage in multiple sclerosis. Glia 2014; 62: 1816-1830.
19. Ljubisavljevic S, Stojanovic I, Pavlovic D, Milojkovic M, Sokolovic D, Stevanovic I, Petrovic A. Suppression of the lipid peroxidation process in the CNS reduces neurological expression of experimentally induced autoimmune encephalomyelitis. Folia Neuropathol 2013; 51: 51-57.
20. Lucchinetti CF, Popescu BF, Bunyan RF, Moll NM, Roemer SF, Lassmann H, Brück W, Parisi JE, Scheithauer BW, Giannini C, Weigand SD, Mandrekar J, Ransohoff RM. Inflammatory cortical demyelination in early multiple sclerosis. N Engl J Med 2011; 365: 2188-2197.
21. Makarewicz D, Sulejczak D, Duszczyk M, Małek M, Słomka M, Lazarewicz JW. Delayed preconditioning with NMDA receptor antagonists in a rat model of perinatal asphyxia. Folia Neuropathol 2014; 52: 270-284.
22. Massella A, D'Intino G, Fernández M, Sivilia S, Lorenzini L, Giatti S, Melcangi RC, Calzà L, Giardino L. Gender effect on neurodegeneration and myelin markers in an animal model for multiple sclerosis. BMC Neurosci 2012; 13: 12.
23. Matute C, Alberdi E, Domercq M, Sánchez-Gómez MV, Pérez-Samartín A, Rodríguez-Antigüedad A, Pérez-Cerdá F. Excitotoxic damage to white matter. J Anat 2007; 210: 693-702.
24. Matute C, Domercq M, Fogarty DJ, Pascual de Zulueta M, Sánchez-Gómez MV. On how altered glutamate homeostasis may contribute to demyelinating diseases of the CNS. Adv Exp Med Biol 1999; 468: 97-107.
25. Morell P, Quarles RH. Myelin Formation, Structure and Biochemistry. In: Basic Neurochemistry: Molecular, Cellular and Medical Aspects. Siegel GJ, Agranoff BW, Albers RW, Fisher SK, Uhler MD (eds.). Lippincott-Raven, Philadelphia 1999; pp. 69-94.
26. Ohgoh M, Hanada T, Smith T, Hashimoto T, Ueno M, Yamanishi Y, Watanabe M., Nishizawa Y. Altered expression of glutamate transporters in experimental autoimmune encephalomyelitis. J Neuroimmunol 2002; 125: 170-178.
27. Otis TS, Brasnjo G, Dzubay JA, Pratap M. Interactions between glutamate transporters and metabotropic glutamate receptors at excitatory synapses in the cerebellar cortex. Neurochem Int 2004; 45: 537-544.
28. Paul C, Bolton C. Modulation of blood-brain-barrier dysfunction and neurological deficits during acute experimental allergic encephalomyelitis by the N-methyl-D-aspartate receptor antagonist memantine. J Pharmacol Exp Ther 2002; 302: 50-57.
29. Pitt D, Werner P, Raine CS. Glutamate excitotoxicity in a model of multiple sclerosis. Nat Med 2000; 6: 67-70.
30. Reindl M, Di Pauli F, Rostásy K, Berger T. The spectrum of MOG autoantibody-associated demyelinating diseases Nat Rev Neurol 2013; 9: 455-461.
31. Sospedra M, Martin R. Immunology of multiple sclerosis Annu Rev Immunol 2005; 23: 683-747.
32. Stys PK, Lipton SA. White matter NMDA receptors: an expected new therapeutic target? Trends Pharmacol Sci 2007; 28: 561-566.
33. Sulkowski G, Dąbrowska-Bouta B, Chalimoniuk M, Strużyńska L. Effects of antagonists of glutamate receptors on pro-inflammatory cytokines in the brain cortex of rats subjected to experimental autoimmune encephalomyelitis. J Neuroimmunol 2013; 261: 67-76.
34. Sulkowski G, Dąbrowska-Bouta B, Strużyńska L. Modulation of neurological deficits and expression of glutamate receptors during experimental autoimmune encephalomyelitis after treatment with selected antagonists of glutamate receptors. Biomed Res Int 2013; article 186068.
35. Sulkowski G, Dąbrowska-Bouta B, Salińska E, Strużyńska L. Modulation of glutamate transport and receptor binding by glutamate receptor antagonists in EAE rat brain. PLoS One 2014; 9: article e113954.
36. Tronci E, Fidalgo C, Zianni E, Collu M, Stancampiano R, Morelli M, Gardoni F, Carta M. Effect of memantine on L-DOPA-induced dyskinesia in the 6-OHDA-lesioned rat model of Parkinson's disease. Neuroscience 2014; 265: 245-252.
37. Volbracht C, van Beek J, Zhu C, Blomgren K, Leist M. Neuroprotective properties of memantine in different in vitro and in vivo models of excitotoxicity. Eur J Neurosci 2006; 23: 2611-2622.
38. Werner P, Pitt D, Raine CS. Multiple sclerosis: altered glutamate homeostasis in lesions correlates with oligodendrocyte and axonal damage. Ann Neurol 2001; 50: 169-180.

Original article

Folia Neuropathologica

Collateral sprouting axons of end-to-side nerve coaptation in the avulsion of ventral branches of the C5-C6 spinal nerves in the brachial plexus

Paweł Reichert[1], Zdzisław Kiełbowicz[2], Piotr Dzięgiel[3], Bartosz Puła[3], Jan Kuryszko[4], Marcin Wrzosek[5], Maciej Kiełbowicz[2], Jerzy Gosk[1]

[1]Department of Traumatology, Clinic of Traumatology and Hand Surgery, Wroclaw Medical University, Wrocław, [2]Department of Surgery, Faculty of Veterinary Medicine, Wroclaw University of Environmental and Life Sciences, Wrocław, [3]Department of Histology and Embryology, Wroclaw Medical University, Wrocław, [4]Department of Animal Physiology and Biostructure, Faculty of Veterinary Medicine, Wroclaw University of Environmental and Life Sciences, Wrocław, [5]Department of Internal Medicine and Clinic of Diseases of Horses, Dogs and Cats, Faculty of Veterinary Medicine, Wroclaw University of Environmental and Life Sciences, Wrocław, Poland

Folia Neuropathol 2015; 53 (4): 327-342 DOI: 10.5114/fn.2015.56547

Abstract

Introduction: *This study assessed the collateral sprouting in avulsion of the ventral branches of the C5 and C6 spinal nerves treated by coaptation of these nerves to the C7 spinal nerve on the brachial plexus of rabbits.*
Material and methods: *Thirty-six New Zealand rabbits were randomly divided into four groups: end-to-side coaptation (ESN) (n = 12), side-to-side coaptation (SSN) (n = 12), direct neurorrhaphy (end-to-end) (EEN) (n = 6) and no coaptation (n = 6). The operations were performed on the left brachial plexus. The contralateral, non-operated right brachial plexi were used as the control group. The groups were compared using morphological, electrophysiological and behavioral methods. The follow-up duration was 20 weeks.*
Results: *Significant differences were observed in all parameters when the experimental groups were compared with the control group and the no coaptation group. The histology of axonal regeneration after ESN, but not after SSN, was comparable to that after EEN. There were no significant differences in the electrophysiological, behavioral assessment or G-ratio parameters between the ESN and EEN groups. There were significant differences in the behavioral assessment, G-ratio and the histomorphometric parameters between the SSN and EEN groups, which disagreed with the electrophysiological results. Sensory axon collateral sprouting was more rapid than motor axon collateral sprouting.*
Conclusions: *The electrophysiological, histomorphometric and behavioral results obtained using end-to-side coaptation of ventral branches of the C5 and C6 spinal nerves to the C7 spinal nerve in the brachial plexi of rabbits confirm the occurrence of collateral sprouting at this level. After further research is performed to confirm the results of this study, end-to-side coaptation might emerge as an alternative method in the treatment of brachial plexus avulsion.*

Key words: *collateral sprouting, spinal nerves, brachial plexus, coaptation.*

Communicating author:
Paweł Reichert, Department of Traumatology, Clinic of Traumatology and Hand Surgery, Wroclaw Medical University, 213 Borowska St., 50-556 Wrocław, Poland, phone: +48 509 570 357, fax: +48 71 734 38 09, e-mail: pawelreichert74@gmail.com

Introduction

The most commonly injured sites in the brachial plexus include the ventral branches of the C5 and C6 spinal nerves and the upper trunk [9,41]. Indeed, most brachial plexus lesions are observed in the supraclavicular area rather than the infraclavicular area. Of these supraclavicular injuries, brachial plexus avulsions are present in 75% of cases [41].

This type of damage cannot be repaired by classical methods, such as "end-to-end" suture with the use of autogenous nerve grafts. Currently, a neurotization procedure is performed [9], in which the intercostal nerve [16], accessory nerve [2], branches of the ipsilateral cervical plexus [11,46], phrenic nerve [26], contralateral C7 [14,26] nerve, selective ulnar nerve to the musculocutaneous nerve [36] and hypoglossal nerve [42] may be used as donor nerves. In such cases, the distal stump of the damaged nerve is sutured to the proximal stump of the donor nerve by direct neurorrhaphy (end-to-end). Unfortunately, donor function is lost when this procedure is performed.

A potential alternative procedure is nerve coaptation, in which the distal stump of the transected nerve is sutured to an undamaged donor nerve via end-to-side coaptation. Efficacy of sensory and motor collateral sprouting after end-to-side coaptation has been confirmed by retrograde double labeling [10,35,37,47,58,59].

Studies have shown that coaptation is more effective when motor axons are coapted to other motor axons [48], when sensory axons are coapted to other sensory axons [33] or when the donor and recipient axons are derived from an identical region of the spinal cord. The results are difficult to predict when mixed nerves are used as donors [29,30,43].

Most previous studies of experimental coaptation have been performed on rats, and these studies have involved the use of long branches of the brachial [47] and lumbar plexus of the peripheral nervous system [34]. The tibial nerve is most often coapted to the peroneal or sural nerve [18], and the ulnar nerve is most frequently coapted to the musculocutaneous nerve [47].

In the rabbit brachial plexus, the ventral branches of the C5 and C6 spinal nerves form the caudal trunk, which creates the suprascapular nerve. The exclusive innervation of the supraspinatus and infraspinatus muscles by the suprascapular nerve and the easy access to these muscles and dermatomes in rabbits might indicate that these animals are a reliable model to use for studying the functions of the C5-C6 spinal nerves. Such innervations provide us with an opportunity to evaluate the recovery of nerve function after coaptation in high brachial plexus injuries.

Due to recent encouraging results coupled with the overall lack of experimental studies examining injuries to the ventral branches of the spinal nerves and brachial plexus trunks, we aimed to evaluate and confirm the treatment efficacies of end-to-side and side-to-side coaptation of the ventral branches of the C5 and C6 spinal nerves to the C7 spinal nerve in brachial plexus avulsion using an experimental rabbit model.

Material and methods

Experimental model

The experiments were approved by the Second Local Ethics Committee for Animals of the University of Life Sciences in Wroclaw. All rabbits (22 weeks old with an average weight of 3.6 kg) were treated using the same anesthesia protocol. Premedication was performed using medetomidine (Cepetor) at a dose of 150 µg/kg body weight, butorphanol (Torbugesic) at a dose of 0.2 mg/kg body weight and ketamine (Bioketan) at a dose of 35 mg/kg body weight. General anesthesia was performed with propofol, which was administered continuously at a dose of 0.1 mg/kg/min. The analgesic effect was supported by fentanyl at a dose of 2-3 µg/kg. After the procedure, buprenorphine (Vetergesic) was used at a dose of 20 µg/kg *i.m.* every 8 h. The animals were administered meloxicam (Metacam) at 0.2 mg/kg body weight for two days after surgery. They were operated on in the lateral position, and the mean duration of surgery was approximately 26 min.

Adequate care was taken to minimize pain and discomfort during and after the operations. The follow-up duration was 20 weeks.

Experimental design

A total of 36 New Zealand rabbits were randomly divided into the following four groups: end-to-side coaptation (ESN) (n = 12), side-to-side coaptation (SSN) (n = 12), direct neurorrhaphy (end-to-end) (EEN) (n = 6) and no coaptation (n = 6). The operations were performed on the left brachial plexus. The contralateral, non-operated right brachial plexi of the rabbits were used as the control group. The groups

were compared using morphological, electrophysiological and behavioral methods. The follow-up duration was 20 weeks.

Surgical procedure

The experimental procedures were performed on the left brachial plexus using a lateral approach (Fig. 1). All of the collateral branches of the C5, C6/caudal truncus and C7 spinal nerves were transected.

The ventral branches of the C5 and C6 nerves were avulsed, and then the distal stumps were incised. An epineural window was created on the cranial side of the C7 spinal nerve for coaptation. For side-to-side coaptation, supplemental epineural windows were created on the caudal sides of the C5 and C6 spinal nerves. End-to-side or side-to-side neurorrhaphy was then performed between the distal stumps of these nerves and the windows by placing two stitches (Ethilon 10-0) in the C7 spinal nerve. To perform direct neurorrhaphy (end-to-end), we sutured two stitches (Ethilon 10-0). In the group without coaptation, we resected 2 cm of the C5 and C6 spinal nerves, and the distal stump was inserted into soft tissue. Then, the skin was sutured with 4-0 sutures. After 20 weeks, the left and right brachial plexi were exposed to obtain sample nerves. The animals were euthanized by pentobarbital intravenous injection (Morbital).

Electrophysiological analysis

The animals were anesthetized by intramuscular injections of medetomidine (dose: 0.5 mg/kg), butorphanol (0.1 mg/kg) and ketamine (25 mg/kg) for electromyographic examination.

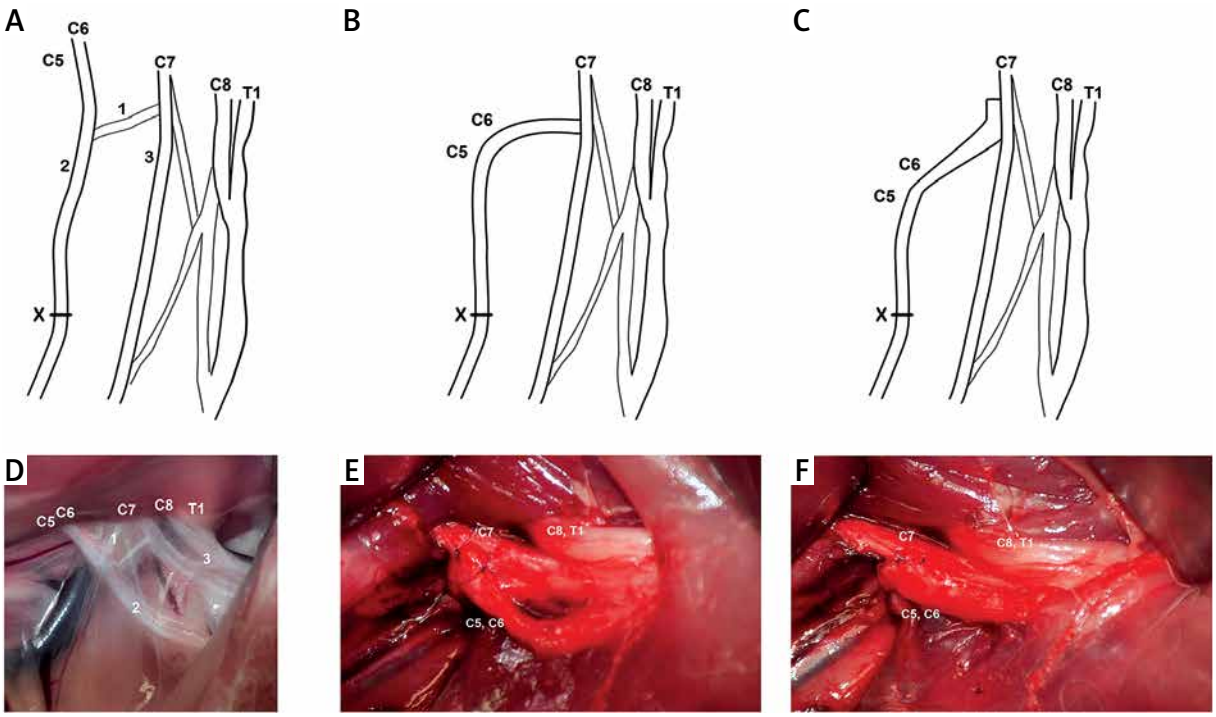

Fig. 1. Intraoperative image and schematic illustration of the surgical picture in each group. **A)** Schematic illustration showing the macroscopic structure of the rabbit's right brachial plexus. C5 – ventral branch of the C5 spinal nerve, C6 – ventral branch of the C6 spinal nerve, C7 – ventral branch of the C7 spinal nerve, C8 – ventral branch of the C8 spinal nerve, Th1 – ventral branch of the Th1 spinal nerve. **B)** Schematic illustration of end-to-side coaptation of C5 and C6 to C7. **C)** Schematic illustration of side-to-side coaptation of C5 and C6 to C7. **D)** Surgical photograph. Macroscopic structure of the rabbit's right brachial plexus. C5, C6, C7, C8, Th1 – ventral branches of the spinal nerves: C5-Th1, 1 – connection branches, 2 – cranial trunk, 3 – caudal trunk. **E)** Surgical photograph. End-to-side coaptation of C5 and C6 to C7. Neurorrhaphy by the epineural window. **F)** Surgical photograph. Side-to-side coaptation of C5 and C6 to C7. Neurorrhaphy by the epineural window joining the lateral part of C5 and C6 with the medial part of C7. X – position of nerve sample.

This examination was performed after 20 weeks at an ambient temperature of 22°C using Nicolet Viking Quest portable electrodiagnostic equipment, version 11.0 (Nicolet Biomedical, Madison, WI, USA). A standard electromyographic concentric needle electrode (used as an active and recording electrode) and a subdermal monopolar ground electrode were used in this study. Electromyography (EMG) was performed by intramuscular insertions of the electrodes into the following muscles: the supraspinatus (innervated by the suprascapular nerve, C5-C6), the infraspinatus (innervated by the suprascapular nerve, C5-C6), the subscapularis (innervated by the subscapular nerve, C6-C8), and the biceps brachii (innervated by the musculocutaneous nerve, C5-C7). During EMG, insertional activity was assessed. Pathological discharge, if present, was recorded and evaluated to determine the type, frequency, duration and amplitude according to a semi-quantitative numerical scale modified by Kimura [31] (Table I). Higher values indicated a lower degree of muscle innervation.

Histomorphometric analysis of sampled nerves

The nerve specimens were immersion-fixed in 2.5% glutaraldehyde for 12 h at 4°C and were then washed with cacodylate buffer (Serva, Heidelberg, Germany). Next, the specimens were post-fixed for 1 h in 1% osmium tetroxide (dissolved in cacodylate buffer), washed with cacodylate buffer, dehydrated in alcohol and embedded in Epon (Chempur, Piekary Slaskie, Poland). A Power Tome XL (RMC Products, Tucson, AZ, USA) was used to cut the fixed nerve specimens into 0.6-µm-thick sections, which were stained with toluidine blue (Serva) and mounted using Euparal (Roth, Mannheim, Germany).

Table I. A modified semi-quantitative numerical scale for the electromyographic evaluation of the degree of muscle denervation

0	No pathological potentials
1	Very rare denervation potentials
2	Sporadic pathological activity, recorded in two or more places
3	Frequent pathological activity, recorded regardless of the position of the needle electrode
4	Abundant pathological activity, recorded regardless of the position of the needle electrode

The stained nerve cross sections were analyzed under a BX41 light microscope equipped with the CellD computer-assisted image analysis program (Olympus, Tokyo, Japan). For analysis, photomicrographs at ×630 magnification were obtained manually without overlap of the microscopic fields. In each nerve cross section, the minimal diameters of the axons and nerve fibers (axon and adjacent myelin) were measured. Only circular-shaped fibers were measured, which allowed for calculation of the myelin sheath thicknesses of the nerve fibers using the following formula: myelin sheath thickness = nerve fiber diameter – axon diameter. The degree of myelination was evaluated using the G-ratio (the ratio of the minimal diameters of the axon and fiber) [45]. Additionally, the myelin sheath and myelinated fiber densities were determined. At least 200 nerve fibers were analyzed per animal. The materials used for histological examination were collected at identical heights of 2 cm per anastomosis in the experimental groups and 4 cm from the spinal canal in the control group.

Skin pinch test

The skin pinch test was performed to determine the return of sensory capacity by examining nociception [33]. The skin of the animals was gently pinched with forceps (in 3-mm intervals) until the first signs of discomfort were noticed, including lifting of the limbs, turning of the head or trembling of the skin. The healthy limb and the limb with nerve coaptation were examined to record a normal reaction to stimulation. We focused on the dermatomes innervated by nerves derived from C5, C6, and C7. This test was performed at 1 day after surgery and at 4, 8, 12, 16, and 20 weeks after surgery. For this study, we used the following 4-point grading scale: 0 – no response; 1 – mild response, the animal presents a very weak reaction; 2 – moderate response, the animal shows a reaction in response to stimuli; and 3 – the animal exhibits a significant response to stimuli.

Nerve pinch test

To assess the statuses of nociceptive axons, the nerve pinch test was performed [33,37]. This test was conducted before euthanasia, when the animals were lightly anesthetized. The EEN, ESN, and SSN sites were carefully dissected from nearby tissue. A series of pinches were then delivered to the recipient caudal trunk/suprascapular nerve with fine-

tipped forceps, proceeding in millimeter increments in the distal-to-proximal direction. The area of the suprascapular nerve stump at which a pinch first elicited the animal's reflexive withdrawal response (a positive pinch test) was recorded, and its distance from the site of the end-to-side or side-to-side coaptation was measured. The pinching of the recipient caudal trunk/suprascapular nerve stump was always stopped at least 15 mm distal from the site of coaptation, thus preserving the remainder of the caudal trunk/suprascapular nerve for use as a histopathological sample.

Modified grooming test

A test for assessing the muscle power of rat forelimbs [34], conducted to ascertain whether and when a reconnected nerve became functional, was adopted for use in rabbits. The test consisted of spraying water over the animal's face to provoke grooming movements of the forepaws toward the head. During normal grooming, the animals raise both forelimbs, lick them and reach behind the ears. The grooming response was graded from 0 to 5 as follows: 0 – no response; 1 – flexion at the elbow, not reaching the snout; 2 – flexion reaching the snout; 3 – flexion reaching below the eyes; 4 – flexion reaching the eyes; and 5 – flexion reaching the ears and beyond. The animals were tested at 4, 8, 12, 16, and 20 weeks following surgery.

Statistical analysis

The data were analyzed using Prism statistical software, version 5.0 (GraphPad, La Jolla, CA, USA). Student's *t*-test for independent samples was performed to compare the significance of the changes between the groups. The Mann-Whitney *U* test was used for non-parametric values. The distribution of the data was tested by the Shapiro-Wilk test. Dissimilarities between the groups were examined using the non-parametric Kruskal-Wallis test with Dunn's post hoc analysis. Differences were considered significant at a $p < 0.05$ for Student's *t*-test and at $p < 0.01$ for the Mann-Whitney *U* test.

Results

Electromyographic analysis

Electromyographic examination revealed the presence of denervation potentials in the ESN, SSN, and EEN groups (A – experimental groups) and in the no coaptation group (B) and did not reveal any pathological myoelectric activity in the control group (C).

Most of the changes in the ESN group were found in the infraspinatus muscle, with a mean value of 2.08 ± 0.64, followed by the supraspinatus (1.54 ± 0.78), biceps (1.54 ± 0.78) and subscapularis muscles (1.38 ± 0.77). The results were dominated by changes in grades 1 and 2 denervation, as graded using the Kimura scale.

The predominantly affected muscles in SSN neurorrhaphy were the biceps brachii (1.86 ± 0.77) and infraspinatus (1.86 ± 0.66) muscles, followed by the subscapularis (1.71 ± 0.83) and supraspinatus (1.57 ± 0.65) muscles. In most cases, the predominant changes were grades 1 and 2.

In the EEN group, pathological changes were discovered in the supraspinatus (1.67 ± 1.53), biceps brachii (1.0 ± 1.0), infraspinatus (1.67 ± 1.53) and subscapularis muscles (1.67 ± 0.58).

In the B group (no coaptation), the supraspinatus (3.33 ± 0.58), biceps brachii (3.33 ± 0.58), and infraspinatus (3.33 ± 0.58) muscles demonstrated the highest degrees of denervation. Minor changes were also found in the subscapularis muscles (median value of 1.33 ± 1.15).

The statistical analysis results for each group are presented in Table II.

Histomorphometric analysis

The numbers of myelinated axons were markedly reduced in the EEN, ESN and SSN groups compared with that in the C group; however, the numbers of myelinated axons were increased in the EEN, ESN and SSN groups compared with that in the B group. The largest axon diameters and myelin sheaths were observed in group C, followed by the EEN, SSN, and ESN groups. The ESN group had a higher G-ratio compared with the SSN group (Table III). The study groups showed statistically significant differences (MW < 0.001, $p < 0.01$) in the following additional parameters: axon diameter, fiber diameter, myelin sheath thickness and the G-ratio, with the exception of the G-ratio in the EEN group compared with that in the ESN group (MW = 0.014, $p < 0.01$), the G-ratio in the ESN group compared with that in the C group (MW = 0.2368, $p < 0.01$), and the G-ratio in the EEN group compared with that in the C group (MW = 0.016, $p < 0.01$).

Table II. Electromyographic comparison among all the groups and the results of the reinnervation of the muscles. C group – control group, EEN – direct neurorrhaphy (end-to-end) group, ESN – end-to-side coaptation group, SSN – side-to-side coaptation group, B group – no coaptation

	Supraspinatus muscle (C5-C6)	Infraspinatus muscle (C5-C6)	Subscapularis muscle (C6-C8)	Biceps brachii muscle (C5-C7)
ESN vs. EEN*	0.831241	0.451858	0.563226	0.318075
ESN vs. B*	0.002236	0.167138	0.924903	0.002236
ESN vs. C**	$p < 0.001$	$p < 0.001$	$p < 0.001$	$p < 0.001$
ESN vs. SSN*	0.905222	0.390024	0.29391	0.29479
SSN vs. EEN*	0.857655	0.723947	0.926405	0.11482
SSN vs. B*	0.000578	0.070006	0.504925	0.007256
SSN vs. C**	$p < 0.001$	$p < 0.001$	$p < 0.001$	$p < 0.001$
EEN vs. B*	0.151835	0.348641	0.677869	0.024896
EEN vs. C**	0.085	0.085	0.009	0.085
B vs. C**	$p < 0.001$	$p < 0.001$	$p < 0.085$	$p < 0.001$

*Student's t-test
**Mann-Whitney U test

Table III. Values of the following parameters in the experimental groups: nerve area (mm^2), nerve diameter (mm), number of axons, myelin fiber density (fiber/mm^2), minimal diameter of myelin fibers (µm), minimal axon diameter (µm), myelin area (µm^2), G-ratio axon/fiber diameter – axon diameter fiber. C group – control group, EEN – direct neurorrhaphy (end-to-end) group, ESN – end-to-side coaptation group, SSN – side-to-side coaptation group, B group – no coaptation

	ESN	SSN	EEN	B	C
Number of axons/myelin fiber density (fiber/mm^2)	170.14 ± 3.71	130.32 ± 4.6	209.96 ± 3.6	23.85 ± 1.6	362.14 ± 2.83
Myelin sheath (µm)	1.325 ± 0.58	1.552 ± 0.72	1.993 ± 0.50	1.390 ± 0.49	2.267 ± 0.53
G-ratio axon/fiber diameter	0.6589 ± 0.08	0.6318 ± 0.09	0.6399 ± 0.008	0.552 ± 0.10	0.6559 ± 0.08
Axon diameter (µm)	5.531 ± 3.10	5.761 ± 3.501	7.630 ± 3.173	3.591 ± 1.56	9.049 ± 2.86
Fiber diameter (µm)	8.180 ± 4.033	8.864 ± 4.613	11.62 ± 3.65	6.371 ± 2.12	13.58 ± 3.19

In all of the groups, the axons within the nerves were grouped into fascicles surrounded by perineural connective tissue (Fig. 2). The small- and large-diameter myelinated axons were evenly distributed in the nerves in the EEN and C groups. Smaller and closely packed myelinated axons were found in both the ESN and SSN groups. The distribution of myelinated axons in the ESN group was more similar to that in the EEN group than to that in the SSN group (Fig. 3). The differences in myelin sheath thickness were greater between the SSN and EEN groups than between the ESN and EEN groups. The frequency distribution of myelin sheath diameter revealed the presence of larger numbers of very small axons in both the EEN and ESN groups compared with the C group (Fig. 4).

Regression analysis revealed that the extent of axon remyelination was more advanced after EEN than after ESN or SSN. The myelin was thicker, and there was less individual scatter around the regression line, resulting in a decreased correlation coefficient and a decreased slope of the regression line of best fit (Fig. 5). Regression analysis showed a decrease in the myelin thickness of large-diameter fiber axons. This decrease was reflected by a slight decrease in the slope of the regression line of best fit (Fig. 6).

Skin pinch test

The spatial pattern of sensitivity recovery was identical in all of the groups; however, the recovery

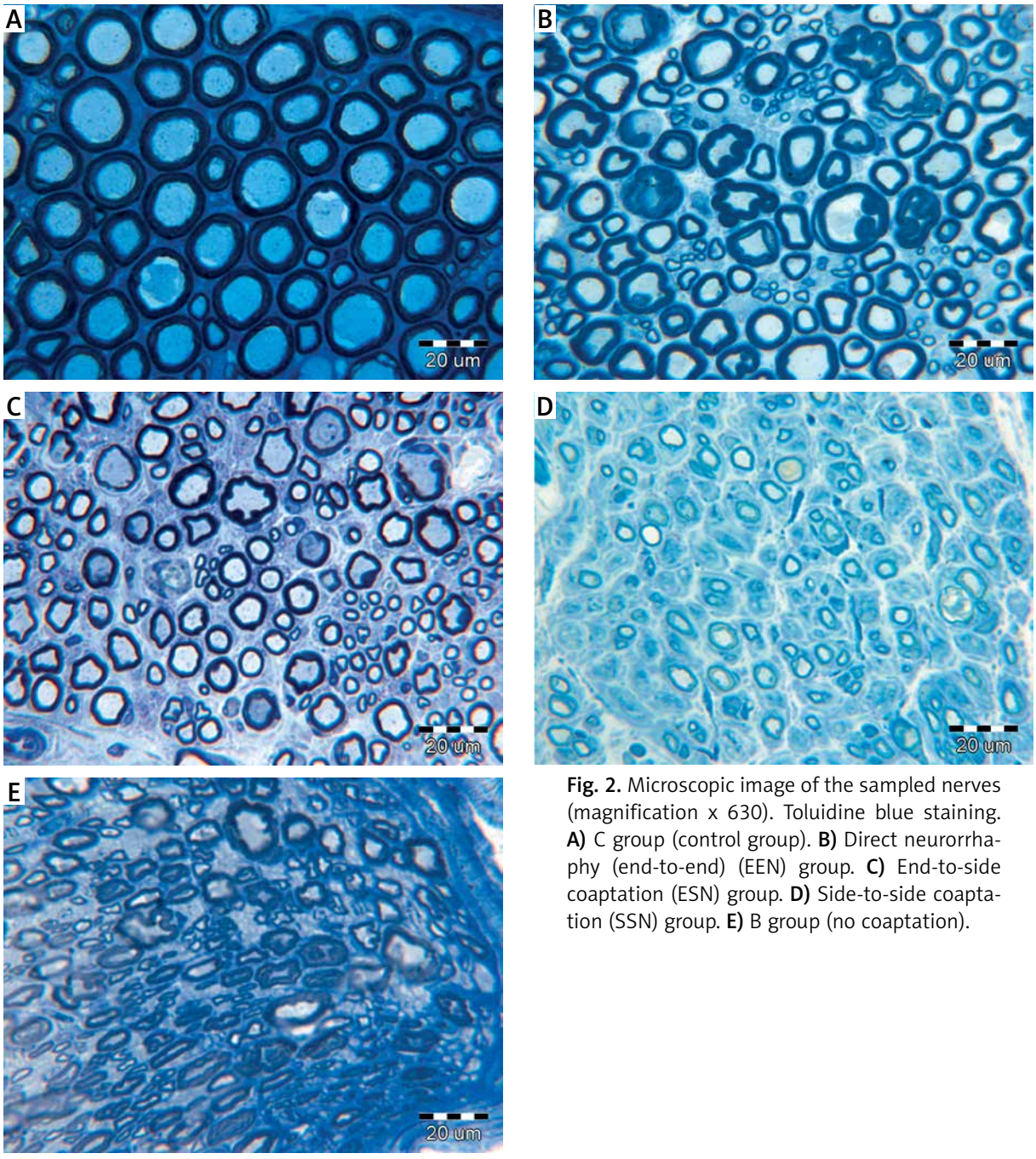

Fig. 2. Microscopic image of the sampled nerves (magnification x 630). Toluidine blue staining. **A)** C group (control group). **B)** Direct neurorrhaphy (end-to-end) (EEN) group. **C)** End-to-side coaptation (ESN) group. **D)** Side-to-side coaptation (SSN) group. **E)** B group (no coaptation).

time and end results were different. Significant differences in these parameters were found between the ESN and control groups ($t < 0.01$, $p < 0.05$), whereas no significant difference was observed between the ESN and EEN groups ($t = 0.20$, $p > 0.05$). In addition, significant differences in these parameters were observed between the SSN group and both the EEN ($t = 0.01$, $p < 0.05$) and C groups ($t < 0.01$, $p < 0.05$) (Table IV). Sensation returned much faster in the group in which innervation of C6-C7, rather than of C5-C6, was performed. The greatest changes occurred at 12 weeks.

Nerve pinch test

The nerve pinch test of the caudal trunk/suprascapular muscle showed positive results in all of the

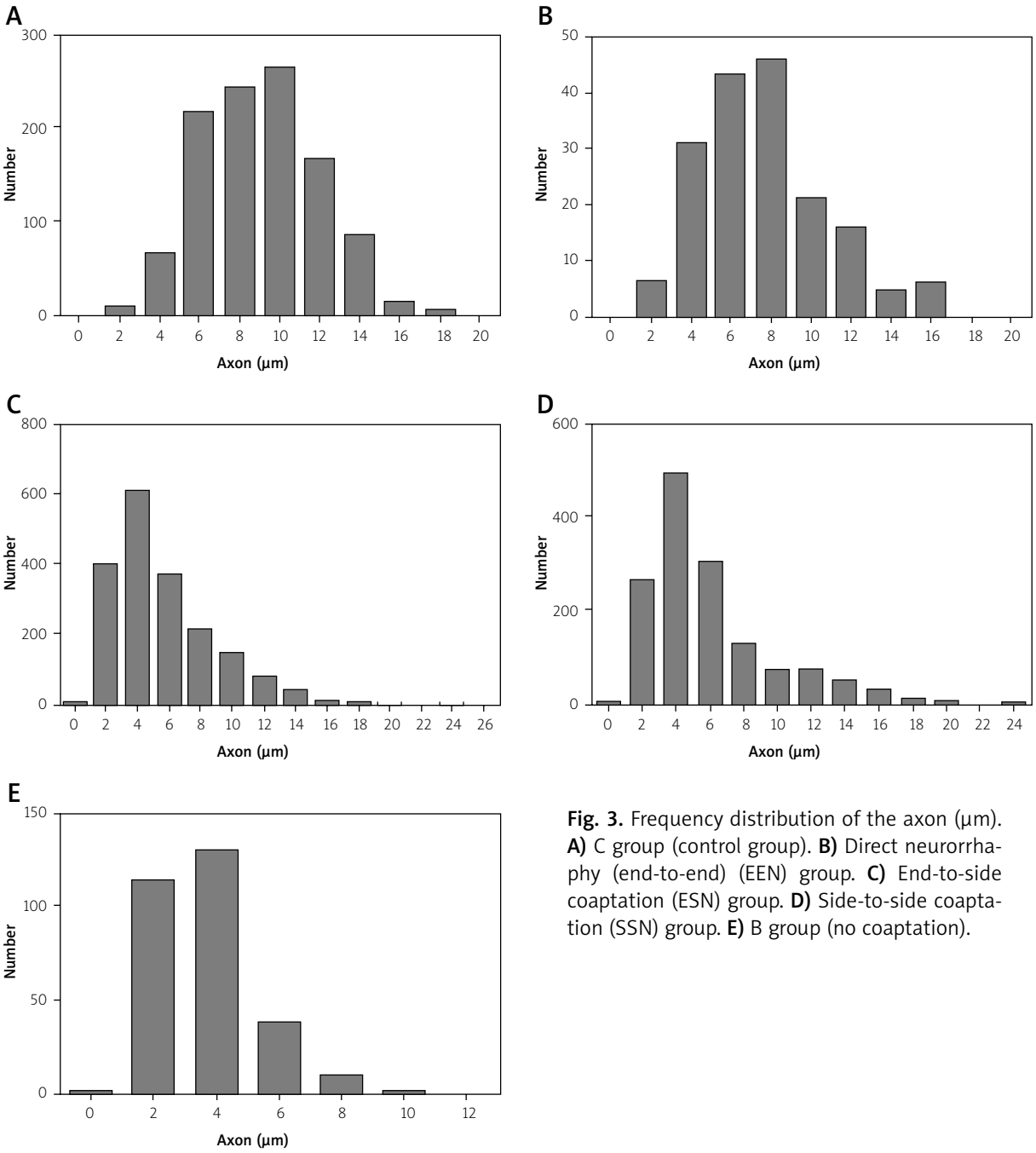

Fig. 3. Frequency distribution of the axon (µm). **A)** C group (control group). **B)** Direct neurorrhaphy (end-to-end) (EEN) group. **C)** End-to-side coaptation (ESN) group. **D)** Side-to-side coaptation (SSN) group. **E)** B group (no coaptation).

rabbits in group C, in all except for 1 rabbit in the EEN group, in all except for 1 rabbit in the ESN group, and in 4 rabbits in the SSN group, and negative results were obtained in all of the animals in the B group. There were no significant differences between the ESN and C groups (t = 0.08, p < 0.05) or between the ESN and EEN groups (t = 0.62, p < 0.05); however, the results after ESN were more similar to those after EEN.

Grooming test

The movement of the forepaw toward the head after water spraying was analyzed, and the results indicated that there were no significant differences between the ESN and EEN groups (t = 0.12, p < 0.05) in contrast with the significant differences observed between the ESN and C groups (t < 0.01, p < 0.05). Statistical analysis also revealed significant differences between the SSN and

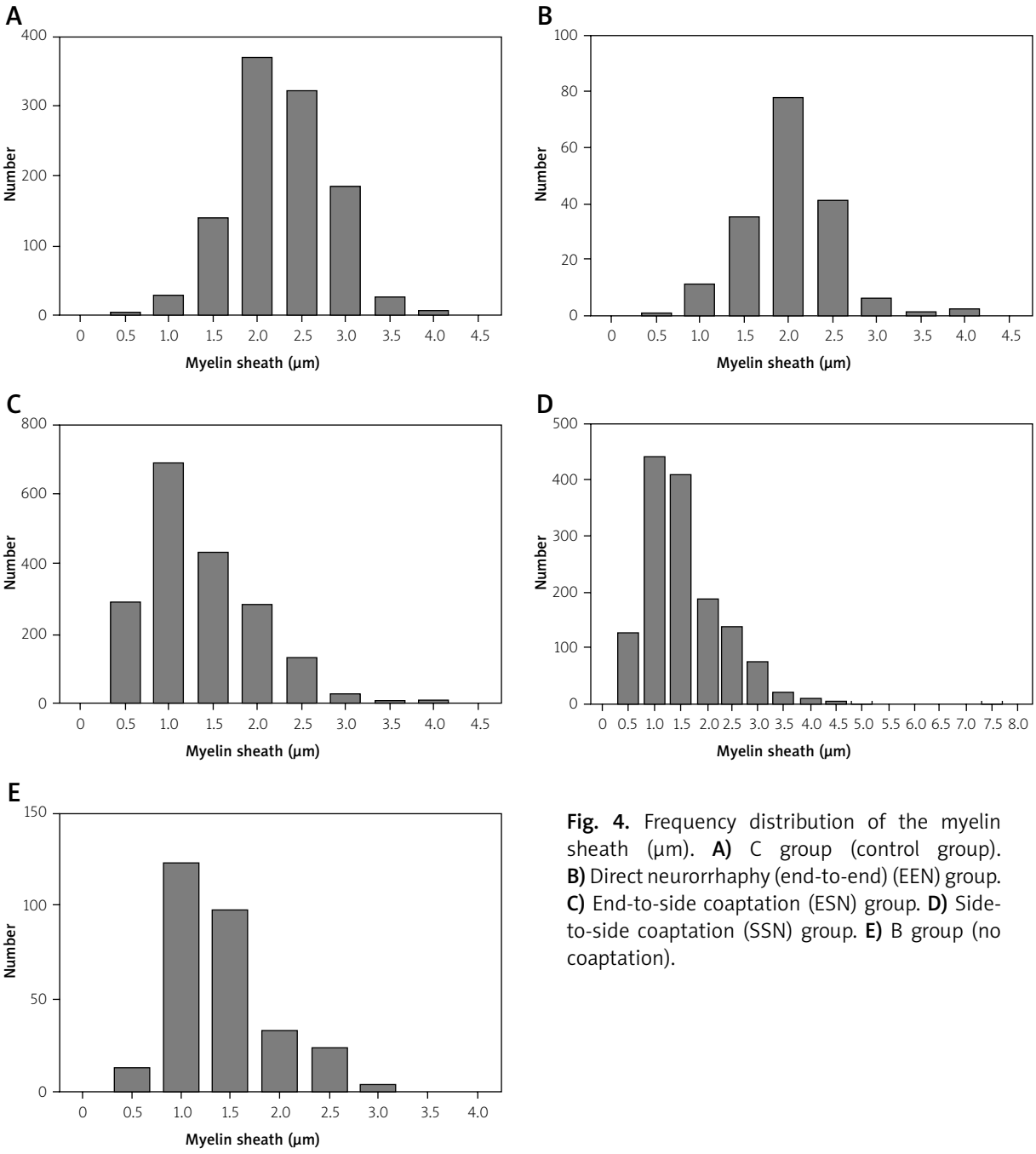

Fig. 4. Frequency distribution of the myelin sheath (µm). **A)** C group (control group). **B)** Direct neurorrhaphy (end-to-end) (EEN) group. **C)** End-to-side coaptation (ESN) group. **D)** Side-to-side coaptation (SSN) group. **E)** B group (no coaptation).

C groups ($t < 0.01$, $p < 0.05$) and between the SSN and EEN groups ($t = 0.04$, $p < 0.05$). The EEN group showed more rapid and better functional recovery compared with the ESN and SSN groups (Table IV).

Discussion

Recent studies of coaptation have shown very interesting results regarding synergistic motor nerve fiber transfer between different nerves [48], end-to-side neurorrhaphy by autonomic nerves and somatic nerves [19], and reverse end-to-side nerve transfer [28]. Additionally, a new type of cortical neuroplasticity after nerve repair of brachial plexus lesions has been described [6].

Although many coaptation studies have been performed, none have examined coaptation of the

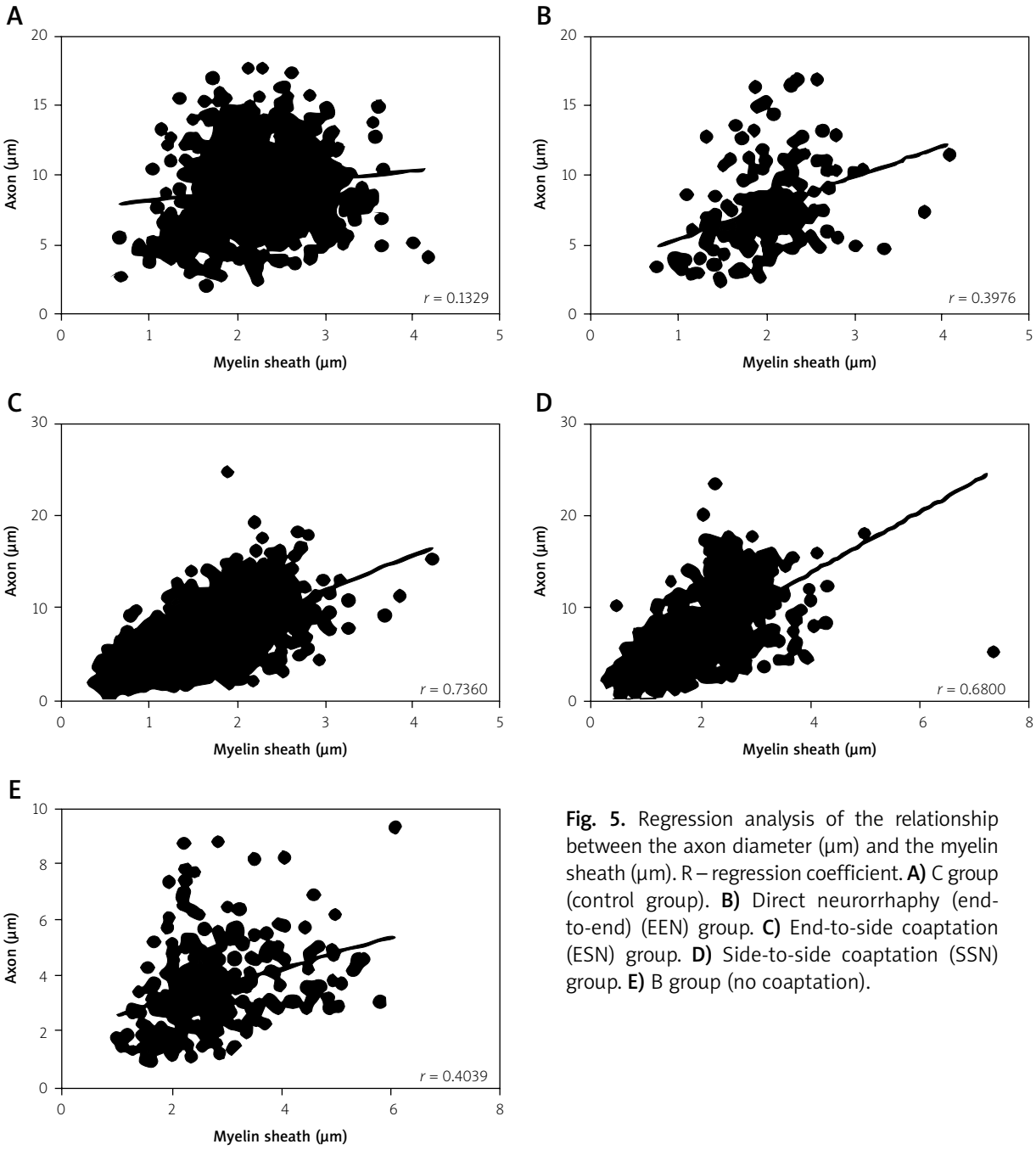

Fig. 5. Regression analysis of the relationship between the axon diameter (µm) and the myelin sheath (µm). R – regression coefficient. **A)** C group (control group). **B)** Direct neurorrhaphy (end-to-end) (EEN) group. **C)** End-to-side coaptation (ESN) group. **D)** Side-to-side coaptation (SSN) group. **E)** B group (no coaptation).

ventral branches of the spinal nerves or the trunks at the brachial plexus level. This lack of research might have resulted from differing views regarding the proximal or distal coaptation procedure or exploitation of the intraplexus or extraplexus nerves. This topic is controversial, and it has been difficult to find a research model that enables reliable nerve assessment after a coaptation procedure. Additionally, the examination results have not been encouraging in cases in which the peripheral nerves correspond to different segments of the spinal cord or in which mixed nerves are used as donors.

We selected a central coaptation model for use in our study, similar to Bentolia [7]. Our results indicated that a better outcome could be attained by

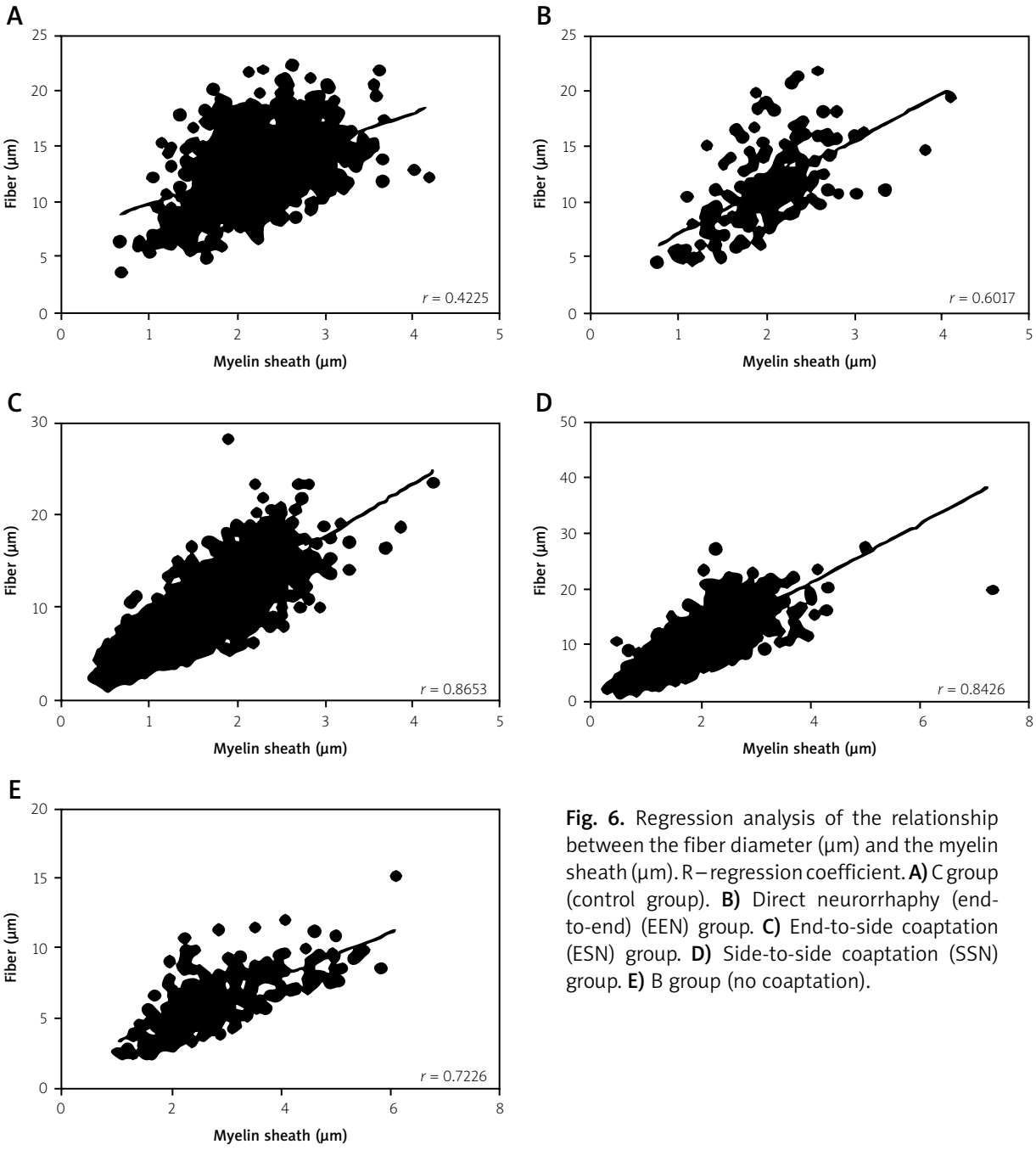

Fig. 6. Regression analysis of the relationship between the fiber diameter (µm) and the myelin sheath (µm). R – regression coefficient. **A)** C group (control group). **B)** Direct neurorrhaphy (end-to-end) (EEN) group. **C)** End-to-side coaptation (ESN) group. **D)** Side-to-side coaptation (SSN) group. **E)** B group (no coaptation).

coapting grafts distal to the lateral or posterior cord to achieve more distal coaptation near the distal objective (i.e., the musculocutaneous nerve). On the other hand, Alnot [3] and Terzis [55] have reported that the use of nerve grafts is more successful when coapting nerve grafts distal to the peripheral nerve rather than distal to the proximal plexus elements (i.e., the cords). At this point most of the nerve fibers would not be lost in fortuitous reinnervation, which would result in achievement of the desired goal.

When a donor is used, many authors [2,42] have preferred to apply intraplexus motor donors for neurotization when they are available because doing so yields better results. In our study, we applied intraplexus motor donors because we agree that intraplexus donors have a greater number of axons than

Table IV. Assessment of the return of sensation (skin pinch test) to the dermatomes and results of the grooming test. EEN – direct neurorrhaphy (end-to-end) group, ESN – end-to-side coaptation group, SSN – side-to-side coaptation group. C5, C6, C7 – ventral branches of spinal nerves C5, C6, C7

		4 weeks	8 weeks	12 weeks	16 weeks	20 weeks	24 weeks
Dermatomes C5-C6	EEN	0.5 ± 0.5	0.8 ± 0.4	2.1 ± 0.4	2.5 ± 0.5	2.5 ± 0.5	2.7 ± 0.5
	ESN	0.2 ± 0.4	0.2 ± 0.4	0.8 ± 0.4	1.4 ± 0.5	2.1 ± 0.4	2.3 ± 0.5
	SSN	0.1 ± 0.2	0.1 ± 0.2	0.6 ± 0.5	1.3 ± 0.5	1.7 ± 0.4	1.9 ± 0.5
Dermatomes C6-C7	EEN	1.7 ± 0.5	2.5 ± 0.5	2.8 ± 0.4	3	3	3
	ESN	1.5 ± 0.5	1.9 ± 0.3	2.1 ± 0.4	2.5 ± 0.5	2.8 ± 0.4	3
	SSN	1.4 ± 0.5	1.6 ± 0.5	1.9 ± 0.3	2.1 ± 0.4	2.2 ± 0.4	2.2 ± 0.4
Dermatomes C7-C8-Th1	EEN	2.3 ± 0.5	2.7 ± 0.5	3	3	3	3
	ESN	1.4 ± 0.5	1.9 ± 0.3	3	3	3	3
	SSN	0.7 ± 0.4	1.1 ± 0.3	3	3	3	3
Grooming test	EEN	2.3 ± 0.5	3.3 ± 0.5	3.7 ± 0.5	3.9 ± 0.4	4.1 ± 0.4	4.3 ± 0.5
	ESN	1.4 ± 0.5	1.9 ± 0.3	2.6 ± 0.5	3.2 ± 0.4	3.6 ± 0.5	3.9 ± 0.5
	SSN	0.7 ± 0.4	1.1 ± 0.3	1.8 ± 0.4	2.4 ± 0.4	3.0 ± 0.3	3.7 ± 0.4

extraplexus donors; thus, the likelihood of successful neurotization is greater. The use of extraplexus nerves was reserved for specific uses for particular targets (e.g., the shoulder and elbow).

The indications for the C7 spinal nerve, which is characterized as a mixed nerve, are controversial, and the surgical results might be difficult to predict [29,30,43]. However, new coaptation strategies have been developed [6,19,28,48].

Interestingly, coaptation involving extension of the probable epineurium or perineurial opening has been performed by many authors. Regarding the surgical technique, we elected to open the epineurium of the donor to expose it to the coapted recipient nerve, as previously described by Viterbo [58] and Lundborg [37]. Although terminolateral nerve regeneration could occur without any surface lesions on the donor nerve [27], experimental research has shown that regeneration is superior when a window is opened in the donor nerve [23,37]. It is widely accepted that resection of a small part of the epineurium improves the efficacy of end-to-side coaptation. Other research has demonstrated that resection of the deeper connective layers of the nerve (the perineurium) further increases the efficacy of terminolateral reconstruction [25,35,61].

We found statistically significant differences in all parameters except for the G-ratio in a comparison of the ESN group with the control group. These similar G-ratios might indicate the possibility of regeneration of myelinated fibers; however, the much smaller amount of these fibers did not allow for conduction to occur, as observed in the control group. This failure might have been the result of scar tissue compression, leading to smaller axons. On the other hand, nerve regeneration was observed in the ESN group, confirming the significant differences compared with the no coaptation group. The ESN and EEN groups did not significantly differ in the EMG examination results ($t = 0.39$, $p < 0.05$), with respect to the G-ratio (MW = 0.014, $p < 0.01$), the grooming test results ($t = 0.12$, $p < 0.05$), the nerve pinch test results ($t = 0.62$, $p < 0.05$) or the skin pinch test results ($t = 0.20$, $p < 0.05$). These findings indicate that similar functional results were obtained for both methods; however, these findings were not found to be correlated with the histomorphometric measurements.

The electrophysiological data for end-to-side coaptation indicated that the axons in the coapted nerves displayed different characteristics from those of intact nerves; however, they were able to induce good functional reinnervation. This phenomenon was most likely caused by the relatively large numbers of thicker axons and thin myelin sheaths.

The SSN group showed statistically significant differences in all parameters compared with both

the control and no coaptation groups. These results were interpreted as much worse outcomes compared with those observed in the C group; however, they indicated the possibility of nerve regeneration. In addition, the lack of statistically significant differences ($t = 0.85$, $p < 0.05$) in the EMG examination results and the statistically significant differences in the G-ratio and histomorphometric measurements in the SSN group compared with the EEN group showed that the SSN method was less effective than the EEN method. The lower G-ratio and the decreased number of myelinated fibers in the SSN group might indicate a very small possibility of regeneration by collateral sprouting.

In our study, we used the end-to-side and side-to-side methods. The anatomical conditions (short spinal nerves and wide perimeters) in some cases (after confirmation of the efficiency of the method in consecutive experimental examinations) necessitated side-to-side coaptation.

In addition, encouraging results on the application of side-to-side coaptation as a complementary technique have been presented by Arm [4] and Shea [50], who observed reduced muscle atrophy with a side-to-side nerve bridge combined with traditional end-to-end neurorrhaphy.

The lack of significant findings for the subscapularis muscle could be explained by the fact that this muscle was also innervated by the ventral branches of the C7 and C8 spinal nerves, which induced partial function. In the biceps brachii muscle, the significant differences in the maintenance of lower amplitudes could be explained by the fact that the connected branches between C5/C6 and C7 were cut and the biceps muscle was deprived of stimulation from the ventral branches of the C5 and C6 spinal nerves.

The number of myelinated axons in the ESN group was 47% of that in the control group. This finding is similar to that of Fogotti, who reported that the mean number of nerve fibers was significantly higher in a control group compared with an ESN group [21]. This finding is also comparable to those of other studies describing end-to-side coaptation. For example, approximately 50-65% of the original axons have been reported to be retained in the recipient nerve by coaptation between the peroneal and tibial nerves [34,47,62]. The results of this study showed that the number of myelinated axons present in recipient nerves in the ESN group was 81% of that in the EEN group.

Similar results have been reported by Gao, who performed a clinical trial, finding that end-to-side coaptation resulted in a significant decrease in myelinated axons by 53% compared with a control group [22].

As previously reported [15,45], the G-ratio in the central nerves of rats is near 0.7, and it is more than 0.6 in the peripheral nerves. For rabbits, this ratio is 0.59-0.63 at the root level, 0.62-0.65 at the trunk level, and 0.63 in the suprascapular nerve [44]. Comparison of these results with those obtained using healthy limbs appears to be sufficient to assess conduction ability. The G-ratio indicates the possibility of conduction; however, the presence of fewer myelinated axons was responsible for the weaker final results. More rapid and better functional recovery occurred in the EEN group because EEN is involved in the regeneration of axotomized nerves, whereas ESN is involved in the collateral sprouting of intact nerves [1,34].

In the case of end-to-side coaptation, regenerated axons appear from the Ranvier nodes of the donor nerve most proximal to the coaptation site, and it is guided into the epineurium of the donor nerve [27, 61]. Before axonal development, Schwann cells are organized into columns at the coaptation site [52]. Then, these cells invade the epineurial layer of the recipient nerve [38]. This is the most important stage in the phenomenon of collateral sprouting [38]. Axons appear from Ranvier nodes of the donor nerve proximal to the site of coaptation [53]. Schwann cells stimulate axonal regeneration from both the distal nerve stump and the nodes of Ranvier of the donor nerve [54, 56]. This mechanism is indirectly controlled by neurotropic factors [61]. After these factors are released from Schwann cells by diffusion, they penetrate through the epineurium into the perineurium. In this way, directed collateral sprouting from the region closest to the injury site occurs at the Ranvier nodes of the donor nerve [61].

Axotomy results in injury to the motor neurons and quickly triggers axonal regeneration; however, in the case of ESN, humoral factors released by damaged or degenerating recipient nerves are likely to play roles in the sprouting of intact donor axons [8].

A linear relationship exists between myelin sheath thickness and axon diameters in nerves at maturity; however, this relationship deviates from the norm in regenerated nerves, depending on the

axonal myelination pattern [15]. The slope of the regression line for regenerated nerves has been demonstrated to be lower than normal because of the myelin-axonal disproportion that persists for a period of time after intervention of regenerated axons that have failed to reinnervate a target [15].

The axon diameter and myelin thickness of the suprascapular nerve after repair and the regression analysis results suggested that the axons were not maximally myelinated. The slightly better parameters observed with EEN and ESN might have resulted from faster regeneration and more advanced myelination of axons; however, long-term studies are needed to determine whether these factors result in a better outcome.

The histological results differed from the behavioral results [48]. Morphological and functional examinations revealed that a limited number of motor axons were capable of producing adequate functional reinnervation of muscles.

The presented results indicate that sensory reinnervation is more effective than motor reinnervation. It has been suggested that it is easier to accomplish sensory reinnervation compared with motor reinnervation after end-to-side nerve repair [35,54]. It is possible that the earlier completion of sensory reinnervation compared with motor reinnervation observed in our study occurred because sensory axons are more prone to sprouting into end-to-side coapted nerves [10,54] and they sprout at a faster rate compared with motor axons [29].

Although consecutive analyses have emphasized the efficacy of coaptation in practice, the underlying mechanism remains to be elucidated. This mechanism is the outcome of the coaptation technique and complex molecular processes.

The most important molecule involved in this process is neurotrophin-3 (NT-3) [53], which acts through its receptor Trk C, followed by growth-associated protein-43 (GAP-43), a marker of growth cone formation, brain-derived neurotrophic factor (BDNF) and Trk B (BDNF receptor) [60]. Another important factor affecting collateral sprouting is nerve growth factor (NGF) [5,51]. NGF is produced in end organs following nerve injury. It is taken up by axon terminals and transported retrogradely to the nerve cell body, stimulating a secondary response. NGF and ciliary neurotrophic factor (CNTF) facilitate axonal regeneration after end-to-side neurorrhaphy [39]. The regulation of matrix metalloproteinase (MMP) expression and activity [20] as well as neurotrophic factors (TIMPs and IGF) [12,40] might also have very important roles in this process. Recent experimental studies have shown that physical and chemical agents stimulate nerve regeneration after end-to-side coaptation, including phototherapy, FK506, and acetyl-L-carnitine [13,24,32,57].

Our results demonstrate the effectiveness of ESN; however, they should be confirmed by retrograde labeling. The main limitation lies in the translation of laboratory results to the clinical setting, which represents a critical step in biomedical research. Unfortunately, promising basic science and preclinical results sometimes fail to meet expectations when they are applied clinically [17,23].

We believe that our results could aid in the development of a differential approach to nerve injury, depending on the nerve trunks involved, the location of the injury, and the methods of repair and reconstruction. We hope that the described method of coaptation, in addition to the neurotropic factors that have been identified, might be used to develop an alternative treatment to surgery of the brachial plexus.

Conclusions

The electrophysiological, histomorphometric and behavioral results obtained using end-to-side coaptation of ventral branches of the C5 and C6 spinal nerves to the C7 spinal nerve in the brachial plexi of rabbits confirm the occurrence of collateral sprouting at this level. After further research is performed to confirm the results of this study, end-to-side coaptation might emerge as an alternative method in the treatment of brachial plexus avulsion.

Acknowledgments

We thank Bartosz Witkowski, who provided medical writing service on behalf of Wroclaw Medical University.

Disclosure

Authors report no conflict of interest.

References

1. Akeda K, Hirata H, Matsumoto M, Fukuda A, Tsujii M, Nagakura T, Ogawa S, Yoshida T, Uchida A. Regenerating axons emerge far proximal to the coaptation site in end-to-side nerve coapta-

tion without a perineurial window using a T-shaped chamber. Plast Reconstr Surg 2006; 117: 1194-1203.
2. Allieu Y, Privat JM, Bonnel F. Paralysis in root avulsion of the brachial plexus: neurotization by the spinal accessory nerve. Clin Plast Surg 1984; 11: 133-136.
3. Alnot J. Traumatic brachial plexus lesions in the adult. Indications and results. Hand Clin 1995; 11: 623-631.
4. Amr SM, Moharram AN. Repair of brachial plexus lesions by end-to-side side-to-side grafting neurorrhaphy: experience based on 11 cases. Microsurgery 2005; 25: 126-146.
5. Bajrović F, Kovacic U, Pavcnik M, Sketelj J. Interneuronal signalling is involved in induction of collateral sprouting of nociceptive axons. Neuroscience 2002; 111: 587-596.
6. Beisteiner R, Höllinger I, Rath J, Wurnig M, Hilbert M, Klinger N, Geissler A, Fischmeister F, Wöber C, Klösch G, Millesi H, Grisold W, Auff E, Schmidhammer R. New type of cortical neuroplasticity after nerve repair in brachial plexus lesions. Arch Neurol 2011; 68: 1467-1470.
7. Bentolia V, Nizard R, Bizot P, Sedel L. Complete traumatic brachial plexus palsy. Treatment and outcome after repair. J Bone Joint Surg Am 1999; 81: 20-28.
8. Beris A, Lykissas M, Korompilias A, Mitsionis G. End-to-side nerve repair in peripheral nerve injury. J Neurotrauma 2007; 24: 909-916.
9. Bonham C, Greaves I. Brachial plexus injuries. Trauma 2011; 13: 353-363.
10. Bontioti E, Kanje M, Lundborg G, Dahlin LB. End-to-side nerve repair in the upper extremity of rat. J Peripher Nerv Syst 2005; 10: 58-68.
11. Brunelli G, Monini L. Neurotization of avulsed roots of brachial plexus by means of anterior nerves of cervical plexus. Clin Plast Surg 1984; 11: 149-152.
12. Chang C, Werb Z. The many faces of metalloproteases: cell growth, invasion, angiogenesis and metastasis. Trends Cell Biol 2001; 11: 37-43.
13. Chen B, Song Y, Liu Z. Promotion of nerve regeneration in peripheral nerve by short-course FK506 after end-to-side neurorrhaphy. J Surg Res 2009; 152: 303-310.
14. Chen L, Gu YD. An experimental study of contralateral C7 root transfer with vascularized nerve grafting to treat brachial plexus root avulsion. J Hand Surg Br 1994; 19: 60-66.
15. Chomiak T, Hu B. What is the optimal value of the g-ratio for myelinated fibers in the rat CNS? A theoretical approach. PLoS One 2009; 4: e7754.
16. Chuang DC, Yeh MC, Wei FC. Intercostal nerve transfer of the musculocutaneous nerve in avulsed brachial plexus injuries: evaluation of 66 patients. J Hand Surg Am 1992; 17: 822-828.
17. Dahlin LB. Nerve injuries. Current Orthopaedics 2008; 22: 9-16.
18. De Sá JM, Mazzer N, Barbieri CH, Barreira AA. The end-to-side peripheral nerve repair. Functional and morphometric study using the peroneal nerve of rats. J Neurosci Methods 2004; 136: 45-53.
19. Dong C, Gao W, Jia R, Li S, Shen Z, Li B. Reconstruction of anorectal function through end-to-side neurorrhaphy by autonomic nerves and somatic nerve in rats. J Surg Res 2013; 180: e63-e71.
20. Dzwonek J, Rylski M, Kaczmarek L. Matrix metalloproteinases and their endogenous inhibitors in neuronal physiology of the adult brain. FEBS Lett 2004; 567: 129-135.
21. Fagotti de Almeida CE, Farina Junior JA, Colli BO. Morphometric and Functional Analysis of Axonal Regeneration after End-to-end and End-to-side Neurorrhaphy in Rats. Plast Reconstr Surg Glob Open 2015; 3: e326.
22. Gao W, Liu Q, Li S, Zhang J, Li Y. End-to-side neurorrhaphy for nerve repair and function rehabilitation. J Surg Res 2015; 197: 427-435.
23. Geuna S, Papalia I, Tos P. End-to-side (terminolateral) nerve regeneration: a challenge for neuroscientists coming from an intriguing nerve repair concept. Brain Res Rev 2006; 52: 381-388.
24. Gigo-Benato D, Geuna S, de Castro Rodrigues A, Tos P, Fornaro M, Boux E, Battiston B, Giacobini-Robecchi MG. Low-power laser biostimulation enhances nerve repair after end-to-side neurorrhaphy: a double-blind randomized study in the rat median nerve model. Lasers Med Sci 2004; 19: 57-65.
25. Goheen-Robillard B, Myckatyn TM, Mackinnon SE, Hunter DA. End-to-side neurorrhaphy and lateral axonal sprouting in a long graft rat model. Laryngoscope 2002; 112: 899-905.
26. Gu YD, Zhang GM, Chen DS, Yan JG, Cheng XM, Chen L. Seventh cervical nerve root transfer from the contralateral healthy side for treatment of brachial plexus root avulsion. J Hand Surg Br 1992; 17: 518-521.
27. Hayashi A, Yanai A, Komuro Y, Nishida M, Inoue M, Seki T. Collateral sprouting occurs following end-to-side neurorrhaphy. Plast Reconstr Surg 2004; 114: 129-137.
28. Kale SS, Glaus SW, Yee A, Nicoson MC, Hunter DA, Mackinnon SE, Johnson PJ. Reverse end-to-side nerve transfer: from animal model to clinical use. J Hand Surg Am 2011; 36: 1631-1639.e2.
29. Kanje M, Arai T, Lundborg G. Collateral sprouting from sensory and motor axons into an end to side attached nerve segment. Neuroreport 2000; 11: 2455-2459.
30. Kelly EJ, Jacoby C, Terenghi G, Mennen U, Ljungberg C, Wiberg M. End-to-side nerve coaptation: a qualitative and quantitative assessment in the primate. J Plast Reconstr Aesthet Surg 2007; 60: 1-12.
31. Kimura J. Electrodiagnosis in diseases of nerve and muscle: Principles and Practice. 3rd ed. Oxford University Press, New York 2001.
32. Kostopoulos VK, Davis CL, Terzis JK. Effects of acetylo-L-carnitine in end-to-side neurorrhaphy: a pilot study. Microsurgery 2009; 29: 456-463.
33. Kovacic U, Tomsic M, Sketelj J, Bajrović FF. Collateral sprouting of sensory axons after end-to-side nerve coaptation – a longitudinal study in the rat. Exp Neurol 2007; 203: 358-369.
34. Liao WC, Chen JR, Wang YJ, Tseng GF. The efficacy of end-to-end and end-to-side nerve repair (neurorrhaphy) in the rat brachial plexus. J Anat 2009; 215: 506-521.
35. Liu K, Chen LE, Seaber AV, Goldner RV, Urbaniak JR. Motor functional and morphological findings following end-to-side neurorrhaphy in the rat model. J Orthop Res 1999; 17: 293-300.
36. Loy S, Bhatia A, Asfazadourian H, Oberlin C. Ulnar nerve fascicle transfer onto to the biceps muscle nerve in C5-C6 or C5-C6-C7 avulsions of the brachial plexus. Eighteen cases. Ann Chir Main Memb Super 1997; 16: 275-284.

37. Lundborg G, Zhao Q, Kanje M, Danielsen N, Kerns JM. Can sensory and motor collateral sprouting be induced from intact peripheral nerve by end-to-side anastomosis? J Hand Surg Br 1994; 19: 277-282.
38. Lykissas MG. Current concepts in end-to-side neurorrhaphy. World J Orthop 2011; 2: 102-106.
39. McCallister WV, Tang P, Smith J, Trumble TE. Axonal regeneration stimulated by the combination of nerve growth factor and ciliary neurotrophic factor in an end-to-side model. J Hand Surg Am 2001; 26: 478-488.
40. McFarlane S. Metalloproteases: carving out a role in axon guidance. Neuron 2003; 37: 559-562.
41. Moran SL, Steinmann SP, Shin AY. Adult brachial plexus injuries: mechanism, patterns of injury, and physical diagnosis. Hand Clin 2005; 21: 13-24.
42. Narakas AO, Hentz VR. Neurotization in brachial plexus injuries. Indication and results. Clin Orthop Relat Res 1988; 237: 43-56.
43. Papalia I, Geuna S, Tos PL, Boux E, Battiston B, Stagno D'Alcontres F. Morphologic and functional study of rat median nerve repair by terminolateral neurorrhaphy of the ulnar nerve. J Reconstr Microsurg 2003; 19: 257-264.
44. Reichert P, Kiełbowicz Z, Dzięgiel P, Puła B, Kuryszko J, Gosk J, Bocheńska A. The rabbit brachial plexus as a model for nerve repair surgery – histomorphometric analysis. Anat Rec (Hoboken) 2015; 298: 444-454.
45. Rushton WA. A theory of the effects of fibre size in medullated nerve. J Physiol 1951; 115: 101-122.
46. Rutowski R. Neurotizations by means of the cervical plexus in over 100 patients with from one to five root avulsions of the brachial plexus. Microsurgery 1993; 14: 285-288.
47. Sanapanich K, Morrison WA, Messina A. Physiologic and morphologic aspects of nerve regeneration after end-to-end or end-to-side coaptation in a rat model of brachial plexus injury. J Hand Surg Am 2002; 27: 133-142.
48. Schmidhammer R, Nógrádi A, Szabó A, Redl H, Hausner T, van der Nest DG, Millesi H. Synergistic motor nerve fiber transfer between different nerves through the use of end-to-side coaptation. Exp Neurol 2009; 217: 388-394.
49. Schmidhammer R, Redl H, Hopf R, van der Nest DG, Millesi H. End-to-side nerve graft repair based on synergistic peripheral terminal motor branches: investigation in a nonhuman primate model. Eur Surg 2005; 37: 308-316.
50. Shea JE, Garlick JW, Salama ME, Mendenhall SD, Moran LA, Agarwal JP. Side-to-side nerve bridges reduce muscle atrophy after peripheral nerve injury in a rodent model. J Surg Res 2014; 187: 350-358.
51. Shen H, Chung JM, Chung K. Expression of neurotrophin mRNAs in the dorsal root ganglion after spinal nerve injury. Brain Res Mol Brain Res 1999; 64: 186-192.
52. Slack JR, Hopkins WG, Williams MN. Nerve sheaths and motoneurone collateral sprouting. Nature 1979; 282: 506-507.
53. Sterne GD, Coulton GR, Brown RA, Green CJ, Terenghi G. Neurotrophin-3-enhanced nerve regeneration selectively improves recovery of muscle fibers expressing myosin heavy chains 2b. J Cell Biol 1997; 139: 709-715.
54. Tarasidis G, Watanabe O, Mackinnon SE, Strasberg SR, Haughey BH, Hunter DA. End-to-side neurorraphy: a long-term study of neural regeneration in a rat model. Otolaryngol Head Neck Surg 1998; 119: 337-341.
55. Terzis JK, Vekris MD, Soucacos PN. Outcomes of brachial plexus reconstruction in 204 patients with devastating paralysis. Plast Reconstr Surg 1999; 104: 1221-1240.
56. Torigoe K, Tanaka HG, Takahashi A, Hashimoto K. Early growth of regenerating neurites in acrylamide neuropathic mice: application of a film model. Brain Res 1997; 746: 269-274.
57. Tos P, Colzani G, Ciclamini D, Titolo P, Pugliese P, Artiaco S. Clinical applications of end-to-side neurorrhaphy: an update. Biomed Res Int 2014; 2014: 646128.
58. Viterbo F, Trindade JC, Hoshino K, Mazzoni Neto A. Latero-terminal neurorrhaphy without removal of the epineural sheath. Experimental study in rats. Rev Paul Med 1992; 110: 267-275.
59. Xiong G, Ling L, Nakamura R, Sugiura Y. Retrograde tracing and electrophysiological findings of collateral sprouting after end-to-side neurorrhaphy. Hand Surg 2003; 8: 145-150.
60. Yamauchi T, Maeda M, Tamai S, Tamai M, Yajima H, Takakura Y, Haga S, Yamamoto H. Collateral sprouting mechanism after end-to-side nerve repair in the rat. Med Electron Microsc 2000; 33: 151-156.
61. Zhang Z, Johnson EO, Vekris MD, Zoubos AB, Bo J, Beris AE, Soucacos PN. Long-term evaluation of rabbit peripheral nerve repair with end-to-side neurorrhaphy in rabbits. Microsurgery 2006; 26: 262-267.
62. Zhang Z, Soucacos PN, Bo J, Beris AE. Evaluation of collateral sprouting after end-to-side nerve coaptation using a fluorescent double-labeling technique. Microsurgery 1999; 19: 281-286.

Original article

Folia Neuropathologica

Polymorphism of the osteopontin gene and clinical course of multiple sclerosis in the Polish population

Justyna Biernacka-Lukanty[1,2], Grazyna Michalowska-Wender[1,2,3], Slawomir Michalak[2,3,4], Beata Raczak[1,2], Wojciech Kozubski[2], Dariusz Urbanski[5], Mieczyslaw Wender[3]

[1]Laboratory of Neurogenetics, Department of Neurology, Poznan University of Medical Sciences, Poznan, [2]Department of Neurology, Poznan University of Medical Sciences, Poznan, [3]Neuroimmunological Unit, Mossakowski Medical Research Centre Polish Academy of Science, Poznan, [4]Department of Neurochemistry and Neuropathology, Poznan University of Medical Sciences, Poznan, [5]Neuropsychiatric Hospital, Department of Neurology, Koscian, Poland

Folia Neuropathol 2015; 53 (4): 343-346 DOI: 10.5114/fn.2015.56548

Abstract

Osteopontin (OPN) is a key cytokine involved in T-cell activation in multiple sclerosis (MS). We investigated whether polymorphism of the osteopontin gene affects MS occurrence and clinical course in a Polish population.
Disability in 100 MS patients was evaluated using the Expanded Disability Status Scale (EDSS). Genotype and allele frequencies at exons 6 and 7 were examined by PCR. Using appropriate statistical tests, the distribution of variables was tested and means ± SD compared.
Genotype distribution and allele frequency differences between patients and control individuals were not statistically significant. No association of OPN with susceptibility to MS was found in the Polish population. The EDSS score was higher in 8090 T/T + 9250 C/C patients than in 8090 C/C + 9250 C/C MS patients (p = 0.0120), and the disability in 8090 C/C + 9250 C/T MS patients was higher than in 8090 C/C + 9250 C/C MS patients (p = 0.0137). Logistic regression analysis revealed age to be an independent factor influencing disability.
The polymorphisms of the OPN gene in positions 8090 T/T + 9250 C/C, 8090 C/C + 9250 C/T, and 8090 C/T + 9250 C/T were linked with higher levels of disability in MS patients.

Key words: *gene, multiple sclerosis, osteopontin, polymorphism.*

Introduction

Osteopontin (OPN) is one of the key cytokines involved in T-cell activation in multiple sclerosis (MS). The *OPN* gene is therefore recognized as an early T-cell activation gene, which underlies immunological events involved in the aetiopathogenesis of MS [15]. In an earlier study, we found *OPN* to be a useful marker to differentiate between malignant and benign ovarian tumours [10]. In patients with optic neuritis, cerebrospinal fluid (CSF) OPN levels have been shown to be correlated with CSF chitinase-3-like protein 1, myelin basic protein, and neurofilament, light polypeptide [9]. *OPN* also enhances the production of interleukin 12 and interferon gamma,

Communicating author
Grazyna Michalowska-Wender, Department of Neurology, Poznan University of Medical Sciences, 49 Przybyszewskiego St., 60-355 Poznan, fax: +48 61 869 16 97, e-mail: grazynawender@wp.pl

and reduces interleukin 10 [8]. Moreover, *OPN* is expressed in MS plaques in the central nervous system [3].

During the course of MS, autoimmune inflammatory processes and associated neurodegeneration develop. The most frequent course of MS is the relapsing-remitting form, but what defines the clinical severity and duration of intervals between the relapses remains unclear. Cerebrospinal fluid OPN concentration is reported to increase during relapse and normalize during remission in MS patients [16]. In a Japanese population, plasma OPN level was used as a marker of disease activity in MS and neuromyelitis optica [14]. However, circulating OPN did not act as a marker of MS activity in participants of the Comprehensive Longitudinal Investigation of MS (CLIMB) study [7]. The important question is whether the above-mentioned discrepancies are associated with genetic factors (such as polymorphisms of cytokine genes, including *OPN*), environmental factors, or both. Genome screening tests for MS support its multifactorial aetiology, including both various genetic and environmental factors and interactions thereof [5,13].

Table I. Frequency of *OPN* genotypes in multiple sclerosis (MS) patients compared to controls

Position		Control group n = 50 (%)	MS patients n = 102 (%)
8090	Genotype		
	C/C	18 (36)	28 (27)
	C/T	5 (10)	22 (22)
	T/T	27 (54)	52 (51)
	Allele		
	C	41 (41)	79 (39)
	T	59 (59)	125 (61)
9250	Genotype		
	C/C	29 (58)	55 (54)
	C/T	18 (36)	39 (38)
	T/T	3 (6)	8 (8)
	Allele		
	C	76 (76)	149 (73)
	T	24 (24)	55 (26)
8090 C/C	9250 C/C	4 (8)	5 (4.90)
8090 C/T	9250 C/C	1 (2)	7 (6.86)
8090 T/T	9250 C/C	24 (48)	43 (42.15)
8090 C/C	9250 C/T	12 (24)	16 (15.68)
8090 C/T	9250 C/T	4 (8)	14 (13.72)
8090 T/T	9250 C/T	2 (4)	9 (8.82)
8090 C/C	9250 T/T	2 (4)	7 (6.86)
8090 C/T	9250 T/T	0 (0)	1 (0.98)
8090 T/T	9250 T/T	1 (2)	0 (0)

The polymorphisms of *OPN* demonstrate variable differences among patients, as well as among various populations, necessitating further studies on this complex issue. We investigated the association, if any, of single-nucleotide polymorphisms (SNPs) of the *OPN* gene with MS course and severity in a Polish population.

Material and methods

We recruited 102 MS patients (25 men and 77 women; mean age, 39.0 ± 10.0 years) of Caucasian origin and Polish ethnicity. MS diagnosis was based on the revised McDonald criteria [12]. Two MS patients presenting with the optic-spinal form were excluded from the study, making the final number of MS participants 100. The EDSS index was established according to the Kurtzke Functional Systems Scores. A control group comprising 50 healthy blood donors, matched for age (mean 30 ± 6.0 years) and ethnicity, was also recruited.

All the study participants provided their informed consent. Blood samples were obtained for DNA extraction from peripheral blood cells, and genotype and allele frequencies in exons 6 and 7 were examined using specific primers in a standard PCR as presented in the paper of Niino *et al*. [11].

The distribution of variables (sex, age, and genotype categories) was tested with the D'Agostino-Pearson test. Mean ± SD values were compared by the χ^2 test. Statistical analysis was performed by one-way ANOVA, Mann-Whitney test, and logistic regression. Differences were considered statistically significant at $p < 0.05$.

The study was approved by the Poznan University of Medical Sciences Committee on Human Research.

Results

Genotype distribution and allele frequencies differed between patients and control individuals, but the differences were not statistically significant. Compared to the control group, MS patients have a higher frequency of the 8090 C/T (exon 6) + 9250 C/C (exon 7) *OPN* genotype ($p = 0.0732$; Table I). The heterozygous C/T genotype at position 8090 was detected in 21.6% of patients and in 10% of control individuals. Our results showed no indication of the

role of *OPN* in susceptibility to MS in the Polish individuals analysed.

However, we identified 8090 T/T + 9250 C/C, 8090 C/C + 9250 C/T, and 8090 C/T + 9250 C/T *OPN* genotypes as being associated with a higher disability in MS patients compared to other genotypes (Table II).

No differences for age between genotype categories were found. However, patients with EDSS scores exceeding 2 points were significantly older (41, 34-48 years; median, interquartile range) than subjects with minor disability (< 2 points) (34, 28-42.75 years) (p = 0.0162). Logistic regression analysis of the effect of variables on EDSS scoring in the model, including sex, age, and genotype categories, revealed age to be an independent factor influencing disability (p = 0.0140).

Discussion

The role of *OPN* in inflammatory diseases, including MS, has been demonstrated in several studies. The polymorphisms of the OPN gene have been established to be associated with MS in Japanese patients [11]. However, these findings could not be replicated in Caucasian MS patients; for instance, the 795 CT polymorphism in the OPN gene was not found to be associated with MS in a Spanish population [8]. In our study on a Polish Caucasian population, the heterozygous C/T genotype at positions 8090 and 9250 tended to have a higher frequency in MS patients compared to the control group. Similar findings were obtained for genotype frequencies of C/C and TT and allele frequencies of C and CT. Thus, haplotype structure might differ across populations. It is not easy to link the differences between Asian and European *OPN* polymorphisms with differences in prevalence rates in the corresponding geographical regions. MS incidence in Japan and other Asian countries is lower than in Europe and North America. Therefore, determining an association of polymorphisms of *OPN* with susceptibility to MS is not that simple.

Several studies provide conflicting results on the impact of OPN gene variations on MS severity. Caillier *et al*. found that patients carrying at least one wild-type 1284 A/4 allele were less likely to have a mild disease course [2]. Hensiek *et al*. found no effect of SNPs located in exons 6 and 7 of *OPN* on the clinical severity of MS [6], while Comi *et al*. reported the role of *OPN* variation on MS development and progression; however, they did not discuss its effect on disease severity [4].

An interesting point was presented in experimental allergic encephalomyelitis by Begum-Haque *et al*. [1]. The authors found that glatiramer acetate biased dendritic cells towards an anti-inflammatory phenotype by modulating OPN, IL-7 and RORγt responses and by increasing IL-10 production. The issue should also be studied in MS patients.

Table II. Disability measure in studied subgroups of multiple sclerosis (MS) patients

Studied group	EDSS score (median; interquartile range)	*p*
Total, *n* = 102	3.0; 2.00-4.00	N/A
Females, *n* = 77/males, *n* = 25	3.00; 2.00-4.25/3.25; 2.00-4.00	0.8743
8090 C/C + 9250 C/C, *n* = 4	1.75; 1.50-2.00	As below
8090 C/T + 9250 C/C, *n* = 7	2.00; 1.50-2.50	As below
8090 T/T + 9250 C/C, *n* = 43	3.00; 2.00-4.00	0.0120 vs. 8090 C/C + 9250 C/C and 0.0482 vs. 8090 C/T + 9250 C/C
8090 C/C + 9250 C/T, *n* = 16	3.75; 2.50-4.50	0.0137 vs. 8090 C/C + 9250 C/C and 0.0482 vs. 8090 C/T + 9250 C/C
8090 C/T + 9250 C/T, *n* = 14	3.25; 2.50-5.00	0.0553 vs. 8090 C/C + 9250 C/C
8090 T/T + 9250 C/T, *n* = 9	2.50; 1.38-4.25	N.S.
8090 C/C + 9250 T/T, *n* = 6	4.00; 3.00-5.50	N.S.
8090 C/T + 9250 T/T, *n* =1	2.0	N/A

N.S. – not significant, N/A – not applicable – insufficient data

To conclude, in our study, we identified 8090 T/T + 9250 C/C, 8090 C/C + 9250 C/T, and 8090 C/T + 9250 C/T *OPN* to be associated with higher levels of disability in MS patients compared to other genotypes. Although we could not establish an association of OPN polymorphisms with MS susceptibility in a population of Polish patients, our results provide a line of evidence on the impact of *OPN* variations on the course of MS. Overall, the differential effects of various combinations of variants in genotypes may contribute to explaining the differences in MS susceptibility between ethnic groups and disability in individual patients. Thus, further research in other populations is needed as well as evaluation of disease severity related to OPN gene polymorphism in single subjects.

Disclosure

Authors report no conflict of interest.

References

1. Begum-Haque S, Christy M, Wang Y, Kasper E, Ochoa-Reparaz J, Smith JY, Haque A, Kasper LH. Glatiramer acetate biases dendritic cells towards an anti-inflammatory phenotype by modulating OPN, IL-17, and RORγt responses and by increasing IL-10 production in experimental allergic encephalomyelitis. J Neuroimmunol 2013; 254 (1-2): 117-124.
2. Caillier S, Barcellos LF, Baranzini SE, Swerdlin A, Lincoln RR, Steinman L, Martin E, Haines JL, Pericak-Vance M, Hauser SL, Oksenberg JR. Multiple Sclerosis Genetics Group. Osteopontin polymorphisms and disease course in multiple sclerosis. Genes Immun 2003; 4: 312-315.
3. Chabas D, Baranzini SE, Mitchell D, Bernard CC, Rittling SR, Denhardt DT, Sobel RA, Lock C, Karpuj M, Pedotti R, Heller R, Oksenberg JR, Steinman L. The influence of the proinflammatory cytokine, osteopontin, on autoimmune demyelinating disease. Science 2001; 294: 1731-1735.
4. Comi C, Cappellano G, Chiocchetti A, Orilieri E, Buttini S, Ghezzi L, Galimberti D, Guerini F, Barizzone N, Perla F, Leone M, D'Alfonso S, Caputo D, Scarpini E, Cantello R, Dianzani U. The impact of osteopontin gene variations on multiple sclerosis development and progression. Clin Dev Immunol 2012; 2012: 212893.
5. Haines JL, Ter-Minassian M, Bazyk A, Gusella JF, Kim DJ, Terwedow H, Pericak-Vance MA, Rimmler JB, Haynes CS, Roses AD, Lee A, Shaner B, Menold M, Seboun E, Fitoussi RP, Gartioux C, Reyes C, Ribierre F, Gyapay G, Weissenbach J, Hauser SL, Goodkin DE, Lincoln R, Usuku K, Oksenberg JR, et al. A complete genomic screen for multiple sclerosis underscores a role for the major histocompatability complex. The Multiple Sclerosis Genetics Group. Nat Genet 1996; 13: 469-471.
6. Hensiek AE, Roxburgh R, Meranian M, Seaman S, Yeo T, Compston DA, Sawcer SJ. Osteopontin gene and clinical severity of multiple sclerosis. J Neurol 2003; 250: 943-947.
7. Kivisäkk P, Healy BC, Francois K, Gandhi R, Gholipour T, Egorova S, Sevdalinova V, Quintana F, Chitnis T, Weiner HL, Khoury SJ. Evaluation of circulating osteopontin levels in an unselected cohort of patients with multiple sclerosis: relevance for biomarker development. Mult Scler 2014; 20: 438-444.
8. Mas A, Martínez A, de las Heras V, Bartolomé M, de la Concha EG, Arroyo R, Urcelay E. The 795CT polymorphism in osteopontin gene is not associated with multiple sclerosis in a Spanish population. Mult Scler 2007; 13: 250-252.
9. Modvig S, Degn M, Horwitz H, Cramer SP, Larsson HB, Wanscher B, Sellebjerg F, Frederiksen JL. Relationship between cerebrospinal fluid biomarkers for inflammation, demyelination and neurodegeneration in acute optic neuritis. PLoS One 2013; 8: e77163.
10. Moszyński R, Szubert S, Szpurek D, Michalak S, Sajdak S. Role of osteopontin in differential diagnosis of ovarian tumors. J Obstet Gynaecol Res 2013; 39: 1518-1525.
11. Niino M, Kikuchi S, Fukazawa T, Yabe I, Tashiro K. Genetic polymorphisms of osteopontin in association with multiple sclerosis in Japanese patients. J Neuroimmunol 2003; 136: 125-129.
12. Polman CH, Reingold SC, Banwell B, Clanet M, Cohen JA, Filippi M, Fujihara K, Havrdova E, Hutchinson M, Kappos L, Lublin FD, Montalban X, O'Connor P, Sandberg-Wollheim M, Thompson AJ, Waubant E, Weinshenker B, Wolinsky JS. Diagnostic criteria for multiple sclerosis: 2010 revisions to the McDonald criteria. Ann Neurol 2011; 69: 292-302.
13. Sawcer S, Jones HB, Feakes R, Gray J, Smaldon N, Chataway J, Robertson N, Clayton D, Goodfellow PN, Compston A. A genome screen in multiple sclerosis reveals susceptibility loci on chromosome 6p21 and 17q22. Nat Genet 1996; 13: 464-468.
14. Shimizu Y, Ota K, Ikeguchi R, Kubo S, Kabasawa C, Uchiyama S. Plasma osteopontin levels are associated with disease activity in the patients with multiple sclerosis and neuromyelitis optica. J Neuroimmunol 2013; 263: 148-151.
15. Steinman L, Zamvil S. Transcriptional analysis of targets in multiple sclerosis. Nat Rev Immunol 2003; 3: 483-492.
16. Szalardy L, Zadori D, Simu M, Bencsik K, Vecsei L, Klivenyi P. Evaluating biomarkers of neuronal degeneration and neuroinflammation in CSF of patients with multiple sclerosis – osteopontin as a potential marker of clinical severity. J Neurol Sci 2013; 331: 38-42.

Original article

Folia Neuropathologica

Toll-like receptor 2 (TLR2) is a marker of angiogenesis in the necrotic area of human medulloblastoma

Danuta Maslinska[1,2], Milena Laure-Kamionowska[1], Sławomir Maslinski[2], Dariusz Szukiewicz[2]

[1]Department of Experimental and Clinical Neuropathology, Mossakowski Medical Research Centre, Polish Academy of Sciences, Warsaw, [2]Department of General and Experimental Pathology, Warsaw Medical University, Warsaw, Poland

Folia Neuropathol 2015; 53 (4): 347-354 DOI: 10.5114/fn.2015.56549

Abstract

Angiogenesis plays a key role in the progression of malignant tumors. In recent years, anti-angiogenic drugs have been shown to be effective against tumors. However, some tumors are able to adopt escape mechanisms, suggesting that the vascular network in these tumors may be formed or may function in a different way. Medulloblastomas are tumors characterized by poor prognosis and low patient survival rates. These tumors rarely metastasize, but the reason why they almost always recur locally is not known. Central to mediating neoplastic changes is the interaction between cell surface receptors and their cognate ligands, which through intracellular signaling induce alternations in gene expression. In this context, the aim of our present study was to examine in medulloblastoma the distribution of Toll-like receptor 2 (TLR2) and receptor for advanced glycosylation end-product (RAGE), and mast cells associated with the tumor neovascularization process. Immunohistochemical study with a battery of specific antibodies was used. The results show that in the tumor necrotic area, TLR2 participates in all steps of vascular network formation, but in regions where the tumor was not affected by necrosis, the capillary network was TLR2 immunonegative. The TLR2 vascular network of the necrotic area was not associated with RAGE and mast cells. However, in the region of the medulloblastoma not affected by necrosis, the RAGE receptor was present in the endothelium of all capillaries, and mast cells were numerous only in the perivascular space of large brain and meningeal vessels at the border of the tumor. In conclusion, our results show that the receptor of innate immunity TLR2 plays an important role in recognition of ligands delivered by dying necrotic medulloblastoma cells and participates in tumor neovascularization. Moreover, the results show that the RAGE receptor and mast cells operate in different medulloblastoma regions and influence different parts of the tumor vascular network.

Key words: *medulloblastoma, receptor for advanced glycosylation end-product (RAGE), mast cells, tumor angiogenesis, Toll-like receptor 2 (TLR2).*

Introduction

The development of the vascular network plays an essential role in physiology and pathology. Three mechanisms – vasculogenesis, angiogenesis and arteriogenesis – participate in this process. Vasculogenesis occurs by angioblast differentiation into endothelial cells to form blood vessels. Angiogene-

Communicating author:
Prof. Danuta Maślińska, Department of Experimental and Clinical Neuropathology, Mossakowski Medical Research Centre, Polish Academy of Sciences, 5 Pawinskiego St., 02-106 Warsaw, Poland, e-mail: maslinskad@imdik.pan.pl

sis is the process in which new blood vessels are formed from pre-existing ones, and arteriogenesis refers to the enlargement of the arterial network to sustain higher metabolic demands of the tissue [19]. In oncology, tumor vascularity is correlated with tumor growth, invasion and initiation of metastasis [2] and is thought to occur mainly by angiogenesis [10], although the role of postnatal vasculogenesis by recruitment of bone marrow-derived endothelial progenitor cells (EPCs) into the tumor vasculature has also been discussed [9,27]. Formation of a new capillary network involves many steps of a cascade in which one event triggers the next through the action of specific mediators. These mediators belong to different sets of factors participating in tumor angiogenesis. One of the sets includes numerous pro-inflammatory mediators such as growth factors, cytokines, proteoglycans and lipid mediators, but all of them are delivered from any cell injured by hypoxia, ischemia, free radicals or infection agents. The other, recently studied, set of angiogenic mediators comprises those that are fragments of destroyed host necrotic cells. Such mediators were recognized as the damage-associated molecular pattern (DAMP) molecules that have been implicated in several inflammatory diseases and activate target cells through the differential engagement of multiple surface receptors including innate immune receptors such as Toll-like receptor 2 (TLR2), or receptor for advanced glycation end-products (RAGE). In addition, mast cells, which are abundant surrounding solid tumors, are a source of numerous compounds that are often suspected of participation in tumor angiogenesis. Recently, we observed that TLR2 is a very sensitive marker of a newly formed tumor capillary network in medulloblastoma [28].

Medulloblastoma is the most common primary solid brain tumor occurring in children, with a strong male preponderance. Histologically, the tumor is composed of sheets or lobules of small cells with prominent nuclei and little cytoplasm. Vascular proliferation may be present but is not a constant feature of this lesion, but as in other tumors neovascularization is an important mechanism underlying medulloblastoma progression. Increased tumor angiogenesis is normally associated with poor prognosis of the disease, and the development of therapeutic agents that can reduce or inhibit angiogenesis or destroy the neovasculature of tumors has recently received considerable interest [31]. One possible advantage of these drugs, compared with conventional chemotherapy, is their potential for reduced susceptibility to acquired drug resistance. This is a major clinical problem observed in patients undergoing chemotherapy and results from the intrinsic genetic instability and heterogeneity of tumor cells [29]. Endothelial cells, on the other hand, on which anti-vascular and anti-angiogenic drugs act, are genetically more stable and more homogeneous and are thus presumed to be not so susceptible to acquired drug resistance. Our growing understanding of the molecular mechanisms underlying angiogenesis, including the role of several growth factors that regulate the process, has enabled the development of a large number of drug candidates against vascular-specific targets that can inhibit angiogenesis.

Since there are numerous unanswered questions concerning the process of angiogenesis which occurs in the pathological microenvironment of cancer, the aim of our present study was to examine in medulloblastoma of the human brain the distribution of TLR2 and RAGE receptors and mast cells associated with the tumor neovascularization.

Material and methods

The study was approved by the local ethical committee and performed on human brains that were obtained following autopsy. Patients died at different ages of life (from 1-5, 17, to 37 years of age), one to two years after ineffective therapy. Brains with medulloblastoma were diagnosed according to the WHO classification [26] in the Institute of Medical Research Centre, Polish Academy of Sciences, Warsaw, Poland. Paraffin blocks were drawn from the file, cut into serial sections (5 µm thick) and stained with H&E for routine histological examination or used for immunohistochemical study.

Immunohistochemistry

Immunohistochemistry was performed using specific primary antibodies and an alkaline phosphatase-avidin-biotin conjugate purchased from Santa Cruz Laboratory (USA) or an avidin-biotin-peroxidase complex system purchased from Vector Laboratories (USA) and used according to the manufacturer's recommendations.

Briefly, sections were dewaxed and hydrated through descending alcohols to water. For non-enzymatic antigen retrieval, some sections were heat-

Table I. Antibodies used in the study

Antibody	Type	Antigen		Source	Dilution
		Origin	Domain		
TLR 2	Polyclonal	Human	*N*-terminus	Santa Cruz	1 : 50
TLR 4	Polyclonal	Human	*C*-terminus	Santa Cruz	1 : 50
MC tryptase	Polyclonal	Human	Not quoted	Chemicon,	1 : 100
RAGE	Polyclonal	Human	*C*-terminus	Santa Cruz	1 : 50
RAGE	Polyclonal	Human	*N*-terminus	Santa Cruz	1 : 50

ed in 0.01 M sodium citrate buffer (pH 6.0) to 95°C and allowed to cool for 20 min at room temperature and washed with PBS. Then, they were incubated in methanol/3% H_2O_2 solution for 20 min to quench endogenous peroxidase. After being washed again in PBS and blocked with solution containing PBS/5% appropriate normal serum (of goat, rabbit or mouse) for 2 h at room temperature, sections were incubated overnight at 4°C in solutions of primary antibodies listed in Table I.

Immunoreactions were visualized using biotinylated secondary antibodies and ABComplex/HRP or an alkaline phosphatase-avidin-biotin conjugate. Then, sections were lightly counterstained with Mayer's hematoxylin.

For negative controls, primary antibodies were replaced with an appropriate isotypic normal mouse, rabbit or goat immunoglobulin fraction at a matched protein concentration. These were included for the examination of each specimen and consistently produced negative results.

Results

Distribution of the TLR2 capillary network, mast cells and RAGE in different regions of medulloblastoma is presented in Table II.

In medulloblastoma of all our patients, neovascularization/angiogenesis (V/A) was observed in areas of tumor cell necrosis. We observed the successive steps of this process. Cells participating in each such step were immunopositive to TLR2. At the beginning, TLR2 immunopositive cells were scattered throughout the tumor necrotic debris (Fig. 1A). In the next step, they formed tubular structures (Fig. 1B) which penetrated to the post-necrotic areas already cleared of dead cells (Fig. 1C). Finally, numerous TLR2-immunopositive capillaries formed a very dense vascular network which closely conforms to the post-necrotic space of the tumor (Fig. 2). In the capillary wall of this network RAGE receptors were not found. In addition, mast cells were not detected in these necrotic or post-necrotic areas of the tumor.

In non-injured regions of the medulloblastoma, the vascular network was immunonegative to TLR2, but RAGE protein was precisely localized in the wall of all capillaries and in proliferating endothelium of some of these vessels (Fig. 3A-B).

Mast cells were distributed at the border of the medulloblastoma and were localized at the perivascular space of large brain vessels (Fig. 4A). Those mast cells that were detected within the solid tumor regions belonged to the host meninges that were incorporated into the tumor mass (Fig. 4B).

Discussion

Reciprocity of inflammation and neovascularization is emerging as an important mechanism underlying numerous processes from tissue healing/remodeling to cancer [3,17].

In recent years, anti-angiogenic therapies have been developed and tested for their effectiveness against tumors. Among such drugs are inhibitors against vascular endothelial growth factor and its receptors, as well as inhibitors targeting the plate-

Table II. Distribution of Toll-like receptor 2 (TLR2) capillary network, mast cells and receptor for advanced glycosylation end-product (RAGE)

	Medulloblastoma regions	
	Post-necrotic areas	Solid tumor areas
TLR2 capillary	Dense network	nd
RAGE	nd	Capillary endothelium
Mast cells	nd	Perivascular area

nd – not detected

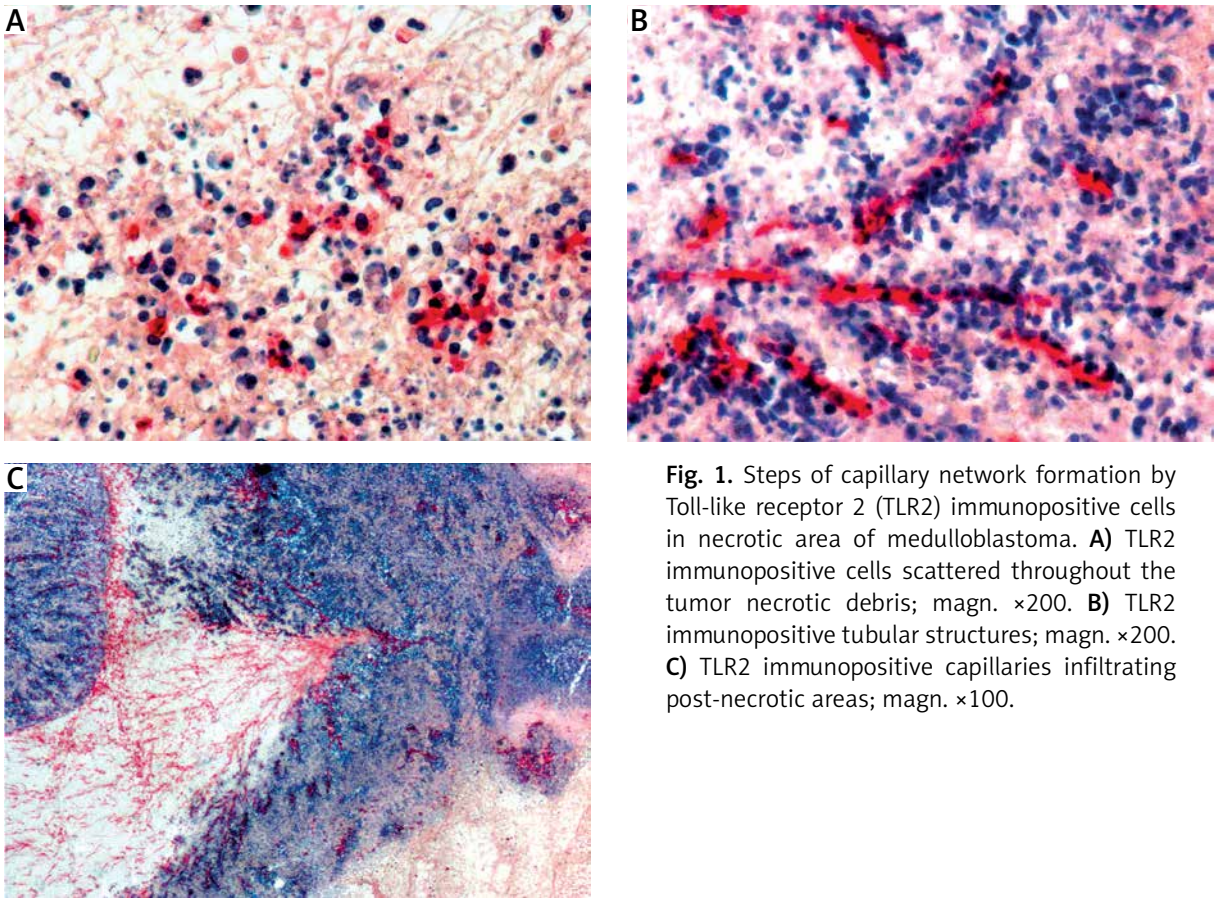

Fig. 1. Steps of capillary network formation by Toll-like receptor 2 (TLR2) immunopositive cells in necrotic area of medulloblastoma. **A)** TLR2 immunopositive cells scattered throughout the tumor necrotic debris; magn. ×200. **B)** TLR2 immunopositive tubular structures; magn. ×200. **C)** TLR2 immunopositive capillaries infiltrating post-necrotic areas; magn. ×100.

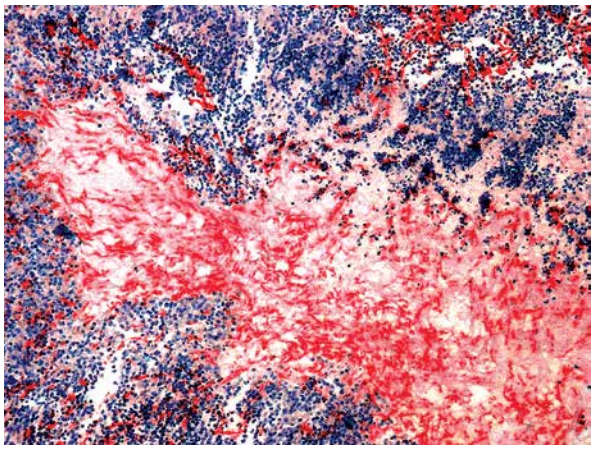

Fig. 2. Toll-like receptor 2 (TLR2) immunopositive vascular network closely conforms to post-necrotic area of the tumor; magn. ×100.

let-derived growth factor family, integrins or histone deacetylase. While many anti-angiogenic drugs have been shown to be effective with limited toxicity, some tumors are able to adopt escape mechanisms [24], suggesting that the vascular network in some tumors could be formed in a different way than normal capillaries. The results of our present study confirm this hypothesis. In regions of medulloblastoma cell necrosis, we observed that TLR2 participates in all steps of vascular network formation, but in regions where the tumor was not affected by necrosis, the capillary network was TLR2 immunonegative. We believe that all those TLR2 immunonegative capillaries were developed during normal host embryogenesis and the space supplied by this capillary network was colonized by medulloblastoma cells. Thus, only in necrotic areas of the medulloblastoma were pathogens delivered from dying undifferentiated tumor cells recognized by TLR2 and activated TLR2 signaling promoted the angiogenic responses in the tumor.

Toll-like receptors (TLRs) are a family of pattern recognition receptors that have emerged as key mediators of innate immunity. These receptors recognize a broad range of protein and lipid ligands [21,33], including a number of host origin ligands [1,18,22,36,37,41], and initiate host defense inflam-

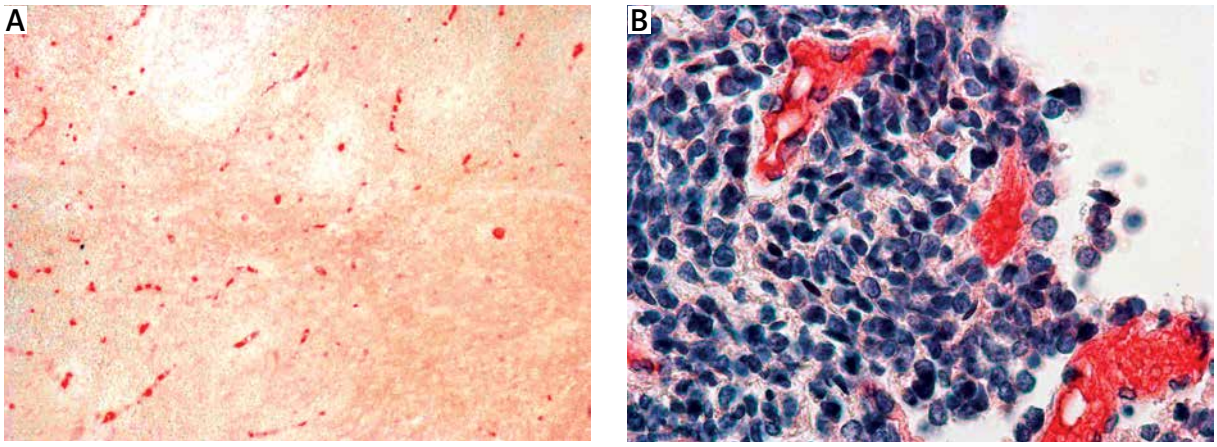

Fig. 3. Receptor for advanced glycosylation end-product (RAGE) immunopositive capillaries in non-injured tumor regions. **A)** RAGE in capillaries (section not counterstained); magn. ×100. **B)** RAGE in proliferating endothelium of tumor blood vessels; magn. ×200.

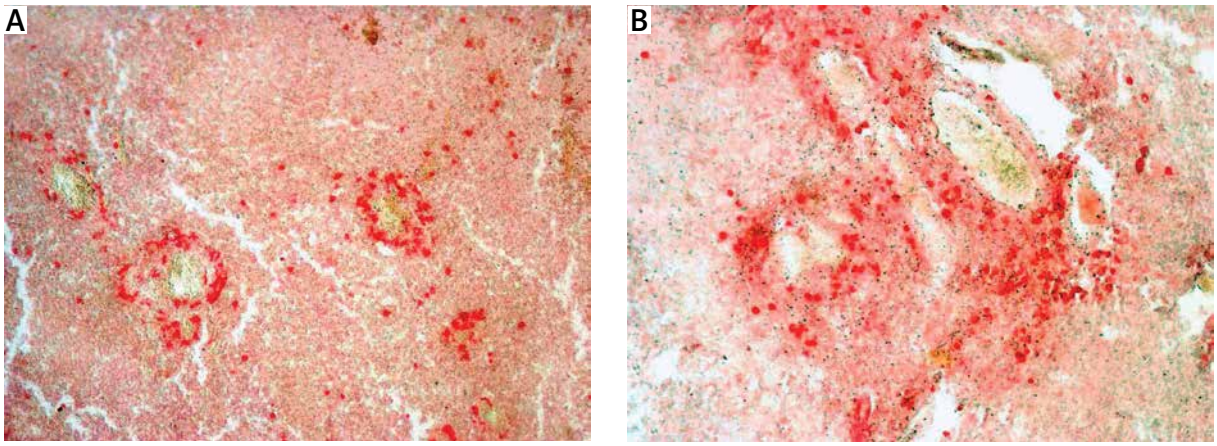

Fig. 4. Tryptase immunopositive mast cells in perivascular space of brain large blood vessels (sections not counterstained). **A)** At the border of medulloblastoma; magn. ×200. **B)** In blood vessels of meninges; magn. ×200.

mation. TLR-mediated inflammation is an important pathogenic link between innate immunity and a diverse panel of clinical disorders including cancer. In addition, expression of TLR2 and TLR4 was found on the endothelium; therefore both receptors, in some circumstances, may be implicated in angiogenesis [8].

Altogether our results indicate that TLR2 is a sensor of pathogens of necrotic tumor cells, which provides a key link connecting innate immunity and cancer angiogenesis.

Tumorigenesis is a multi-step process involving the alternation of a number of key cellular properties including uncontrolled proliferation, evasion of cell death (apoptosis), vascularization (angiogenesis) and subsequent invasion and migration of tumor cells into the surrounding tissues [10]. Understanding the molecular processes underlying these cellular phenotypic changes is critical in order to develop novel therapies. Central to mediating these changes is the interaction between cell surface receptors and their cognate ligands, which through intracellular signaling induce alternations in gene expression. In this context, recent studies have identified that the receptor for advanced glycation end-products (RAGE) and its ligands may play an important role in cancer [7,25,38,39]. RAGE is a multi-ligand receptor that has been implicated in the pathogenesis of numerous diseases [20,38,42]. RAGE-ligand interaction triggers activation of a diverse array of signaling pathways that lead to processes integrally linked to the tumorigenic sequelae including cellular migration, invasion, proliferation and survival [25,29]. Furthermore,

studies have indicated that RAGE and its ligands are expressed in human tumors, and often the extent of tumor invasiveness and metastatic potential was correlated with the degree of RAGE/ligand up-regulation [11-16,23,30,35,40].

Brain compartments are effectively isolated from the plasma proteins and various ligands by the blood-brain barrier (BBB), localized on the endothelium of the brain capillaries. However, at this barrier, there are specialized receptors including RAGE that may shuttle all such proteins in efflux and influx directions [4,5]. The results of our present study suggest that RAGE does not participate in the blood-brain function of the capillary network formed in post-necrotic regions of the medulloblastoma and ligands of this receptor cannot affect the healing process of the tumor. However, in all other regions of the tumor, RAGE is present on capillary endothelium, and thus the blood-brain barrier functions differently than in post-necrotic areas. In addition, mast cells, known as a source of early-response cytokines decisive in initiating the immune and host defense reaction to pathogens, were not found in the vicinity of capillaries in any regions of the tumor. Despite many reports concerning the association of mast cells (MC) with a variety of tumors, the functional significance of these cells in tumor biology remains obscure. The presence of mast cells has been interpreted as an immunological anti-tumor response or as a more direct interaction with tumor cells, especially an interaction which facilitates tumor growth [32]. The results of our study suggest that mast cells have little if any influence on development of angiogenesis in post-necrotic regions of the medulloblastoma.

Mast cells are a heterogeneous cell population categorized as either mucosal type or connective tissue type, based on their tissue locations, staining patterns, content of proteases and reactivity. In humans, mature mast cells in the brain contain tryptase as a protease and are known as the MC tryptase phenotype (MCT) [34]. Mast cells provide different multifunctional cytokines and potent mediators can mediate a variety of antimicrobial functions and possess certain unique features that make MC function particularly crucial for host defense [6]. Mast cells are always located at the host-environment interface, and they belong to the first line of cells that encounter pathogens. In our study, we found many of these cells at the border of the tumor and in meninges that covered the tumor. All MC were located at the perivascular space of large blood vessels. Therefore we conclude that MC were not directly involved in the function of the blood-brain barrier or in the process of angiogenesis of medulloblastoma post-necrotic areas. However, MC are long-lived cells with the capacity to respond repeatedly to the same stimulus, and we suspect that in our patients they had a potent influence on the function of the vascular network at the peripheral regions of the tumor.

Medulloblastomas are characterized by poor prognosis and low patient survival rates. In particular, strong induction of angiogenesis marks the transition from a lower-grade medulloblastoma to a more aggressive and lethal form of the tumor. Although these tumors rarely metastasize, they almost always recur locally. Data from our study suggest that this may be linked with angiogenesis and the healing process in medulloblastoma necrotic areas.

Despite advanced clinical approaches with surgery, radiotherapy and chemotherapy, inhibition of angiogenesis might represent a key strategy in the treatment of this neoplasm.

Nevertheless, the success with existing compounds in the managements of brain tumors is limited, and further study is required. We present new data focused on tumor angiogenesis. They show that capillary network formation and function of the blood-brain barrier differ depending on the medulloblastoma region and that receptors of innate immunity play an essential role in these processes.

Disclosure

Authors report no conflict of interest.

References

1. Apetoh L, Ghiringhelli F, Tesniere A, Obeid M, Ortiz C, Criollo A, Mignot G, Maiuri MC, Ullrich E, Saulnier P, Yang H, Amigorena S, Ryffel B, Barrat FJ,Saftig P, Levi F, Lidereau R, Nogues C, Mira JP, Chompret A, Joulin V, Clavel-Chapelon F, Bourhis J, André F, Delaloge S, Tursz T, Kroemer G, Zitvogel L. Toll-like receptor 4-dependent contribution of the immune system to anticancer chemotheraoy and radiotherapy. Nat Med 2007; 13: 1050-1059.
2. Carmeliet P, Jain RK. Angiogenesis in cancer and other diseases. Nature 2000; 407: 249-257.
3. Coussens LM, Werb Z. Inflammation and cancer. Nature 2002; 420: 860-867.
4. Deane R, Du Yan S, Submamaryan RK, LaRue B, Jovanovic S, Hogg E, Welch D, Manness L, Lin C, Yu J, Zhu H, Ghiso J, Frangione B, Stern A, Schmidt AM, Armstrong DL, Arnold B, Liliensiek B, Nawroth P, Hofman F, Kindy M, Stern D, Zlokovic B. RAGE

mediates amyloid-beta peptide transport across the blood-brain barrier and accumulation in brain. Nat Med 2003; 9: 907-913.
5. Deane R, Wu Z, Zlokovic BV. RAGE (yin) versus LRP (yang) balance regulates Alzheimer amyloid beta-peptide clearance through transport across the blood-brain barrier. Stroke 2004; 35 (11 Suppl 1): 2628-2631.
6. Dong H, Zhang X, Qian Y. Mast cells and neuroinflammation. Med Sci Monit Basic Res 2014; 20: 200-206.
7. Gebhardt C, Riehl A, Durchdewald M, Németh J, Fürstenberger G, Müller-Decker K, Enk A, Arnold B, Bierhaus A, Nawroth PP, Hess J, Angel P. RAGE signaling sustains inflammation and promotes tumor development. J Exp Med 2008; 205: 275-285.
8. Grote K, Schuett H, Salguero G, Grothusen C, Jagielska J, Drexler H, Mühlradt PF, Schieffer B. Toll-like receptor 2/6 stimulation promotes angiogenesis via GM-CSF as a potential strategy for immune defense and tissue regeneration. Blood 2010; 115: 2543-2552.
9. Hanahan D, Folkman J. Patterns and emerging mechanisms of the angiogenic switch during tumorigenesis. Cell 1996; 86: 353-364.
10. Hanahan D, Weinberg RA. The hallmarks of cancer. Cell 2000; 100: 57-70.
11. Harpio R, Einarsson R. S100 proteins as cancer biomarkers with focus on S100B in malignant melanoma. Clin Biochem 2004; 37: 512-518.
12. Hermani A, De Servi B, Medunjanin S, Tessier PA, Mayer D. S100A8 and S100A9 activate MAP kinase and NF-kappaB signaling pathways and trigger translocation of RAGE in human prostate cancer cells. Exp Cell Res 2006; 312: 184-197.
13. Hofmann MA, Drury S, Fu C, Qu W, Taguchi A, Lu Y, Avila C, Kambham N, Bierhaus A, Nawroth P, Neurath MF, Slattery T, Beach D, McClary J, Nagashima M, Morser J, Stern D, Schmidt AM. RAGE mediates a novel proinflammatory axis: a central cell surface receptor for s100/calgranulin polypeptides. Cell 1999; 97: 889-901.
14. Hori O, Brett J, Slattery T, Cao R, Zhang J, Chen JX, Nagashima M, Lundh ER, Vijay S, Nitecki D, et al. The receptor for advanced glycation end products (RAGE) is a cellular binding site for amphoterin. Mediation of neurite outgrowth and co-expression of RAGE and amphoterin in the developing nervous system. J Biol Chem 1995; 270: 25752-25761.
15. Hsieh HL, Schafer BW, Sasaki N, Heizmann CW. Expression analysis of S100 proteins and RAGE in human tumors using tissue microarrays. Biochem Biophys Res Commun 2003; 307: 375-381.
16. Ishiguro H, Nakaigawa N, Miyoshi Y, Fujinami K, Kubota Y, Uemura H. Receptor for advanced glycation end products (RAGE) and its ligand, amphoterin are overexpressed and associated with prostate cancer development. Prostate 2005; 64: 92-100.
17. Jackson JR, Seed MP, Kircher CH, Willoughby DA, Winkler JD. The codependence of angiogenesis and chronic inflammation. FASEB J 1997; 11: 457-465.
18. Jiang D, Liang J, Fan J, Yu S, Chen S, Luo Y, Prestwich GD, Mascarenhas MM, Garg HG, Quinn DA, Homer RJ, Goldstein DR, Bucala R, Lee PJ, Medzhitov R, Noble PW. Regulation of lung injury and repair by Toll-like receptors and hyaluronan. Nat Med 2005; 11: 1173-1179.
19. Jouanneau E. Angiogenesis and gliomas current issues and development of surrogate markers. Neurosurgery 2008; 62: 31-50.
20. Kalea AZ, Schmidt AM, Hudson BI. RAGE: a novel biological and genetic marker for vascular disease. Clin Sci (Lond) 2009; 116: 621-637.
21. Kawai T, Akira S. Pathogen recognition with Toll-like receptors. Curr Opin Immunol 2005; 17: 338-344.
22. Kim HS, Han MS, Chung KW, Kim S, Kim E, Kim MJ, Jang E, Lee HA, Youn J, Akira S, Lee MS. Toll-like receptor 2 senses beta-cell death and contributes to the initiation of autoimmune diabetes. Immunity 2007; 27: 321-333.
23. Kuniyasu H, Oue N, Wakikawa A, Shigeishi H, Matsutani N, Kuraoka K, Yokozaki H, Yasui W. Expression of receptors for advanced glycation end-products (RAGE) is closely associated with the invasive and metastatic activity of gastric cancer. J Pathol 2002; 196: 163-170.
24. Kunnakkat S, Mathew M, Narayana A. Antiangiogenic therapy in the management of brain tumors : a clinical overview. Cancer Chemother Pharmacol 2012; 70: 353-363.
25. Logsdon CD, Fuentes MK, Huang EH, Arumugam T. RAGE and RAGE ligands in cancer. Curr Mol Med 2007; 7: 777-789.
26. Louis DN, Ohgaki H, Wiestler OD, Cavenee WK (eds.). WHO classification of tumours of the central nervous system. 4th ed. IARC Press, Lyon 2007.
27. Lyden D, Hattori K, Dias S, Costa C, Blaikie P, Butros L, Chadburn A, Heissig B, Marks W, Witte L, Wu Y, Hicklin D, Zhu Z, Hackett NR, Crystal RG, Moore MAS, Hajjar KA, Manova K, Benezra R, Rafii S. Impaired recruitment of bone-marrow-derived endothelial and hematopoietic precursor cells blocks tumor angiogenesis and growth. Nat Med 2001; 7: 1194-1201.
28. Maslinska D, Laure-Kamionowska M, Maslinski S. Toll-like receptors as an innate immunity bridge to neuroinflammation in medulloblastoma. Folia Neuropathol 2012; 50: 375-381.
29. Michor F, Nowak MA, Iwasa Y. Evolution of resistance to cancer therapy. Curr Pharm Des 2006; 12: 261-271.
30. Neeper M, Schmidt AM, Brett J, Yan SD, Wang F, Pan YC, Elliston K, Stern D, Shaw A. Cloning and expression of a cell surface receptor for advanced glycosylation end products of proteins. J Biol Chem 1992; 267: 14998-15004.
31. Neves AA, Brindle KM. Assessing responses to cancer therapy using molecular imaging. Biochem Biophis Acta 2006; 1766: 242-261.
32. Oldford SA, Haild ID, Howatt MA, Leiva CA, Johnston B, Marshall JS. A critical role for mast cells and mast cell-derived IL-6 in TLR2-mediated inhibition of tumor growth. J Immunol 2010; 185: 7067-7076.
33. Palm NW, Medzhitov R. Pattern recognition receptors and control of adaptive immunity. Immunol Rev 2009; 227: 221-233.
34. Ribatti D, Ranieri G. Tryptase, a novel angiogenic factor stored in mast cell granules. Exp Cell Res 2015; 332: 157-262.
35. Sasahira T, Akama Y, Fujii K, Kuniyasu H. Expression of receptor for advanced glycation end products and HMGB1/amphoterin in colorectal adenomas. Virchows Arch 2005; 446: 411-415.
36. Schaefer L, Babelova A, Kiss E, Hausser HJ, Baliova M, Krzyzankova M, Marsche G, Young MF, Mihalik D, Götte M, Malle E,

Schaefer RM, Gröne HJ. The matrix component biglycan is proinflammatory and signals through Toll-like receptors 4 and 2 in macrophages. J Clin Invest 2005; 115: 2223-2233.
37. Shi H, Kokoeva MV, Inouye K, Tzameli I, Yin H, Flier JS. TLR4 links innate immunity and fatty acid-induced insulin resistance. J Clin Invest 2006; 116: 3015-3025.
38. Sparvero LJ, Asafu-Adjei D, Kang R, Tang D, Amin N, Im J, Rutledge R, Lin B, Amoscato AA, Zeh HJ, Lotze MT. RAGE (Receptor for Advanced Glycation Endproducts), RAGE ligands, and their role in cancer and inflammation. J Transl Med 2009; 17: 7-17.
39. Taguchi A, Blood DC, del Toro G, Canet A, Lee DC, Qu W, Tanji N, Lu Y, Lalla E, Fu C, Hofmann MA, Kislinger T, Ingram M, Lu A, Tanaka H, Hori O, Ogawa S, Stern DM, Schmidt AM. Blockade of RAGE-amphoterin signalling suppresses tumour growth and metastases. Nature 2000; 405: 354-360.
40. van Heijst JW, Niessen HW, Hoekman K, Schalkwijk CG. Advanced glycation end products in human cancer tissues: detection of Nepsilon-(carboxymethyl)lysine and argpyrimidine. Ann N Y Acad Sci 2005; 1043: 725-733.
41. Vogl T, Tenbrock K, Ludwig S, Leukert N, Ehrhardt C, van Zoelen MA, Nacken W, Foell D, van der Poll T, Sorg C, Roth J. Mrp8 and Mrp14 are endogenous activators of Toll-like receptor 4, promoting lethal endoxin-induced shock. Nat Med 2007; 13: 1042-1049.
42. Yan SF, Ramasamy R, Schmidt AM. Mechanisms of disease: advanced glycation end-products and their receptor in inflammation and diabetes complications. Nat Clin Pract Endocrinol Metab 2008; 4: 285-293.

Original article

Folia Neuropathologica

Sporadic inclusion body myositis: clinical, pathological, and genetic analysis of eight Polish patients

Biruta Kierdaszuk[1], Mariusz Berdynski[2], Piotr Palczewski[3], Marek Golebiowski[3], Cezary Zekanowski[2], Anna Maria Kaminska[1]

[1]Department of Neurology, Medical University of Warsaw, [2]Department of Neurodegenerative Disorders and Neurogenetic Unit, Mossakowski Medical Research Center, Polish Academy of Sciences, Warsaw, [3]1st Department of Clinical Radiology, Medical University of Warsaw, Poland

Folia Neuropathol 2015; 53 (4): 355-366 DOI: 10.5114/fn.2015.56550

Abstract

Introduction: *Sporadic inclusion body myositis (sIBM) is one of the most common myopathies in patients above 50 years of age. Its progressive course finally leads to immobilisation, and no effective therapy exists. Its pathogenesis includes both degenerative and inflammatory processes, however, its direct causes remain unknown. Therefore, a possible genetic background of the disease must also be considered.*

Material and methods: *Here we report on twelve patients: eight with sporadic inclusion body myositis and four with other myopathies with rimmed vacuoles in muscle biopsy. All patients were evaluated clinically, morphologically, radiologically, and genetically.*

Results: *All patients with sIBM presented both shoulder and pelvic girdle muscle involvement. In addition, distal upper and lower limb muscle weakness was noted. Patients with other muscle disorders showed effects mainly in proximal muscles and marked calf muscle hypertrophy. In sIBM cases computed tomography of lower limb muscles revealed atrophy that was most pronounced within the quadriceps femoris and gracilis muscles in the thighs and within the medial head of the gastrocnemius muscle and the tibialis anterior muscle in the lower legs. On light microscopy mononuclear cell invasion of muscle fibres was present in six patients with sIBM. On electron microscopy myofibrillar disorganisation and mitochondrial abnormalities were noted in all sIBM patients, whereas cytoplasmic tubulofilamentous inclusions were seen in three patients and both cytoplasmic and nuclear inclusions in one of them. According to the criteria by Rose et al. (2011) six patients were classified as "clinico-pathologically defined IBM", one as "clinically defined IBM", and one as "probable IBM". Pathological deposits of TDP-43 were found in muscles in all sIBM as well as in control cases. Additionally, accumulation of other proteins thought to be associated with sIBM, like β-amyloid, α-synuclein, and tau protein, was present in the most of examined biopsies. All twelve patients were screened for the presence of causative mutations in TARDBP, VCP, HNRNPA1, and HNRNPA2B1 genes. Additionally, analysis of C9ORF72 hexanucleotide repeat expansion was performed. No causative mutations were found in any of the patients.*

Conclusions: *Our study provides the first – to our knowledge – comprehensive clinical, pathological, and genetic workup of a group of Polish patients.*

Key words: *inclusion body myositis, muscle biopsy, TDP-43, muscles' CT, genetic diagnostics.*

Communicating author:

Prof. Anna M. Kaminska, Department of Neurology, Medical University of Warsaw, 1A Banacha St., 02-097 Warsaw, Poland, phone: +48 22 599 28 58, fax: +48 22 599 18 57, e-mail: amkaminska@wum.edu.pl

Introduction

Sporadic inclusion body myositis (sIBM) is an untreatable muscle disorder with weakness beginning after 50 years of age. It is more common in men than in women. Its pathogenesis remains undiscovered and the coexistence of inflammatory, degenerative, genetic, and environmental factors has been proposed. A possible genetic background is also considered. Its progressive course usually leads to immobilisation and severe dysphagia [3]. Both proximal and distal muscle weakness is observed, and the quadriceps, foot extensors, and deep finger flexors are most severely weakened. Creatine kinase (CK) activity may be slightly elevated. Electromyography studies (EMG) show myogenic or mixed myogenic and neurogenic pattern. Since clinical features of sIBM are not clearly delineated, morphological assessment of muscle biopsy is extremely important. Light microscopy examination reveals eosinophilic inclusions, necrotic fibres, and sometimes inflammatory infiltrates. Rimmed vacuoles are considered a hallmark of the disease. Additionally, immunohistochemistry shows deposits of various proteins such as β-amyloid, TDP-43 (TAR DNA-binding protein 43), tau protein, and α-synuclein [3,19]. Electron microscopy (EM) examination reveals the presence of tubulofilamentous inclusions – both cytoplasmic and nuclear, degeneration of myofibrils, accumulation of abnormal mitochondria, and cytoplasmic bodies.

Inclusion body myositis diagnostic criteria were first proposed by Griggs *et al*. in 1995 [11]. In 2007 Needham and Mastaglia included additional muscle biopsy features, such as expression of MHC-I [13]. Later criteria were repeatedly modified, and the latest version comes from 2011 [14]. It is worth mentioning that among the major changes were the increase in the age of onset (to 45 years) and the introduction of three categories of IBM, namely "clinico-pathologically defined IBM", "clinically defined IBM", and "probable IBM". The authors emphasised that, due to sampling error or the early stage of the disease, not all pathological changes might be present in muscle biopsy [15]. Therefore, the diagnosis should be made according to both clinical and morphological features.

Over the last decades numerous pathogenic genes potentially involved in sporadic inclusion body myositis have been suggested. However, phenotype-genotype correlations are still poorly understood. Up to now all attempts to successfully treat inclusion body myositis failed. Neither corticosteroids and other immunosuppressive drugs nor intravenous immunoglobulins and plasma exchange were shown to improve clinical symptoms and prognosis.

Our study provides the first – to our knowledge – comprehensive clinical, pathological, and genetic workup of a group of eight sIBM Polish patients.

Material and methods

Patients

Clinical data of eight male patients aged 49 to 67 years with the diagnosis of sporadic IBM, hospitalised between 2002 and 2013 in the Department of Neurology of the Medical University of Warsaw were evaluated retrospectively. The course of the disease, distribution of muscle weakness, serum creatine kinase activity, and results of electrophysiological studies were evaluated. Additionally, four male patients aged 18 to 59 years with other primary muscle disorders were included in the study. The basis for including those patients was the presence of rimmed vacuoles in muscle biopsy. Among them there were three patients with clinically typical limb-girdle muscular dystrophy (LGMD) and one patient with genetically confirmed proximal myotonic myopathy (myotonic dystrophy type 2 – DM2). The "radiological control group" consisted of six men aged 58 to 65 years, with no signs and symptoms of neuromuscular disease. The study was approved by the Bioethical Committee at the Medical University of Warsaw.

Computed tomography studies

All computed tomography (CT) studies were performed using a 64-row scanner (Aquilion, Toshiba) without administration of contrast medium. The proximal one third of the thighs and lower legs were scanned. A low-dose protocol with automatic tube current modulation was used to minimise the radiation dose received by the patients.

Images in the axial (10 mm reconstructed slices) and coronal plane (5 mm reconstructed slices) were reviewed by an experienced musculoskeletal radiologist on the soft tissue (to grade muscles' atrophy) and bone window (to exclude bone pathology that may lead to muscle atrophy). Muscle atrophy was assessed on a five-point scale based on the scale

originally developed by Goutallier *et al*. for grading muscular fatty degeneration in the rotator cuff (Table I) [10]. The control group consisted of six age-matched healthy volunteers (male, aged 58 to 65 years). The exclusion criteria for healthy volunteers included history of chronic lower back pain and significant trauma of the lower extremities.

Muscle biopsy

The open muscle biopsies were performed under local anaesthesia. The samples were obtained from the quadriceps in all eight patients with sIBM and in three patients with other myopathies. A biopsy from biceps brachii muscle was carried out in one patient. The muscle specimens were processed for further analyses using routine methods [6].

Light microscopy

All 12 muscle biopsies were assessed on light microscopy (LM). Biopsied tissue was frozen in isopentane cooled in liquid nitrogen, cut on a cryomicrotome with a slice thickness of 8 µm and stained for a battery of routine histological and histochemical methods as well as for immunohistochemistry.

Electron microscopy

Ultrastructural examination was done in all patients. Samples for electron microscopy (EM) were fixed in glutaraldehyde and post-fixed in osmium tetroxide before embedding in Spurr embedding medium. Ultrathin sections of the selected areas were stained with uranyl acetate and counterstained with lead citrate. The samples were viewed with a JEM 1200 EX2 electron microscope.

Immunohistochemical studies

In six patients with inclusion body myositis the immunostaining for the β-amyloid (NCL-B-Amyloid antibody, Novocastra), TDP-43 (TARDBP monoclonal antibody, Abnova), tau protein (NCL-Tau-2 antibody, Novocastra), and α-synuclein (Anti-Synuclein antibody, Chemicon) was performed using guidelines provided by each company. Additionally, the same procedures were applied in three of four patients with other myopathies. In two patients with sIBM and in one patient with LGMD the immunohistochemistry evaluation was not done according to the remote time of muscle biopsy.

Table I. Scale used for the grading of muscle atrophy in computed tomography (CT) (adapted from Goutallier *et al*., 1994) [10]

Atrophy grade	CT findings
0	No atrophy
1	Minimal atrophy, muscle contains some streaks of fat
2	Marked fatty degeneration with still more muscle than fat
3	Advanced fatty degeneration with more fat than muscle
4	Complete atrophy, muscle fibres replaced by fat, only tendinous components preserved

Genetic analyses

All 12 patients were screened for the presence of known sIBM-causative mutations. Genomic DNA was isolated from peripheral blood leukocytes using standard methods. Intronic primers were used to amplify protein-coding exons of *TARDBP* and *VCP*, and exons coding for the prion-like domain of *HNRNPA1* and *HNRNPA2B1*. Amplicons were purified with Exonuclease I/FastAP (Fermentas) and sequenced on an ABI PRISM 3130 Genetic Analyser (Applied Biosystems) using a BigDye Terminator v1.1 Cycle Sequencing Kit (Applied Biosystems). Primers for *VCP* and *HNRNPA1*, and *HNRNPA2B1* were prepared as described by Hirano *et al*. 2015, and Seelen *et al*. 2014, respectively [12,16]. For *TARDBP* gene primers were designed using Primer 3 programme (Untergasser *et al*., 2012) [17]. Analysis of *C9ORF72* hexanucleotide repeat was performed in two stages: fragment lengths analysis and the repeat-primed PCR reaction previously described (DeJesus-Hernandez *et al*., 2011) [4].

Results

Clinical characteristics

Sporadic inclusion body myositis was diagnosed in eight male patients (number 1-8) with negative family history. Clinical characteristics are summarised in Table II. The age of onset varied from 46 to 65 years and the age of diagnosis from 49 to 67 years. The most often affected were the shoulder girdle (SG) and pelvic girdle (PG) muscles; however, in all patients distal upper limb (dUL) and distal lower limb (dLL) muscles involvement was also

Table II. Patients' clinical characteristics

Patient	Diagnosis	Age of onset/ Age of diagnosis	Affected muscles	CK (U/l)	NCS	EMG
1	sIBM/c-p-def.	59/63	SG, PG, dUL	55	n	M+N
2	sIBM/ c-p-def.	46/49	SG, PG, dLL	107	n	N
3	sIBM/ c-p-def.	65/67	SG, PG, dUL	89	n	n
4	sIBM/ c-p-def.	54/56	SG, PG, dUL, dLL	237	n	M
5	sIBM/c-def.	49/60	SG, PG, dLL	55	n	n
6	sIBM/prob.	58/61	dLL	19	n	n
7	sIBM/ c-p-def.	54/60	SG, PG, dUL, dLL	110	n	n
8	sIBM/ c-p-def.	55/55	SG, PG, dUL, dLL	49	n	M
9	LGMD	36/38	SG, PG	96	n	M
10	LGMD	12/18	SG, PG	248	n	M
11	LGMD	30/42	SG, PG	527	n	M
12	DM2	49/59	SG, PG, dUL	222	A-m	N

sIBM – inclusion body myositis, c-p-def. – clinico-pathologically defined IBM, c-def. – clinically defined IBM, prob. – probable IBM, LGMD – limb-girdle muscular dystrophy, DM2 – myotonic dystrophy 2, SG – shoulder girdle muscles, PG – pelvic girdle muscles, dUL – distal muscles of upper limb, dLL – distal muscles of lower limb, CK – creatine kinase, NCS – nerve conduction studies, EMG – electromyography studies, n – normal, A-m – axonal motor neuropathy, M – myogenic, N – neurogenic, M+N – myogenic and neurogenic

present. No calf muscle hypertrophy was observed. The course of the disease was progressive; nevertheless, all of the patients were mobile and only two of them used a walking stick. There were no reported difficulties in swallowing. Serum creatine kinase (CK) activity was moderately elevated, maximally up to seven times above the upper range (laboratory norm up to 34 U/l). Electromyography disclosed a myogenic pattern from biceps brachii and vastus lateralis muscles in two patients, a neurogenic pattern from biceps brachii, vastus lateralis, interosseous I, and tibialis anterior muscles in one patient, and a myogenic pattern in the tibialis anterior muscle and neurogenic pattern in vastus lateralis muscle in one patient. In four cases electromyography was normal. Nerve conduction studies showed no abnormalities.

Additionally, four male patients (number 9-12) with other primary muscle disorders and with rimmed vacuoles on light microscopy examination were included. Three patients had clinically typical LGMD phenotype, without genetic confirmation of the subtype of LGMD. One patient had genetically confirmed proximal myotonic myopathy (myotonic dystrophy type 2 – DM2) (Table II). The age of onset ranged from 12 to 49 years and the age of diagnosis from 18 to 59 years in that group. The weakness of shoulder and pelvic girdle muscles was more pronounced than in sIBM patients. Calf muscles hypertrophy was present in all four patients. Serum creatine kinase activity was markedly elevated, maximally up to fifteen times above the upper range (laboratory norm up to 34 U/l). Nerve conduction studies showed motor axonal neuropathy signs only in the patient with DM2. Electromyography from biceps brachii or vastus lateralis muscles presented a myogenic pattern in all patients with LGMD. In a patient with DM2 neurogenic pattern from biceps brachii and pseudomyotonic discharges in proximal muscles in the upper limb and in distal muscles in the lower limb were present.

Computed tomography studies

In the group of sIBM patients CT revealed a different degree of muscle atrophy in all but two patients. Muscle atrophy was symmetric and showed a slight predilection to the distal parts of muscle bellies in all but one patient. In the thighs, the atrophy was most pronounced within the quadriceps femoris and gracilis muscles, while in the lower legs it was within the medial head of the gastrocnemius muscle and within the tibialis anterior muscle (Fig. 1A-B). A summary of the degree of muscle atrophy results for the eight sIBM patients is presented in Fig. 2.

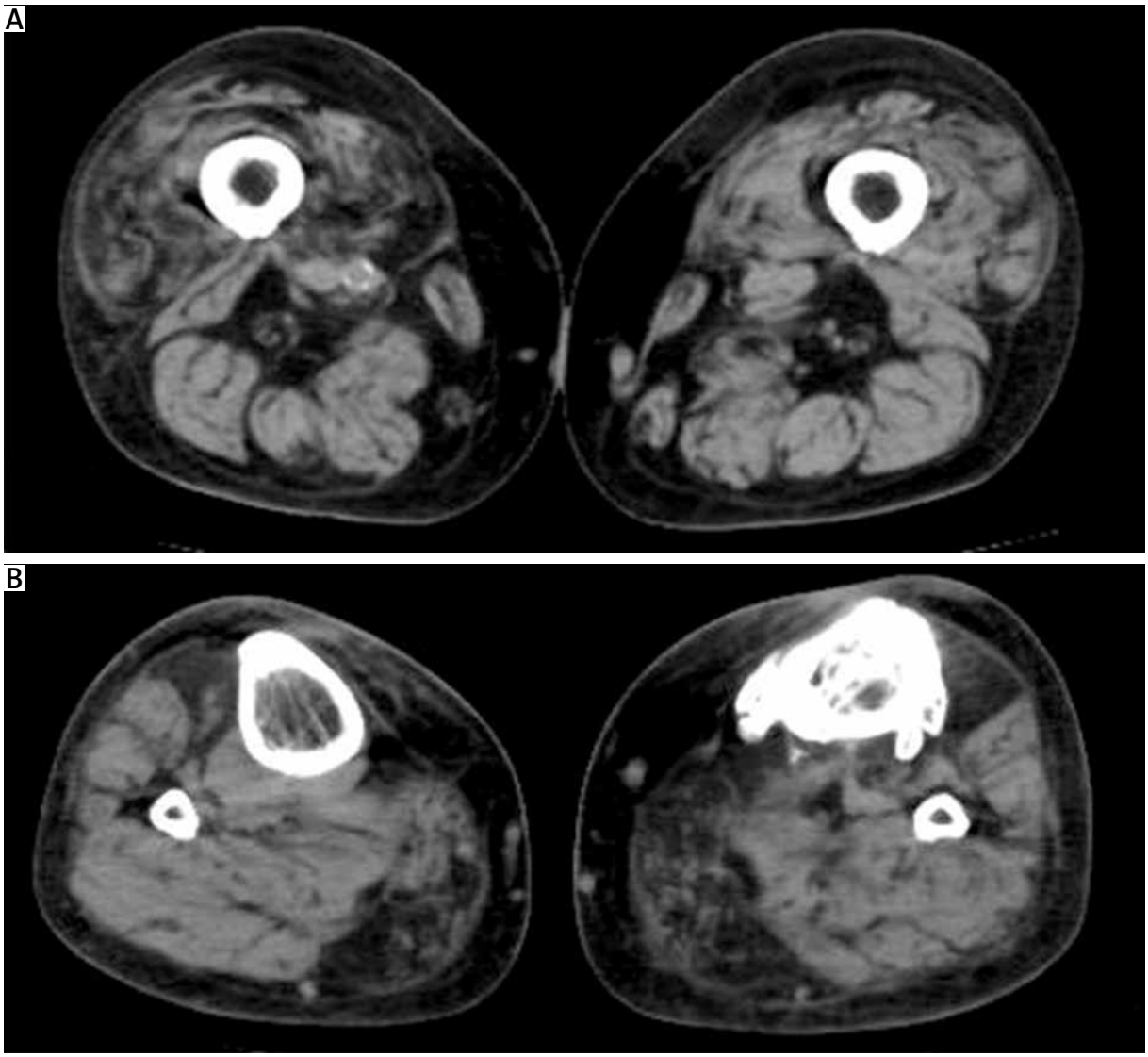

Fig. 1. Computed tomography images in a patient with "clinico-pathologically defined" sIBM: **A)** atrophy of quadriceps femoris muscle (grade 3 on the right, grade 2 on the left), **B)** atrophy of the medial head of the gastrocnemius muscle and within the tibialis anterior muscle (grade 4 on both sides).

In the control group, minimal muscle atrophy limited to the medial heads of the gastrocnemius muscle (grade 1 on the right, grade 2 on the left) was found in one 63-year-old man with no signs and symptoms of neuromuscular disease. All remaining participants of the control group had no muscle atrophy.

Muscle biopsies assessment

The results of light microscopic and ultrastructural evaluation are summarised in Table III and IV, respectively. The assessment of muscle samples on light microscopy revealed variation in fibre size in all 12 patients. There were many atrophic or hypertrophic fibres, fibres with internal nuclei, and muscle fibre splitting. Infiltration of mononuclear cells was observed in six patients with sIBM. "Rimmed vacuoles" considered characteristic for sIBM were noted in all 12 samples (Fig. 3A-D). Electron microscopy studies were performed in all patients (Fig. 4A-D). Myofibrillar disorganisation and mitochondrial abnormalities were observed in all biopsies. Lipofuscin accumulation was seen in all samples except for one patient with LGMD. Tubulofilamentous cytoplasmic inclusions composed of 15-18-nm tubulofil-

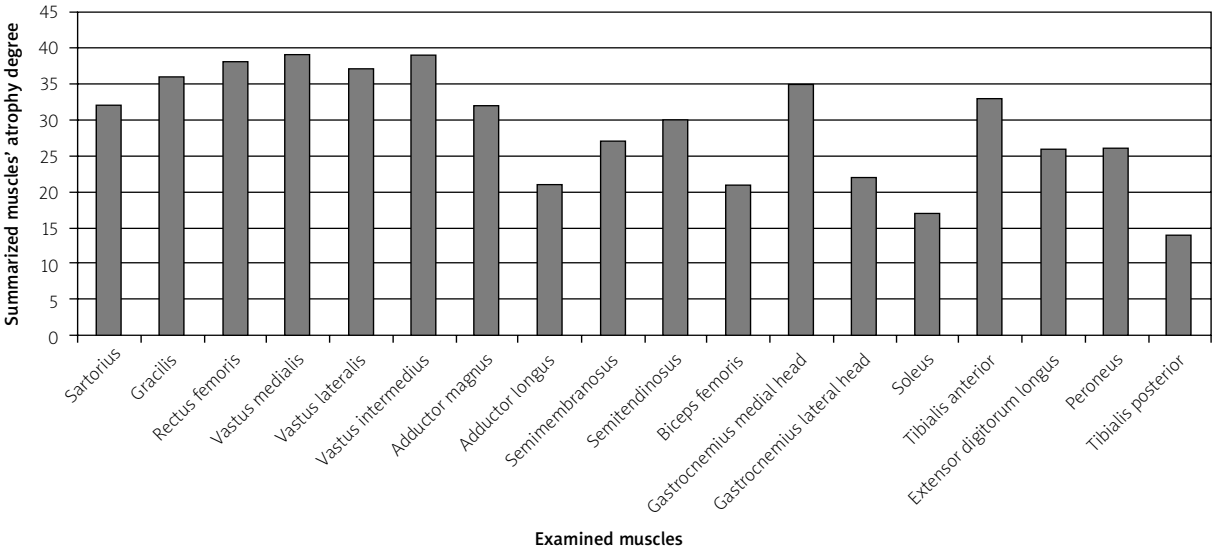

Fig. 2. Summarised muscle atrophy degree results.

aments were noted in two patients with sIBM. Both nuclear and cytoplasmic tubulofilamentous inclusions were observed in one sIBM and were present in one LGMD 18-year-old patient with biopsy and with other clinical and morphological findings supporting LGMD diagnosis.

Different patterns of accumulation of pathological proteins were observed in the examined biopsies. Immunohistochemical stains presented strong accumulation of TDP-43 in the subsarcolemmal and intracytoplasmic regions, in the atrophied fibres, in rimmed vacuoles, and in the blood vessels in half of the examined sIBM cases and in the patient with DM2 (Fig. 5A). β-amyloid aggregates, located in the subsarcolemmal and intracytoplasmic regions and in the atrophied fibres, were observed in all performed biopsies, being most prominent in the patient with DM2 (Fig. 5B). Tau protein accumulation, mostly located in the subsarcolemmal region, was present in six sIBM and in two control patients (Fig. 5C). Also

Table III. Light microscopy results

Patient	Varied fibre size or shape	Necrosis or necrosis with phagocytosis	Mononuclear cell invasion	Rimmed vacuoles	Inclusions	Lobulated fibres	Other
1	+	+	+	+	+	+	Connective tissue hypertrophy
2	+	+	+	+	+	–	–
3	+	+	+	+	+	–	–
4	+	+	+	+	+	–	–
5	+	–	–	+	–	–	Ring fibres
6	+	–	–	+	+	–	–
7	+	+	+	+	+	–	–
8	+	+	+	+	+	–	–
9	+	+	+	+	+	+	–
10	+	–	+	+	–	+	–
11	+	+	+	+	+	–	–
12	+	–	–	+	+	–	Internal nuclei

+ presence of abnormality, – absence of abnormality

Table IV. Electron microscopy results

Patient	Cytoplasmic inclusions	Nuclear inclusions	Myofibril abnormalities	Mitochondrial abnormalities	Cytoplasmic bodies	Lipofuscin accumulation	Myelin structures
1	+	–	+	+	–	+	+
2	–	–	+	+	+	+	–
3	–	–	+	+	–	+	–
4	+	+	+	+	+	+	+
5	–	–	+	+	–	+	–
6	–	–	+	+	–	+	–
7	+	–	+	+	–	+	+
8	–	–	+	+	+	+	+
9	–	–	+	+	–	–	–
10	+	+	+	+	+	+	+
11	–	–	+	+	–	+	–
12	–	–	+	+	–	+	–

+ presence of abnormality, – absence of abnormality

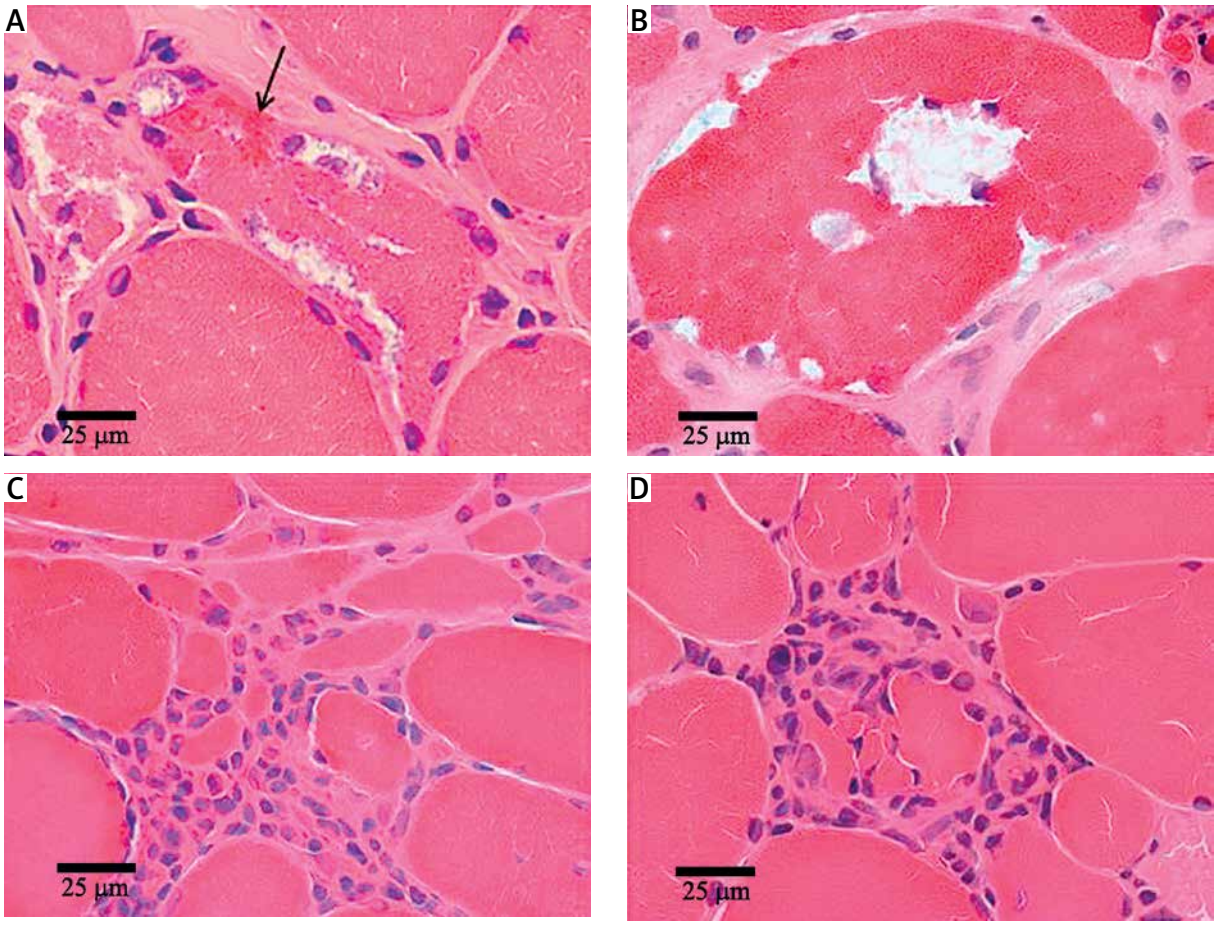

Fig. 3. Haematoxylin-eosin staining from sIBM patients: **A)** cytoplasmic inclusions (arrow), **B)** rimmed vacuoles, **C)** mononuclear cells invasion, **D)** necrosis with phagocytosis. Bar 25 µm.

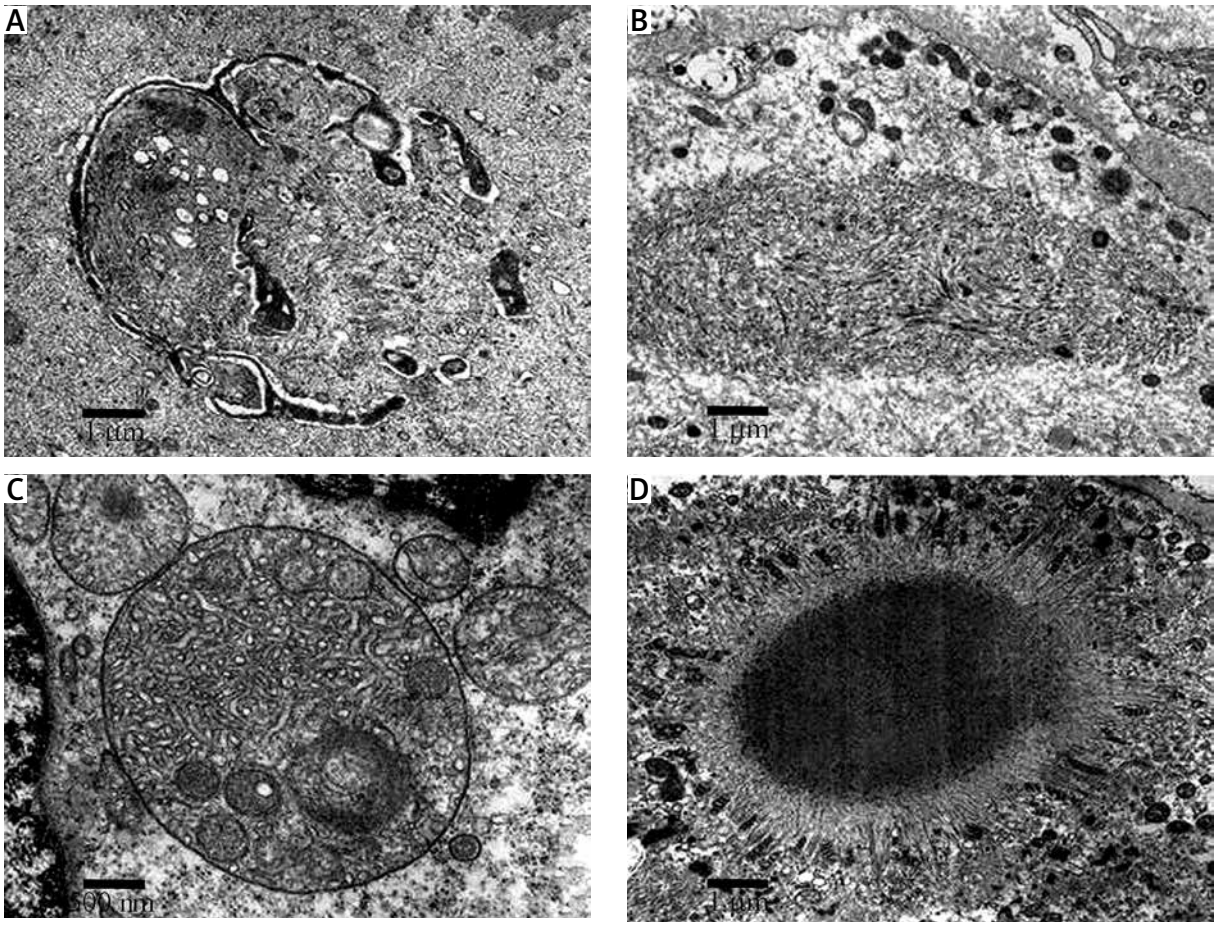

Fig. 4. Electron microscopy results from sIBM patients: **A)** nuclear inclusions, **B)** cytoplasmic inclusions, **C)** mitochondrial abnormalities, **D)** cytoplasmic body. Bar 1 µm for **A)**, **B)**, and **D)**; bar 500 nm for **C)**.

α-synuclein aggregates, located in the subsarcolemmal and intracytoplasmic regions mostly in the atrophied fibres, were noted in all examined cases (Fig. 5D). The results of immunohistochemical studies are listed in Table V.

Based on such comprehensive evaluation, according to Rose *et al.*'s criteria, six patients (numbers 1-4, 7, and 8) were classified as "clinico-pathologically defined IBM", one patient (number 5) as "clinically defined IBM", and one patient (number 6) as "probable IBM" [14].

Genetic analyses

No causative mutations were found in the protein-coding sequences of *TARDBP*, *VCP*, *HNRNPA1*, *HNRNPA2B1*, and *C9ORF72* genes in any of the examined patients with sIBM and other myopathies. Two novel and probably not pathogenic intronic insertions and known exonic and intronic polymorphisms were identified in *VCP* and *HNRNPA2B1* genes (see Table VI).

Discussion

The pathogenic mechanisms of sIBM are still unknown. It is believed that both environmental and genetic factors can contribute to the disease process. Clinical diagnosis of sIBM presents many problems and in most cases requires additional morphological, radiological, and genetic assessment. No single procedure is unreservedly precise, and only occasionally can the disease be confirmed by specific mutation. The primary diagnostic criteria for sporadic IBM were first proposed by Griggs *et al*. in 1995 and they emphasised the role of skeletal muscle biopsy [11]. Inclusion criteria covered duration of the disease above six months, age of onset above 30 years, both proximal and distal muscle weakness of upper and lower limbs, and negative family history.

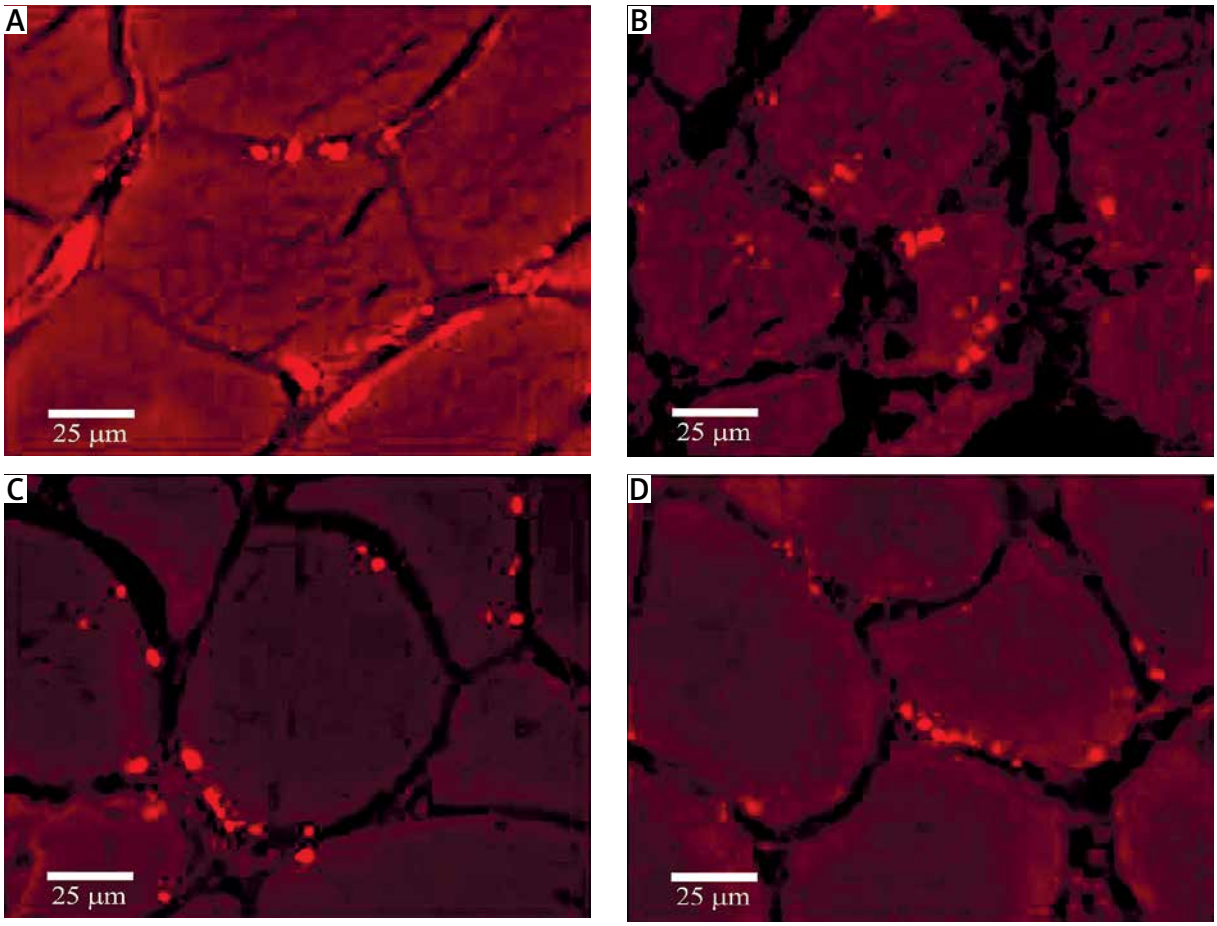

Fig. 5. Immunohistochemical results from sIBM patients: **A)** TDP-43 aggregates, **B)** β-amyloid aggregates, **C)** tau protein aggregates, **D)** α-synuclein aggregates. Bar 25 µm.

Table V. Immunohistochemistry results

Patient	TDP-43	β-amyloid	tau protein	α-synuclein
1	++; SS, AF, IC	+; SS, AF	+; SS, AF	+; SS, AF, IC
2	ND	ND	ND	ND
3	+; SS, AF, V	+; SS, AF	+; SS, AF	+; SS, AF
4	ND	ND	ND	ND
5	++; SS, IC	++; SS	+++; SS	ND
6	++; SS	+; SS	++; SS	+; SS
7	+; SS, AF, V	++; SS, AF, IC	+; AF	+; SS, AF
8	++; AF, RV, V	+; SS	+; SS, AF	+; SS, AF, IC
9	+; SS	+; SS	ND	ND
10	ND	ND	ND	ND
11	+; SS, AF, V	+; AF, IC	+; SS	+; SS, AF
12	++; SS, V	+++; SS, AF, IC	+++; SS, AF, IC, V	+; SS, AF

+ slight accumulation, ++ strong accumulation, +++ excessive accumulation
SS – subsarcolemmal, AF – atrophied fibres, IC – intracytoplasmic, V – blood vessels, RV – rimmed vacuoles
ND – not done

Table VI. Genetic analyses results

Gene	dbSNPs	Localization	Most severe potential consequence	MAF
TARDBP	rs968545	Intron	Unknown	0.125 (T)
	rs4133584	Intron	Unknown	0.458 (C)
VCP	rs10972300	Intron	Unknown	0.208 (A)
	rs514492	Intron	Splice region variant	0.167 (G)
	g.16046_16047insTTGTGTACTGT*	Intron	Unknown	0.292 (INS)
	rs2258240	Intron	Unknown	0.500 (G)
	rs562381	Exon	Non-coding transcript exon variant	0.333 (T)
	rs684562	Intron	Splice region variant	0.125 (A)
HNRNPA1	rs7967622	Intron	Unknown	0.500 (T)
HNRNPA2B1	g.12606_12607insGAAGATAA*	Intron	Unknown	0.042(INS)

MAF – minor allele frequency
**Novel variant, VCP NCBI Reference Sequence: NG_007887.1, HNRNPA2B1 NCBI Reference Sequence: NG_029680.1*

Laboratory abnormalities included serum creatine kinase activity not more than 12-times normal, typical muscle biopsy changes, and diversified pattern of electromyography. "Definite" inclusion body myositis was recognised when muscle biopsy presented mononuclear cell invasion of non-necrotic muscle fibres, vacuolated muscle fibres and intracellular amyloid deposits, or 15-18 nm tubulofilaments. In such cases no additional clinical and laboratory criteria were necessary. "Possible" inclusion body myositis was considered when muscle biopsy presented only inflammatory features and the patient exhibited all of the clinical and laboratory symptoms mentioned above. Later Needham and Mastaglia applied different morphological criteria [13]; however, they emphasised that the lack of particular changes in muscle biopsy cannot exclude IBM. They introduced the term "probable" inclusion body myositis to characterise patients with incomplete biopsy criteria, and the term "possible" IBM to distinguish patients with atypical muscle involvement and non-specific muscle biopsy findings. Finally, Rose in cooperation with the European Neuromuscular Centre (ENMC) developed the so-called "IBM Research Diagnostic Criteria 2011", published as a workshop report in 2013 [14]. The symptoms had to last for at least 12 months, the age of onset was increased to 45 years, and serum creatine kinase activity had to be no greater than 15-times above the upper limit of normal. The knee extension and finger flexion weakness had to be more pronounced than hip flexion weakness and shoulder abduction weakness, respectively. If these features were accompanied by all pathological changes (which covered endomysial inflammatory infiltrates, rimmed vacuoles, β-amyloid or TDP-43 accumulation, or inclusions composed of 15-18 nm tubulofilaments in EM), then "clinico-pathologically defined IBM" could be recognised. When not all pathological changes were present, the diagnosis was classified as "clinically defined IBM". And when not all clinical features were expressed, "probable IBM" was diagnosed. Although patients included in our study were hospitalised between 2002 and 2013 in the Department of Neurology, their clinical and morphological data were re-evaluated according to Rose *et al.*'s criteria developed in 2011. Application of those criteria in our study allowed us to recognise "clinico-pathologically defined IBM" in six cases, "clinically defined IBM" in one case, and "probable IBM" in one.

According to the literature, the muscle assessment on light microscopy should be focused on vacuolar degeneration and atrophy of muscle fibres with mononuclear cell infiltrations. The so-called "rimmed vacuoles" are considered the hallmark for sIBM; nevertheless, they are seen in many other muscle disorders, for example in inclusion body myopathy with Paget's disease and frontotemporal dementia (IBMPFD), in oculopharyngeal muscular dystrophy, or in myofibrillar myopathies [1]. Additionally, tubulofilamentous inclusions in the cytoplasm or in the nuclei can be found on electron microscopy in a variety of neuromuscular diseases [7,8]. Numerous studies have showed deposits of

different proteins in sIBM and none was disease specific [19]. The presence of TDP-43 aggregates in sIBM was highlighted in several articles [5]. In healthy subjects TDP-43 is present mostly in the nucleus, whereas in sIBM cases it is seen as non-nuclear sarcoplasmic deposits [15]. However, the precise role of TDP-43 accumulation is still unknown; it may cause neuronal dysfunction and disturb transcriptional regulation and RNA processing. We detected no *TARDBP* mutation associated with IBM, which is consistent with Qian Gang *et al*.'s study (Qian Gang *et al*., 2014) [9]. We did not detect pathogenic hexanucleotide expansion in *C9ORF72*, which is the most common cause of amyotrophic lateral sclerosis (ALS) and frontotemporal dementia (FTD) with TDP-43 inclusions (Weihl *et al*., 2015) [18]. Other possible genes associated with the disease may be *HNRNPA1* and *HNRNPA2B1* [16].

Mutations in prion-like domain of the RNA binding genes heterogeneous nuclear ribonucleoproteins A1 and A2B1 were shown to cause multi-system proteinopathy (MSP), which may be clinically presented as IBM, FTD, ALS, or Paget's disease (Seelen *et al*., 2014) [16]. However, our results, as well as the analysis of 31 patients from the Dutch population have shown no causative mutation in clinically defined IBM [16]. Our study also reveals no mutation in *VCP*, known to be causative for IBM.

The presented study describes eight patients with sporadic inclusion body myositis and four with other primary muscle disorders. This is the first, to our knowledge, such comprehensive workup of Polish patients with sIBM. Clinical findings were similar to those described in the literature and correlated with criteria proposed by Rose *et al*. [14]. The muscle involvement highlighted on computed tomography studies was comparable to that known from previous reports [2].

Morphological and immunohistochemical assessments proved that none of the changes are disease specific. The presence of TDP-43 and other protein aggregates were seen in all examined sIBM patients as well as in patients with other myopathies. It seems that, regardless of the primary cause, muscle fibre degeneration may be connected with the formation of various protein aggregates [14].

Conclusions

Our analysis of eight sIBM patients and four patients with other myopathies did not indicate the role of TDP-43 in sIBM pathogenesis. Muscle biopsy, although in some cases not conclusive for sIBM diagnosis, remains important for excluding other possible diagnoses of neuromuscular disorders. The analysis of known genes involved in sIBM pathogenesis did not confirm the genetic background in the examined group of eight Polish patients.

Disclosure

Authors report no conflict of interest.

Acknowledgments

This work has been supported by grant N N402 434238 from the Ministry of Science and Higher Education.

Dr Jo Lewkowicz edited our paper from the language point of view.

References

1. Cai H, Yabe I, Sato K, Kano T, Nakamura M, Hozen H, Sasaki H. Clinical, pathological, and genetic mutation analysis of sporadic inclusion body myositis in Japanese people. J Neurol 2012; 259: 1913-1922.
2. Cox FM, Reijnierse M, van Rijswijk CSP, Wintzen AR, Verschuuren JJ, Badrising UA. Magnetic resonance imaging of skeletal muscles in sporadic inclusion body myositis. Rheumatology 2011; 50: 1153-1161.
3. Dalakas MC. Sporadic inclusion body myositis – diagnosis, pathogenesis and therapeutic strategies. Nat Clin Pract Neurol 2006; 2: 437-447.
4. DeJesus-Hernandez M, Mackenzie IR, Boeve BF, Boxer AL, Baker M, Rutherford NJ, Nicholson AM, Finch NA, Flynn H, Adamson J, Kouri N, Wojtas A, Sengdy P, Hsiung GY, Karydas A, Seeley WW, Josephs KA, Coppola G, Geschwind DH, Wszolek ZK, Feldman H, Knopman DS, Petersen RC, Miller BL, Dickson DW, Boylan KB, Graff-Radford NR, Rademakers R. Expanded GGGGCC hexanucleotide repeat in noncoding region of C9ORF72 causes chromosome 9p-linked FTD and ALS. Neuron 2011; 72: 245-256.
5. Dubourg O, Wanschitz J, Maisonobe T, Béhin A, Allenbach Y, Herson S, Benveniste O. Diagnostic value of markers of muscle degeneration in sporadic inclusion body myositis. Acta Myol 2011; 30: 103-108.
6. Dubowitz V, Sewry CA. The procedure of muscle biopsy. Histological and histochemical stains and reactions. In: Muscle biopsy: A Practical Approach. 3rd ed. Saunders Elsevier, Philadelphia 2007; pp. 3-40.
7. Fidziańska A, Kamińska A, Ryniewicz B. Congenital myopathy with tubular aggregates and tubulofilamentous IBM-type inclusions. Neuropediatrics 2005; 36: 35-39.
8. Fidzianska A, Ryniewicz B, Shen XM, Engel AG. IBM-type inclusions in a patient with slow-channel syndrome caused by

a mutation in the AChR epsilon subunit. Neuromuscul Disord 2005; 15: 753-759.
9. Gang Q, Bettencourt C, Machado P, Hanna MG, Houlden H. Sporadic inclusion body myositis: the genetic contributions to the pathogenesis. Orphanet J Rare Dis 2014; 9: 88.
10. Goutallier D, Postel JM, Bernageau J, Lavau L, Voisin MC. Fatty muscle degeneration in cuff ruptures. Pre- and postoperative evaluation by CT scan. Clin Orthop Relat Res 1994; 304: 78-83.
11. Griggs RC, Askanas V, DiMauro S, Engel A, Karpati G, Mendell JR, Rowland LP. Inclusion body myositis and myopathies. Ann Neurol 1995; 38: 705-713.
12. Hirano M, Nakamura Y, Saigoh K, Sakamoto H, Ueno S, Isono C, Mitsui Y, Kusunoki S. VCP gene analyses in Japanese patients with sporadic amyotrophic lateral sclerosis identify a new mutation. Neurobiol Aging 2015; 36: 1604.e1-6.
13. Needham M, Mastaglia FL. Inclusion body myositis: current pathogenic concepts and diagnostic and therapeutic approaches. Lancet Neurol 2007; 6: 620-631.
14. Rose MR, ENMC IBM Working Group. 188th ENMC International Workshop: Inclusion Body Myositis, 2-4 December 2011, Naarden, The Netherlands. Neuromuscul Disord 2013; 23: 1044-1055.
15. Salajegheh M, Pinkus JL, Taylor JP, Amato AA, Remedios N, Baloh RH, Greenberg SA. Sarcoplasmic redistribution of nuclear TDP-43 in inclusion body myositis. Muscle Nerve 2009; 40: 19-31.
16. Seelen M, Visser AE, Overste DJ, Kim HJ, Palud A, Wong TH, van Swieten JC, Scheltens P, Voermans NC, Baas F, de Jong JM, van der Kooi AJ, de Visser M, Veldink JH, Taylor JP, Van Es MA, van den Berg LH. No mutations in hnRNPA1 and hnRNPA2B1 in Dutch patients with amyotrophic lateral sclerosis, frontotemporal dementia, and inclusion body myopathy. Neurobiol Aging 2014; 35: 1956.e9-1956.e11.
17. Untergasser A, Cutcutache I, Koressaar T, Ye J, Faircloth BC, Remm M, Rozen SG. Primer3 – new capabilities and interfaces. Nucleic Acids Res 2012; 40: e115.
18. Weihl CC, Baloh RH, Lee Y, Chou TF, Pittman SK, Lopate G, Allred P, Jockel-Balsarotti J, Pestronk A, Harms MB. Targeted sequencing and identification of genetic variants in sporadic inclusion body myositis. Neuromuscul Disord 2015; 25: 289-296.
19. Weihl CC, Pestronk A. Sporadic Inclusion Body Myositis: Possible pathogenesis inferred from biomarkers. Curr Opin Neurol 2010; 23: 482-488.

Original paper

Folia Neuropathologica

NF-κB deficit in spinal motoneurons in patients with sporadic amyotrophic lateral sclerosis – a pilot study

Dorota Sulejczak[1], Stanisław J. Chrapusta[1], Dorota Dziewulska[2,3], Janina Rafałowska[2]

[1]Department of Experimental Pharmacology, Mossakowski Medical Research Centre, Polish Academy of Sciences, Warsaw, [2]Department of Experimental and Clinical Neuropathology, Mossakowski Medical Research Centre, Polish Academy of Sciences, Warsaw, [3]Department of Neurology, Medical University of Warsaw, Warsaw, Poland

Folia Neuropathol 2015; 53 (4): 367-376 DOI: 10.5114/fn.2015.56551

Abstract

Amyotrophic lateral sclerosis (ALS) is a fatal incurable neurodegenerative disease whose etiology is unknown and pathogenesis is still not fully understood. A great majority of its cases are sporadic. Clinical ALS signs are caused by damage and dying-out of the lower and upper motor neurons. This study was aimed at identifying possible sporadic ALS-associated aberrations in the spinal cord expression of the transcription nuclear factor κ light-chain-enhancer of activated B cells (NF-κB). NF-κB is widely distributed among various cell types, including those specific for the central nervous system (CNS), and is involved in the control of many physiological and pathological processes, including, inter alia, inflammatory response, proliferation, angiogenesis, and cell survival and death. It is constitutively expressed and its inactive form resides in the cytoplasm. After activation, it enters the cell nucleus and promotes the transcription of target genes. NF-κB is a dimer and its most common form is a heterodimer made of subunits p50 and p65. In this study, we estimated and compared by immunohistochemical means the contents of these subunits in spinal cord motoneurons in a few archival cases of sporadic ALS of varying disease duration and the respective age-matched control cases with no CNS pathology. The major goal of the study was to seek possible changes in the expression of these proteins in the course of the disease. The control cases showed a strong expression of both p50 and p65 in spinal cord motoneurons, with both cytoplasmic and nuclear localization. In contrast, the ALS cases studies revealed a considerably lower and varying intensity of specific immunohistochemical staining for the two subunits, which suggested an increased deficit of their expression linked to longer disease duration. Moreover, there was an apparent shift toward mostly cytoplasmic localization of the two subunits. These preliminary data suggest that the changes in the expression of theses NF-κB subunits may be involved in pathogenesis of sporadic ALS.

Key words: *amyotrophic lateral sclerosis, motoneuron, neurodegeneration, NF-κB, spinal cord.*

Introduction

Nuclear factor κ light-chain-enhancer of activated B cells (nuclear factor κB – NF-κB) is a protein complex functioning as a transcription factor. It has been discovered in 1986 in mouse lymphocytes B as a constitutively expressed complex that binds to the promoter of the gene encoding the light chain κ of immu-

Communicating author:
Dorota Sulejczak, Department of Experimental Pharmacology, Mossakowski Medical Research Centre, Polish Academy of Sciences, 5 Pawińskiego St., 02-106 Warsaw, Poland, phone: +48 22 608 65 23, fax: +48 22 668 65 27, e-mail: dsulejczak@imdik.pan.pl

noglobulins and is indispensable for the expression of the gene [41]. Inactive NF-κB resides in the cytoplasm, but enters the cell nucleus upon activation, binds to the so-called κB elements located in the promoter region of target genes and activates expression of the genes [27]. Extensive studies on NF-κB have revealed that it is widely distributed in various cell types in both the vertebrates and invertebrates and takes part in many cellular processes. Its action is closely connected to multiple intracellular signaling pathways ending in the synthesis of proteins linked to: 1) responses to a variety of stimuli, including, but not limited to, ischemia, free radical stress, cytokine and UV actions, and some antigens [5,11,12,36,45], 2) oncogenesis, regulation of inflammatory processes and responses to infections [21,22], and 3) processes related to learning and memory as well as synaptic plasticity [2]. Studies performed during the last decade have extended the list of NF-κB commitments with the processes linked to angiogenesis and cell proliferation, survival and death (including roles in both the prevention and promotion of apoptosis) [32,43]; most recently, NF-κB was also credited with a role in the pathogenesis of a growing number of neurodegenerative diseases [6].

NF-κB acts as a homo- or heterodimer of members of the Rel family that includes five proteins: p65 (RelA), RelB, c-Rel, p50 and p52 that are divided between two sub-families. One of the latter comprises p65, RelB and c-Rel, which all possess a transcription activation domain and due to this characteristic are able of activating NF-κB target genes. The other sub-family comprises p50 and p52 that originate from their respective precursors p100 and p105 and are devoid of this domain. All the Rel proteins possess the evolutionary highly conserved Rel homology domain. This domain is responsible for subunit dimerization and binding to DNA, which allows activation of the target genes [15], and encompasses a nuclear localization sequence that enables the Rel proteins entering the cell nucleus [32]. In the inactive state, the nuclear localization sequences are blocked by the Rel homology domain-bound inhibitory proteins of the IκB family. Activation of NF-κB relies on phosphorylation of the respective IκB inhibitor that is next subject to ubiquitination and proteosomal degradation. The inhibitor-free dimeric NF-κB translocates then to the nucleus [15].

In mammalian cells, the most common isoform of NF-κB is the p50-p65 heterodimer [32]. In the central nervous system (CNS), this isoform has been identified in the Schwann cells [7], astrocytes [44], microglia [35] and neurons [14,17,18,26,29,40]. The p65 subunit is considered the most important NF-κB subunit in the nervous system [26,27]. NF-κB plays an important role in multiple physiological processes in the nervous system both during the ontogeny and after reaching maturity. It is well-known that this factor is responsible both for the control of apoptosis [31,40] and the promotion of the survival of nervous system cells [23]. This duality in NF-κB action is the consequence of a wide spectrum of the targets of this transcription factor, which includes both some pro-apoptotic (e.g., *Bax*) and anti-apoptotic genes (e.g., *bcl-2*). An NF-κB target is also the *Survival Motor Neuron* (*SMN*) gene that plays an essential role in motoneuron function and survival.

Amyotrophic lateral sclerosis (ALS) is a fatal incurable neurodegenerative disease with relatively fast clinical course. Its etiology is unknown and pathogenesis is far from fully elucidated. Its progress and the fatal outcome rely on the damage and dying-out of the neurons of the spinal cord anterior horns, motor nuclei of the cranial nerves within the brain stem as well as motoneurons in the cerebral cortex, that is, of the lower and the upper motor neuron [20,34]. About 90% of all ALS cases are sporadic (sALS). The remaining cases represent the so-called familial ALS (fALS), a minor subset of which are linked to identifiable heritable genetic damage. Our earlier investigation has revealed a probable role of aberration(s) in the expression of the SMN complex proteins, in sALS pathogenesis. This is because we found a major decrease in gemin 2 level correlating with sALS duration [37]. The present study was aimed at identifying possible aberrations in the expression of the key transcription factor NF-κB subunits p50 and p65 in the spinal cord motoneurons of sALS patients with differing duration of the disease.

Material and methods

The study material included archival paraffin blocks with spinal cord samples harvested from the cervical enlargements (C4-C8 level) of four patients from 52 to 74 years of age, who died 1-8 years after the clinical onset of sALS. Before death, all the patients revealed lower motor neuron damage with tetraparesis and bulbar syndrome. The controls comprised spinal cords from two age-matched patients who died from CNS-unrelated causes and with no

Table I. Clinical characteristics of the sporadic amyotrophic lateral sclerosis (sALS) cases and controls and estimation of motoneuron loss in the spinal cord anterior horns

Group	Case No.	Gender	Age (years)	Cause of death	sALS duration (years)	*Post-mortem* time (h)	Motoneuron loss
Controls	1	F	60	Digestive system hemorrhage	–	41	–
	2	F	67	Heart infarction	–	14	–
sALS	1	M	52	sALS	1	30	Mild
	2	F	59	sALS	1	22	Mild
	3	F	73	sALS	2	12	Moderate
	4	M	74	sALS	8	15	Extensive

record of neurological problems. Basic clinical characteristics of the cases and estimation of motoneuron loss in the spinal cord anterior horns in the studied samples are shown in Table I.

All experiments involving the human material were in agreement with the respective ethical principles as stipulated in the Helsinki Declaration and with the current law of Poland regarding the use of human organs and tissues in research. The study protocol has been filed with the Bioethics Committee of the Medical University of Warsaw. The Committee has raised no objection, and – because of the archival nature of the involved human tissue-containing material, full anonymization of the samples and the retrospective retroactive character of the study – has waived the need for consent from the next of kin of the donors (Permit No. AKBE/20/14).

The paraffin blocks with the formalin-fixed spinal cord samples were cut tranversely into 8 µm-thick sections, deparaffinized and rehydrated by routine procedures and then subjected to hematoxylin-eosin or cresyl violet staining or immunohistochemical labelings for p50 or p65 subunit of NF-κB. Immunohistochemistry was performed by the avidin-biotin-peroxidase method. Briefly, the rehydrated spinal cord slices were microwaved (3 × 10 min, in 10 mM citrate buffer pH 6.0) for antigen retrieval, and then were stained with primary antibodies (Santa Cruz Biotechnology, Dallas, TX, USA) against p50 (cat. no. sc-114; dilution 1 : 250) or p65 (cat. no. sc-109; dil. 1 : 250). Next, the samples were incubated with biotinylated goat F(ab)2 fragment of anti-rabbit IgG (Beckman Coulter, cat. no. PN IM0830; dil. 1 : 1500), and consequently with streptavidin-horseradish peroxidase solution. The final immune complexes were developed with diaminobenzidine as the chromogen and assessed in a light microscope (Nikon, Japan) equipped with a model CCD camera (Nikon) and a computerized image analyzer system. Specifity of the reaction was tested using a negative control procedure (with primary antibodies omitted); the test showed no immunostaining. The intensities of specific p50 and p65 immunoreactivities were assessed in the respective slices (4-6 slices per case), in all visible spinal cord motoneurons, employing an 8-bit scale (256 levels of gray). The gray scale levels for p50 immunoreactivity from all the analyzed slices from a given case were next averaged and used as one observation for statistical analysis; the same was done for the respective p65 immunoreactivity data. The sALS cases analyzed were divided between two groups: the group with short (1-year, n = 2) and the group with long (2- or 8-year, n = 2) course of the disease; the two control cases with no ALS comprised the control group. The quantitative immunostaing data were subject to a one-way ANOVA with group as the between-subject factor followed by the Tukey test.

Cell morphology in the studied samples was assessed in a separate series of the spinal cord samples that were subject to routine hematoxylin-eosin (H&E) and cresyl violet stainings, air-dried, coverslipped using Permount™ and then examined in the aforementioned computerized Nikon light microscopy system.

Results

Spinal cord sections from controls showed no symptoms of degeneration, and the motoneurons were of normal morphology (Fig. 1). The sections from sALS cases, both those with short (1 year) and longer (2 and 8 years) disease history, on the contrary, revealed obvious aberrations in the mor-

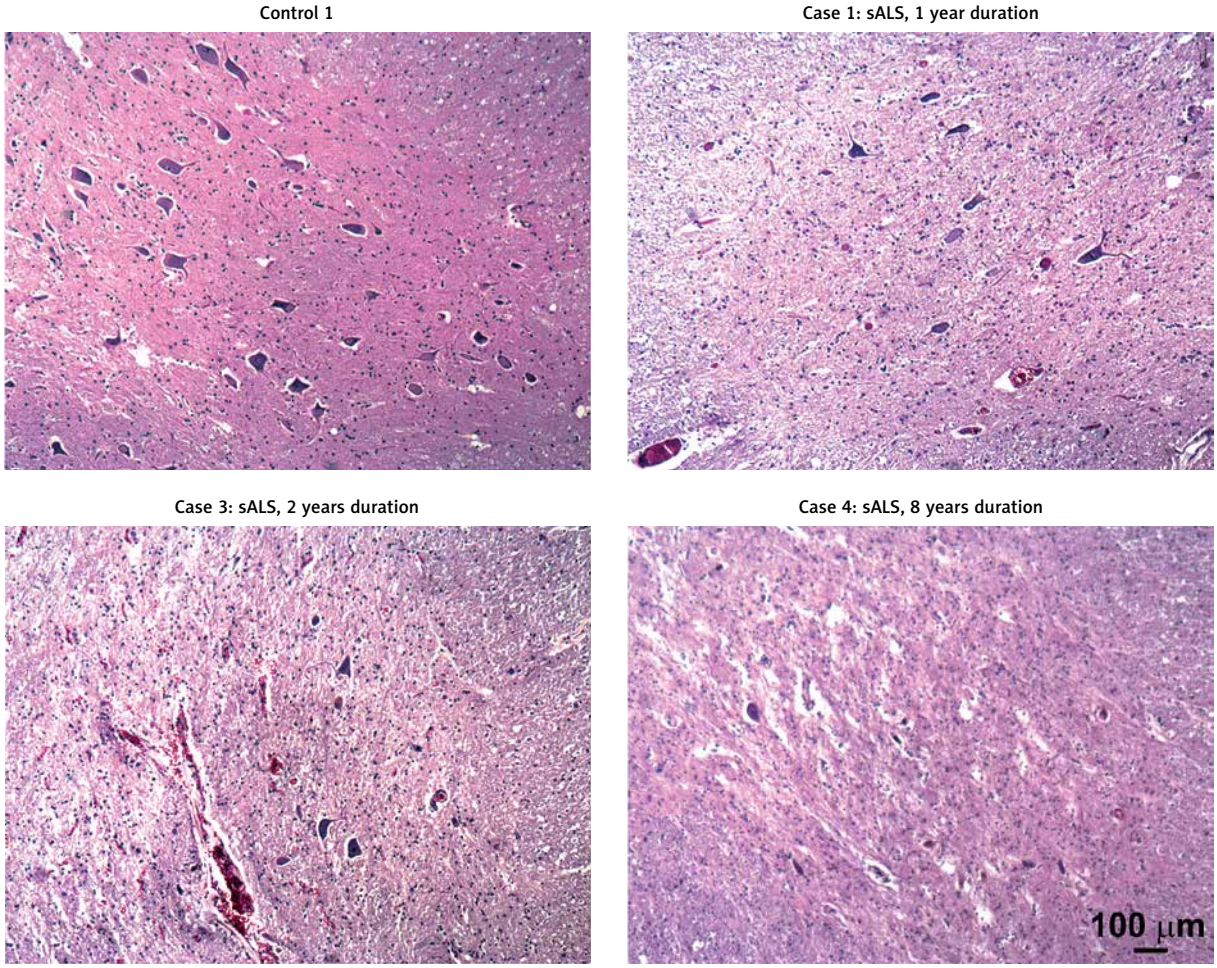

Fig. 1. H&E staining of spinal cord anterior horn sections from a control and sporadic amyotrophic lateral sclerosis (sALS) cases. The control section shows the presence of many motoneurons of normal morphology (left top panel). The sections from sALS cases reveal much lower motoneuron numbers.

phology of the surviving motoneurons: changes in both the shape and size (shrinkage), hiperchromatosis, and (typical of damaged neurons) tigrolysis of intensity that showed a great variability with regard both to individual case and cell (Fig. 2). The two sALS cases with 1-year history of the disease showed the presence of few tigrolysis-affected motoneurons; the numbers of these cells were considerably higher in the sALS cases with longer disease duration. Interestingly, the spinal cord sections from the former showed also the presence of few motoneurons with enlarged Nissl bodies, which might be related to a transient reinervation that occurs during the initial stage of the disease and may represent a compensation for degeneration of the other motoneurons (Fig. 2). Compared to the controls, the sections from sALS cases showed also clearly lower total motoneuron numbers, but no signs of apoptosis. This difference was rather small for the cases with short disease history, but was much higher in those with longer disease duration (see Fig. 1 and Table I).

For both p50 and p65, immunohistochemistry revealed a moderate cytoplasmic staining in non-neuronal cells, and an intense staining of the cytoplasm and even more intense staining of the nuclei of motoneurons in the controls; the apparent immunoreactivity was higher for p50 (Figs. 3 and 4). The motoneurons in spinal cord sections from sALS cases showed lower immunoreactivity levels for both p50 (Fig. 3) and p65 (Fig. 4). The sections from sALS cases compared to those from controls contained also considerably lower numbers of motoneurons with p50- or p65-positive nuclei. This difference was particularly evident in the two sALS cases with

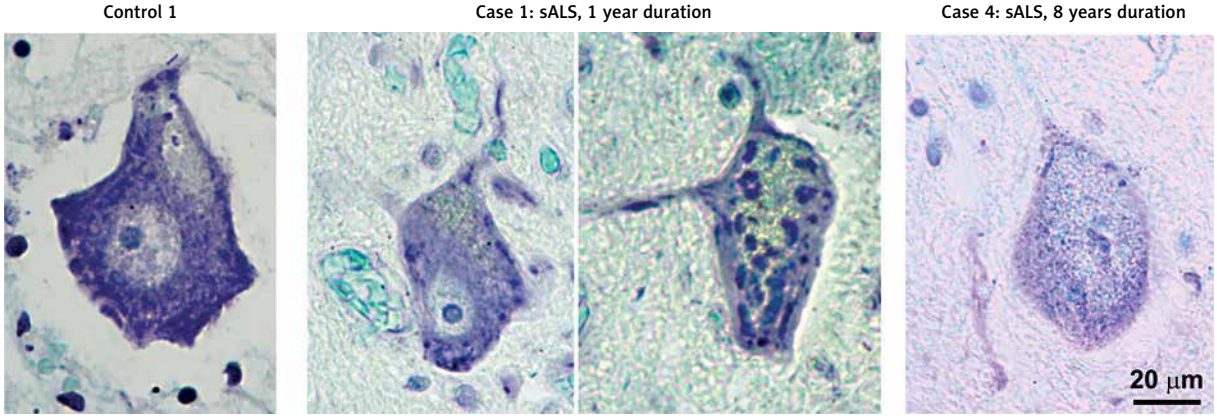

Fig. 2. Cresyl violet staining of spinal cord anterior horn sections from a control and selected sporadic amyotrophic lateral sclerosis (sALS) cases. The microphotograph of a section from a control (far left) shows a motoneuron of normal morphology, including typical-looking Nissl granules. The two middle microphotographs of a section from an sALS case with 1-year history show an enlargement (right) and decay (left) of Nissl bodies. The microphotograph of a section from an sALS case with 8-year history reveals extensive tigrolysis.

longer disease history. In the two cases with 1-year sALS duration there were a few motoneurons with p50- or p65-positive nucleus in each section analyzed. The remaining motoneurons showed p50 or p65 positivity only in the cytoplasm. The other two sALS cases (with longer disease history) revealed even lower numbers of motoneurons. Notably, the surviving motoneurons showed but a weak cytoplasmic staining, and only a minor fraction of these (a few in the case with 2-year, and only one in the case with 8-year ALS history, in all the studied sections combined) showed the presence of p50 or p65 in the nucleus.

Interestingly, the non-neuronal cells present in the spinal cord anterior horns sections showed heavy immunolabeling for both p50 and p65 in all sALS cases studied (Figs. 3 and 4). Many of these cells revealed nuclear localization of the NF-κB subunits.

Statistical analysis revealed significantly lower intensities of both the p50 and p65 immunoreactivities in the sALS cases with either 1-year or longer disease duration compared to the controls, while there was no statistically significant difference in this respect between the two sALS subsets (Table II). There was a high positive linear correlation between the p50 and p65 staining intensities as assessed across all the cases (sALS and controls combined) included in this study (n = 6; Pearson's correlation coefficient: R = 0.97, p = 0.0014). This correlation was in line with the presumed co-expression of the two NF-κB subunits in the same cells and their presumed heterodimerization.

Discussion

A large body of evidence indicates that NF-κB-mediated signaling plays an important role in neuron survival in many pathological entities, for review see [19,32]. The decrease in NF-κB expression and the shift toward its prevailing cytoplasmic localization associated with increased duration of the disease in our material of sALS strongly suggests a failing function of this transcription-regulating factor. This result may put in doubt the presumed importance of NF-κB for the processes that promote either the death or the survival of the analyzed cells. However, the absence of this factor in the nuclear compartment may indirectly contribute to the deficient neuroprotection, e.g. due to a diminished NF-κB-dependent expression of the anti-apoptotic *Bcl-2* gene [27]. The link between motoneuron death and function of anti- (e.g., Bcl-2) and proapoptotic proteins (e.g., Bax) is supported by a steadily growing number of studies [1,10,25,33,39,42].

Another important target gene of NF-κB is *SMN* that plays an essential role in both motoneuron survival and function. However, our earlier studies have revealed similar SMN immunoreactivity in sALS autopsy cases greatly differing in disease duration. The only exception was a single case with 8-year history of ALS with prominent symptoms of neurodegeneration in the few surviving motoneurons and

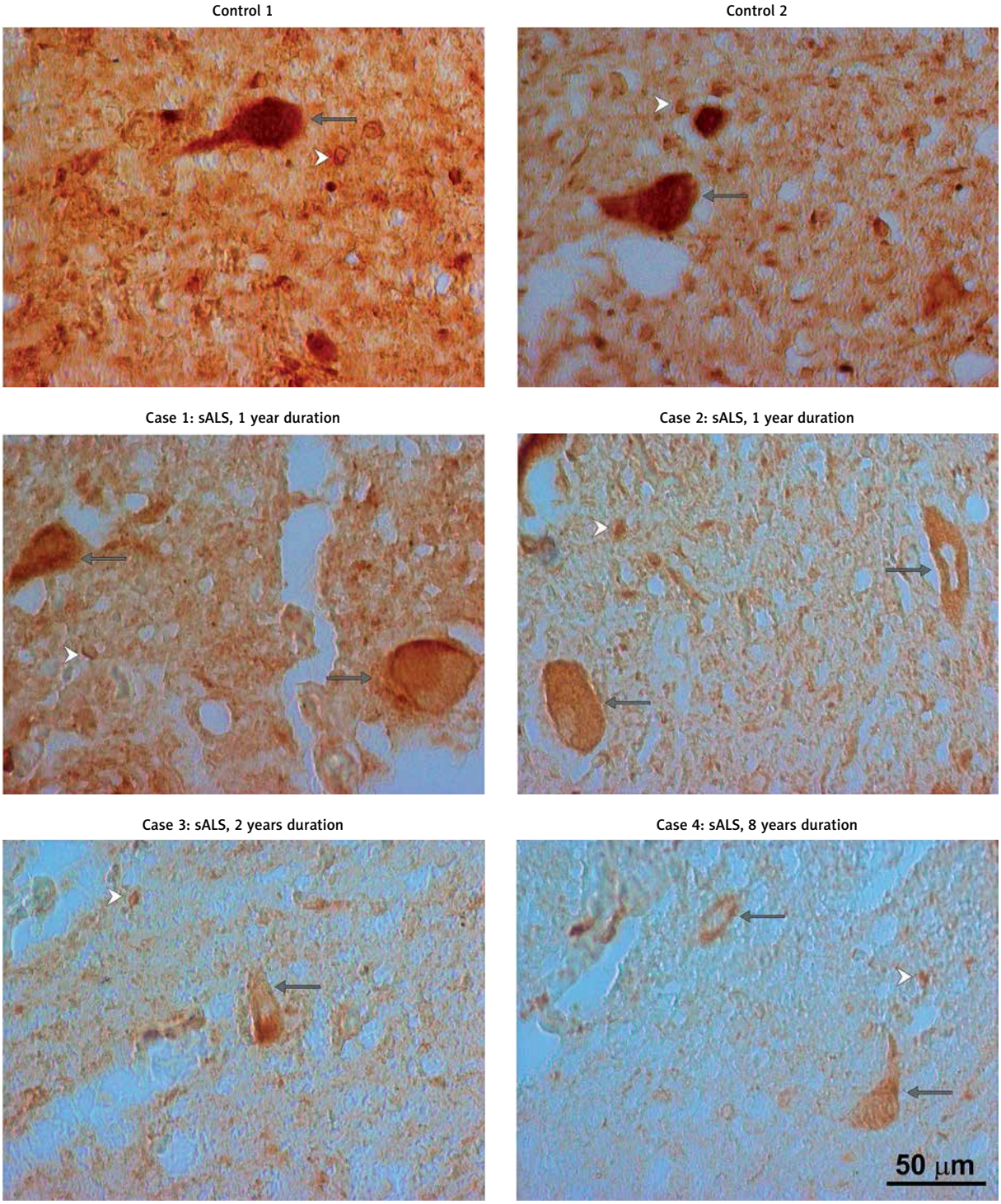

Fig. 3. NF-κB p50 subunit immunoreactivity in the anterior horn of spinal cords from controls and sporadic amyotrophic lateral sclerosis (sALS) cases. The sections from controls (top panel) show the presence of heavily stained motoneurons (long arrows) with both cytoplasmic and nuclear p50 staining. The sections from sALS cases (middle and bottom panels) reveal little or no p50 staining, particularly of cell nuclei; white arrowheads point to glial cells.

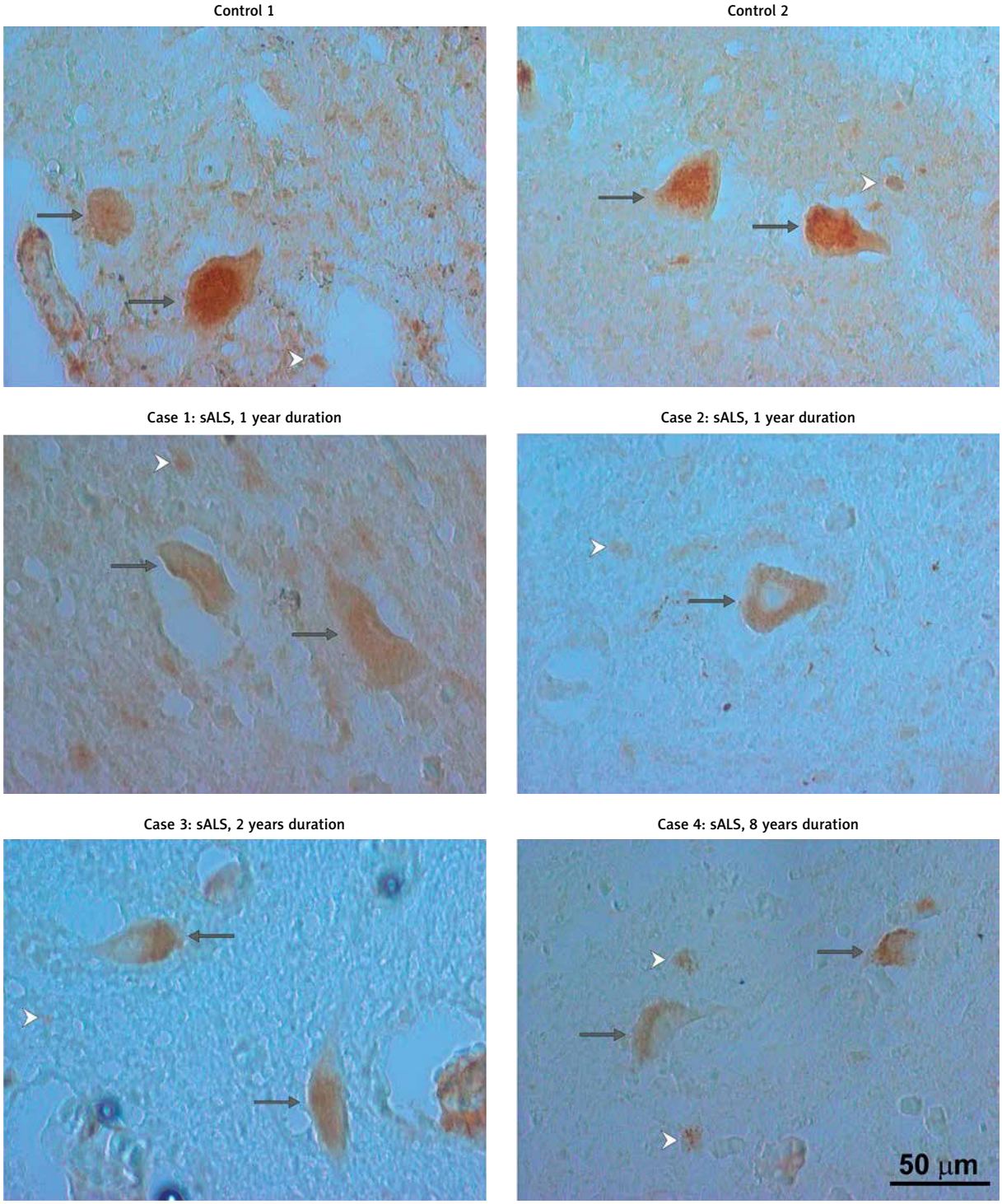

Fig. 4. NF-κB p65 subunit immunoreactivity in the anterior horn of spinal cords from control and sporadic amyotrophic lateral sclerosis (sALS) cases. The sections from controls (top panel) show the presence of intensively stained motoneurons (long arrows) with both cytoplasmic and nuclear p65 staining. The sections from sALS cases (middle and bottom panels) demonstrate little or no p65 labeling intensity, particularly of cell nuclei; white arrowheads point to glial cells.

Table II. A comparison of total (cytoplasmic + nuclear) NF-κB subunit immunoreactivities between spinal cord anterior horns' motoneurons from controls and sporadic amyotrophic lateral sclerosis (sALS) cases of varying disease duration

Group	NF-κB subunit immunoreactivity (8-bit gray scale levels)	
	p50	p65
Controls (n = 2)	178.2 ± 0.5	142.0 ± 5.5
1-year sALS history (n = 2)	142.9 ± 2.9*	108.7 ± 5.8*
Over 1-year sALS history (n = 2)	129.4 ± 8.6*	94.7 ± 2.8*

*Results are shown as the mean ± S.E.M.; *p < 0.05 versus the respective control value*

clearly lowered SMN level; the latter was obviously related to the poor condition of the cells [37].

The continuing SMN expression at the absence of NF-κB in the nucleus suggests that the expression under these conditions is controlled by different transcription factor(s); it has been shown that *SMN* is a target gene also for Elk-1 [9] and CREB [24]. However, the functionality of the SMN protein complex-dependent motoneuron survival pathway is in serious doubt. This is because of the evidence indicating a deficient production in sALS of gemin 2 that is a key subunit responsible for SMN binding with the other subunits of the SMN protein complex [37].

The actual role of NF-κB in the ALS-related neurodegeneration is presently under intense scrutiny, but the existing data are equivocal. Studies in transgenic mice overexpressing a mutated form of human SOD-1 have shown that blocking apoptosis by pharmacological induction of NF-κB in motoneurons prolongs survival of the cells [38]. Surprisingly, a neuroprotective effect on spinal cord motoneurons was also achieved in a mouse ALS model with NF-κB inhibition [46]. The results of the present study suggest that the progress of ALS may linked to a dysfunction in the mechanisms governing NF-κB activation.

The sALS cases studied revealed heavy cytoplasmic and nuclear staining for both the p50 and p65 subunits of NF-κB in non-neuronal cells. This high immunoreactivity could be related to the increased production of pro- and anti-inflammatory cytokines in glial cells, which has been suggested in previous studies [3,4,13,28]. It is also believed that NF-κB activation in non-neuronal cells (micro- and astroglia), which is a common finding in various CNS pathologies, may promote dying-out of neurons. This could be due to detrimental action of excessive amounts of pro-inflammatory cytokines, excitotoxins and free radicals produced and released by the glial cells [6,16,27].

Some studies in a rat model of traumatic CNS injury have shown that blockade of the NF-κB-mediated signaling pathway in astrocytes can exert a neuroprotective effect [30]. However, an attempt to use the same strategy for motoneuron protection in a mouse model of ALS has failed. It appeared that the pathomechanism of the neuronal damage in this model was much more complex and the inhibition of but one out of a number of pathways contributing to motoneuron damage was insufficient for an effective neuroprotection [8].

Conclusions

The role of NF-κB in sALS remains far from elucidated. The apparent decline in its immunoreactivity in spinal cord motoneurons with increasing duration of the disease may result either from a diminished expression or from an increased turnover of the respective NF-κB subunits, or both. The major shift toward prevailing cytoplasmic localization of NF-κB suggests that there is also a considerable disruption of the machinery governing the activation of this transcription factor in the motoneurons. Both these phenomena may contribute to the pathogenesis of the neurodegeneration process in sALS, but this issue needs further studies.

An impared NF-κB function in spinal cord motoneurons is most likely but one of multiple factors involved in ALS pathogenesis. The effect of perturbations affecting the function of this transcription factor in the motoneurons may also be related to its performance in the other cell types in the spinal cord. An important role in this regard may be played by enhanced NF-κB expression/activity in glial cells, which may result in a boosted production and release of factors with a potential detrimental action, e.g., of pro-inflammatory cytokines, excitotoxins and free radicals.

Acknowledgment

This study was supported by the National Centre for Research and Development Project NN 401 014640 and by statutory funds from the Mossakowski Medical Research Centre, Polish Academy of Science.

Disclosure

Authors report no conflict of interest.

References

1. Akhtar RS, Ness JM, Roth KA. Bcl-2 family regulation of neuronal development and neurodegeneration. Biochim Biophys Acta 2004; 1644: 189-203.
2. Albensi BC, Mattson MP. Evidence for the involvement of TNF and NF-κB in hippocampal synaptic plasticity. Synapse 2000; 35: 151-159.
3. Appel SH, Beers DR, Henkel JS. T cell-microglial dialogue in Parkinson's disease and amyotrophic lateral sclerosis: are we listening? Trends Immunol 2010; 31: 7-17.
4. Baeuerle PA, Baltimore D. NF-κB: ten years after. Cell 1996; 87: 13-20.
5. Brasier AR. The NF-κB regulatory network. Cardiovasc Toxicol 2006; 6: 111-130.
6. Camandola S, Mattson MP. NF-κB as a therapeutic target in neurodegenerative diseases. Expert Opin Ther Targets 2007; 11: 123-132.
7. Carter BD, Kaltschmidt C, Kaltschmidt B, Offenhäuser N, Böhm-Matthaei R, Baeuerle PA, Barde YA. Selective activation of NF-κB by nerve growth factor through the neurotrophin receptor p75. Science 1996; 272: 542-545.
8. Crosio C, Valle C, Casciati A, Iaccarino C, Carrì MT. Astroglial inhibition of NF-κB does not ameliorate disease onset and progression in a mouse model for amyotrophic lateral sclerosis (ALS). PLoS One 2011; 6: e17187.
9. Demir O, Aysit N, Onder Z, Turkel N, Ozturk G, Sharrocks AD, Kurnaz IA. ETS-domain transcription factor Elk-1 mediates neuronal survival: SMN as a potential target. Biochim Biophys Acta 2011; 1812: 652-662.
10. Ekegren T, Grundström E, Lindholm D, Aquilonius SM. Upregulation of Bax protein and increased DNA degradation in ALS spinal cord motor neurons. Acta Neurol Scand 1999; 100: 317-321.
11. Gilmore TD. The Rel/NF-κB signal transduction pathway: introduction. Oncogene 1999; 18: 6842-6844.
12. Gilmore TD. Introduction to NF-κB: players, pathways, perspectives. Oncogene 2006; 25: 6680-6684.
13. Glass CK, Saijo K, Winner B, Marchetto MC, Gage FH. Mechanisms underlying inflammation in neurodegeneration. Cell 2010; 140: 918-934.
14. Guerrini L, Blasi F, Denis-Donini S. Synaptic activation of NF-κB by glutamate in cerebellar granule neurons in vitro. Proc Natl Acad Sci USA 1995; 92: 9077-9081.
15. Huxford T, Malek S, Ghosh G. Structure and mechanism in NF-κB/IκB signaling. Cold Spring Harb Symp Quant Biol 1999; 64: 533-540.
16. John GR, Lee SC, Brosnan CF. Cytokines: powerful regulators of glial cell activation. Neuroscientist 2003; 9: 10-22.
17. Kaltschmidt B, Kaltschmidt C. Constitutive NF-κB activity in neurons. Mol Cell Biol 1994; 14: 3981-3992.
18. Kaltschmidt C, Kaltschmidt B, Baeuerle PA. Brain synapses contain inducible forms of the transcription factor NF-κB. Mech Dev 1993; 43: 135-147.
19. Kaltschmidt B, Widera D, Kaltschmidt C. Signaling via NF-κB in the nervous system. Biochim Biophys Acta 2005; 1745: 287-299.
20. Kiernan MC, Vucic S, Cheah BC, Turner MR, Eisen A, Hardiman O, Burrell JR, Zoing MC. Amyotrophic lateral sclerosis. Lancet 2011; 377: 942-955.
21. Kumar A, Takada Y, Boriek AM, Aggarwal BB. Nuclear factor- κB: its role in health and disease. J Mol Med 2004; 82: 434-448.
22. Li X, Stark GR. NFκB-dependent signalling pathways. Exp Hematol 2002; 30: 285-296.
23. Maggirwar SB, Sarmiere PD, Dewhurst S, Freeman RS. Nerve growth factor-dependent activation of NF-κB contributes to survival of sympathetic neurons. J Neurosci 1998; 18: 10356-10365.
24. Majumder S, Varadharaj S, Ghoshal K, Monani U, Burghes AHM, Jacob ST. Identification of a novel cyclic AMP-response element (CRE-II) and the role of CREB-1 in the cAMP-induced expression of the survival motor neuron (SMN) gene. J Biol Chem 2004; 279: 14803-14811.
25. Martin LJ. Neuronal death in amyotrophic lateral sclerosis is apoptosis: possible contribution of a programmed cell death mechanism. J Neuropathol Exp Neurol 1999; 58: 459-471.
26. Mattson MP. NF-κB in the survival and plasticity of neurons. Neurochem Res 2005; 30: 883-893.
27. Mattson MP, Meffert MK. Roles for NF-κB in nerve cell survival, plasticity, and disease. Cell Death Differ 2006; 13: 852-860.
28. McGeer PL, McGeer EG. Inflammatory processes in amyotrophic lateral sclerosis. Muscle Nerve 2002; 26: 459-470.
29. Meffert MK, Chang JM, Wiltgen BJ, Fanselow MS, Baltimore D. NF-κB functions in synaptic signaling and behavior. Nat Neurosci 2003; 6: 1072-1078.
30. Meunier A, Latrémolière A, Dominguez E, Mauborgne A, Philippe S, Hamon M, Mallet J, Benoliel JJ, Pohl M. Lentiviral-mediated targeted NF-κB blockade in dorsal spinal cord glia attenuates sciatic nerve injury-induced neuropathic pain in the rat. Mol Ther 2007; 15: 687-697.
31. Mincheva S, Garcera A, Gou-Fabregas M, Encinas M, Dolcet X, Soler RM. The canonical nuclear factor-κB pathway regulates cell survival in a developmental model of spinal cord motoneurons. J Neurosci 2011; 31: 6493-6503.
32. Mincheva-Tasheva S, Soler RM. NF-κB signaling pathways: role in nervous system physiology and pathology. Neuroscientist 2013; 19: 175-194.
33. Mu X, He J, Anderson DW, Trojanowski JQ, Springer JE. Altered expression of bcl-2 and bax mRNA in amyotrophic lateral sclerosis spinal cord motor neurons. Ann Neurol 1996; 40: 379-386.
34. Naganska E, Matyja E. Amyotrophic lateral sclerosis – looking for pathogenesis and effective therapy. Folia Neuropathol 2011; 49: 1-13.
35. Nakajima K, Kohsaka S. Functional roles of microglia in the central nervous system. Hum Cell 1998; 11: 141-155.

36. Perkins ND. Integrating cell-signalling pathways with NF-κB and IKK function. Nat Rev Mol Cell Biol 2007; 8: 49-62.
37. Rafałowska J, Sulejczak D, Chrapusta SJ, Gadamski R, Dziewulska D. Diverse expression of selected SMN complex proteins in humans with sporadic amyotrophic lateral sclerosis and in a transgenic rat model of familial form of the disease. PLoS One 2014; 9: e104614.
38. Ryu H, Smith K, Camelo SI, Carreras I, Lee J, Iglesias AH, Dangond F, Cormier KA, Cudkowicz ME, Brown RH Jr, Ferrante RJ. Sodium phenylbutyrate prolongs survival and regulates expression of anti-apoptotic genes in transgenic amyotrophic lateral sclerosis mice. J Neurochem 2005; 93: 1087-1098.
39. Schinzel A, Kaufmann T, Borner C. Bcl-2 family members: integrators of survival and death signals in physiology and pathology. Biochim Biophys Acta 2004; 1644: 95-105.
40. Schmidt-Ullrich R, Mémet S, Lilienbaum A, Feuillard J, Raphaël M, Israel A. NF-κB activity in transgenic mice: developmental regulation and tissue specificity. Development 1996; 122: 2117-2128.
41. Sen R, Baltimore D. Multiple nuclear factors interact with the immunoglobulin enhancer sequences. Cell 1986; 46: 705-716.
42. Shinoe T, Wanaka A, Nikaido T, Kanazawa K, Shimizu J, Imaizumi K, Kanazawa I. Upregulation of the pro-apoptotic BH3-only peptide harakiri in spinal neurons of amyotrophic lateral sclerosis patients. Neurosci Lett 2001; 313: 153-157.
43. Skórka K, Giannopoulos K. The structure and the role of NF-κB proteins and their significance in chronic lymphocytic leukemia. Acta Haematol Pol 2012; 43: 54-62.
44. Sparacio SM, Zhang Y, Vilcek J, Benveniste EN. Cytokine regulation of interleukin-6 gene expression in astrocytes involves activation of an NF-κB-like nuclear protein. J Neuroimmunol 1992; 39: 231-242.
45. Tian B, Brasier AR. Identification of a nuclear factor κ B-dependent gene network. Recent Prog Horm Res 2003; 58: 95-130.
46. Xu Z, Chen S, Li X, Luo G, Li L, Le W. Neuroprotective effects of (–)-epigallocatechin-3-gallate in a transgenic mouse model of amyotrophic lateral sclerosis. Neurochem Res 2006; 31: 1263-1269.

Original article

Folia Neuropathologica

Effects of supplementation with branched chain amino acids and ornithine aspartate on plasma ammonia and central fatigue during exercise in healthy men

Tomasz Mikulski[1], Jan Dabrowski[1], Wojciech Hilgier[2], Andrzej Ziemba[1], Krzysztof Krzeminski[1]

[1]Department of Applied Physiology, Mossakowski Medical Research Centre, Polish Academy of Sciences, Warsaw,
[2]Department of Neurotoxicology, Mossakowski Medical Research Centre, Polish Academy of Sciences, Warsaw, Poland

Folia Neuropathol 2015; 53 (4): 377-386 DOI: 10.5114/fn.2015.56552

Abstract

Introduction: *Our previous studies showed only slight improvement in central fatigue, measured indirectly by psychomotor performance, after branched chain amino acids (BCAA) supplementation during various efforts in healthy men. It is hypothesised that hyperammonaemia resulting from amino acids metabolism may attenuate their beneficial effect on psychomotor performance; therefore, the L-ornithine L-aspartate (OA) as an ammonia decreasing agent was used. The aim of this study was to investigate the effectiveness of oral BCAA + OA supplementation to reduce plasma ammonia concentration and enhance psychomotor performance during exhaustive exercise in healthy men.*
Material and methods: *Eleven endurance-trained men (mean age 32.6 ± 1.9 years) performed two sessions (separated by one week) of submaximal cycloergometer exercise for 90 minutes at 60% of maximal oxygen uptake followed by graded exercise until exhaustion with randomised, double-blind supplementation with a total of 16 g BCAA and 12 g OA (BCAA + OA trial) or flavoured water (placebo trial). Before exercise, during both efforts and after 20 minutes of recovery multiple choice reaction time (MCRT), perceived exertion, heart rate and oxygen uptake were measured and venous blood samples were taken for plasma leucine, valine, isoleucine, ornithine, aspartate, free tryptophan (fTRP), ammonia, lactate and glucose determination.*
Results: *After ingestion, during both efforts and after 20 minutes of recovery the plasma concentrations of all supplemented amino acids were significantly increased, while the fTRP/BCAA ratio decreased in the BCAA + OA trial more than in the placebo trial. At the end of graded exercise plasma fTRP was lower and MCRT shorter in BCAA + OA than in the placebo trial ($p < 0.05$). At the end of prolonged exercise the plasma ammonia concentration was higher in BCAA + OA than in placebo trial ($p < 0.05$). Decreases in plasma ammonia during recovery were significantly higher in BCAA + OA than in the placebo trial. Plasma ammonia positively correlated with the total plasma BCAA and MCRT only in the BCAA + OA trial. The fTRP/BCAA ratio positively correlated with MCRT only in the placebo trial.*
Conclusions: *Supplementation with BCAA and OA is a useful way to improve MCRT during high-intensity exercise and accelerate the elimination of ammonia at the recovery stage after exercise in healthy young men.*

Key words: *hyperammonaemia, tryptophan, brain, psychomotor performance, reaction time, effort.*

Communicating author:
Tomasz Mikulski, Mossakowski Medical Research Centre, 5 Pawinskiego St., 02-106 Warszawa, Poland, phone: +48 22 608 65 17, fax: +48 22 668 54 45, e-mail: tomik@imdik.pan.pl

Introduction

Exercise fatigue usually involves both peripheral muscle and central fatigue. Peripheral fatigue is relatively well understood, while the knowledge of mechanisms underlying central fatigue is still limited. Stress central fatigue may arise from changes in various neurotransmitters in the brain secondary to the changes that occur in the body, especially in the working muscles and in the mind. There are several theories concerning central fatigue, including modulation of glutamatergic and GABA-ergic synaptic signal transmission, as well as increased serotonin, which works as a neurotransmitter in the brain [3,26]. Since administration of selective serotonin reuptake inhibitors in humans has shown increased fatigue and perceived exertion [41,49] it seems likely that central fatigue may result from enhanced synthesis and release of serotonin from some neurons in the brain [14,26,50]. Serotonin is synthesised from L-tryptophan by a metabolic pathway consisting *inter alia* of tryptophan hydroxylase, the rate-limiting enzyme of serotonin synthesis [27,32,37]. Tryptophan circulates in blood in both albumin-bound and free forms. The free form crosses the blood-brain barrier and is converted into serotonin. Increased plasma free tryptophan (fTRP) enhances the rate of entry of tryptophan into the brain. Free tryptophan, the branched-chain amino acids (BCAA), as well as other amino acids share a common transporter across the blood-brain barrier [17,28,38]. Similarly, tryptophan and free fatty acids (FFA) compete for the same binding sites to albumin [24].

Thus, the reduction in BCAA and elevation in FFA may lead to an increase of tryptophan uptake into the brain. Some studies in human subjects [19] and in animals [13,37] have shown that exercise-induced increases in fTRP/BCAA ratio, due to higher BCAA oxidation in skeletal muscles and FFA mobilisation from adipose tissue, are associated with an increased rate of serotonin synthesis in brain neurons [12,49]. The rate of serotonin synthesis can be lowered by raising the blood BCAA concentration, which reduces tryptophan uptake into the brain. Studies in human subjects have shown that ingestion of BCAA reduces the perceived exertion and mental fatigue during standardised cycle ergometer exercise and sustained heavy exercise (a competitive 30-km cross-country race), as well as improves cognitive performance after exercise in human subjects [12,15,16,29,39,49]. However, the BCAA supplementation did not affect physical fatigue and was ineffective in preventing muscle power loss and perceived muscle pain during strenuous exercise such as in a marathon race [5,49]. Our previous studies in soccer players [39,54] showed a slight improvement in psychomotor performance after BCAA supplementation during both graded exercise until exhaustion and treadmill running simulating a football game.

Several studies demonstrated that both ingested BCAA and prolonged exercise itself can enhance the circulating level and the cerebral uptake of ammonia [4,25,40]. Strüder *et al*. [49] demonstrated that the increase in plasma ammonia during strenuous activity is significantly higher in subjects supplemented with BCAA than in the group supplemented with tyrosine or placebo. Elevated ammonia concentration is a result of both increased catabolism of amino acids and purine nucleotide deamination within the working muscles [34,43]. Since ammonia is crossing the blood-brain barrier [6], its high circulating level can cause detrimental effects on neurotransmitter metabolism (glutamate, GABA), neurotransmission as well as cerebral metabolism, which in turn may lead to central fatigue [3,4,9]. The enhanced cerebral ammonia uptake was observed during both prolonged and maximal exercise [4,9]. Thus, it was concluded that hyperammonaemia may cause central fatigue. Since in most experimental studies [7,35,42,44,48] the greatest effect on ammonia reduction was achieved with L-ornithine L-aspartate (OA), it seems likely that oral intake of BCAA together with OA may reduce ammonia accumulation and cerebral absorption, thereby delaying fatigue.

The present study was designed to investigate the effectiveness of a BCAA + OA containing drink to reduce plasma ammonia concentration and enhance the psychomotor performance (assessed by measurement of multiple-choice reaction time) during high-intensity exercise in healthy young men. It has been reported that the multiple-choice reaction time closely reflects the flow rate of neurophysiological, cognitive, and information processes that are created by the action of stimulus on the subject's sensory system [10,30].

Material and methods

Eleven healthy, endurance-trained male volunteers (mean age 32.6 ± 1.9 years, height 180 ± 2.0 cm, weight 73.6 ± 1.6 kg, BMI 22.3 ± 0.3 kg × m^{-2} (range 20.60-24.19 kg × m^{-2}), peak oxygen uptake 59 ± 1 ml ×

$kg^{-1} \times min^{-1}$ (range 56-73 ml × $kg^{-1} \times min^{-1}$) and mean arterial blood pressure 79 ± 3 mmHg; the values are means ± SEM) participated in this study. They were asked to refrain from strenuous activity and caffeine or alcohol consumption three days prior to the study. All subjects gave their informed consent to participate in the study. The investigation conforms to the principles outlined in the Declaration of Helsinki and was approved by the Local Ethics Committee (permission No. KB/48/2009). All procedures were carried out under similar environmental conditions (23-24°C and 50-60% humidity) between 8:00 and 12:00 AM. The subjects visited the laboratory three times with one-week intervals between the tests.

On the first occasion, the subjects were submitted to an incremental, graded exercise test performed on a bicycle ergometer (EM 840, Siemens, Germany) until volitional exhaustion, to determine their maximal oxygen uptake (VO_2 max). The workloads were increased by 50 Watts (W) every 3 minutes starting with 50 W. Oxygen uptake, carbon dioxide production and heart rate (HR) were continuously recorded using a V_{max} 29 (Sensormedics, USA) analyser. Before exercise and during the last two minutes of each workload a multiple-choice reaction time (MCRT) test was conducted in order to familiarise the subjects with the procedure chosen for evaluation of psychomotor performance [10,30,39]. The subjects were asked to react to visual and audio stimuli by pressing as fast as possible the corresponding buttons on the handlebars of the bicycle ergometer. Three coloured lights and sound were emitted in various time intervals by a psychomotor performance measurement device (CRR-APR-2/05, Unipar, Poland) with the signaller placed two metres in front of the subject at eye level. There were 15 stimuli for which the reaction time was recorded in milliseconds (red light for right hand and sound for left hand), while other 15 stimuli (green and orange light) were supposed to be ignored.

On the second and third occasion, according to the same protocol, the subjects were submitted to submaximal exercise performed on a bicycle ergometer lasting 90 minutes at 60% HR_{max} followed by graded exercise performed until volitional exhaustion as during the first visit. Before exercise each subject performed an MCRT test. Afterwards, a catheter was inserted into the antecubital vein in one arm for sampling of the plasma concentrations of amino acids (valine, leucine, isoleucine, tryptophan, ornithine, aspartic acid), ammonia, lactate, and glucose. The blood samples were collected into the tubes containing EDTA as an anticoagulant. Then, the subjects were randomised in a double-blind cross-over manner to receive amino acids with ornithine aspartate (BCAA + OA trial, n = 11) or flavoured water as placebo (placebo trial, n = 11). The supplements were given in a cross-over fashion, i.e. six of the subjects started with BCAA and OA and the other five started with placebo, in the second experiment, after one week, the order was changed. Before exercise the subjects ingested 500 ml of either a flavoured solution containing 10 g of BCAA (leucine, valine, isoleucine; 2 : 1 : 1, Olimp Labs) with 6 g of OA (Hepa-Merz 3000, Merz Pharmaceuticals GmbH, Germany) or flavoured water. Both drinks contained artificial sweetener, fruit flavour – orange syrup mixed with citric acid – and were indistinguishable in taste.

After a 30-minute rest period in a sitting position, baseline blood sample was taken and the subjects were submitted to prolonged submaximal exercise for 90 minutes at 60% of HR_{max}.

In the 30^{th} minute of exercise the second portion of 500 ml solution containing 6 g of BCAA and 6 g of OA or placebo was administered. After three minutes of rest, upon completion of the prolonged exercise, the subjects started graded exercise until volitional exhaustion, as they did at the first visit. Blood samples for determinations of the plasma amino acids, ammonia, glucose and lactate concentrations were taken in the 45^{th} minute and at the end of prolonged exercise as well as at the end of each workload of graded exercise until exhaustion and after 20 minutes of recovery. Before exercise, in the 45^{th} minute and at the end of prolonged exercise, as well as during last two minutes of each workload of graded exercise until exhaustion MCRT was measured. Additionally, at the end of each workload of graded exercise the rate of perceived exertion with a 20-point Borg scale was recorded.

Amino acids were assayed in deproteinised blood samples using HPLC with fluorescence detection after derivatisation in a timed reaction with o-phthalaldehyde plus mercaptoethanol, as described by Kilpatrick [36]. Derivatised samples were injected onto a 150 × 4.6-mm 5-µ Hypersil Gold BDS C18 column with a mobile phase of 50-mM phosphate buffer containing 10% v/v methanol, pH 6.2 (solvent A), and methanol (solvent B). Blood ammonia and lactate concentrations were analysed using a photometer Dr Lange LP420 (Konisburg, Germany) and cuvette

tests AM1054 (Randox, UK) and LKM140 (Hach Lange, Germany), respectively. Blood glucose concentration was measured using a glucometer (Optium Xido, UK). The fTRP/BCAA ratio was calculated by dividing the concentration of free tryptophan by the summarised concentrations of valine, leucine, and isoleucine (expressed in the same units).

Statistical analysis

The data are expressed as means with standard errors of the mean (SEM). Distribution of results was analysed by Shapiro-Wilk's test and paired *t* test or Wilcoxon test was used to compare results, accordingly. Changes over time were examined with two-way ANOVA for repeated measures, and $p < 0.05$ was accepted as the level of significance. In addition, correlation coefficients were calculated between variables using linear regression analysis. For calculations, Statistica (2001) version 6 (Statsoft Inc., Tulsa, OK, USA) was used.

Results

The aerobic capacities of the young men were within the upper normal range for men of their respective ages. There were no significant differences in HR, oxygen uptake and rating of perceived exertion, as well as in blood lactate or glucose between BCAA + OA and placebo trials at all stages of the study. Supplementation with BCAA + OA caused significant increases in the pre-exercise resting plasma concentrations of valine, leucine, isoleucine and ornithine. The concentration of these amino acids in the plasma remained significantly elevated during both types of exercise (prolonged – of moderate intensity and graded – until exhaustion) as well as after 20 minutes of the recovery period (Table I and II). Plasma aspartic acid concentration was significantly higher at the end of prolonged moderate-intensity exercise and after 20 minutes of recovery period only in the BCAA + OA trial (Table II). At the end of graded exercise until exhaustion plasma tryptophan was significantly lower in the BCAA + OA than in the placebo trial (19.2 ± 2.7 μM vs. 29.1 ± 2.0 μM, $p < 0.05$). The ratio of fTRP/BCAA was significantly lower in the BCAA + OA than in the placebo trial at all stages of the study (Table II). At the end of prolonged submaximal exercise the plasma ammonia concentration was significantly higher in the BCAA + OA than in the placebo trial (Fig. 1). Plasma ammonia decrease after graded exer-

Table I. Plasma valine, leucine, and isoleucine concentrations (branched chain amino acids – BCAA) at rest and during prolonged exercise followed by graded exercise until exhaustion with or without BCAA and ornithine aspartate (OA) supplementation

	Placebo (*n* = 11)			BCAA + OA (*n* = 11)		
	Valine (μM)	Leucine (μM)	Isoleucine (μM)	Valine (μM)	Leucine (μM)	Isoleucine (μM)
Pre	138 ± 19	67 ± 5	36 ± 3	141 ± 26	82 ± 15	46 ± 9
Post	140 ± 10	70 ± 5	39 ± 3	335 ± 42***	164 ± 19***	129 ± 16***
45'	136 ± 22	62 ± 9	37 ± 7	328 ± 53**	133 ± 24*	111 ± 21**
90'	122 ± 29	56 ± 11	33 ± 8	409 ± 52***	159 ± 25**	133 ± 22**
50 W	127 ± 20	58 ± 7	33 ± 5	385 ± 51**	147 ± 24**	115 ± 21**
100W	124 ± 23	55 ± 8	31 ± 5	342 ± 46**	108 ± 16**	87 ± 14**
150W	124 ± 20	56 ± 6	30 ± 6	373 ± 48***	123 ± 18**	99 ± 15**
200W	133 ± 33	55 ± 8	32 ± 6	409 ± 45**	131 ± 15**	105 ± 14***
250W	128 ± 25	57 ± 6	33 ± 5	365 ± 45***	113 ± 16**	91 ± 15***
300W	125 ± 20	57 ± 5	33 ± 4	439 ± 48**	110 ± 16*	82 ± 14**
350W	121 ± 11	58 ± 4	32 ± 3	324 ± 46**	112 ± 18**	78 ± 12**
Rec	117 ± 19	52 ± 6	29 ± 3	337 ± 52**	119 ± 25*	81 ± 16**

*Pre – rest, Post – 30 minutes after ingestion of BCAA and OA (BCAA + OA) or placebo, 45' and 90' – minutes during prolonged submaximal exercise, 50-350 Watts – workloads of graded exercise until exhaustion, Rec – at the 20th min of the recovery period, BCAA + OA – amino acids with ornithine aspartate trial. Values are means ± SEM. * – denote significant differences between trials: *p < 0.05, **p < 0.01, ***p < 0.001*

Table II. Plasma ornithine and aspartic acid concentrations and the ratio of free tryptophan to branched chain amino acids (fTRP/BCAA) at rest and during prolonged exercise followed by graded exercise until exhaustion with or without BCAA and ornithine aspartate (OA) supplementation

	Placebo (n = 11)			BCAA + OA (n = 11)		
	Ornithine (μM)	Aspartic acid (μM)	fTRP/BCAA	Ornithine (μM)	Aspartic acid (μM)	fTRP/BCAA
Pre	48 ± 6	3.3 ± 0.7	0.137 ± 0.012	47 ± 7	4.0 ± 0.8	0.134 ± 0.013
Post	49 ± 6	2.8 ± 0.5	0.137 ± 0.013	107 ± 14***	3.4 ± 0.6	0.056 ± 0.006***
45’	45 ± 6	2.5 ± 0.5	0.149 ± 0.015	119 ± 22**	3.1 ± 0.5	0.053 ± 0.010***
90’	41 ± 5	2.5 ± 0.4	0.155 ± 0.017	187 ± 31***	4.5 ± 0.8*	0.047 ± 0.010***
50 W	41 ± 5	3.1 ± 0.5	0.139 ± 0.014	155 ± 27***	4.4 ± 0.9	0.047 ± 0.011**
100 W	40 ± 5	2.9 ± 0.4	0.151 ± 0.016	124 ± 18***	3.5 ± 0.7	0.056 ± 0.140**
150 W	40 ± 5	2.7 ± 0.5	0.148 ± 0.009	134 ± 18***	3.7 ± 0.7	0.055 ± 0.019**
200 W	39 ± 6	2.9 ± 0.5	0.151 ± 0.015	147 ± 20***	4.0 ± 0.8	0.051 ± 0.012**
250 W	41 ± 6	2.6 ± 0.4	0.148 ± 0.016	122 ± 18***	3.7 ± 0.7	0.058 ± 0.017**
300 W	44 ± 6	3.0 ± 0.7	0.139 ± 0.011	112 ± 21**	3.5 ± 0.7	0.052 ± 0.011**
350 W	42 ± 5	2.9 ± 0.6	0.144 ± 0.014	102 ± 15**	4.0 ± 0.6	0.049 ± 0.014**
Rec	42 ± 7	2.1 ± 0.5	0.136 ± 0.012	98 ± 21*	3.7 ± 0.6***	0.058 ± 0.015**

*Pre – rest, Post – 30 minutes after ingestion of BCAA and OA (BCAA+ OA) or placebo, 45’ and 90’ – minutes during prolonged submaximal exercise, 50-350 Watts – workloads of graded exercise until exhaustion, Rec – at the 20th min of the recovery period, BCAA+OA – amino acids with ornithine aspartate trial. Values are means ±SEM. *– denote significant differences between trials: *p < 0.05, **p < 0.01, ***p < 0.001*

cise until exhaustion was significantly higher in the BCAA + OA than in the placebo trial (Δ 99.5 ± 16.6 μM vs. Δ 51.4 ± 11.5 μM, $p < 0.05$; Fig. 2). After 20 minutes of the recovery period the plasma ammonia concentration did not differ significantly from the resting values only in the BCAA + OA trial (Fig. 1). At work-

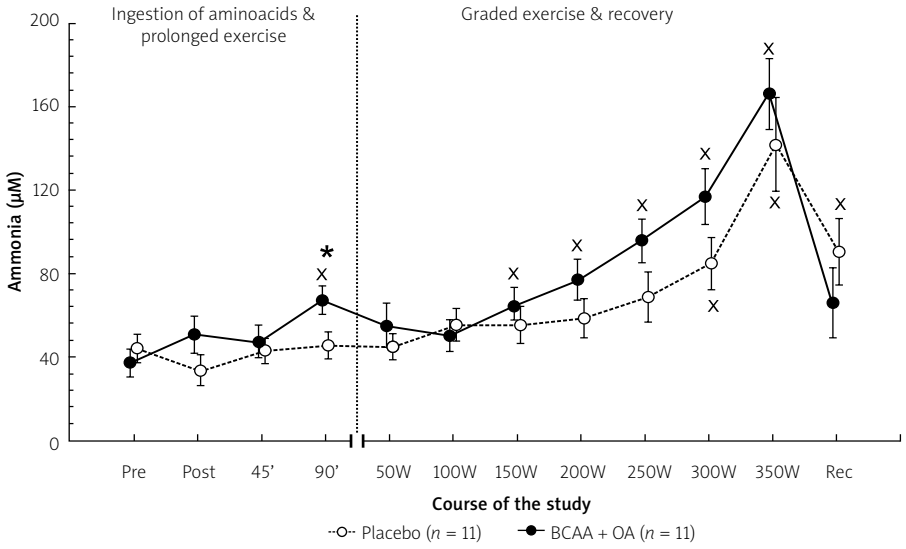

Fig. 1. Plasma ammonia concentration at rest (Pre) 30 minutes after ingestion of branched chain amino acids (BCAA) and ornithine aspartate (OA) (BCAA + OA) or placebo (Post), during both prolonged submaximal exercise (45’ and 90’) and graded exercise until exhaustion (50-350 Watts workloads) and at the 20th min of the recovery period (Rec). Values are means ± SE. * – denotes significant differences between trials: *$p < 0.05$; x – denotes significant differences from the resting values: x$p < 0.05$.

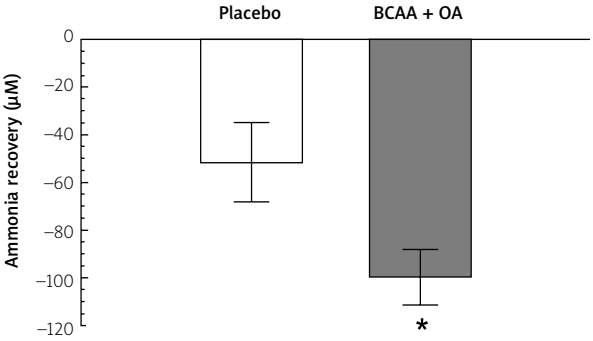

Fig. 2. Restitution of plasma ammonia concentration after graded exercise in placebo and amino acids-supplemented (branched chain amino acids and ornithine aspartate; BCAA + OA) trials. Δ – the difference between concentration achieved at the end of maximal exercise and after 20 minutes of recovery. Values are means ± SE. * – denote significant differences between trials: *$p < 0.05$.

loads of 100 W, 150 W and at the end of graded exercise until exhaustion MCRT was significantly shorter in the BCAA + OA than in the placebo trial (272 ± 8 ms vs. 286 ± 8 ms, $p < 0.05$; 271 ± 9 ms vs. 287 ± 8 ms, $p < 0.05$; and 281 ± 7 ms vs. 310 ± 8 ms, $p < 0.01$, respectively; Fig. 3). Plasma ammonia concentration correlated positively with the total plasma BCAA in both trials, and with MCRT only in the BCAA + OA trial ($r = 0.40$, $p < 0.05$; $r = 0.20$, $p < 0.05$; $r = 0.35$; $p < 0.05$, respectively). The fTRP/BCAA ratio correlated positively with MCRT only in the placebo trial ($r = 0.38$, $p < 0.05$; Fig. 4).

Discussion

The new finding of this study is that, despite similar levels of ammonia in both trials, shorter multiple-choice reaction time at the end of strenuous, exhaustive exercise and faster return of ammonia concentration to the pre-exercise resting values were observed in the BCAA + OA trial. Furthermore, significant positive correlations were found between plasma ammonia and the total plasma BCAA concentration in both trials and between plasma ammonia and MCRT in the BCAA + OA trial. Similar correlation was found between the fTRP/BCAA ratio and MCRT only in the placebo trial. The study showed also that BCAA + OA supplementation, although effective in increasing blood concentrations of BCAA and OA, did not influence aerobic performance or the rating of perceived exertion.

Several studies showed that ammonia is tightly regulated in response to exercise, being affected by factors such as exercise duration and intensity and energy substrates availability [4,9,40]. During high-intensity or exhaustive exercise ammonia is mainly

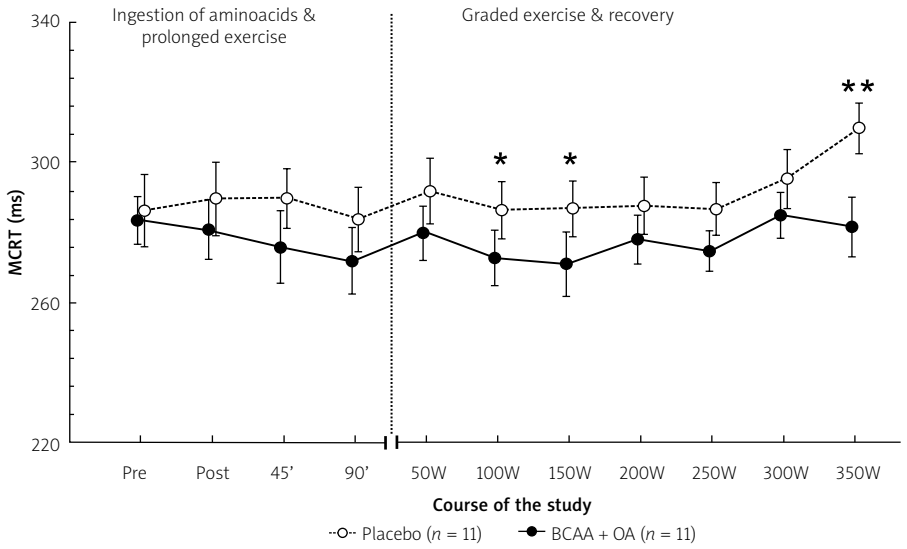

Fig. 3. Multiple choice reaction time (MCRT) at rest (Pre) 30 minutes after ingestion of branched chain amino acids (BCAA) and ornithine aspartate (BCAA + OA) or placebo (Post), during both prolonged submaximal exercise (45' and 90') and graded exercise until exhaustion (50-350 Watts workloads) and at the 20th min of the recovery period (Rec). Values are means ± SE. * – denotes significant differences between trials: *$p < 0.05$, **$p < 0.01$.

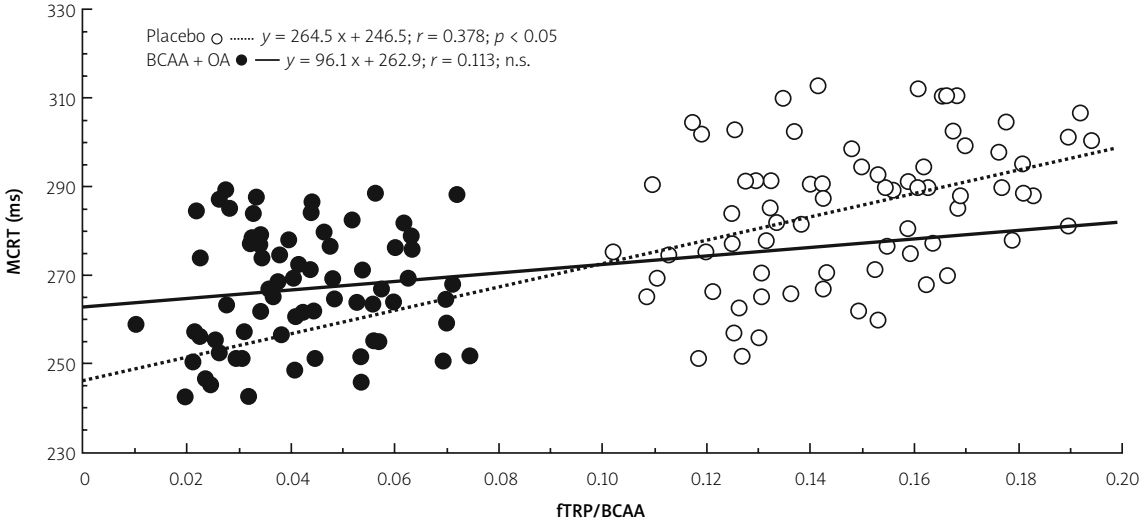

Fig. 4. Correlation between plasma free tryptophan to branched chain amino acids ratio (fTRP/BCAA) and multiple-choice reaction time (MCRT) during exercise in placebo and amino acids supplemented (branched chain amino acids and ornithine aspartate; BCAA + OA) trials.

produced by deamination of AMP in the purine nucleotide cycle, which takes place in the contracting muscles.

The relationship between plasma ammonia and total plasma BCAA observed in this study may be at least partly associated with deamination of the branched chain amino acids for additional energy provision. Based on previous studies [51,52], it might be speculated that increased oxidation of BCAA limited the tricarboxylic acid cycle activity and fatty acid oxidation, and therefore plays an important role in fatigue mechanisms during prolonged exercise, leading to glycogen depletion at intensities above 60% VO_2max. Nybo *et al*. [40] demonstrated that high levels of systemic ammonia during prolonged exercise enhanced the uptake of ammonia by the brain in endurance-trained male subjects. Positive correlations were observed between the arterial ammonia concentration and both the cerebral uptake and the cerebrospinal fluid ammonia. Weaker correlation was found between the cerebrospinal fluid ammonia and perceived exertion at the end of prolonged exercise (at 60% of VO_2max). The authors suggested that exercise-induced hyperammonaemia may induce a transient state of acute ammonia toxicity with concomitant disturbances in brain neurotransmitters, leading to central fatigue. The findings obtained in trained rats showed that an enhanced brain ammonia level evoked by exhaustive exercise stimulates glutamine synthesis as a result of detoxification and subsequently decreases both brain glutamate levels in all brain structures and gamma-aminobutyric acid (GABA) levels in the striatum. Thus, changes in neurotransmitters metabolism and subsequent central fatigue depend on the effect of ammonia on the excitatory amino acids [31]. Although the weak correlation between plasma ammonia concentration and MCRT in the BCAA + OA trial observed in the present study supports this mechanism, shortened MCRT at the end of exhaustive exercise in the BCAA + OA trial indicates that other factors are involved in the development of central fatigue.

An additional finding of the present investigation is that in the BCAA + OA trial the ratio of fTRP/BCAA was significantly lower than in placebo trial at all stages of the study. Since tryptophan was not administered, the changes in fTRP/BCAA ratio resulted from the BCAA supplementation [28,32], which prevented the described decrease of these amino acids in the latter stages of exercise [15,18,28]. However, the present study has not confirmed such a decrease that should have been observed in the placebo trial. The decrease in the fTRP/BCAA ratio would lead to decreased tryptophan transport across the blood-brain barrier because BCAA and tryptophan compete for entry by the same large neutral amino acid transporter [15-17]. This should lead to a lower level of 5-hydroxytryptamine responsible for

central fatigue [15,23,50]. Thus, the ingestion of BCAA could reduce the exercise-induced increase in brain tryptophan uptake and delay fatigue. The shortening of the multiple-choice reaction time at the end of exhaustive exercise in the BCAA + OA trial observed in the present study supports this "central fatigue" hypothesis.

However, it is unclear why the fTRP/BCAA ratio did not correlate with MCRT in the BCAA + OA trial. In this regard, it seems worth mentioning that MCRT reflects not only one pathway of the selected neurotransmitter or the flow rate of neurophysiological and information processes, but also several cognitive modalities (attention, impulse control, processing speed, cognitive flexibility) that are created by the action of stimulus on the subject's sensory system [10,30]. During heavier but still submaximal workloads other involved pathways might dominate, for example BCAA also competitively inhibits tyrosine uptake into the brain, and thus catecholamine synthesis, which reduce physical performance [23].

In the placebo trial reflecting the physiological concentrations of amino acids and the balance in nitrogen turnover, MCRT correlated with fTRP/BCAA ratio and probably was not influenced by ammonia (Fig. 4). In the BCAA + OA trial this relationship disappeared, and enhanced nitrogen turnover adversely affected psychomotor performance, because MCRT became slower with increased blood ammonia concentration, which was not diminished during exercise by OA. This finding suggests that exogenous amino acids can easily exceed autoregulatory capacity, disturb nitrogen homeostasis and contribute to the development of central fatigue. Thus, very careful selection of doses of BCAA should be applied in order to shift the fTRP/BCAA ratio but not to increase the nitrogen turnover beyond the limits resulting in significantly enhanced ammonia production.

Administration of OA prevented the expected increase in blood ammonia concentration after the BCAA supplementation during the graded exhaustive exercise and therefore probably prevented the deterioration of multiple choice reaction time usually occurring in the final stage of the exhaustive exercise [20-22,39,54], which reflects improved psychomotor performance (Fig. 3).

During prolonged exercise of constant intensity and graded exercise with subsequent workloads without any breaks the influence of OA on ammonia was limited, possibly due to decreased splanchnic (especially liver) blood flow [46]. The supposed site of detoxification action of OA in hepatocytes [47] by stimulation of urea cycle and glutamine synthesis [33] can be systematically effective only when sufficient blood flow through the liver is maintained. However, in the BCAA + OA trial after 20 minutes of the recovery period a beneficial effect of reduced ammonaemia was observed. It is very likely that the supplemented OA was available for ammonia metabolism in the liver, but the splanchnic blood flow was so limited by exercise that its action could not be significant. After cessation of exercise when liver blood flow increased [46,53] ammonia degradation became significantly faster in BCAA + OA than in the placebo trial. Improved recovery capacity is very important in daily activities or sports with repeated efforts with short breaks between them. On the other hand, application of OA is questionable in high-intensity efforts performed as one bout of exercise without any breaks. In current trends for faster mobilisation of patients suffering from any diseases care should be taken in treatment of patients with hyperammonaemia. Activities of moderate intensity with frequent breaks can be considered, whereas intense exercise, especially of constant intensity and without breaks is not recommended as it can increase ammonia production and impair its breakdown and effectiveness of treatment with ammonia-decreasing drugs acting in the liver, e.g. OA. Supplements based on proteins and amino acids are currently one of the most overused and overdosed, so any recommendations for their use should be calculated very carefully. In certain cases the use of OA seems to be rational and in agreement with the results of most studies [1,7,8,11,42,44]; however, some critical works are also present [2,45].

Conclusions

In summary, this study demonstrated that BCAA + OA supplementation, although effective in increasing blood concentrations of BCAA and OA, did not influence aerobic performance or rating of perceived exertion. The most important finding is that, despite similar levels of ammonia in both trials, shorter multiple-choice reaction time at the end of strenuous exhaustive exercise and faster return to the pre-exercise resting values were observed only in the BCAA + OA trial.

These results suggest that oral supplementation with BCAA + OA delays central fatigue during pro-

longed exhaustive exercise in endurance-trained young men, but this requires more detailed studies.

Acknowledgments

The study was financed by the grant of Ministry of Science and Education N N404 051337.

Disclosure

Authors declare no conflict of interest.

References

1. Abid S, Jafri W, Mumtaz K, Islam M, Abbas Z, Shah HA, Hamid S. Efficacy of L-ornithine-L-aspartate as an adjuvant therapy in cirrhotic patients with hepatic encephalopathy. J Coll Physicians Surg Pak 2011; 21: 666-671.
2. Acharya SK, Bhatia V, Sreenivas V, Khanal S, Panda SK. Efficacy of L-ornithine L-aspartate in acute liver failure: a double-blind, randomized, placebo-controlled study. Gastroenterology 2009; 136: 2159-2168.
3. Albrecht J, Norenberg MD. Glutamine: a Trojan horse in ammonia neurotoxicity. Hepatology 2006; 44: 788-794.
4. Ament W, Huizenga JR, Kort E, van der Mark TW, Grevink RG, Verkerke GJ. Respiratory ammonia output and blood ammonia concentration during incremental exercise. Int J Sports Med 1999; 20: 71-77.
5. Areces F, Salinero JJ, Abian-Vicen J, Gonzalez-Millan C, Gallo-Salazar C, Ruiz-Vicente D, Lara B, Del Coso J. A 7-day oral supplementation with branched-chain amino acids was ineffective to prevent muscle damage during a marathon. Amino Acids 2014; 46: 1169-1176.
6. Bachmann C. Mechanisms of hyperammonemia. Clin Chem Lab Med 2002; 40: 653-662.
7. Bai M, Yang Z, Qi X, Fan D, Han G. L-ornithine-l-aspartate for hepatic encephalopathy in patients with cirrhosis: a meta-analysis of randomized controlled trials. J Gastroenterol Hepatol 2013; 28: 783-792.
8. Bai M, He C, Yin Z, Niu J, Wang Z, Qi X, Liu L, Yang Z, Guo W, Tie J, Bai W, Xia J, Cai H, Wang J, Wu K, Fan D, Han G. Randomised clinical trial: L-ornithine-L-aspartate reduces significantly the increase of venous ammonia concentration after TIPSS. Aliment Pharmacol Ther 2014; 40: 63-71.
9. Banister EW, Cameron BJ. Exercise-induced hyperammonemia: peripheral and central effects. Int J Sports Med 1990; 11: S129-142.
10. Batra A, Vyas S, Gupta J, Gupta K, Hada R. A comparative study between young and elderly indian males on audio-visual reaction time. Indian Journal of Scientific Research and Technology 2014; 2: 25-29.
11. Blanco Vela CI, Poo Ramírez JL. Efficacy of oral L-ornithine L-aspartate in cirrhotic patients with hyperammonemic hepatic encephalopathy. Ann Hepatol 2011; 10 Suppl 2: S55-59.
12. Blomstrand E, Hassmen P, Ekblom B, Newsholme EA. Influence of ingesting a solution of branched-chain amino acids on perceived exertion during exercise. Acta Physiol Scand 1997; 159: 41-49.
13. Blomstrand E, Perrett D, Parry-Billings M, Newsholme EA. Effect of sustained exercise on plasma amino acid concentrations and on 5-hydroxytryptamine metabolism in six different brain regions of the rat. Acta Physiol Scand 1989; 136: 473-481.
14. Blomstrand E, Saltin B. BCAA intake affects protein metabolism in muscle after but not during exercise in humans. Am J Physiol Endocrinol Metab 2001; 281: E365-374.
15. Blomstrand E. A role for branched-chain amino acids in reducing central fatigue. J Nutr 2006; 136: S544-547.
16. Blomstrand E. Amino acids and central fatigue. Amino Acids 2001; 20: 25-34.
17. Boado RJ, Li JY, Nagaya M, Zhang C, Pardridge WM. Selective expression of the large neutral amino acid transporter at the blood-brain barrier. Proc Natl Acad Sci USA 1999; 96: 12079-12084.
18. Borgenvik M, Nordin M, Mikael Mattsson C, Enqvist JK, Blomstrand E, Ekblom B. Alterations in amino acid concentrations in the plasma and muscle in human subjects during 24 h of simulated adventure racing. Eur J Appl Physiol 2012; 112: 3679-3688.
19. Chaouloff F. Effects of acute physical exercise on central serotonergic systems. Med Sci Sports Exerc 1997; 29: 58-62.
20. Chmura J, Krysztofiak H, Ziemba AW, Nazar K, Kaciuba-Uściłko H. Psychomotor performance during prolonged exercise above and below the blood lactate threshold. Eur J Appl Physiol Occup Physiol 1998; 77: 77-80.
21. Chmura J, Nazar K. Kaciuba-Uściłko H. Próg psychomotoryczny zmęczenia. Sport Wyczynowy 2007; 4-6: 508-510.
22. Chmura J, Nazar K. Parallel changes in the onset of blood lactate accumulation (OBLA) and threshold of psychomotor performance deterioration during incremental exercise after training in athletes. Int J Psychophysiol 2010; 75: 287-290.
23. Choi S, DiSilvio B, Fernstrom MH, Fernstrom JD. Oral branched-chain amino acid supplements that reduce brain serotonin during exercise in rats also lower brain catecholamines. Amino Acids 2013; 45: 1133-1142.
24. Curzon G, Friedel J, Knott PJ. The effect of fatty acids on the binding of tryptophan to plasma protein. Nature 1973; 242: 198-200.
25. Dalsgaard MK, Volianitis S, Yoshiga CC, Dawson EA, Secher NH. Cerebral metabolism during upper and lower body exercise. J Appl Physiol 2004; 97: 1733-1739.
26. Davis JM, Alderson NL, Welsh RS. Serotonin and central nervous system fatigue: nutritional considerations. Am J Clin Nutr 2000; 72: S573-578.
27. Du L, Bakish D, Hrdina PD. Tryptophan hydroxylase gene 218A/C polymorphism is associated with somatic anxiety in major depressive disorder. J Affect Disord 2001; 65: 37-44.
28. Fernstrom JD. Branched-chain amino acids and brain function. J Nutr 2005; 135: S1539-1546.
29. Greer BK, White JP, Arguello EM, Haymes EM. Branched-chain amino acid supplementation lowers perceived exertion but does not affect performance in untrained males. J Strength Cond Res 2011; 25: 539-544.
30. Grrishma B, Gaur G S, Velkumary S, Gurunandan U, Dutt A, Dinesh T. Comparison of hand and foot reaction times among females-a methodological study using recognition auditory

reaction time. International Journal of Current Research 2013; 5: 4272-4274.
31. Guezennec CY, Abdelmalki A, Serrurier B, Merino D, Bigard X, Berthelot M, Pierard C, Peres M. Effects of prolonged exercise on brain ammonia and amino acids. Int J Sports Med 1998; 19: 323-327.
32. Hamon M, Bourgoin S, Artaud F, El Mestikawy S. The respective roles of tryptophan uptake and tryptophan hydroxylase in the regulation of serotonin synthesis in the central nervous system. J Physiol 1981; 77: 269-279.
33. Haussinger D. Nitrogen metabolism in liver: structural and functional organization and physiological relevance. Biochem J 1990; 267: 281-290.
34. Hellsten Y, Richter EA, Kiens B, Bangsbo J. AMP deamination and purine exchange in human skeletal muscle during and after intense exercise. J Physiol 1999; 3: 909-920.
35. Jalan R, Wright G, Davies NA, Hodges SJ. L-Ornithine phenylacetate (OP): a novel treatment for hyperammonemia and hepatic encephalopathy. Med Hypotheses 2007; 69: 1064-1069.
36. Kilpatrick IC. Rapid, automated HPLC analysis of neuroactive and other amino acids in microdissected brain regions and brain slice superfusates using fluorimetric detection. In: Neuroendocrine research methods. Vol. 2. Greenstein B (ed.). Harwood Academic Publishers, Chur, 1991; pp. 555-578.
37. MacGillivray L, Reynolds KB, Rosebush PI, Mazurek MF. The comparative effects of environmental enrichment with exercise and serotonin transporter blockade on serotonergic neurons in the dorsal raphe nucleus. Synapse 2012; 66: 465-470.
38. Meeusen R, Watson P. Amino acids and the brain: do they play a role in "central fatigue"? Int J Sport Nutr Exerc Metab 2007; 17: S37-46.
39. Mikulski T, Ziemba A, Chmura J, Wiśnik P, Kurek Z, Kaciuba-Uściłko H, Nazar K. The effect of supplementation with branched chain amino acids (BCAA) on psychomotor performance during graded exercise in human subjects. Biol Sport 2002; 19: 295-301.
40. Nybo L, Dalsgaard MK, Steensberg A, Møller K, Secher NH. Cerebral ammonia uptake and accumulation during prolonged exercise in humans. J Physiol 2005; 563: 285-290.
41. Parise G, Bosman MJ, Boecker DR, Barry MJ, Tarnopolsky MA. Selective serotonin reuptake inhibitors: Their effect on high-intensity exercise performance. Archives of Physical Medicine and Rehabilitation 2001; 82: 867-871.
42. Pérez Hernández JL, Higuera de la Tijera F, Serralde-Zúñiga AE, Abdo Francis JM. Critical analysis of studies evaluating the efficacy of infusion of L-ornithine L-aspartate in clinical hepatic encephalopathy in patients with liver failure. Ann Hepatol. 2011; 10 Suppl 2: S66-69.
43. Pitkanen H, Nykanen T, Knuutinen J. Free amino acid pool and muscle protein balance after resistance exercise. Med Sci Sports Exerc 2003; 35: 784-792.
44. Rees CJ, Oppong K, Al Mardini H, Hudson M, Record CO. Effect of L-ornithine-L-aspartate on patients with and without TIPS undergoing glutamine challenge: a double blind, placebo controlled trial. Gut 2000; 47: 571-574.
45. Schmid M, Peck-Radosavljevic M, König F, Mittermaier C, Gangl A, Ferenci P. A double-blind, randomized, placebo-controlled trial of intravenous L-ornithine-L-aspartate on postural control in patients with cirrhosis. Liver Int 2010; 30: 574-582.
46. Shephard RJ, Johnson N. Effects of physical activity upon the liver. Eur J Appl Physiol 2015; 115: 1-46.
47. Sikorska H, Cianciara J, Wiercińska-Drapało A. Physiological functions of L-ornithine and L-aspartate in the body and the efficacy of administration of L-ornithine-L-aspartate in conditions of relative deficiency. Pol Merkur Lekarski 2010; 28: 490-495.
48. Staedt U, Leweling H, Gladisch R, Kortsik C, Hagmüller E, Holm E. Effects of ornithine aspartate on plasma ammonia and plasma amino acids in patients with cirrhosis. A double-blind, randomized study using a four-fold crossover design. J Hepatol 1993; 19: 424-430.
49. Strüder HK, Hollmann W, Platen P, Donike M, Gotzmann A, Weber K. Influence of paroxetine, branched-chain amino acids and tyrosine on neuroendocrine system responses and fatigue in humans. Horm Metab Res 1998; 30: 188-194.
50. Strüder HK, Weicker H. Physiology and pathophysiology of the serotonergic system and its implications on mental and physical performance. Int J Sports Med 2001; 22: 482-497.
51. Wagenmakers AJ, Coakley JH, Edwards RH. Metabolism of branched-chain amino acids and ammonia during exercise: clues from McArdle's disease. Int J Sports Med 1990; 11 Suppl 2: S101-113.
52. Wagenmakers AJ, Beckers EJ, Brouns F, Kuipers H, Soeters PB, van der Vusse GJ, Saris WH. Carbohydrate supplementation, glycogen depletion, and amino acid metabolism during exercise. Am J Physiol 1991; 260 (6 Pt 1): E883-890.
53. van Wijck K, Lenaerts K, van Loon LJ, Peters WH, Buurman WA, Dejong CH. Exercise-induced splanchnic hypoperfusion results in gut dysfunction in healthy men. PLoS One 2011; 6: e22366.
54. Wiśnik P, Chmura J, Ziemba AW, Mikulski T, Nazar K. The effect of branched chain amino acids on psychomotor performance during treadmill exercise of changing intensity simulating a soccer game. Appl Physiol Nutr Metab 2011; 36: 856-862.

Case report

Folia Neuropathologica

Holoprosencephaly with agenesia of the prosencephalic ventricle

Milena Laure-Kamionowska[1], Krystyna Szymanska[1,2], Teresa Klepacka[3]

[1]Department of Experimental and Clinical Neuropathology, Mossakowski Medical Research Centre, Polish Academy of Sciences, Warsaw, [2]Department of Child Psychiatry, Medical University of Warsaw, [3]Department of Pathomorphology, Institute of Mother and Child, Warsaw, Poland

Folia Neuropathol 2015; 53 (4): 387-394 DOI: 10.5114/fn.2015.56553

Abstract

Malformations of the forebrain are characterized by abnormalities in size, shape, and arrangement of the cerebral hemispheres and ventricles. We present the morphological picture of a brain with failure of the forebrain complementary to holoprosencephaly coexisting with absence of the anterodorsal part of the prosencephalic ventricles. The anomaly can be graded within the holoprosencephalic spectrum due to the main morphological features. However, such alterations as aplasia of the forebrain ventricles and prominent leptomeningeal gliomesodermal proliferation are related to atelencephaly. The observations confirm the common pathogenic mechanism of aprosencephaly/atelencephaly and holoprosencephaly. The malformation corresponds to a wide continuous spectrum with no clear-cut boundaries of abnormal formation of the prosencephalon.

Key words: *holoprosencephaly, aprosencephaly, atelencephaly, aventriculi, aplasia of the prosencephalic ventricle.*

Introduction

Prosencephalon is the primordial forebrain vesicle at the cephalic part of the neural tube following closure of the anterior neuropore. During the next developmental steps the cerebral hemispheres and diencephalon will be formed. Abnormal ventral induction may result in disorders of formation, cleavage and midline development of prosencephalic structures [22,30]. Malformations of the forebrain are characterized by abnormalities in size, shape, and arrangement of the cerebral hemispheres and ventricles. Developmental failure characterized by deficient midline division of the forebrain into two hemispheres with accompanying midline defects results in holoprosencephaly (HPE). The main features are characterized by the variable loss of midline structures of the brain and face, as well as fusion of the cerebral hemispheres into the holosphere and the lateral ventricles into a single midline monoventricle. The monoventricle spreads anteriorly as a crescent-shaped cavity and divides posteriorly into temporal horns [22]. A few cases with partial or completely missing ventricular lumina in holoprosencephalic brains have been described [7,12,25]. Diagnosis of absence of supratentorial ventricles was based on neuroimaging analysis. Cerebral ventricles were not identifiable in ultrasound and magnetic resonance imaging scans.

Communicating author

Milena Laure-Kamionowska, Department of Clinical and Experimental Neuropathology, Mossakowski Medical Research Centre, PASci, 5 Pawinskiego St., 02-106 Warsaw, e-mail: mkamionowska@imdik.pan.pl

We had the opportunity to describe the morphological picture of a brain with failure of the forebrain and agenesia of the anterodorsal part of the prosencephalic ventricles.

Case description

The premature female infant was born by cesarean section because of labor in progress at the 32nd week of gestation. It was a twin pregnancy; the baby was born second. The 21-year-old mother was in her first pregnancy. The birth weight of the newborn was 840 g (1 percentile), length 38 cm, crown-rump length 22 cm, head circumference 19 cm, chest circumference 20 cm. Apgar score was 1.2 after 1 and 5 minutes. The child presented craniofacial abnormalities: cyclopia, nasal hypoplasia, cleft palate, failure of the forehead. The girl died after one hour. The first born twin is alive.

Postmortem examination revealed abnormal features of the face – small flattened nose, single nostril, two palpebral fissures, the right completely sealed, right eyeball impalpable. In the lungs severe alveolar emphysema, hyperemia and disseminated coagulation in small capillaries were noted. The internal organs did not present malformations.

Neuropathological examination: Macroscopically the formalin-fixed brain weighed 29 g (below 1 percentile). The front part of the brain was abnormal in size and shape. The telencephalon was small, undivided, disc shaped, situated in front of the cerebellum instead of overlaying it. The interhemispheric fissure was absent. The convolutional pattern of the holosphere was aberrant, and the cerebral lobes were not defined. Cross-sections of this part revealed a C-shaped narrow solid mass. The ventricular cavity was not visible (Fig. 1).

The frontal part, in its rear portion, was connected with a short middle spherical shape structure comparable to the diencephalon (Fig. 1B). It was covered, particularly on its dorsal surface, by thick hypervascularized meninges. The picture may correspond to a collapsed dorsal sac cyst. Into this dorsal subarachnoid space an infundibulum-shaped orifice was opened. At this anatomical structure two mammillary bodies were well recognizable. The telencephalon-diencephalon junction was irregular and very small. Thin-walled vascular channels mixed with disorganized neural tissue closely adhered to the diencephalon at this level. At the diencephalic-mesencephalic junction cross-section, paired red nuclei were observed. The slit narrow third ventricle was observed at that level.

In the brainstem hypoplastic corticospinal tracts were observed. The cerebellum was relatively normal.

Microscopic examination was performed on paraffin-embedded slides stained with hematoxylin-eosin, cresyl violet, the Klüver-Barrera method, and immunohistochemically with glial fibrillary acidic protein (GFAP) and synaptophysin antibodies.

In the middle of the solid frontal mass, clusters of glial cells resembling subependymal glia and congested thin walled blood vessels were seen (Fig. 2). Single small ependymal rosettes and some thin channels composed of ependymal cells were arranged linearly mostly in the rear part (Fig. 3). Adjacent to them the germinative zone of small cells with hyperchromatic nuclei and scant cytoplasm was observed. Distribution of these cells was irregular. Neuroblasts were loosely dispersed without any specific arrangement or formed dense nodules depending on localization. White matter was narrow with an intense proliferation of fibrous astrocytes. A few mature disoriented neurons were misplaced in the white matter. The cerebral cortex band occupied the rim of the structure and presented a disturbed cortical pattern (Fig. 4). Cytoarchitecture of the cortex differed between the frontal and rear surface of the telencephalon. Layer I was hypocellular, while in the other superficial layers neurons were radially arranged in clusters. In layer V multiple neuropil islands devoid of neurons were observed. The cortex of the rear telencephalic surface was more disorganized. The cortical band was thick with neurons concentrated in the deepest layers. In the superficial layers only a few small islands of neurons were seen. The cortical architectonic of inferior-medial gyri resembled dysplastic hippocampal and entorhinal cortex. Striatum was indiscernible.

Beneath the telencephalon dorsal diencephalon was covered by gliomesenchymal membranes with ependymal cells and choroid plexus elements consistent with the appearance of the dorsal sac membrane. Cell-rich mesenchymal and glial tissue with angiomatous cavernoma-like structures and multiple congested vessels surrounded the ventral diencephalon. The structures of the diencephalon were rudimentary. An indistinct fused mass and indiscernible anatomical nuclei were observed. The third ventricle appeared in the lowest midline part of the diencephalon, close to the diencephalon-mesencephalon

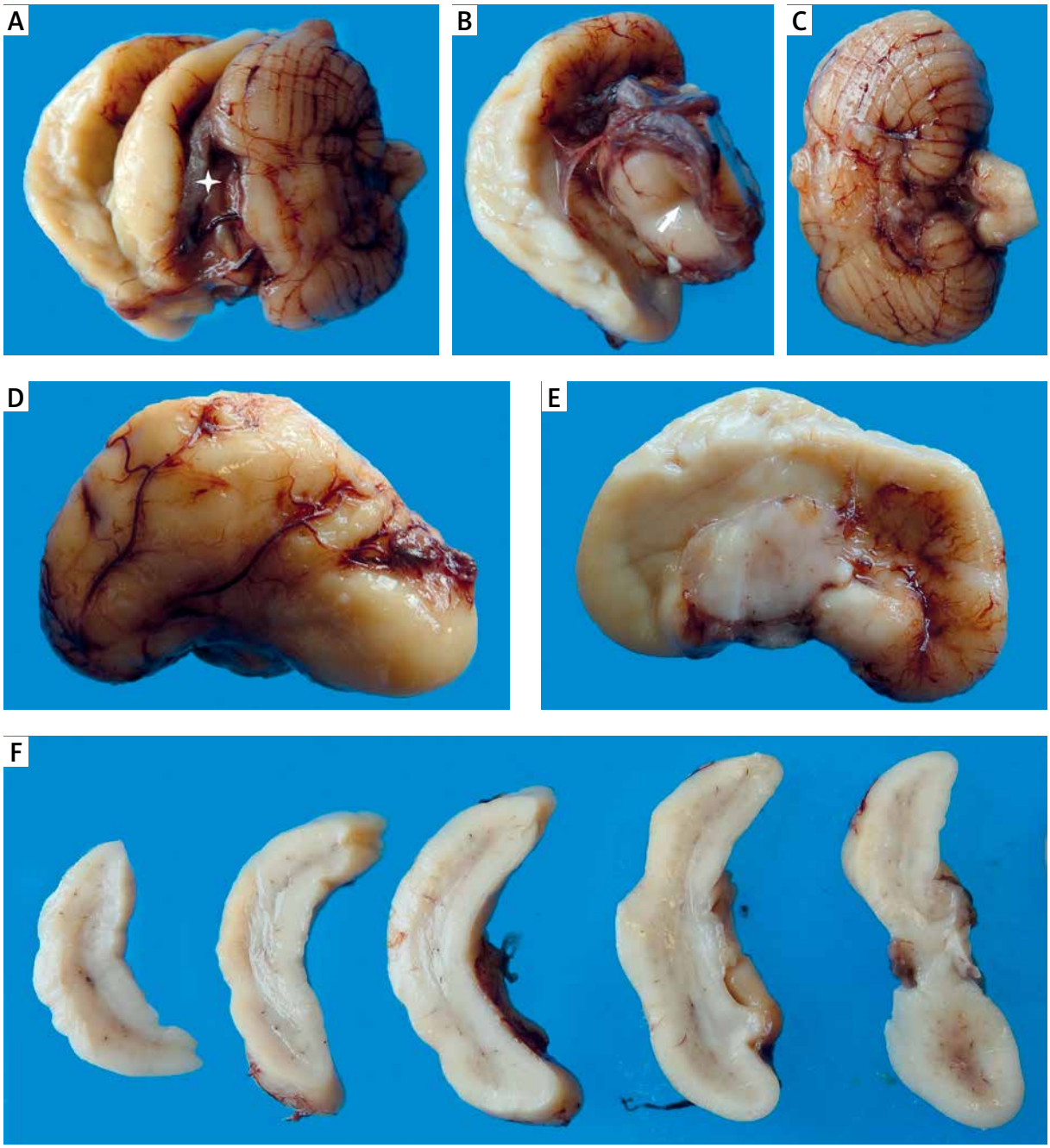

Fig. 1. Macroscopic view of the malformed brain. **A)** Dorsal view of the whole brain, collapsed dorsal cyst (asterisk). **B)** Undivided telencephalon and diencephalon, infundibulum-shaped orifice opened to the subarachnoid space (arrow). **C)** The well-formed cerebellum, development compatible with gestational age. **D)** Continuous across the midline telencephalon with aberrant convolutional pattern; there is no interhemispheric fissure-frontal view. **E)** Telencephalon, view from the back on the telencephalon-diencephalon junction. **F)** Cross-section through telencephalon, C-shaped narrow solid mass without recognizable ventricle.

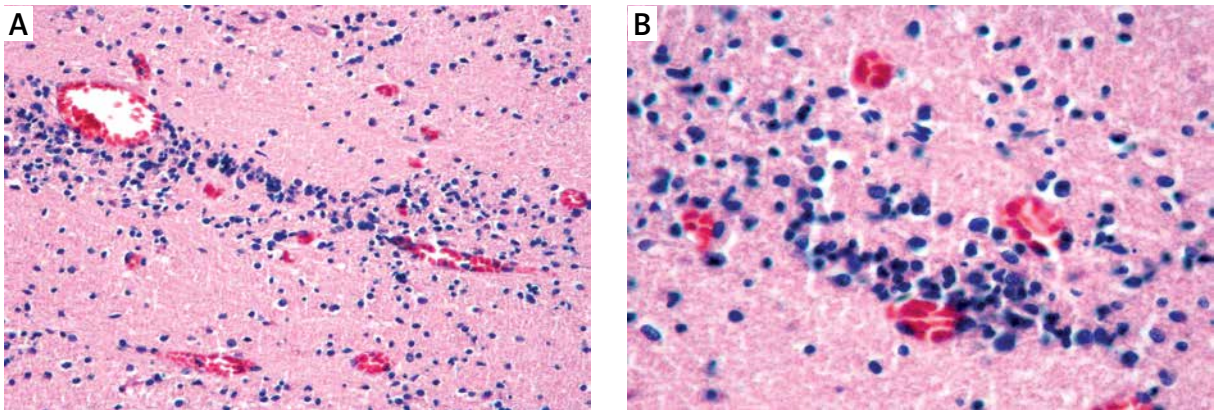

Fig. 2. Aligned glial cells resembling subependymal glia and congested thin-walled blood vessels located in the middle of the solid frontal mass. Hematoxylin-eosin. **A)** Magn. ×200; **B)** magn. ×400.

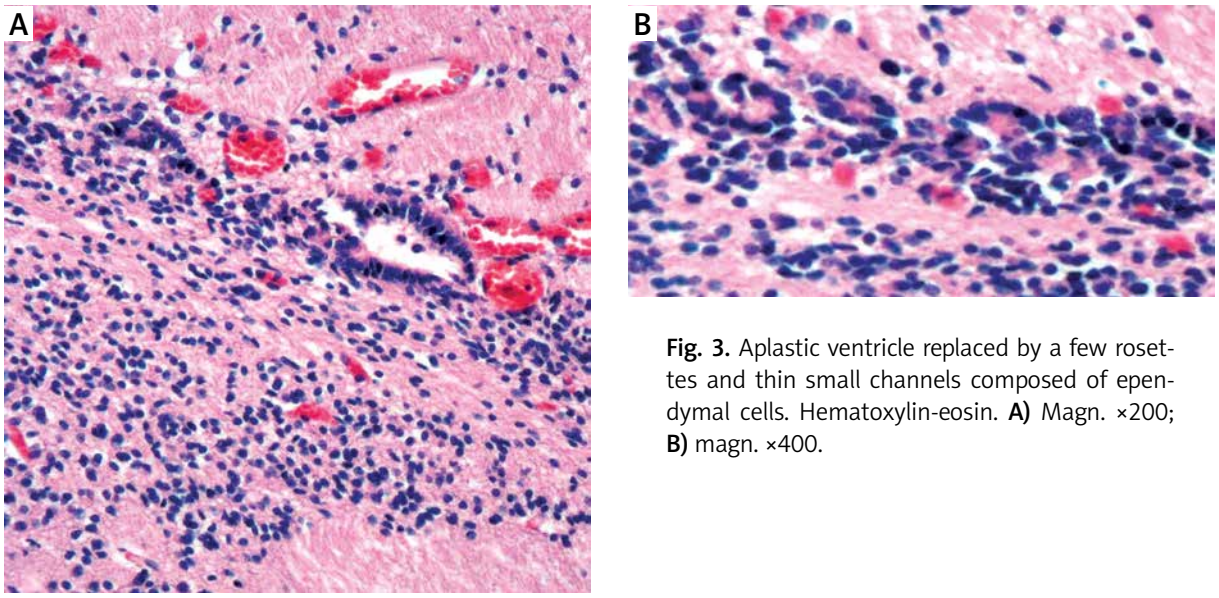

Fig. 3. Aplastic ventricle replaced by a few rosettes and thin small channels composed of ependymal cells. Hematoxylin-eosin. **A)** Magn. ×200; **B)** magn. ×400.

junction. The aqueduct was narrow, and the 4th ventricle was normal. The pons, medulla oblongata and cerebellum were properly developed.

Discussion

Severe brain malformations may present a wide spectrum of variants. Difficulties in classification require detailed analysis of their morphological picture with regard to normal development of the central nervous system.

During embryological development the prosencephalon is the primitive forebrain vesicle at the rostral end of the neural tube following closure of the anterior neuropore [18]. The lamina terminalis is the membrane that closes the anterior neuropore. An intact notochord is important for the induction of lamina terminalis. The prosencephalon develops around the lamina terminalis [24]. The primordial ventricular system originates also at the time of neural tube closure. The wall of the forebrain vesicle is composed by the neuroepithelium around the primordial ventricle. All forebrain structures begin their development in the zone around the ventricles. Neuronal migration is the way by which neurons travel from their origin to their final position in the brain. At 33 gestational days the first wave of neuroblasts migrates radially from the periventricular zone to the pial surface. The prosencephalon gives rise to the telencephalon and diencephalon. The telencephalon and diencephalon are formed from the fore-

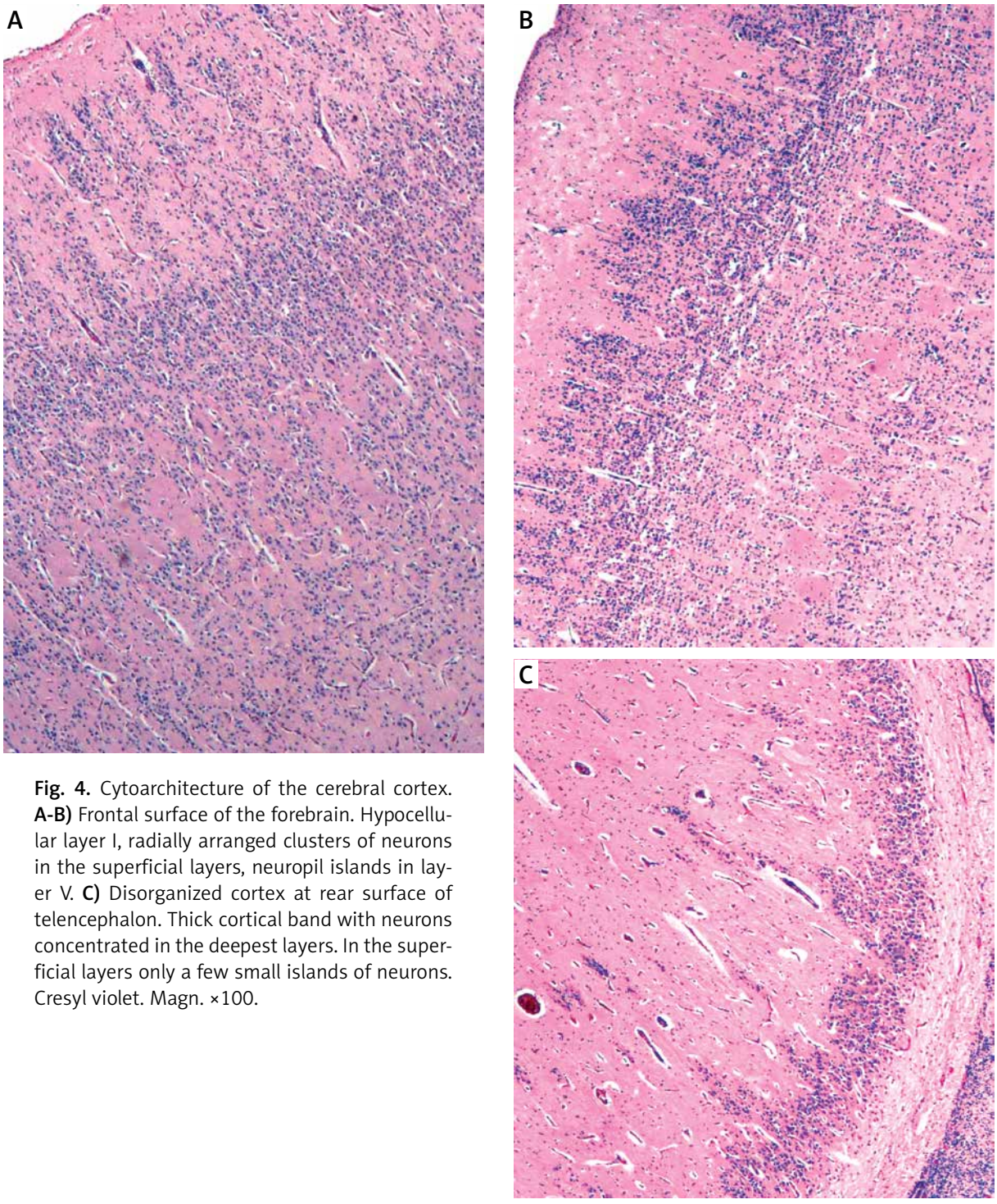

Fig. 4. Cytoarchitecture of the cerebral cortex. **A-B)** Frontal surface of the forebrain. Hypocellular layer I, radially arranged clusters of neurons in the superficial layers, neuropil islands in layer V. **C)** Disorganized cortex at rear surface of telencephalon. Thick cortical band with neurons concentrated in the deepest layers. In the superficial layers only a few small islands of neurons. Cresyl violet. Magn. ×100.

brain during the 5th week of development. At that developmental stage the telencephalon starts to grow to form the cerebral hemispheres, corpus striatum and the lateral ventricles. The rapid growth of the telencephalon modifies the size, shape and internal arrangement of the forebrain and its cavities. The dorsal and lateral growth of the neopallium forms the parietal and frontal lobes, and the posterior and ventral expansions form the occipital and temporal lobes. Following dynamic backwards

expansion the hemispheres cover the thalami by 3rd month, by the 4th the midbrain, and by the 6th gestational month the occipital lobes begin to cover the cerebellum. In the meantime the hypothalamus, thalamus and basal ganglia differentiate and settle in their normal anatomical localization. Simultaneously the cavities corresponding to the lateral ventricles enlarge backwards and downwards, forming the occipital and temporal horns, and the anterior horns and bodies become compressed by the expanding basal ganglia and callosal body [13,17,22,24].

The morphogenetic steps are controlled and coordinated by signaling pathways such as Sonic hedgehog, bone morphogenetic protein, fibroblast growth factor, and nodal signaling [21]. Nodal signaling is essential for the initial specification of the prechordal plate, hedgehog signaling is crucial for the ventral forebrain development, retinoid signaling is critical in anterior-posterior patterning, fibroblast growth factor signaling is pivotal in growth of the developing forebrain due to cell proliferation and midline formation, and bone morphogenetic protein signaling participates in the organization of the medial-lateral axis of the developing telencephalon and is necessary for formation of the dorsal midline [21,26]. Mutations in these pathways have been determined in human patients and animal models of holoprosencephaly [1,3-5,15,17]. Polygenic mechanisms and gene-environmental interactions play a major role in the formation of holoprosencephaly [27].

Holoprosencephaly is a developmental failure of the forebrain characterized by its faulty midline division with concomitant associated midline defects [8]. Defect of neural induction at the lamina terminalis and inappropriate patterning of the rostral neural tube into the prosencephalon with a significant role of the prechordal plate play crucial roles [18,23].The prosencephalon fails to divide sagittally into the cerebral hemispheres, transversely into the telencephalon and diencephalon, and horizontally into the olfactory tracts and bulbs [3]. An abnormally small prosencephalic protrusion with a single ventricle was observed early during embryogenesis [26,31]. A critical period for holoprosencephaly occurs prior to neural tube closure, about the gastrulation or primitive streak stage, around the sixteenth day after fertilization. Perturbation of gene expression at this stage can disturb later development of the forebrain and result in holoprosencephaly-like malformations.

The presented case demonstrated characteristic features of classical holoprosencephaly [14]. The brain was evidently hypoplastic, with a very small, undivided, disc-shaped telencephalon without an interhemispheric fissure. The cerebral lobes could not be defined. The gyral pattern was abnormal. The frontal part was small and did not cover the midbrain.

The middle part of the brain corresponding to the diencephalon was covered in its dorsal part by meninges forming the dorsal cyst. Into this subarachnoid space the infundibulum of the third ventricle opened. A common feature in holoprosencephaly is the presence of a dorsal sac membrane, which represents the unfolded diencephalic roof plate and covers the dorsocaudal part of the prosencephalic ventricle [22,29]. Simon [28] suggested that the unseparated thalamus in holoprosencephaly blocks the way out for cerebrospinal fluid leakage from the third ventricle, resulting in expansion of the posterodorsal portion of the ventricle to form the cyst. Probst and Sarnat combined the origin of the dorsal cyst with the dilated suprapineal recess of the third ventricle [22,23]. The roof plate, which forms at the dorsal midline of the neural tube, is a well-known signaling center in central nervous system (CNS) development. Multiple developmental processes in the dorsal telencephalon depend on the roof plate. The roof plate is essential for normal external cortical mantle formation and dorsal cortical patterning. Bone morphogenetic protein signaling plays a role in the roof plate patterning functions [2]. Roof plate cell loss causes reduction of the Bmp activity gradient and failed midline induction.

On coronal sections through the front part of the brain the lack of a ventricular cavity drew attention. Instead of a single ventricular lumen there were only a few small ependymal rosettes and thin narrow channels lined with ependymal cells. It is difficult to comment on whether the prosencephalic part of the ventricular system developed primarily or was secondarily obliterated. During the normal development of the ventricular system there are transient fetal ventricular protrusions into olfactory bulbs and into centers of the optic nerves. These sacs lined with ependyma become obliterated in early gestation [24].

The fetal ependyma matures in a precise temporal and spatial pattern in the human CNS [23]. In the vicinity of ependymal lined channels dispersed

germinative small cells were seen. Disturbance in ependymal differentiation connected with the anomalous ventricle secondarily interferes with defective neuronal migration. Deficient neurogenesis and defective migration result in failure of neuroblasts to reach the surface and form a proper cortical plate. Some neurons lost their migratory way and settled in the white matter. White matter in the solid telencephalon was narrow with intensified gliosis, similar to that described in cases of classical holoprosencephaly [11,14]. The cerebral cortex band revealed cytoarchitecture characteristic for holoprosencephaly [14,16]. The segmentation of superficial neurons into irregular clusters and deeply placed glomerular islands devoid of nerves were observed in the dorsal surface of the telencephalon. The cortex of the ventral surface was severely disorganized.

The diencephalon presented an indistinct fused mass. Anatomical nuclei were indiscernible. Thick gliomesodermal tissue was attached to the diencephalon. Some variations in the severity of dysfunctions of the fused diencephalon and basal ganglia among the alobar HPE cases have been described in the literature [8]. Lack of separation of the thalamus in holoprosencephaly is thought to result from an imbalance of dorsal and ventral patterning signals in the embryonic forebrain – the cells that should occupy the midline of the prosencephalon never form, and the structures that should normally be lateral to the midline are fused [28].

The morphological picture of the presented brain can be properly graded within the holoprosencephalic spectrum. However, some elements matching other prosencephalic malformations occurred.

At the telencephalon-diencephalon junction a proliferation of thin-walled vascular channels mixed with disorganized neural tissue without recognizable structure corresponding to the "area cerebrovasculosa" was observed. The area cerebrovasculosa replaces the telencephalon of the anencephalic brain [24].

Anomalous ventricles correspond to aprosencephaly/atelencephaly (AP/AT). Aprosencephaly/atelencephaly is defined by the lack of prosencephalic derivatives [3,9,10,14]. An early failure of the neural tube in forming a normal prosencephalon plays a role in pathogenesis [30]. The failure occurs after neurulation and before the prosencephalon begins to grow [10]. In aprosencephaly both prosencephalic and diencephalic derivatives fail to develop. In atelencephaly the tiny forebrain remnant is composed of disorganized grey and white matter and prominent leptomeningeal gliomesodermal proliferation without a ventricular cavity. Ependymal lined tubules are observed. Complete absence of the cytoarchitecture of both the telencephalic and diencephalic structures is observed [24].

Pasquier [20] suggested a common pathogenic mechanism of aprosencephaly/atelencephaly and holoprosencephaly. Their neuropathological and mutational analysis with phenotype and genotype evaluation provides strong evidence for a link between AP/AT and holoprosencephaly and the role of the *SIX3* gene in the genesis of AP/AT.

In summary, the presented malformation corresponds to a wide continuous spectrum with no clear-cut boundaries of abnormal formation of the prosencephalon. Disturbance in the sequence of interrelated and interdependent developmental pathways has influenced the abnormal course of forebrain formation. Failure in primary induction and improper patterning of the rostral neural tube during the early embryogenesis resulted in morphological alterations related to holoprosencephaly and atelencephaly. Coexistence of cerebral anomalies characteristic for holoprosencephaly and atelencephaly in the same case confirms the suggestion of a common pathogenic mechanism of these malformations.

Disclosure

Authors report no conflict of interest.

References

1. Bertrand N, Dahmane N. Sonic hedgehog signaling in forebrain development and its interactions with pathways that modify its effects. Trends Cell Biol 2007; 16: 597-605.
2. Cheng X, Hsu C, Currle S, Hu S, Barkovich AJ, Monuki ES. Central roles of the roof plate in telencephalic development and holoprosencephaly. J Neurosci 2006; 26: 7640-7649.
3. Cohen MM. Holoprosencephaly: Clinical, anatomic, and molecular dimensions. Birth Defects Res (Part A) 2006; 76: 658-673.
4. Cordero DR, Tapadia M, Helms JA. The etiopathologies of holoprosencephaly. Drug Discovery Today 2005; 2: 529-537.
5. Dubourg C, Bendavid C, Pasquier L, Henry K, Odent S, David V. Holoprosencephaly. Orphan J Rare Dis 2007; 2: 8.
6. Garfinkle WB. Aventriculy: a new entity? AJNR 1996; 17: 1649-1650.
7. Geng X, Oliver G. Pathogenesis of holoprosencephaly. J Clin Invest 2009; 119: 1403-1413.
8. Hayashi M, Araki S, Kumada S, Itoh M, Morimatsu Y, Matsuyama H. Neuropathological evaluation of the diencephalon,

basal ganglia and upper brainstem in alobar holoprosencephaly. Acta Neuropathol 2004; 107: 190-196.
9. Ippel PF, Breslau-Siderius EJ, Hack WWM, van der Blij HF, Bouve S, Bijlsma JB. Atelencephalic microcephaly: a case report and review of the literature. Eur J Pediatr 1998; 157: 493-497.
10. Kakita A, Hayashi S, Arakawa M, Takahashi H. Aprosencephaly: histopathological features of the rudimentary forebrain and retina. Acta Neuropathol 2001; 102: 110-116.
11. Kinsman SL. White matter imaging in holoprosencephaly in children. Curr Opin Neurol 2004; 17: 115-117.
12. Kumar S, Jaiswal JA, Rastogi M. Aventriculi associated with holoprosencephaly. J Clin Neurosci 2006; 13: 378-380.
13. Lowery LA, Sive H. Totally tubular: the mystery behind function and origin of the brain ventricular system. Bioessays 2009; 31: 446-458.
14. Marcorelles P, Laquerriere A. Neuropathology of holoprosencephaly. Am J Med Genet Part C Semin Med Genet 2010; 154C: 109-119.
15. Mercier S, Duborg C, Belleguic M, Pasquier L, Loget P, Lucas J, Bendavid C, Odent S. Genetic counseling and "molecular" prenatal diagnosis of holoprosencephaly. Am J Med Genet Part C Semin Med Genet 2010; 154C: 191-196.
16. Mizuguchi M, Morimatsu Y. Histopatological study of alobar holoprosencephaly.1.Abnormal laminar architecture of the telencephalic cortex. Acta Neuropathol 1989; 78: 178-182.
17. Muenke M, Beachy PA. Genetics of ventral forebrain development and holoprosencephaly. Curr Opin Genet Dev 2000; 10: 262-269.
18. Müller F, O'Rahilly R. Mediobasal prosencephalic defects, including holoprosencephaly and cyclopia in relation to the development of the human forebrain. Am J Anat 1989; 185: 391-414.
19. O'Rahilly R, Müller F. The developmental anatomy and histology of the human central nervous system. In: Handbook of Clinical Neurology. Vol 6. Malformations. Myrianthopoulos NC (ed.). Elsevier Science Publishers, Amsterdam, New York 1987; pp. 1-17.
20. Pasquier L, Duborg C, Gonzales M, Lazaro L, David V, Odent S, Encha-Razavi F. First occurrence of aprosencephaly/atelencephaly and holoprosencephaly in a family with a SIX3 gene mutation and phenotype/genotype correlation in our series of SIX3 mutations. J Med Genet 2005; 42: e4.
21. Petryk A, Graf D, Marcucio R. Holoprosencephaly: signaling interactions between the brain and the face, the environment and the genes, and the phenotypic variability in animal models and humans. WIREs Dev Biol 2015; 4: 17-32.
22. Probst FP. The prosencephalies. Morphology, neuroradiological appearances and differential diagnosis. Springer-Verlag, Berlin, Heidelberg, New York 1979.
23. Sarnat HB, Flores-Sarnat L. Neuropathologic research strategies in holoprosencephaly. J Child Neurol 2001; 16: 918-931.
24. Sarnat HB. Disorders of the lamina terminalis:midline malformations of the brain. In: Cerebral dysgenesis. Embryology and clinical expression. Oxford University Press, New York 1992; pp. 167-207.
25. Sener RN. Aventriculi associated with holoprosencephaly. Comp Med Imaging Graph 1998; 22: 345-347.
26. Shiota K, Yamada S, Komada M, Ishibashi M. Embryogenesis of holoprosencephaly. Am J Med Genet Part A 2007; 143A: 3079-3087.
27. Shiota K, Yamada S. Early pathogenesis of holoprosencephaly. Am J Med Genet Part C Semin Med Genet 2010; 154C: 22-28.
28. Simon EM, Hevner RF, Pinter JD, Clegg NJ, Deglado M, Kinsman SL, Hahn JS, Barkovich AJ. The dorsal cyst in holoprosencephaly and the role of the thalamus in its formation. Neuroradiology 2001; 43: 787-791.
29. Utsunomiya H, Yamashita S, Takano K, Ueda Y, Fujii A. Midline cystic malformations of the brain: imaging diagnosis and classification based on embryologic analysis. Radiat Med 2006; 24: 471-481.
30. Volpe P, Campobasso G, De Robertis V, Rembouskos G. Disorders of prosencephalic development. Prenat Diagn 2009; 29: 340-354.
31. Yamada S. Embryonic holoprosencephaly: pathology and phenotypic variability. Congenit Anom 2006; 46: 164-171.

DOI: 10.5114/fn.2015.56554

Neurochemical Conference 2015

The Days of Neurochemistry

"Neuropsychoimmunological mechanisms in the pathology of neurodegenerative diseases: From biomarkers to therapeutics"

October 22-23, 2015

Warsaw, Poland

ORGANIZERS

Polish Academy of Sciences, Mossakowski Medical Research Centre
Polish Academy of Sciences, Division V Medical Sciences
and The Committee of Neurological Sciences

LOCAL ORGANIZING COMMITTEE

Agata Adamczyk
Joanna B. Strosznajder
Grzegorz A. Czapski
Anna Wilkaniec
Magdalena Gąssowska
Henryk Jęśko
Robert P. Strosznajder
Beata Łuczyńska

Editorial note:
The communications presented at the Conference are printed without alterations from the manuscripts submitted by the authors, who bear the full responsibility for their form and content.

ORAL

|A1|

Synaptic Shank proteins alterations in rat offspring following maternal immune activation: implications for autism spectrum disorders

Agata Adamczyk[1]*, Henryk Jęśko[1], Magdalena Gąssowska[1], Agnieszka Dominiak[2], Paweł M. Boguszewski[3], Magdalena Cieślik[1]

[1]Department of Cellular Signalling, Mossakowski Medical Research Centre Polish Academy of Sciences, Warsaw, Poland
[2]Department of Drug Bioanalysis and Analysis, Medical University of Warsaw, Warsaw, Poland
[3]Laboratory of Animal Models, Neurobiology Center, Nencki Institute of Experimental Biology, Polish Academy of Sciences, Warsaw, Poland

Agataadamczyk72@gmail.com

Autism spectrum disorders (ASDs) are a heterogeneous group of neurodevelopmental brain diseases that are clinically defined by emotional and social deficits, impairments in social interaction and stereotyped behaviours such as repetitive movements or speech. The recent study suggested that alterations of ProSAP/Shank proteins located at the post-synaptic density and involved in synaptic formation, development, and function may play a crucial role in ASD pathomechanism. Mutations in the family of SHANK genes, SHANK1, SHANK2, and SHANK3, are strongly associated with ASD. However, the specific role of the various Shank proteins in the pathogenesis of ASD is still unclear. Prenatal maternal immune activation (MIA) is a risk factor for ASD and is commonly used as animal model of this disorders. In the present study pregnant dams of Wistar rats were injected intraperitoneally (i.p.) at gestational day 9.5 with 0.1mg/kg lipopolysaccharide (LPS), which mimics infections by gram-negative bacteria. We investigated the effect of MIA on the expression and protein level of ProSAP/Shank family proteins in male offspring of rats. Additionally, protein levels of postsynaptic organizing molecule PSD-95 associated with Shank, phosphorylated and total Akt, and brain-derived neurotrophic factor (BDNF) expression were measured in LPS-treated animals versus control subjects. Moreover, redox potential and pro-oxidative/pro-inflammatory proteins were analysed along with the autism-associated behaviour.

The data showed MIA-induced down-regulation of SHANK1, SHANK2, and SHANK3 in the cerebral cortex, without changes in other brain structures. Therefore, the further studies were carried out using only brain cortex. Western blotting revealed significant alteration of pre- and post-synaptic proteins level. Moreover, a statistically significant decrease in phosphorylated Akt (pAkt) and pAkt/Akt ratio in MIA subjects was indicated. In addition, the GSH/GSSG ratio used as an indicator of oxidative stress was reduced. Furthermore, the gene expression for interleukin-6 (IL-6), cyclooxygenase-2 (COX-2) as well as 12-lipoxygenase (LOX-12) were up-regulated. Along with the biochemical investigation behavioural tests were conducted to assess social communication, motions and anxiety, play behaviours as well as learning and memory. The results showed no bedding preference in prenatal LPS exposure animals at post-natal day 14 compared to control rats, indicating the impairment of need being in proximity of the mother. In conclusion, our findings indicate MIA-induced down-regulation of SHANK family and alteration of others synaptic proteins, reduced antioxidative capacity as well as activation of proinflammatory genes. These changes may disturb synaptic structure and function as well as social communication behaviour.

Supported from MMRC statutory theme 8.

|A2|

A search for mechanisms of Parkinson's disease (PD)-associated depression in an animal model

Klemencja Berghauzen-Maciejewska*[1], Urszula Głowacka[1], Helena Domin[2], Maria Śmiałowska[2], Katarzyna Kuter[1], Barbara Kosmowska[1], Krystyna Ossowska[1], Jadwiga Wardas[1]

[1]Department of Neuropsychopharmacology and [2]Department of Neurobiology, Institute of Pharmacology, Polish Academy of Sciences, Krakow, Poland

klemberg@if-pan.krakow.pl

Depression may appear in a preclinical period of PD. Alterations of serotonin (5-HT) transporter (SERT) and BDNF signaling have been suggested to be associated with major depression. However their role in PD associated depression is unknown.

The aim of the study was to examine if a partial dopaminergic lesion modeling pre-clinical phase of PD may induce 'depressive-like' behaviour of rats. Furthermore, a role of SERT and BDNF in this behaviour and antidepressant drug action were evaluated.

Rats were injected with 6-OHDA into the ventral part of the caudate-putamen (CP). Pramipexole [(PRA), a dopamine D3/D2 receptor agonist, the most effective compound in the treatment of depression in PD] or imipramine [(IMI) a classic tricyclic antidepressant] were administered for 2 weeks. 24 h later the behavioural tests were performed and rats were decapitated.

6-OHDA induced moderate DA depletion in CP, nucleus accumbens (NAC) and frontal cortex, loss of DA neurons in the substantia nigra, ventral tegmental area (VTA) and dorsal raphe (DR), decreases in binding to DA transporter (DAT) in CP and NAC. Contrariwise, 6-OHDA influenced neither the number of DR 5-HT neurons, nor forebrain 5-HT levels. The lesion prolonged the immobility in FST but did not influence motility of rats. PRA, but not IMI shortened the immobility in lesioned rats. PRA but not IMI increased levels of DA metabolites and its turnover.

The lesion reduced the BDNF and trkB mRNAs in the hippocampus and amygdala. PRA increased BDNF mRNA but decreased trkB mRNA in VTA in lesioned rats. Furthermore, it reduced BDNF and/or trkB mRNA expression in NAC, amygdala and CP in these animals. The lesion lowered the [3H]citalopram binding to SERT in DR, and in all structures of 5-HT terminals. Similarly, PRA decreased the binding to SERT in the above regions.

These results indicate that a moderate DA lesion, which does not produce motor disturbances, may induce "depressive-like" symptoms which are reversed by DA agonist but not by a classic antidepressant. Mechanisms responsible for the above behaviour may be associated with decreased DA but not 5-HT transmission. Moreover, the increase of DA transmission and reduced BDNF signaling in NAC and amygdala induced by PRA may contribute to its antidepressant efficacy.

Financing: DEMETER (POIG.01.01.02-12-004/09-00) from the European Regional Development Fund (Operative Programme "Innovative Economy 2007-2013) and the Statutory Funds of the Institute of Pharmacology.

|A3|

Towards treatment of amyloid toxicity in dementia

Konrad Beyreuther*

Network Aging Research (NAR), Heidelberg University, Heidelberg, Germany

beyreuther@nar.uni-heidelbeg.de

The correlation between the total amount of fibrillar aggregates and cognitive decline depends not only on the quantity of the amyloid protein deposited but also on the number of synapses to be destroyed. Indeed, patient with Alzheimer's disease (AD) exhibiting similar level of clinical severity, higher levels of education are associated with more severe disease related changes of β-amyloid PET or CSF Aβ42 levels suggesting that amyloid toxicity may be the same in patients with matched clinical severity but gross differences in AD pathology. Pre-fibrillary Aβ species rather than elongated amyloid fibrils are likely to represent the primary pathogenic agents simply because the former provide on their surfaces more chemical groups than the latter, such as hydrophobic side chains and unbound hydrogen bonds that would not be accessible within amyloid. The origine of the toxicity of the oligomers may arise from inappropriate interaction in trans with the folding of cellular and extracellular structures including proteins, lipid membranes and nucleic acids. Therefore, prevention and treatment of protein misfolding disorders needs to address aggregation and misfolding in cis and trans by decreasing the concentration and disrupting the formation of these toxic species. This can be achieved, as we have shown firs, with Aβ-analogues that selectively bind to the native state of the peptide that suppress nucleation and proliferation of toxic pre-amyloid species, by antibodies to reduce the level of highly trans-aggregation prone species (such as Aβ oligomers), and by stimulating clearance by proteolytic degradation.

|A4|

Pathogenic microRNA (miRNA) signaling in Alzheimer's disease (AD) and age-related macular degeneration (AMD) target common genetic pathways leading to amyloidogenesis and inflammatory neurodegeneration

Surjyadipta Bhattacharjee[1], Evgeny I. Rogaev[2,3], Brandon Jones[1], James M. Hill[1,4], Yuhai Zhao[1], Prerna Dua[5], Walter J.Lukiw[1]

[1]Neuroscience & Ophthalmology, Louisiana State University Health Science Center, New Orleans, LA, USA
[2]Department of Neurogenetics, Vavilov Institute of General Genetics, Russian Academy of Medical Sciences, Moscow, Russian Federation
[3]University of Massachusetts School of Medicine, Worcester, MA, USA
[4]Departments of Microbiology and Pharmacology, Louisiana State University Health Science Center, New Orleans, LA, USA
[5]Health Information Management, Louisiana Technical University, Ruston, LA, USA
[6]Department of Neurology, Louisiana State University Health Science Center, New Orleans, LA, USA

wlukiw@lsuhsc.edu

Overview: Progressive amyloidogenesis and inflammation in the neocortex and retina are associated with aberrant innate-immune signaling and inflammatory degeneration in both Alzheimer's disease (AD) and age-related macular degeneration (AMD). Two pivotal players in this pathogenic system are the immune-repressor protein complement factor H (CFH) and the triggering receptor expressed in myeloid/microglial cells (TREM2), each found to be reduced in abundance in AD and AMD. Here we investigated the mechanism of CFH and TREM2 expression regulation in AD and AMD involving the up-regulated, NF-κB-sensitive miRNA-34a, miRNA-146a and miRNA-155, and the effects of specific anti-NFkB and anti-miRNA therapeutic strategies which may be useful in the clinical management of these disorders.

Methods: Aβ42-peptide- and/or TNFα-induced stress; AD/AMD tissues; bioinformatics; DNA array/RNA sequencing; human retinal/brain cells; LED-Northern dot blot analysis; micro-RNA array; NF-kB-inhibitors luciferase-reporter transfection; Western analysis.

Results: A major ~4200 nucleotide (nt) human CFH mRNA included a 232 nt 3'UTR, containing recognition features for 27 miRNA-mRNA interactions. Similarly, multiple miRNA binding sites were found in the 299 nt TREM2 mRNA 3'UTR. Binding of miRNA-34a, miRNA-146a and/or miRNA-155 to the CFH- or TREM2-3'UTR dramatically decreased CFH or TREM2 expression. This deficit was in part reversed using NF-kB inhibitors or anti-miRNA pharmacological strategies.

Conclusions: Our perception on the mechanism and relevance of miRNA signaling in brain and retina continues to evolve. For the first time these data provide evidence for novel miRNA-mediated genetic switches in the CFH and TREM2 mRNA 3'UTRs that are differentially regulated in the brain and retina. These data further suggest that epigenetic mechanisms involving inducible miRNAs contribute to immune-inflammatory degeneration and amyloidogenesis characteristic of age-related disorders, and further support the use of novel transcription factor- and nucleic acid-based therapeutic strategies in the clinical management of AD and/or AMD.

Support: Research on miRNA in the Lukiw laboratory involving the innate-immune response in AD, AMD and in retinal disease, amyloidogenesis and neuroinflammation was supported through an unrestricted grant to the LSU Eye Center from Research to Prevent Blindness (RPB); the Louisiana Biotechnology Research Network (LBRN) and NIH grants NEI EY006311 and NIA AG038834.

|A5|

PPAR-gamma: therapeutic prospects in Parkinson's disease

Anna R. Carta*, Daniela Lecca, Giovanna Mulas

Department of Biomedical Sciences, University of Cagliari, Cagliari, Italy

acarta@unica.it

Skewed microglia activation with pro-inflammatory prevailing over anti-inflammatory phenotypes may contribute to neurotoxicity in Parkinson's disease (PD), via the production of cytokines and neurotoxic species. Targeting the microglia polarization process is a proposed strategy for neuroprotection. The peroxisome proliferator-activated receptor (PPAR)gamma is expressed in microglia and peripheral immune cells, where they are involved in macrophages polarization. PPARγ agonists mediate neuroprotection in PD models. We investigated the neuroprotective activity of PPARγ agonists in the chronic MPTP/probenecid (MPTPp) models of PD, and their action on microglia polarization via the evaluation of pro- and anti-inflammatory molecules. PPARγ agonists rosiglitazone and the novel compound MDG548, were neuroprotective in the MPTPp model and reduced microglia activation and iNOS produc-

tion in the substantia nigra compacta (SNc). Moreover, we found a gradual increase of pro-inflammatory cytokines tumor necrosis factor (TNF)-α and interleukin (IL)-1β, over anti-inflammatory molecules such as transforming growth factor (TGF)-β, IL-10 and CD206, within Iba-1-positive microglia, suggesting that a skewed polarization was associated with disease progression. Rosiglitazone and MDG548 administered during the full MPTPp treatment or for the last 10 days, reduced pro-inflammatory cytokines while increasing anti-inflammatory molecules as compared with the MPTPp treatment. Therefore, neuroprotective treatment with PPAR-γ agonists exerts an anti-inflammatory action via a modulation of microglia polarization correcting the imbalance between pro- over anti-inflammatory molecules, offering a novel immunomodulatory approach to neuroprotection.

|A6|

Regulated cell death pathways converging at mitochondria are promising therapeutic targets for neuroprotection

Carsten Culmsee

Institut für Pharmakologie und Klinische Pharmazie, Philipps-Universität Marburg, Germany

culmsee@staff.uni-marburg.de

Mitochondria play crucial roles in energy metabolism, regulation of free radical formation and calcium storage, thereby determining essential metabolic functions and cell survival, in particular in neurons. Under physiological conditions, mitochondria are highly dynamic organelles that undergo constant fission and fusion and these dynamic morphological changes are essential for mitochondrial functions. Consistent with the critical role of mitochondrial dynamics in neurons, impairments of mitochondrial fission and fusion are associated with a wide array of inherited or acquired neurodegenerative diseases. In order to elucidate impaired mitochondrial dynamics in different paradigms neuronal cell death, including oxytosis, ferroptosis and necroptosis, our studies focus on the regulation of mitochondrial integrity in neuronal cells in vitro and after cerebral ischemia in vivo. In neuronal HT22 cells, glutamate and erastin induce pronounced production of ROS followed by mitochondrial fission through mechanisms of oxytosis and ferroptosis, respectively. The fragmented mitochondria accumulate around the nucleus and release apoptosis inducing factor (AIF) which executes cell death in a caspase-independent manner. The mechanisms upstream of detrimental mitochondrial fission involve concomitant mitochondrial translocation of Bid and dynamin related protein 1 (Drp-1) which mediate mitochondrial membrane permeabilization. Inhibition of Bid or Drp-1, as well as inhibition of ferroptosis by ferrostatin or inhibition of necroptosis by necrostatin-1 preserve mitochondrial morphology and provide neuroprotective effects, also after oxygen glucose deprivation in primary cultured neurons and in models of cerebral ischemia in vivo. In conclusion, our data suggest that regulators of pathological mitochondrial fragmentation such as Bid and Drp-1 as well as pathways of ferroptosis and necroptosis are promising therapeutic targets for neuroprotection.

|A7|

Cyclin-dependent kinase 5 signaling in neuroinflammation and neurodegeneration

Grzegorz A. Czapski*

Department of Cellular Signalling, Mossakowski Medical Research Centre PAS, Warsaw, Poland

gczapski@imdik.pan.pl

The common feature of age-related neurodegenerative disorders is accumulation, improper folding and aggregation of specific proteins, with amyloid beta (Aβ) and alpha synuclein (ASN) being the most prominent representatives. The growing body of evidence suggests that significant component of molecular mechanisms of misfolded proteins' toxicity may be dysfunction of cyclin-dependent kinase 5 (Cdk5). Cdk5 is fundamental for central nervous system's development, but also actively contributes in regulating neuronal function in adult brain. Cdk5 controls neurite elongation, synaptogenesis, synaptic plasticity, oxidative stress and neuronal survival, though its deregulation has detrimental effects for neuronal function. In our studies we analyzed the role of Cdk5 in toxicity of two major misfolded proteins, Aβ and ASN. We used PC12 cells stably transfected with human APP gene or incubated with exogenous ASN. For in vivo analysis we used mouse model of systemic inflammatory response and model of acute toxicity of Aβ after intracerebroventricular administration.

The in vitro studies discovered two pathways responsible for Cdk5 overactivation in cytotoxicity of ASN: i) calcium-induced, calpain-dependent proteolysis of Cdk5-activating protein p35 leading to formation of excessive activator of Cdk5-p25, ii) phosphorylation of Cdk5 at

Tyr15. Enhanced activity of Cdk5 was responsible for mitochondrial dysfunction, oxidative stress and cell death evoked by ASN. However, the studies carried out in cells overexpressing Aβ revealed that decrease in Cdk5 activity evokes a decline in the level of phosphorylation of glycogen synthase kinase-3β at Ser9, leading to its activation and to hyperphosphorylation of Tau protein. These results indicate that not only an increase but also a decline of Cdk5 activity may lead to detrimental effects.

The recent data suggest that Cdk5 may actively assist inflammatory signaling. Our in vivo studies showed overactivation of Cdk5 and its involvement in controlling the expression of inflammation-related genes in the brain during systemic inflammatory response. Moreover, we demonstrated the significant role of Cdk5 in regulation of gene transcription in mouse model of Aβ toxicity.

In summary, our results demonstrated that Cdk5 actively contributes to pathomechanism of protein misfolding-linked disorders, being involved in both neurodegeneration and neuroinflammation.

Supported by The National Science Centre grant 2011/03/B/NZ3/04549.

|A8|

Neurosteroids and Alzheimer' disease: mitochondria at the interface

Anne Eckert*, Amandine Grimm

Neurobiology Laboratory for Brain Aging and Mental Health, Transfaculty Research Platform Molecular & Cognitive Neuroscience (MCN), University of Basel, Psychiatric University Clinics Basel, Basel, Switzerland

Anne.Eckert@upkbs.ch

Alzheimer's disease (AD) is an age-related neurodegenerative disorder that currently accounts for more than 60% of all dementia cases and is characterized by a progressive cognitive and physical deterioration. This neuropathology will become increasingly burdensome and costly in the coming years as AD prevalence is expected to double within the next two decades.

Mitochondrial dysfunction is a prominent and early event of the disease, since energy deficiency is a fundamental characteristic of AD that was observed in the brain of AD patients as well as in transgenic AD mouse models. Indeed, an impaired mitochondrial function can already be detected before the onset of cognitive impairments and the appearance of the two histopathological hallmarks of the disease – the presence of extracellular amyloid-β (Aβ) deposits and intracellular neurofibrillary tangles (NFT). Of note, Aβ and abnormally hyperphosphorylated tau protein, which composes the NFT, may act synergistically to trigger mitochondrial dysfunction in AD.

Neurosteroids are steroid molecules that are synthetized within the nervous system independently of peripheral endocrine glands and are involved in brain-specific functions. Neurosteroids have recently shown promise in alleviating cognitive and neuronal sequelae of AD. In particular, extensive studies only focused on estradiol as a promising neurosteroid compound that is able to ameliorate cellular bioenergetics, while the effects of other steroids on brain mitochondria are still poorly understood.

To gain insights into the underlying mechanism of neuroprotection by neurosteroids, in particular those belonging to the sex hormone family, we focused on their effects on AD-related mitochondrial dysfunction. First, we showed that the binding of Aβ to the mitochondrial enzyme ABAD (Aβ-binding alcohol dehydrogenase) disturbed estradiol homeostasis and that a treatment with AG18051, a novel small ABAD-specific compound inhibitor, prevented cell death induced by the presence of Aβ thereby normalizing estradiol levels in vitro. Second, we showed that the bioenergetic deficits induced by either Aβ or abnormally hyperphosphorylated tau protein can be alleviated by a treatment with sex hormones-related neurosteroids, with testosterone representing the lead steroid acting against mitochondrial deficits induced by Aβ, while progesterone and estrogens were more efficient against AD-related tauopathies.

Together, our findings lend further evidences to the neuroprotective effects of neuroactive steroids in AD pathology and indicate that these molecules represent promising tools able to increase mitochondrial bioenergetics in pathological conditions. Our results may open new avenues for the development of gender-based therapeutic approaches in AD.

|A9|

M1 muscarinic agonists and a novel and highly potent activator of the M1R/sigma-1R complex: future therapeutics of Alzheimer's (AD) and Parkinson's disease (PD)

Abraham Fisher[1,2,*], Ilya Bezprozvanny[3,4], Lili Wu[3], Daniel A. Ryskamp[3], Nira Bar-Ner[1], Niva Natan[1], Rachel Brandeis[1], Hanoch Elkon[1], Victoria Nahum[1], Eitan Gershonov[1], Frank M. Laferla[5,6] and Rodrigo Medeiros[5,6]

[1]Israel Institute for Biological Research (IIBR), PO Box 19, Ness-Ziona, Israel (*retired)
[2]Weizmann Institute of Science, Rehovot, Israel (*Academic adviser)
[3]Department of Physiology, University of Texas Southwestern Medical Center, Dallas, TX, USA
[4]Laboratory of Molecular Neurodegeneration, St. Petersburg State Polytechnical University, St. Petersburg, Russia
[5]Department of Neurobiology & Behavior
[6]Institute for Memory Impairments and Neurological Disorders, University of California, Irvine (UCI), USA

fisher_a@netvision.net.il

The M1 muscarinic receptor (M1R) has a major therapeutic role in AD and PD. The sigma-1 receptor (S1R), a molecular chaperone, is another drug target as it plays a fundamental role in cognitive function, mitochondrial functioning and in protein conformation diseases. We previously developed orthosteric M1R agonists (*e.g.*, AF102B, AF267B, and AF292), which act as cognitive enhancers and potential disease modifiers in AD and PD *(review: Fisher, J. Neurochem, 2012)*. Notably, i) AF102B and AF267B decreased CSFAbeta levels in vivo and reduced brain alpha-synuclein in transgenic mice over-expressing human alpha-synuclein; ii) AF267B was effective against cognitive deficits, Abeta42 and tau pathologies in 3xTg-AD mice; and iii) AF102B decreased CSF Abeta in AD patients. We now report on AF710B, a highly potent and selective allosteric M1R and S1R receptor agonist. AF710B exhibits an allosteric agonistic profile on M1R; AF710B (0.1nM, *in vitro*) significantly potentiated the binding and efficacy of carbachol on M1R and their downstream effects (phopho-ERK1/2, phospho-CREB). AF710B (nM range) decreased Tau-hyperphosphorylation, GSK3beta activation, and reduced apoptosis and mitochondrial dysfunction *via* increased Bcl2/Bax. AF710B (1-30 microg/kg, po) was a potent and safe cognitive enhancer in rats treated with the M1R antagonist trihexyphenidyl (passive avoidance impairment). These effects of AF710B involve S1R activation. In agreement with its anti-amnesic properties, AF710B (at 30 nM), via activation of M1R and a possible involvement of S1R, rescued mushroom synapse loss in PS1-KI and APP-KI neuronal cultures, while AF267B (1 microM) was less potent in PS1-KI and ineffective in APP-KI models, respectively. In female 3xTg-AD mice AF710B (10 μg/kg, ip/daily/2 months) – i) mitigated cognitive impairments in Morris water maze; ii) decreased BACE1, GSK3beta activity, p25/CDK5, neuroinflammation, soluble and insoluble Abeta40, Abeta42, plaques and tau pathologies. The effects of AF710B can be attributed to concomitant activation of S1R and a super-sensitized M1R, via a hypothetical heteromerization of these receptors. AF710B represents a comprehensive therapy on cognitive deficits, synaptic loss, beta-amyloid and tau pathologies, neuroinflammation, ER-stress and mitochondrial dysfunctions. AF710B may also be effective in several other protein conformation diseases (e.g. PD, LBD, ALS and more).

|A10|

Tissue Stress Phenomena in the Brain in the Context of Mechanisms of Neurological Diseases and Therapeutic Neuroprotection

Paweł Grieb

Department of Experimental Pharmacolgy, Mossakowski Medical Research Centre, Polish Academy of Sciences, Warsaw, Poland

pgrieb@imdik.pan.pl

Although its basic meaning was different, the word "stress" is frequently used to describe either exposure to, or response of organs (e.g. brain), tissues, cells or subcellular organelles to adverse influences. The overarching definition of this understanding of "stress" may be thus be given as "a strain of circumstances". Many neurologic diseases, both chronic and acute, are believed to involve certain types of stress, e.g. hypoxic/ischemic, oxiadative/peroxidative, mitochondrial and endoplasmatic reticulum stress, etc. It is less emphasized that brief exposure to stressful stimuli precondition cells and organs to variety of different stressors and produce tolerace to otherwise lethal stress conditions, providing robust protection of cells. Acute responses to stress, taking place within second-to-minute time intervals, involve changes in blood flow and (in)activation (through (de)phosphorylation) of enzymes or receptors already present in cells ("preformed"). Chronic responses involve modifications of gene expression, synthesis and/or degradation of proteins, and take distincly more time. Responses to hypoxia or ischemia are of particular importance for the brain, which

critically depends upon continuous delivery of oxygen to maintain normal function and survival. Apparently they occur against a background of global depression of cellular protein synthesis, executed in order to save energy. It had been assumed that hypoxia-respnsive genes are controlled by hypoxia-inducible factor-1alpha (HIF-1a), which is quickly activated by hypoxia. More recently it has been found that in the brain up-regulation of transcriptional signaling by HIF-1a is supplemented by activation of patways involving insulin growth factor, vitamin D3 receptor/retinoid X nuclear receptor and glucocorticoid signaling. Hypoxia-responsive genes are predominantly up-regulated in hindbrain and down-regulated in forebrain – possibly to support hindbrain survival functions at the expense of forebrain cognitive functions. Of possible practical importance is response to chemical stressors, which involves induction of heat-shock proteins that counteract proteotoxic stress. Considering that tolerance evoked by a given stressor is effective also to other stress types, means of inducing tolerance in order to provide neuroprotection are being sought. For example, inducers of Hsp70 proterin expression may be effective in chronic neurodegenerative diseases which involve proteotoxic stress, such as ALS.

|A11|

Effects and mechanisms of prenatal stress on neuro-development: applications to autism

Patrick Hecht[1,2], Eldin Jasarevic[1,3], Fumihiro Matsui[1,4], Matthew Will[1,5], Laruen Welby[6], Jennifer Mink[6], David Beversdorf[1,5,7]*

[1]Interdisciplinary Neuroscience Program, University of Missouri, Columbia, Missouri, USA
[2]Zilkha Neurogenetic Institute, University of Southern California, Los Angeles, California, USA
[3]Department of Biomedical Sciences, University of Pennsylvania, Philadelphia, Pennsylvania, USA
[4]Department of Pediatrics, Kyoto Prefectural University of Medicine, Kyoto, Japan
[5]Department of Psychological Sciences, University of Missouri, Columbia, Missouri, USA
[6]College of Arts and Sciences, University of Missouri, Columbia, Missouri, USA
[7]Departments of Radiology, Neurology, and Psychological Sciences, University of Missouri, Columbia, Missouri, USA
beversdorfd@health.missouri.edu

Prenatal stress has been shown to have a profound and lasting impact on neurodevelopment and leads to an increased risk for several neuropsychiatric conditions, including autism spectrum disorder (ASD). It is crucial to understand how genetics may interact with this environmental trigger to identify those most susceptible to the increased risk and to create a better understanding of the underlying mechanisms and potential treatments of such disorders. A 44 base-pair deletion polymorphism located in the promoter region (5-HTTLPR) of the serotonin transporter gene (SLC6A4) results in decreased gene expression and has been associated with several anxiety related disorders. In an animal model, pregnant dams heterozygous for the serotonin transporter gene (Slc6a4 +/–) exposed to stress produced offspring that exhibited several autistic-like behaviors. It has been suggested that the GABAergic system plays a key role in the underlying pathophysiological process of ASD. Previous research has shown that prenatal stress and manipulation of the serotonergic system affects the proper development of the GABAergic system individually. However, the combined effects are unknown. In the present study, wild-type female mice and females heterozygous for the serotonin transporter gene (Slc6a4 +/–) were bred with wild-type males. Upon detection of a mating plug, mice were either placed in a prenatal stress or control condition. In the stress condition, animals were exposed to restraint stress beginning on embryonic day 12 and continued every day until embryo tissue collection or parturition. GABAergic interneuron development was then analyzed using immunofluorescence. Results suggest that manipulations of the maternal serotoninergic system further exacerbate the deleterious effects of stress on the developing brain. Embryonic tissue in this group exhibited delayed interneuron migration and abnormal cortical layering into the cortex. These findings begin to reveal how stress exposure and genetics may interact to impact the development of neural circuits believed to be critical for social interaction.

|A12|

Differential susceptibility of microglial cells and cholinergic neurons to neurodegenerative signals

Joanna Klimaszewska-Łata*, Sylwia Gul-Hinc, Anna Ronowska, Dorota Bizon-Zygmańska, Aleksandra Dyś, Andrzej Szutowicz, Hanna Bielarczyk

Department of Laboratory Medicine, Medical University of Gdańsk, Gdańsk, Poland
joannaklimaszewska@gumed.edu.pl

Neurodegenerative lesions in cholinergic encephalopathies include an excessive activation of microglia, which may aggravate this process. Microglial inflamma-

tory response to neurotoxic signals may contribute to neuronal degeneration through excessive production of nitric oxide (NO) and a vast range of pro-inflammatory cytokines. Little is known about the sensitivity of microglia to neurotoxins in combination with changes in their energy metabolism. The aim of this work was to investigate wheather and how lipopolysaccharide (LPS), and its key mediator NO, may differentially affect energy and acetyl-CoA metabolism of microglial and cholinergic neuronal cells. We demonstrated the differences between enzymes of acetyl-CoA metabolism, acetyl-CoA and ATP levels and toll-like receptor 4 contents in non-activated N9 microglial and cholinergic SN56 neuroblastoma cells. Exposition of microglial N9 cells to LPS caused concentration-dependent several-fold increases of nitrogen oxide synthesis, accompanied by inhibition of pyruvate dehydrogenase complex (PDHC), aconitase and α-ketoglutarate dehydrogenase complex (KDHC) activities, and by depletion of acetyl-CoA, but by small losses in ATP content and cell viability. On the other hands, SN56 cells were insensitivity to LPS, which was probably caused by lower than in N9, expression of TLR4. However, exogenous NO caused inhibition of PDHC and aconitase activities, depletion of acetyl-CoA and loss of SN56 cells viability. Microglial cells appeared to be more resistant than neuronal cells to acetyl-CoA and ATP depletion evoked by these neurodegenerative condition. This date indicate the existence of substantial differences in TLR4 levels and activities of key enzymes of acetyl-CoA synthesis and utilization, as well as in energy metabolism in cholinergic neuronal and microglial cells. This factors contribute to differential distribution of acetyl-CoA/ATP in microglial and cholinergic neuronal compartments of the brain, resulting in their smaller and greater susceptibility to neurodegenerative conditions, respectively. One of the reasons for greater resistance of microglial cells to cytotoxic inputs could be their lower energy demand. The preferential susceptibility of cholinergic neurons to neurodegenerative insults may results from competition for acetyl-CoA between mitochondrial energy-producing and cytoplasmic acetylocholine synthesizing pathways.

Supported by MN 01-0067/08 and ST57 from MU of Gdańsk.

|A13|

Noradrenergic signaling in Parkinson's disease

Grzegorz Kreiner

Dept. Brain Biochemistry, Institute of Pharmacology,
Polish Academy of Sciences

kreiner@if-pan.krakow.pl

Parkinson's disease (PD), the second most common neurodegenerative disorder, is characterized by subsequent loss of the dopaminergic neurons of substantia nigra (SN) and ventral tegmental area (VTA, directly responsible for the observed symptomatology (bradykinesia, rigidity, and tremor). Most of the PD cases (90%) have a sporadic occurrence, and even for those in which the genetic factors have been determined, the distinct molecular pathways leading to the final, inevitable cell death remain unclear. As a consequence, currently available pharmacotherapies are based on disease symptomatology, and, although they do alleviate the typical symptoms, they do not restore neuronal function nor prevent neuronal loss.

However, PD is well known to be associated with factors beyond dopaminergic transmission. The involvement of extranigral structures in PD also includes the noradrenergic system as well. Noradrenaline is one of the most important neurotransmitters in the brain, and the projections of noradrenergic neurons originating in the locus ceruleus (LC) penetrate nearly all brain structures. It was shown, that degeneration of noradrenergic neurons in the LC is observed in PD patients to an even greater extent and exacerbates the loss of dopaminergic neurons of SN/VTA. Experimental data from toxin-treated PD animal models seems to confirm the important involvement of the noradrenergic system in PD brain damage. These data prompt the hypothesis that noradrenergic neurodegeneration may be regarded as an early pre-symptomatic phase of PD that progresses in neuropathological stages and finally reaches the threshold responsible for symptomatology directly associated with a profound loss of SN/VTA dopaminergic cells Noradrenaline was also proposed to serve as a compensatory mechanism in PD dopaminergic neurodegeneration.

Elucidating these mechanisms may further our understanding of the preclinical deficits observed in neurodegenerative diseases and provide insight into the pathogenic mechanisms underlying the initial, symptomless phase of their onset. These could lead to opportunities for more successful, neuroprotective and neurorestorative anti-PD therapies, not only those restricted to the compounds that simply delay the onset of degeneration.

|A14|

Therapeutic relevance of local hypothermia after spinal cord compression: a characterization of neurofilaments in white matter pathology

Nadezda Lukacova*, Monika Zavodska, Stefania Gedrova, Igor Sulla, Andrea Stropkovska, Jaroslav Pavel, Jan Galik

Institute of Neurobiology, Slovak Academy of Sciences, Kosice, Slovakia

lukacova@saske.sk

The resurgence of interest in the use of hypothermia in spinal cord injury (SCI) is due to evidence that moderate hypothermia may improve electrophysiologic, histologic, and neurological outcomes. We studied the effect of local hypothermia (initiated half hour after spinal cord compression) on changes of neurofilaments (NF) and neurological outcome. Adult Gottingen-Minnesota-Liběchov minipigs underwent SCI (18N force) by computer-controlled compression apparatus at L3 level causing paraplegia of lower extremities. Hypothermia was performed locally through perfusion chamber with 4°C saline solution perfusion, oxygenated culture medium (DMEM/F12) or DMEM/F12 in combination with growth factors, energy metabolism factors and compounds with antioxidant effects. The animals were behaviorally assessed during 9 weeks of survival (neurological scale for minipigs; points range 0-20). We show that local hypothermia with 4°C saline solution (perfusion lasting first 5 hours after SCI) significantly protected against locomotor deficits and reduced area of tissue damage in minipigs 9 weeks after injury. Staining with SMI-312 antibody have shown significant decrease in number of NF/mm2 in sensory and motor tracts after SCI. The results clearly correlate with the development of paraplegia. Systematic quantification of SMI-312 positive axons in L2-L4 spinal cord sections after local hypothermia have shown the increase in number of structural components of myelinated axons in motor areas 1 cm rostrally (23% in lateral and 13% in ventral white matter) and 3 cm caudally (17% in both white matter columns) from the epicenter of injury, when the results were compared to SCI group. The results show that the regeneration of NF in spinal cord after trauma and subsequent treatment clearly indicate an important role of local hypothermia in initiation of functional improvement. Hypothermia with 4°C saline, but not with DMEM/F12 or DMEM/F12 in combination with growth factors, energy metabolism factor and compounds with antioxidant effects, if combined with early physical therapy could be promising treatment for improvement of the neurological behavior of animals after SCI. Hypothermia initiated after traumatic insult in preclinical model of minipigs may improve both, behavioral and histological outcome.

Supported by OP VV EÚ, ITMS: 26220220127.

|A15|

Synaptic plasticity impairments in a BTBR $T^{+}Iptr3^{tf}/J$ mouse model of idiopathic autism

Ksenia Meyza

Laboratory of Emotions' Neurobiology, Nencki Institute of Experimental Biology, Polish Academy of Sciences, Warsaw, Poland

ksenia.meyza@gmail.com

Autism spectrum disorders (ASD) are the most commonly diagnosed neurodevelopmental disorder affecting more than 1 % of children. Despite many years of research it is still diagnosed entirely based on behavior as its molecular basis is not clear. Only 5-10% of cases seem to have genetic background with many of the associated genes involved in forming and maintenance of synapses. Mice lacking these genes often do not represent a full ASD phenotype, therefore in the current study we took an opposite approach. We studied the extracellular matrix components crucial for proper neuronal development and neuronal plasticity, in the BTBR T+ tf/J mouse, an idiopathic model of autism (BTBR). BTBR mice have been extensively studied and show all of the behavioral symptoms of ASD: social interaction and communication impairments as well as strong insistence on sameness combined with repetitive behaviors. We found that unlike the prosocial c57BL6/J (B6) mice, BTBR mice have very little heparan sulfate content in the neurogenic niches and that they display increased matrix metalloproteinase-9 activity in the central nucleus of amygdala, Both of these findings have implication for the function of the synapse and neuronal connections in the development of autism-like phenotype of these mice.

|A16|

Sphingolipid signalling in experimental model of Parkinson's disease

Joanna Motyl[1]*, Łukasz Przykaza[2], Paweł M. Boguszewski[3], Joanna B. Strosznajder[1]

[1]Department of Cellular Signalling
[2]Department of Neurosurgery, Laboratory of Experimental Neurosurgery, Mossakowski Medical Research Centre Polish Academy of Sciences
[3]Laboratory of Limbic System, Department of Neurophysiology, Nencki Institute of Experimental Biology, Polish Academy of Sciences

asiapyszko@o2.pl

The last study highlight the importance of sphingolipids in the pathomechanism of neurodegenerative disorders. The alterations of sphingolipids biostat between ceramide and sphingosine-1-phosphate (S1P) might play a crucial role in neuronal cell death in Alzheimer's disease (AD). The significant lowering of S1P level and down-regulation of sphingosine kinases (Sphk1/2) has been recently reported in AD brain. S1P is very potent messenger that regulate cell proliferation, differentiation, migration and apoptosis. This bioactive lipid mediator, which is mainly synthetized by Sphk1 is easily transported outside the cell and act in autocrine or paracrine manner through five specific G-protein-coupled receptors, termed S1P1-S1P5. Moreover, S1P is also important intracellular messenger, which regulate gene expression, mitochondria function and Ca2+ ions concentration. However, the significance of S1P/Sphk1 in Parkinson's diseases (PD) is not fully elucidated. Our in vitro study, using dopaminergic SH-SY5Y cell PD model, induced by 1-methyl-4-phenylpyridinium (MPP+), indicated for the first time the inhibition of Sphk1 expression and activity. Our data showed also higher expression of S1P lyase, which irreversibly leads to S1P degradation and significantly reduces this bioactive sphingolipid concentration. Additionally, we have found that alterations of S1P signalling in PD cell model leads to activation of caspase-dependent apoptotic neuronal death. In current study using mice in vivo PD model evoked by i.p. injection of 1-methyl-4-phenyl-1,2,3,6-tetrahydropyridine (MPTP) we have confirmed the alterations of bioactive sphingolipids observed in in vitro PD model. The lower Sphk1 activity and its expression were observed in mice midbrain after MPTP administration. Concomitantly, the inhibition of pro-survival kinase Akt and up-regulation of pro-apoptotic Bax protein were indicated. Moreover, the significant changes in motor activity in rota-rod test were found. The modulator of S1P receptors Fingolimod (FTY720) which exerted neuroprotective effect in *in vitro* study, in this in vivo model has also ameliorating effect. The agonist of dopaminergic receptors D2/D3 pramipexole (PPX) protects midbrain against Sphk1 activity/expression disturbances, apoptosis and motor activity alterations. Our data indicated impaired sphingolipid rheostat in PD model and suggest sphingolipid signalling as a promising target in PD therapy.

Supported by NCN grant 2013/09/N/NZ4/02045

|A17|

Dangerous Liaisons: tau interaction with muscarinic receptors

Grazyna Niewiadomska

Department of Neurophysiology, Nencki Institute of Experimental Biology, Warsaw, Poland

g.niewiadomska@nencki.gov.pl

The microtubule-binding protein tau has numerous binding partners, including signaling molecules, cytoskeletal elements and lipids, suggesting that it is a multifunctional protein. Indeed, tau can bind to and affect cytoskeletal components and regulate signaling pathways by acting as a protein scaffold for signaling complexes; tau binding also activates or inhibits several enzymes. Tau may also exert toxic effect acting as a agonist of cholinergic muscarinic receptors. There are different alternatives to explain tau pathology spreading in tauopathies like AD, a disease that long time ago was associated with severe loss of cholinergic markers in the brain, and that such loss may be due to the toxic interaction of tau with muscarinic receptors. By using specific antagonists of muscarinic receptors it was found that extracellular tau binds to M1 and M3 receptors and that it may explain the increase of intracellular calcium found in neuronal cells upon tau-binding. It is suggested that increase of calcium mediated by the interaction of tau with muscarinic receptors could result in cell death. M1 and M3 receptors are coupled with Gq/G11 proteins leading to activation of phospholipase C and an increase in the level of intracellular calcium. This calcium increase could activate some protein kinases, and these kinases could modify tau protein rendering the protein toxic. M1 receptors are involved in all key pathological changes found in AD – parenchymal and cerebrovascular amyloid deposition, neurofibrillary tangles, neuroinflammation, and cognitive decline studying 3xTgAD mice with

the deletion of M1 receptor gene. Notably, tau overphosphorylation and potentiation of amyloidogenic processing in the mice with AD lacking M1 were attributed to changes in the GSK-3β and protein kinase C activities. Corroborating these findings, genetic deletion of M1 receptor has recently increased Aβ pathological features in APPSwe/Ind mice. Finally, deleting the M1 receptor increased the astrocytic and microglial response associated with Aβ plaques. These data highlight the significant effect of M1 receptors disruption in exacerbating AD-related cognitive decline and pathological features and provide critical preclinical evidence to justify further development and evaluation of selective M1 agonists for treating AD. However so far, significance of tau signaling through muscarinic receptor in solely in vivo tauopathic models remains uncertain.

|A18|

PKCβII in mitochondria as a potential neuroprotective factor. Proteomics strategy to elucidate protein-protein interactions involved in PKCβII signaling

Olga Poleszak[1], Małgorzata Beręsewicz[1]*, Ewa Sitkiewicz[2], Michał Dadlez[2], Anna Sarnowska[1], Barbara Zabłocka[1]

[1]Molecular Biology Unit and Stem Cell Bioengineering Unit, Mossakowski Medical Research Centre, Polish Academy of Sciences, Warsaw, Poland
[2]Laboratory of Mass Spectrometry, Institute of Biochemistry and Biophysics, Polish Academy of Sciences, Warsaw, Poland

mberesewicz@imdik.pan.pl

Mitochondria are principal mediators of cell death that occurs during cerebral ischemia. Recent reports indicate participation of the PKC in regulation of mitochondrial metabolism what can determine the fate of the cell following ischemic stress. We demonstrated that PKCβII, due to ischemia/reperfusion injury (I/R), translocates to mitochondrial fraction, mainly in ischemia-resistant part of hippocampus. We hypothesize that this translocation is responsible for endogenous neuroprotection. Therefore, we aim: to prove the possible relationship of PKCβII translocation with endogenous neuroprotection and to understand the mechanism of this process. To reveal the role of PKCβ we used widely acknowledged models of brain ischemia: *in vitro* – rat organotypic hippocampal slice culture exposed to excitotoxic injury and *in vivo* – 5' transient brain ischemia in gerbils. We observed ischemia-induced increase of PKCβII isozyme immunoreactivity in mitochondrial fraction in ischemia-resistant part of hippocampus. Moreover, we determined that PKCβII enzymatic activity is preserved after its translocation to mitochondria. The PKCβII-isozyme selective inhibitor administration showed: inhibition of postischemic translocation of PKCβII to particulate fraction and an increase of neuronal death after I/R in an in vitro and in vivo models. It may bespeak neuroprotective role for PKCβII. Pull-down chromatography and mass spectrometry (MS) revealed potential mitochondrial PKC βII-interactors which are involved in regulation of mitochondrial metabolism. We assume that a biological effects of the PKCβII translocation are associated with the phosphorylation of mitochondrial proteins by it. Therefore, mitochondrial phosphoproteomic analysis using titanium affinity chromatography and MS is under investigation. Until now, two proteins identified as potential PKCβII-partners, have been confirmed by co-immunoprecipitation method. Moreover, in silico analysis (http://networkin.info) confirmed that due to amino acid structure, this two proteins can be potentially phosphorylated by PKCβ. Taken together, we suggest that at least these two proteins might be regulated by PKCβII phosphorylation and might be involved in PKCβII-mediated neuroprotection. The exact mechanisms by which PKCβII phosphorylation leads to neuroprotection still needs to be elucidated.

Funding: National Science Centre grant 2012/05/B/NZ3/00415 and KNOW-MMRC projectA search for mechanisms of Parkinson's disease (PD)-associated depression in an animal model.

|A19|

Insights for botanical polyphenols to target signaling pathways and regulate microglial activation

Grace Sun

Biochemistry Department, University of Missouri, Columbia, Missouri, USA,

sung@missouri.edu

Many neurodegenerative diseases and brain injuries are marked by increased oxidative stress that results in neuron cell death and glial cell activation. In recent years, intense interest has been directed to unveiling the role of microglial cells, which are the major innate immune cells

in brain. Microglial cells not only are capable of performing host defense mechanisms, but also exhibit multiple functions for regulating cellular redox homeostasis. Microglial activation has been implicated in a number of neurodegenerative diseases, in particular, in Alzheimer's disease, Parkinson disease, stroke and traumatic brain injury. Our studies have demonstrated microglial activation in cerebral ischemia in gerbil and mouse brain. Many botanical polyphenols including grape polyphenols, curcumin as well as elderberry and Sutherlandia can suppress microglia activation and mitigate expression of oxidative and inflammatory marker proteins in these cells. Studies using the BV2 microglial cells also demonstrated a number of botanical polyphenols including EGCG from green tea, honokiol from Magnolia bark and quercetin from berries to inhibit lipopolysaccharides (LPS)-induced production of nitric oxide (NO) and reactive oxygen species (ROS), and alter signaling pathways involving NADPH oxidase, NF-κB and MAPKs. In addition, there is evidence that some polyphenols, such as quercetin, not only are capable of inhibiting inflammatory responses through the NF-κB pathway, but also can stimulate the antioxidant pathway involving Nrf2 and upregulation of antioxidant response element (ARE) and synthesis of heme oxygenase-1 (HO-1), a potent antioxidant enzyme. Therefore, understanding the mechanisms for these polyphenols to modulate the oxidative and antioxidative pathways in microglial cells may be important for providing therapeutic potential for prevention or treatment of neuroinflammatory disorders.

|A20|

Neuroprotective and immunomodulatory properties of oligodendrocyte progenitors as a tool for neuroregenerative strategies

Joanna Sypecka[1], Anna Sarnowska[2]

[1]NeuroRepair Department and [2]Translative Platform for Regenerative Medicine, Mossakowski Medical Research Centre PAS, Warsaw, Poland

jsypecka@imdik.pan.pl

Oligodendrocyte progenitor cells (OPCs) are known to undergo a multi-stage maturation to gain a myelinating potential. Their role however is supposed to go beyond the process of myelinating nerve fibers in the central nervous system. Pre-clinical studies based on oligodendrocyte progenitor cell (OPCs) therapies revealed significant behavioral improvement in spite of failure in the remyelination process in animal models of demyelinating diseases. Basing on the reported observations, a trophic support provided by OPCs has been hypothesized as an explanation of the beneficial effects resulting from OPCs transplantation. To address the issue, series of co-culture experiments with neonatal rat OPCs and organotypic hippocampal slices were designed. For this purpose, rat organotypic hippocampal slices were exposed to a brief oxygen and glucose deprivation (OGD) which allowed mimicking an ischemic injury ex vivo. Soon after the OGD procedure, the hippocampal slices were co-cultured together with differentiating oligodendroglial progenitors. The molecular analysis revealed that the mRNA levels for several cytokines, transcription factors and neurotrophins is up-regulated in OPCs in the response to the vicinity of the injured nervous tissue. During the following biochemical analysis and functional assays, some of the factors were proved to be secreted extracellularly and to exert either neuroprotective or immunomodulatory effect. In response to the OPC-derived IL-10, the number of microglial cells increased within the OGD-subjected slices, while the BDNF and SCF were shown to up-regulate the proliferation of the neuroblasts and their subsequent differentiation into the cells with the neuronal phenotype. The results obtained in the study prove that OPCs indeed are potent to secrete soluble factors and exert the neuroprotective effect, additionally promoting cell survival and proliferation in the damaged nervous tissue. In conclusion, the OPCs might support the preservation/restoration of a tissue structure. The immunomodulation of locally ongoing inflammatory process might also contribute to the initiation of neuroregenerative mechanisms which could be the other beneficent effect of the therapies based on OPC transplantation.

Supported by NCN (National Science Centre, Poland) grant 2014/15/B/NZ4/01875.

|A21|

Cholinergic hypothesis of dementia

Andrzej Szutowicz.*, Hanna Bielarczyk, Anna Ronowska, Sylwia Gul-Hinc, Joanna Klimaszewska-Łata, Aleksandra Dyś, Marlena Zyśk

Chair of Clinical Biochemistry, Department of Laboratory Medicine, Medical University of Gdańsk, Poland

aszut@gumed.edu.pl

Cholinergic neurons require continuous provision of acetyl-CoA and choline to their synaptoplasmic com-

partment for synthesis of acetylcholine (ACh) by choline acetyltransferase (ChAT) in order to maintain their neurotransmitter functions. Glucose- derived pyruvate, through pyruvate dehydrogenase complex (PDHC) reaction in mitochondria, is almost exclusive source of brain acetyl-CoA. The latter is used mainly for energy production in mitochondria of neurons and other types of brain cells. However, only in cholinergic neurons certain fraction of acetyl-CoA is used for ACh synthesis. Therefore, they appear to be particularly vulnerable to several neurodegenerative conditions (e.g. Alzheimer's disease, thiamine deficits) presumably due to competition for acetyl-CoA between energy and ACh synthesizing pathways. On the other hand, second substrate - choline has to supplied to the site of ACh synthesis from extracellular space exclusively by specific high affinity choline transporter. During neurotoxin-evoked excessive depolarization, when transporter is inhibited, choline for ACh synthesis may be provided by hydrolysis of structural phospholipids in neuronal membranes by activated phospholipases, thereby affecting cholinergic neurons viability. Studies on Tg2576 mice, as well as cell lines revealed that, several neurodegenerative inhibited PDHC and other enzymes linked with energy production. It caused loss of viability and transmitter functions in cholinergic neurons, being less or non toxic to non-cholinergic neurons or glial cells. Viability of mature cholinergic neuronal cells displayed direct significant correlations with activities of PDHC and mitochondrial acetyl-CoA levels under various cytotoxic and cytoprotective conditions. No such dependencies were observed for non cholinergic cells. In the same conditions, choline acetyltransferase activity and ACh content/release displayed direct correlations with acetyl-CoA levels in cytoplasmic/synaptoplasmic compartment of cholinergic neurons. Also choline depletion or supplementation in whole animal or cellular models of dementia, decreased or increased neuronal viability, their ACh metabolism, respectively. Thus, combinations of these two autocanibalism-like mechanisms, involving acetyl-CoA and choline shortages present in degenerating brain, may contribute to preferential functional and structural impairments of cholinergic neurons in these conditions.

|A22|

α-Synuclein and its role in synaptic function

Wilkaniec Anna

Mossakowski Medical Research Centre Polish Academy of Sciences, Department of Cellular Signaling, Warsaw, Poland

aniakazmierczak@gmail.com

The cytosolic protein α-synuclein (ASN) is enriched at the pre-synaptic terminals of almost all types of neurons in the central nervous system. In physiological conditions this protein is involved in the synapses formation, neurotransmitter release and re-uptake, vesicle recycling and regulation of the synaptic cytoskeleton assembly. A growing body of evidence has underlined ASN missfolding and oligomerisation as important events that contribute to synaptic abnormalities (synaptopathies) occurring in various neurodegenerative diseases. Our previous studies demonstrated that this protein in monomeric/oligomeric form induces Ca^{2+} influx and NMDA receptor-dependent activation of neuronal nitric oxide (NO) synthase. Subsequently, it was shown that ASN enhanced Aβ toxicity leading to acceleration of oxidative stress, mitochondria failure and caspase-dependent apoptotic cell death. Our recent findings showed, that ASN-evoked oxidative/nitrosative stress leads to S-nitrosylation of multifunctional E3 ubiquitin ligase-parkin, resulting in the inhibition of this enzyme's function. Moreover, using ATRA-differentiated SH-SY5Y cells, we observed that ASN alters ATP-dependent signalling. Exogenously added ASN induced release of ATP from nerve endings, leading to activation of synaptic purinergic P2X7 receptor, intracellular Ca^{2+} influx and cell death. Interestingly, in SH-SY5Y cells stably transfected with ASN we observed that agonist of purinergic receptor, extracellular ATP significantly increased intracellular ASN level. Further investigation revealed that ASN accumulation is a result of alteration of its secretion and probably lysosomal as well as proteasomal dysfunction. The alteration of ASN level may subsequently affect the function of synaptic vesicles and mitochondria and may be implicated in synaptosis. Taken together, these findings provide new insight into our knowledge of the relationship between purinergic signalling and ASN in synaptic failure and may be helpful in identifying new therapeutic targets for neurodegenerative disorders.

Supported by NCN grant 2013/09/D/NZ3/01359.

POSTERS

|B1|

Monitoring of human mesenchymal stem cells overexpressing vla-4 after their intracarotid administration in a rat model of deep brain structure damage

Anna Andrzejewska[1]*, Sylwia Koniusz[1], Adam Nowakowski[1], Miroslaw Janowski[1,2,3], Barbara Lukomska[1]

[1]NeuroRepair Department, Mossakowski Medical Research Centre, PAS, Warsaw, Poland
[2]Cellular Imaging Section and Vascular Biology Program, Institute for Cell Engineering, the Johns Hopkins University School of Medicine, Baltimore, Maryland, USA
[3]Russel H. Morgan Vascular Biology Program, Division of MR Research, The Johns Hopkins University School of Medicine, Baltimore, USA

aandrzejewska@imdik.pan

Introduction: Mesenchymal stem cells (MSC)-based therapy is one of the most promising approaches in the treatment of wide range of diseases. However up to now clinical trials with MSC transplanted in neurodegenerative diseases provided inconclusive results. One of the reason may be insufficint migration of donor cells after systemic infusion and lack of their homing in the brain. Thus the modification of adhesive proteins on the surface of transplanted cells might be beneficial. VLA-4 is one of the most important proteins involved in leukocyte diapedesis and migration to inflamed area, therefore our research is focused on use it to enhance homing of MSCs.

Material and methods: In our study we used mRNA-ITGA4 transfected human bone marrow-derived MSC (hBM-MSC) (Lonza) overexpressing A4 subunit of VLA-4 intergin. The modified and naïve cells were labelled with SPIO (MIRB, BioPAL) and delivered into right internal carotid artery in rats withdeep brain structure damage. The infusion of hBM-MSC was monitored with 7T Biospec 70/30 MR scanner (Bruker) directly after transplantation and 24h later. The analysis of signal intensity was performed in ImageJ program then rat brains were collected and analysed by immunohistochemistry using antibodies against CD44 (specific for human MSC), von Willebrand factor and Claudin-5 antigens (recognized endothelial cells).

Results: Both naïve and A4 overexpressing MSC reached brain lesion area after intra-arterial delivery. Directly after transplantation and 24 hours later hBM-MSC were present in the right hemisphere of the recipients but significant decrease in signal level originating from transplanted cells between these two time points was noticed. However, the decline of the signal in rats transplanted with modified hBM-MSC was much smaller as compared to naïve cell recipients. The presence of transplanted hBM-MSC in the rat brain was confirmed by using of CD44 antibody. Staining with von Willebrand factor and Claudin-5 antibodies revealed that both types of cells (modified and naïve) remained inside brain blood vessels 24 hours after transplantation.

Conclusions: Our results showed that arterially transplanted hBM-MSC effectively reach the brain lesion area. The overexpression of VLA-4 increases homing of MSCs to the brain, however no diapedesis of transplanted cells was present. The role of peripheral sensory pathways and NKA1 and NKA2 receptors in cardiorespiratory effects induced by neurokinin A.

|B2|

Treatment of neural stem cells (HUCB-NSC) with methylmercure chloride results with cytotoxic and genotoxic effect

Justyna Augustyniak, Marzena Zychowicz, Martyna Podobińska, Leonora Bużańska

Stem Cell Bioengineering Unit, Mossakowski Medical Research Centre, Polish Academy of Sciences

jaugustyniak1@o2.pl

Several studies have demonstrated that exposure to toxic levels of MeHgCl during pre- and post-natal life causes neurological abnormalities, cognitive impairment, and behavioral disturbance. In this study we present that the mechanism of cell damage induced by MeHgCl involves generation of free radicals, which trigger a double and a single DNA strand breakage and is related with cytotoxic and genotoxic effect. We have tested exposition of MeHgCl on HUCB-NSC in different culture conditions: monolayer 2D culture at various conditions resembling different developmental stages (serum free culture, low serum medium and low serum with dBcAMP) and 3D culture on collagen scaffolds, all in 21% or 5% of oxygen tension. Treatment of HUCB-NSC on MeHgCl showed a decrease in cell viability (Alamar blue test), in both oxygen conditions (21% of oxygen or 5% of oxygen) and both dimension of culture (monolayer vs culture on collagen scaffolds). The most sensitive to MeHgCl were cells cultured under 5% oxygen tension in medium without serum, where cells exhibit ear-

ly neural phenotype. Examination of HUCB-NSC exposition on MeHgCl showed numerous dose-dependent chromosomal abnormalities. Methylmercury chloride increases level of chromosome break or lost what produces micronuclei (MN) and chromosomal rearrangement – nucleoplasmic bridge (NPBs) and gen amplification – nuclear bud formation (Nbud). This effect suggest that methymercury chloride is mutagenic agent, causes the DNA damage and in consequence produces chromosome changes in Human Umbilical Cord Blood Neural Stem Cells.

The work is supported by statutory funds to MMRC and National Science Centre via Grant No DEC-2011/03/B/ST8/05867.

|B3|

The role of peripheral sensory pathways and NKA1 and NKA2 receptors in cardiorespiratory effects induced by neurokinin A

Monika Białkowska*, Małgorzata Szereda-Przestaszewska, Katarzyna Kaczyńska

Laboratory of Respiration Physiology, Mossakowski Medical Research Centre, Polish Academy of Sciences, Warsaw, Poland
mbialkowska@imdik.pan.pl

Neurokinin A (NKA) is a peptide neurotransmitter that participates in the regulation of breathing and cardiovascular system. It is established that NKA released from the vagal excitatory NANC fibers innervating respiratory tract acts via NK2 receptors, causing contractions of the smooth muscle of the tracheobronchial tree. Neurokinin A is also present in the ganglion nodosum of the vagus nerve and the petrosal ganglion of the glossopharyngeal nerve which both project to the nucleus of the solitary tract in the medulla oblongata. However its impact on the cardiorespiratory pattern is not clear. The purpose of our study was to determine the cardiorespiratory pattern exerted by the systemic injection of neurokinin A, to look at contribution of neurokinin NK1 and NK2 receptors, and to show the engagement of the vagal pathway in mediation of these responses. The effects of intravenous injections of NKA (50 µg/kg) were studied in anaesthetized, spontaneously breathing rats in the following experimental schemes: in neurally intact rats, and vagotomized at either midcervical or supranodosal level. Intravenous injections of NKA in the intact rats evoked sudden and short-lived increase in the respiratory rate, followed by a prolonged depression coupled with slow continuous augmentation of the tidal volume. Respiratory alterations were accompanied by short-lived tachycardia and a prolonged hypotension. Midcervical vagotomy eliminated only respiratory rate response, while supranodosal vagi section abrogated all respiratory reactions. NK2 receptor antagonist eliminated the respiratory frequency and tidal volume changes not affecting the fall in arterial blood pressure. NKA1 receptor blockade revealed an avert effect significantly reducing hypotension with no influence on the respiratory system. These results indicate that NKA induced changes in the breathing result from an excitation of the NKA2 receptors of the vagal endings and also from modulation of NKA2 receptors within the nodose ganglia. Fall in blood pressure triggered by NKA occurs outside of the vagus nerve and is probably mediated via a direct action of the neurokinin A on vascular smooth muscles supplied with NK1 receptors.

|B4|

Differential effect of KU55933, an inhibitor of ATM kinase, against hydrogen peroxide-, doxorubicin- and staurosporine-induced cell damage in neuronal-like and astrocyte-like cell lines

Jakub Chwastek*, Danuta Jantas, Władysław Lasoń

Department of Experimental Neuroendocrinology, Institute of Pharmacology, Polish Academy of Sciences, Cracow, Poland
chwastek@if-pan.krakow.pl

ATM (ataxia-telangiectasia mutated) kinase belongs to family of phosphatidylinositol 3-kinase-related kinases (PIKKs) and its dysfunction is a cause of rare neurodegenerative disorder- ataxia-telangiectasia. It is involved in processes like DNA repair system, cellular response to oxidative stress, insulin signaling and mitochondrial homeostasis. Taking these properties into account, ATM started to be the subject of research in diabetes, cancer and neurodegenerative diseases. Our previous data demonstrated that pharmacological inhibition of ATM kinase by specific inhibitor – KU55933, protects the retinoic acid differentiated human neuroblastoma SH-SY5Y cells (RA-SH-SY5Y) against the cell damage induced by hydrogen peroxide (H_2O_2) and doxorubicin (Dox), but not by staurosporine (St). In order to study the cell specificity of the above results in the present study we tested the effect of ATM kinase inhibitor in mouse hippocampal (HT-22) and rat glioma C6 cell lines. The data showed that KU55933

(1-10 μM) was not toxic to HT-22 cells when given alone, but induced cell damage in C6 cells at concentration of 10 μM. Moreover, it partially attenuated the cell death induced by (H_2O_2) (by 11-15%) and doxorubicin (by 20-26%) in HT-22 cells, whereas in glioma cells it mediated only a slight protection in Dox-model (1 μM with 8% protection). However, in the model of oxidative stress-evoked cell damage in C6 cells it was not only without protective effects but at concentration of 10 μM it enhanced the H_2O_2 toxicity (by 24%). In contrast to results obtained from RA-SH-SY5Y cells, in St-model of cell damage we found a slight protection mediated by KU55933 in both, HT-22 (10 μM with 10% protection) and glioma (0.1-1 μM with 7-10% protection) cells. Taking together results from neuronal-like (RA-SH-SY5Y and HT-22 cells) and glioma cells, a differential protective effect of ATM kinase inhibitor in dependence on the used model of cell damage has been demonstrated. The most significant protective effects of KU55933 were observed in neuronal-like cells (RA-SH-SY5Y and HT-22) in the model of H_2O_2- and Dox-induced cell damage.

The study was supported by statutory funds of the Institute of Pharmacology, Polish Academy of Sciences. Jakub Chwastek is a holder of scholarship from the KNOW sponsored by Ministry of Science and Higher Education, Republic of Poland.

|B5|

The interplay between amyloid β42 peptide, sphingosine kinase-1 and mitochondrial sirtuins in cell survival and death: implication in Alzheimer's disease

Magdalena Cieślik*, Grzegorz A. Czapski, Joanna B. Strosznajder

Department of Cellular Signaling, Mossakowski Medical Research Centre, Polish Academy of Sciences, Warsaw, Poland
mcieslik@imdik.pan.pl

Amyloid beta (Aβ) is a key player in pathomechanism of Alzheimer's disease (AD). The recent studies demonstrated that soluble oligomers are the most toxic form of Aβ. The oligomers are responsible for synaptic dysfunction, memory loss and neurodegeneration, but the mechanisms of their toxicity largely remain unsolved. The Aβ precursor protein and the enzymes involved in Aβ release are situated in lipid rafts rich in sphingolipids. Recent data underline the role of sphingolipid rheostat alterations in AD pathology. In this study we analyse the interaction between $A\beta_{1-42}$ and sphingosine kinases (SphKs) – the key enzymes in sphingolipid biostat. Moreover, we investigated the role of mitochondrial sirtuins and other antioxidative enzymes in cell survival under Aβ toxicity.

PC12 cells were incubated with $A\beta_{1-42}$ oligomers (AβO) and SphK inhibitor SKI II for 24-96 h. AβO increased SphK1 expression and activity after 24 h, but down-regulated them after 96 h and had no effect on Sphk2. AβO and SKI II accelerated oxidative stress and affected the pro- and anti-apoptotic signalling leading to cell death. At the same time, up-regulation of anti-oxidative enzymes catalase and superoxide dismutase 2 was observed. AβO significantly increased the level of mitochondrial proteins: apoptosis-inducing factor (AIF) and Sirt3, -4, -5. To decipher the molecular pathways involved in AβO toxicity, several pharmacologically active compounds were tested. It was shown that at very early stages of AβO toxicity, p53 protein plays a major role. However, during prolonged exposure, alterations of caspases, MEK/ERK, mitochondrial permeability transition pores, oxidative stress, S1P signalling pathway and down-regulation of Sirts were responsible for cell death.

Our data demonstrated the molecular relationship between Aβ peptide, Sphk in cell survival and death, and indicated that inhibitor of p53 and activators of S1P receptors and Sirts may be useful in cell protection against Aβ toxicity.

This study was supported by The National Science Centre Grant 2013/09/B/NZ3/01350.

|B6|

The oxidative stress in myelin of the rat brain exposed to silver nanoparticles

Beata Dąbrowska-Bouta[1], Grzegorz Sulkowski[1], Mateusz Zięba[2], Jolanta Orzelska[2], Lidia Strużyńska[1]

[1]Laboratory of Pathoneurochemistry, Department of Neurochemistry, Mossakowski Medical Research Centre, Polish Academy of Sciences, Warsaw, Poland
[2]Chair and Department of Pharmacology and Pharmacodynamics, Medical University of Lublin, Lublin, Poland
bbouta@imdik.pan.pl

Nanotechnology has become a major research project in the last decade and scientists world-wide are continuing to discover unique properties and applications of nanomaterials. Among the metal nanoparticles, nanosilver (AgNPs) has the highest degree of commercialization because of

its antimicrobial properties. However, the unique properties of AgNPs could potentially lead to unexpected hazards to both the environment and human health. In the present study we investigate the pro-oxidative potential of AgNPs in chronically exposed rats. Markers of oxidative stress such as lipid peroxidation, the level of sulfhydryl groups (-SH), and the mRNA expression of superoxide dismutase (SOD) were examined in myelin of the CNS. Small (10 nm) citrate-stabilized silver nanoparticles were administered once daily via the gastric tube at a dose of 0.2 mg/kg b.w. per day for 14 days. Control groups received silver citrate or saline in the same dose. Our results indicated that exposure to AgNPs decreased level of sulfhydryl groups. We noticed statistically significant reduction of both protein- and non-protein –SH groups level by about 35% and 20%, respectively. Similar effect was also observed after administration of ionic form of silver. Exposure to AgNPs increased the rate of lipid peroxidation expressed by the level of malondialdehyde (MDA) – final products of polyunsaturated fatty acids peroxidation in the cell memranes. The level of MDA was significantly elevated (by about 40%) in myelin of AgNPs-treated rats. Exposure to AgNPs also changed mRNA expression of SOD – an antioxidative enzyme. Obtained results indicate that in AgNPs-exposed rats antioxidative mechanisms are inefficient to counter reactive oxygen species (ROS)-mediated cellular stress.

|B7|

8-Oxoguanine DNA glycosylase 1 and TP53 genetic variants and apolipoprotein E (APOE) genotype and oxidative stress in the patients with Alzheimer's disease

Jolanta Dorszewska[1]*, Michał Prendecki[1], Daria Truszczyńska[1], Jolanta Florczak-Wyspiańska[2], Urszula Łagan-Jędrzejczyk[2], Anna Oczkowska[1], Wojciech Kozubski[2]

[1]Laboratory of Neurobiology, Department of Neurology, Poznan University of Medical Sciences
[2]Chair and Department of Neurology, Poznan University of Medical Sciences, Poznań, Poland

dorszewskaj@yahoo.com

Alzheimer's disease (AD) leads to generation of β-amyloid (Aβ) and oxidative stress. Oxidative stress and apolipoprotein E (ApoE) are associated with DNA damage which leads to apoptosis induction e.g. in cells expressing wild-type p53 protein encoded by TP53 gene. 8-Oxoguanine DNA glycosylase 1 (OGG1) is a main DNA repair enzyme that removes of 8-oxo-2'-deoxyguanosine (8-oxo2dG) from DNA. It is known that OGG1 and TP53 genetic variants, and APOE genotypes are involved in dementia diseases pathogenesis.

The purpose of this study was to analyze OGG1 and TP53 genetic variants, and APOE genotypes in peripheral lymphocytes and the extent of oxidative DNA damage (8-oxo2dG) in AD patients and controls.

The studies were conducted on 60 patients with AD, aging 47-90 years. The control group consisted of 200 individuals, aging 25-86 years, including 80 related (RC) and 120 unrelated (UC) persons with AD patients. The OGG1 and TP53 genetic variants and APOE genotyping analysis was performed using PCR and DNA sequencing, and Real-Time PCR method. The plasma levels of 8-oxo2dG were determined using ELISA technique.

Our studies revealed the presence only in AD patients of two different mutations in TP53 gene: a silence C708T mutation (21%) [$p < 0.05$] and a missense C748A mutation (4%) as well as first described in OGG1 gene a silence C798T mutation (6%). Additionally, significant differences in the frequency of the APOE ε4 in patients with AD and UC ($p < 0.001$), and RC ($p < 0.01$), respectively, as well as RC and UC ($p < 0.05$) were observed. AD patients with silent or missense mutation in the TP53 and OGG1 gene have protective (ε2) and/or neutral (ε3) and/or pathogenic (ε4) allel of APOE gene. The plasma level of 8-oxo2dG was almost 2 times lower in AD patients with APOE ε4/ε4 as compared to AD subjects with APOE ε3/ε3 genotype.

It seems that APOE ε4 as well as APOE ε2, ε3 associated with OGG1 and TP53 genetic variants may be involved in the AD pathology.

|B8|

New bifunctional peptides with both, opioid agonist and tachykinin antagonist components as new analgesics

Jolanta Dyniewicz[1], Piotr Kosson[2]*, Piotr Lipiński[1], Aleksandra Misicka[1,3], Andrzej W. Lipkowski[1]

[1]Neuropeptide Department, Mossakowski Medical Research Centre Polish Academy of Science, Warsaw, Poland
[2]Laboratory for Genetically Modified Animals, Mossakowski Medical Research Centre Polish Academy of Science, Warsaw, Poland
[3]Faculty of Chemistry, Biological and Chemical Research Centre, University of Warsaw, Warsaw, Poland

pkosson@imdik.pan.pl

Morphine and its derivatives are the most widely used narcotic analgesics for relieving severe acute pain. Unfortunately, the use of opioids in treating is limited due to significant side effects e.g. analgesic tolerance, addiction, respiratory depression. Since many years Neuropeptide Department search for new bifunctional compounds, acting on two (or more) different receptors, which will have fewer side effects than compounds acting at a single target. Substance P plays an important role in pain signals generation and transmission from periphery to CNS. In contrast, opioids suppress pain signals mainly through suppression of substance P release. These mechanisms of neurophysiological actions were fundamentals for invention of hybrid compounds that act as both antagonists of substance P to reduce postsynaptic activation of NK1 receptors as well as opioid agonists to activate presynaptic opioid receptors that result in decrease substance P release. We will present bifunctional compounds acting on opioid and tachykinin system. In all presented compounds opioid pharmacophore is covalently hybridized with tachykinin pharmacophore that positively modulate effects of the opioid part. Synergistic enhancement of opioid analgesia and/or decrease of unwanted side-effects should result from such hybridization. Therefore, to the list of already synthesized and characterized compounds presented in the literature we elaborated new series of compounds that combine peptide opioid pharmacophore (biphalin) with 3,5 bis-trifluoromethyl-benzyl derivative, responsible for antagonism at NK1 receptor. Opioid and tachykinin pharmacophores are connected by few kinds of linkers which are derivative of hydrazine. We will present pharmacological and analgesic properties of new bifunctional peptides, which exhibit affinity to opioid (mu and delta) and NK1 receptors. For the most active compound the hypothetical model of interaction of bifunctional compound and the NK receptor will be shown.

|B9|

Nanofiber mat dressing-mediated glutamate delivery to the spinal cord damages blood-brain barrier

Dorota Dziewulska[1,2*], Dorota Sulejczak[3], Stanisław J. Chrapusta[3], Anna Taraszewska[2], Paweł Nakielski[4], Małgorzata Modrzewska-Lewczuk[5], Lidia Wąsowska[2], Janina Rafałowska[2]

[1]Department of Neurology, Medical University of Warsaw, Warsaw, Poland
[2]Department of Experimental and Clinical Neuropathology, Mossakowski Medical Research Centre, Polish Academy of Sciences, Warsaw, Poland
[3]Department of Experimental Pharmacology, Mossakowski Medical Research Centre, Polish Academy of Sciences, Warsaw, Poland
[4] Department of Mechanics and Physics of Fluids, Institute of Fundamental Technological Research, Polish Academy of Sciences, Warsaw, Poland
[5]Scientific Documentation Unit, Mossakowski Medical Research Centre, Polish Academy of Sciences, Warsaw, Poland

dorota.dziewulska@wum.edu.pl

Excessive interstitial glutamate levels cause injury and death of CNS cells, and are involved in many CNS disorders. Excitotoxic neuronal injury may correlate with blood-brain barrier (BBB) damage. The aim of this study was to investigate the effects of glutamate released into the cerebrospinal fluid from electrospun nanofiber mat dressing of the spinal cord. Adult male Wistar rat were subjected to subarachnoid application of an 'empty' (carrying no active principle) nanofiber mat or a glutamate-loaded nanofiber mat at the lumbar enlargement level. Half of the latter group was additionally given a systemic treatment with the histone deacetylase inhibitor valproic acid. A group of age-matched intact rats served as an additional control. All rats were killed 21 days after dressing application, and the L1-L6 parts of their spinal cords were collected and processed for electron microscopy, histological and immunohistochemical (IHC) studies by routine procedures. Spinal cords from the intact rats and rats carrying 'empty' nanofiber mat dressing showed proper parenchyma and BBB morphology. Spinal cords from the rats carrying glutamate-loaded spinal cord dressing revealed the presence of multiple intraparenchymal hemorrhages of varying sizes. The capillaries in the vicinity of the dressing (both in the

meninges and the white matter) were leaky and showed considerable swelling; there was no difference in these characteristics between rats with and without systemic valproic acid treatment. IHC studies revealed no difference in the staining intensity or the labeling pattern for basal lamina markers (laminin, collagen IV and fibronectin) between the study groups. Endothelial nitric oxide synthase immunolabeling showed an increased staining intensity in rats carrying glutamate-loaded dressing, irrespective of the valproic acid treatment. Electron microscopy revealed signs of excitotoxic neuronal injury and perivascular edema in both rat subgroups with glutamate-loaded mat dressing. Endothelial cells in these animals showed considerable mitochondrial swelling, increased numbers of plasmalemmal pinocytic vesicles and cytoplasmic vacuoles, and the formation of membrane-bound intraluminal protrusions and blebs; the integrity of tight junctions was generally preserved. No similar changes were seen in controls. These results indicate that glutamate-loaded nanofiber mat dressing can create glutamate concentrations capable of damaging spinal cord BBB.

|B10|

The phenotypic characterization and therapeutic application of human mesenchymal stem cells derived from adipose tissue

Anna Figiel-Dąbrowska[1], Patrycja Siedlecka[1], Krystyna Domańska-Janik[1], Anna Sarnowska[1,2]

[1]Stem Cell Bioengineering Unit, Mossakowski Medical Research Centre Polish Academy of Sciences, Warsaw, Poland
[2]Translative Platform for Regenerative Medicine, Mossakowski Medical Research Centre Polish Academy of Sciences, Warsaw, Poland

ania.dabrowska2703@gmail.com

The application of mesenchymal stem cells (MSCs) in regenerative medicine offers hope for effective treatment of yet incurable diseases. The therapeutic effect of stem cells has been confirmed in numerous independent studies, but their widespread clinical use requires the development of unified protocols of safe and efficient cells acquisition. The adipose tissue is one of the most promising sources of MSC for regenerative medicine.

The aim of this study was to isolate MSC from human subcutaneous adipose tissue (ASC) in real clinical surrounding, and setting the optimal conditions for their further propagation or direct transplantation into the wound.

The ASC isolated by the enzymatic method established previously in our laboratory were characterized by flow cytometry and immunocytochemistry. Long term cell culture was carried out in two variants: 5% or 21% of oxygen concentration, for which population doubling time (PDT), the cumulative time of population doublings (CPDs) and the rates of cell senescent were estimated. The cells ability to differentiate into the adipocytes, chondrocytes and osteocytes were evaluated together with their potential to vasculogenesis. In order to develop methods for topical transplantation of ASC, the cells were co-cultured with human fibroblasts or plated directly on the top of skin patchs.

The cell survival, integration and differentiation were evaluated in vitro after direct application of ASC on the top of co-cultured fibroblast surfaces by the use of irrigator.

The results demonstrated that modified enzymatic method of ASC isolation is reproducible and efficient. The cells possess all features typical for MSCs and have capacity to vasculogenesis in vitro. The low oxygen condition determines faster proliferation and slower cells senescence. The ASC delivered by use of irrigator survived well and were able to stimulate the growth of fibroblasts. Moreover, ASC can be administered on the wound surfaces directly by use of irrigator or special skin patches.

We can conclude that ASC obtained and applied according to the described protocol can be easily used for cell therapy of non-healing skin wounds in clinic.

The work was supported by National Science Centre grant No 2011/01/B/NZ3/05401 and Ministry of Science and Higher Education funds No 3757/E-32/R/2014-1.

|B11|

Energy metabolism in neurons exposed to hypoxia-inducing chemicals

Beata Gapys*, Marlena Zyśk, Anna Ronowska, Hanna Bielarczyk

Department of Laboratory Medicine, Medical University of Gdańsk

beata_gapys@gumed.edu.pl

Excess of Zn ions under hypoxic episodes may lead to neurodegeneration by disruption the neuronal cells energy metabolism.

Aim of the project was to evaluate the effect of Zn excess on energy metabolism in neuronal cells during hypoxia.

Experimental model was human neuroblastoma SH-SY5Y cell line, modified to cholinergic phenotype by using RA and cAMP (DC) or unmodified (NC). To induce hypoxia Co was used, added 3 h prior to Zn. Cells viability was measured by lactic dehydrogenase assay. Also activities of enzymes: pyruvate dehydrogenase complex (PDHC), aconitase, NADP-isocitrate dehydrogenase (IDH) were measured. Following the total level of acetyl-CoA was determined.

Exposition of NC to 0.125 mM Zn or 0.20 mM Co ions used apart didn't increase cells mortality, however when cells were 3 h preincubated with 0.20 mM Co mortality increased to 17.5% in response to 0.125 mM Zn. After exposition to 0.125 mM Zn activities of selected enzymes IDH and PDHC were decreased: by 18% and by 30% respectively while activity of aconitase remained unchanged. Exposition to 0.20 mM Co caused decrease of enzymes activities: – aconitase by 17%, PDHC by 38%. There was no inhibition of IDH. However when cells were preincubated with 0.20 mM Co prior to 0.125 mM Zn, the inhibition of the enzyme's activity was aggravated to 69% for aconitase and 30% for IDH. Activity of PDHC in these conditions was inhibited by 22%. The level of acetyl-CoA in the cells was changed neither after the Zn or Co alone nor after the preincubative conditions.

DC exposed to 0.125 mM Zn or 0.20 mM Co didn't exert changes in their mortality. After preincubation of the cells with Co mortality increased to 30% under 0.125 mM Zn. Activities of IDH, PDH were inhibited by 40%, 17% under 0.125 mM Zn and 34%, 44% after 0.20 mM Co. Activity of aconitase was not inhibited by 0.125 mM Zn while 0.20 mM Co inhibited its activity by 23%. Zn added 3 h after Co significantly increased the inhibitory effect on selected enzymes. The acetyl-CoA level was only diminished after 0.125 mM Zn under hypoxic conditions.

These results indicate that highly differentiated cholinergic cells are more prone to Zn-overload in hypoxic conditions, expressed by aggravation of inhibition of their energy metabolism.

Supported by M&R and H. E. projects: MN 01-0058/08 and ST-57, IP 2011046071.Differential susceptibility of microglial cells and cholinergic neurons to neurodegenerative signals.

|B12|

The effect of Perinatal Exposure to lead (Pb) on trafficking and scaffolding proteins dysfunction in rat brain

Magdalena Gąssowska[1]*, Irena Baranowska-Bosiacka[2], Joanna Moczydłowska[1], Lidia Strużyńska[3], Izabela Gutowska[2], Dariusz Chlubek[2], Agata Adamczyk[1]

[1]Mossakowski Medical Research Centre Polish Academy of Sciences, Department of Cellular Signaling, Warsaw, Poland
[2]Pomeranian Medical University, Department of Biochemistry and Medical Chemistry, Szczecin, Poland
[3]Mossakowski Medical Research Centre Polish Academy of Sciences, Department of Neurochemistry, Laboratory of Pathoneurochemistry, Warsaw, Poland

magy80@gmail.com

Lead (Pb) is a highly reactive heavy metal found in air, soil, drinking water and food widely recognized as a potent toxin of central nervous system. The most critical effects of Pb toxicity occur among children exposed during fetal and/or postnatal development leading to impairment learning and memory, cognition and behavioural control. However, the precise mechanism by which Pb exerts its neurotoxic effect and induces deficit in learning and memory processes are not fully elucidated. The objective of the present study was to evaluate the effect of perinatal low level Pb exposure on the expression of pre- and postsynaptic proteins as well as Tau protein changes in the young brain. Experiments were carried out on Wistar rats. Pregnant females were divided into two groups: control and Pb-treated animals. The control group was maintained on distilled water until weaning of the offspring while females from the experimental group received 0.1% lead acetate (PbAc) in drinking water *ad libitum*, starting from the first day of gestation. Offspring stayed with their mothers and were fed by them. During the feeding of pups, mothers from the experimental group were still receiving PbAc in drinking water *ad libitum*. Pups were weaned at postnatal day 21. 28-day old pups were sacrificed and expression of presynaptic syntaxin-1 and VAMP1/2 and postsynaptic PSD95, as well as the BDNF concentration and ultrastructural alterations were analysed in three brain areas: forebrain cortex (FC), cerebellum (C) and hippocampus (H). Concomitantly, we examined the effect of perinatal exposure to Pb on Tau pathology in these regions. Our data revealed that pre- and neonatal exposure of rats to Pb (concentration in rat offspring's blood below a 'safe level') evoked significant decrease in the expression of key synaptic proteins: syntaxin-1 in (H) and (C), VAMP1/2 in (C) and PSD95 in (C) and (FC) without changes in other brain

parts. Moreover, we observed the lower concentration of BDNF in all analysed structures in comparison to control. Molecular alterations were accompanied by pathological changes in ultrastructure of all examined brain structures from rats subjected to Pb. Parallel with synapses dysfunction, our results showed that Pb treatment caused significant increase of Tau expression and its phosphorylation at Ser396 in (FC) and (C). In these structures, we observed activation of two major Tau kinases: GSK-3b and CDK5, through increase in phosphorylation of Tyr-216 and formation of p25 protein, respectively. Concluding, perinatal exposure to lead induces disturbances of synaptic endings structure and functions that is implicated in neurodegenerative disorders including Alzheimer's and Parkinson's disease as well as in autism. We suggest that neurotoxic effect of Pb might be mediated, at least in part, by GSK-3β and CDK5-dependent Tau hyperphosphorylation, cytoskeleton disruption and synapses dysfunction.

Supported from MMRC statutory theme 8.

|B13|

Changes of sFas, its ligand – sFasL and Bcl-2 in cerebrospinal fluid and serum of multiple sclerosis patients, during relapse and after glucocorticoid therapy

Wanda Gordon-Krajcer[1], Krystyna Mitosek-Szewczyk[2]

[1]Department of Neurodegenerative Disorders, Mossakowski Medical Research Centre, Polish Academy of Science, Warsaw, Poland
[2]Department of Neurology, Medical University in Lublin, Lublin, Poland

wkrajcer@imdik.pan.pl

The mechanisms underlying cell death in MS (multiple sclerosis) are not fully understood. Apoptosis is believed to be one mechanism contributing to a marked and prolonged neuronal cell loss following MS. Recent data suggest a role for soluble Fas (sFas) (sAPO-1, sCD95) and soluble FasL (sFasL), a type I transmembrane receptor glycoprotein of nerve growth factor/tumor necrosis factor (TNF/NGF) superfamily, and its ligand sFasL in the central nervous system in MS before and after glucocorticoid therapy. In addition, we evaluate the potential therapeutic effects of the glucocorticoids. A truncated form of the Fas receptor, soluble Fas (sFas) may indicate activation of the Fas/FasL system and act as a negative feedback mechanism, thereby inhibiting Fas mediated apoptosis. We measured the expression rate of Fas in cerebrospinal fluid (CSF) and serum collected from 37 patients. The patients were evaluated at three different timepoints: at relapse (active stage), after 5 days of glucocorticoid therapy and in the remitting period – not shorter than 30 days of neurological status stability (inactive stage). No sFas was detected in CSF samples from persons without neurological pathologies – control group, consisted of 10 volunteers. CSF samples of MS patients at relapse showed elevated Fas concentrations (mean 458.26 ± SD 157.42 pg/ml). Serum samples showed slightly elevated sFas at relapse, five days after glucocorticoid therapy and in the remitting period. Serum levels of sFas were always much higher than CSF levels. However, there was no correlation between concentrations measured in CSF and in serum of appropriate groups of patient at relapse, suggesting that the concentrations in the two compartments are independently regulated. Concomitantly we estimated sFasL in the serum and CSF. We noted increase of sFasL levels in relapse and in the remitting period compared to controls. We observed significantly higher immunoreaction of Bcl-2 in the active stage of MS than in the inactive stage after glucocorticoid therapy or in controls.

|B14|

Adrenergic control of membrane potential in medial prefrontal cortex (mPFC) pyramidal neurons

Katarzyna Ewa Grzelka*, Paweł Szulczyk

Department of Physiology and Pathophysiology, Centre for Preclinical Research and Technology, Medical University of Warsaw, Warsaw, Poland

katarzyna.grzelka@wum.edu.pl

Aims: Impairment of the signal transduction from adrenergic receptors to cellular effectors in prefrontal cortex (PFC) neurons occurs in many neuropsychiatric disorders (acute stress disorder, ADHD). Application of clonidine (alpha2-adrenergic receptor agonist) evokes hyperpolarisation of the resting membrane potential in mPFC pyramidal neurons. The aim of the study was to define the cellular effectors and the exact signal transduction pathway from the receptor to the effector, which still remains unclear.

Methods: The membrane potential was recorded in layer V mPFC pyramidal neurons in slices isolated from 3-week-old rats. Recordings were performed in perforated-patch configuration at a temperature of 34°C. Adre-

nergic antagonists, inhibitors of cellular effectors and intracellular signalling were applied to the bath medium before, during and after clonidine application (100 μM). Their effects on clonidine-dependent membrane potential changes were analysed.

Results: The alpha2-receptor antagonists yohimbine (60 μM, *n* = 15) and atipamezole (20 μM, *n* = 6) did not completely block clonidine-dependent hyperpolarisation. The effect of clonidine was attenuated by the blocker of hyperpolarisation-activated cyclic nucleotide-gated (HCN) channels (ZD7288, 50 μM, *n* = 10) and by the selective Na^+/K^+-ATPase inhibitor (ouabain, 100 μM, *n* = 7). The hyperpolarisation was affected neither by the adenylyl cyclase inhibitor (SQ22536, 100 μM, *n* = 6), protein kinase A inhibitor (H-89, 40 μM, *n* = 6), phospholipase C inhibitor (U73122, 10 μM, *n* = 7) nor the protein kinase C inhibitor (chelerythrine, 5 μM, *n* = 5), but it was attenuated by the G-protein beta-gamma-subunit inhibitor (gallein, 20 μM, *n* = 12).

Conclusions: alpha2-adrenergic receptor activation evokes hyperpolarisation due to HCN channel inhibition and modification of the Na+/K+-ATPase function. The transduction pathway occurs in a membrane-delimited fashion and involves the G beta-gamma subunit released from the G-protein.

Supported by grants no: NN401584638 and NN3015 72940.

|B15|

Human and bovine nuclear matrix protein complexes bind to the first intron of the tyrosine hydroxylase gene

Joanna Jabłońska[1]*, Piotr Wasąg[1], Anna Goc[1], Robert Lenartowski[2]

[1]Department of Genetics, Nicolaus Copernicus University, Toruń, Poland
[2]Laboratory of Isotope and Instrumental Analysis, Nicolaus Copernicus University, Toruń, Poland

bajanaoj@gmail.com

Tyrosine hydroxylase (TH) [EC 1.4.16.2] is a rate-limiting enzyme required for catecholamine synthesis. The TH gene and its product are under strict, multilevel regulation to control tissue-specific expression and enzymatic activity in neurons. Our previous work showed that the TH gene interacts with protein components of the nuclear structure called the nuclear matrix (NM). We showed that the proximal region (+725 to +1678) of the bovine TH gene bound to bovine NM proteins (NMPs) isolated from both TH-expressing (TH+) and non-expressing (TH–) tissues. In contrast, the -2300 to +2300 region of the human TH gene bound to bovine NMPs isolated from TH+ tissue but not from TH- tissue. We hypothesize that these interactions affect the spatial organization of the TH gene chromatin and thereby control its transcription. To determine whether NMP-mediated epigenetic regulation of the TH gene is species-specific, here we aimed to: (i) map the minimal sequence of the bovine TH gene responsible for interactions with bovine NMPs and (ii) identify regions of the human TH first intron that interact with human NMPs.

To accomplish our objectives, we isolated NMPs from the bovine adrenal medulla and the human SH-Sy5y cell line, which are both TH+, and the bovine liver and human HepG2 cell line, which are both TH-. Radiolabeled probes encompassing parts of the TH first intron (+113/+613, +589/+1085, +807/+1016, +1122/+1602, and +1449/+1973) were incubated with NMPs isolated from TH+ or TH- cells or tissues in the presence of non-specific competitor and increasing excess of unlabeled probe. EMSA, in which complexes were separated on 3 or 5% non-denaturing polyacrylamide gels, was used to assess binding.

We found that a minimal 210 nt intronic fragment (+807/+1016) of the bovine TH gene interacted with bovine NMPs isolated from both the adrenal medulla and the liver. Interactions between regions of the human TH first intron and human NMPs were more complex. The proximal fragment (+113/+613) interacted with NMPs isolated from both SH-Sy5y and HepG2 cells, whereas the +1122/+1602 region did not interact with NMPs from either cell line. The +589/+1085 region only interacted with NMPs from SH-Sy5y cells, and the distal region (+1449/+1973) only interacted with NMPs from HepG2 cells. Together with our previous results, these data indicate that NMPs isolated from HepG2 cells contain species-specific proteins that are able to bind the human TH first intron.

|B16|

Neuroprotective effects of necrostatin-1 against oxidative stress- and pro-apoptotic factors-induced cell damage in human neuroblastoma SH-SY5Y cells

Danuta Jantas*, Jakub Chwastek, Beata Grygier, Władysław Lasoń

Department of Experimental Neuroendocrinology, Institute of Pharmacology, Polish Academy of Sciences
jantas@if-pan.krakow.pl

Recent data suggest that necroptosis, a novel form of non-apoptotic programmed cell death, could be implicated in many pathological conditions including neuronal death in experimental models of stroke and brain trauma. Moreover, an inhibition of this process by necrostatin-1 (Nec-1) has been shown to be neuroprotective in in vitro and in vivo models of cerebral ischemia. However, the involvement of this type of cell death in other neurodegenerative conditions and its interplay with other cell death types (apoptosis, autophagy) is less recognized. Thus in the present study we tested the effect of necrostatin 1 (Nec-1), an inhibitor of necroptosis, in the models of oxidative stress (H_2O_2)- and pro-apoptotic factors-induced human neuroblastoma SH-SY5Y cell damage. The data showed that Nec-1 (0.1-20 μM) partially attenuated the cell death induced by H2O2, staurosporine and doxorubicin as confirmed by MTT reduction assay. The range of protection mediated by Nec-1 was similar to the effect of caspase-3 inhibitor, Ac-DEVD-CHO in all tested models of cell injury. Moreover, the neuroprotective effect of Nec-1 was not connected with reduction of the toxin-induced caspase-3 activity. The concomitant treatment of cells with necroptosis and apoptosis inhibitors evoked similar protection in all tested models as did each agent given alone, suggesting a shared common downstream intracellular cell death mechanisms for both processes. Our data showed an involvement of necroptosis in oxidative stress- and pro-apoptotic factors-induced cell damage of SH-SY5Y cells and that inhibition of this pathway could be neuroprotective.

Acknowledgment: The study was supported by statutory funds of the Institute of Pharmacology, Polish Academy of Sciences.

|B17|

The stimulation of hippocampal neurogenesis by a histone deacetylase inhibitor – Trichostatin A, after neonatal hypoxia-ischemia

Joanna Jaworska*, Małgorzata Ziemka-Nałęcz, Teresa Zalewska

NeuroRepair Department, Mossakowski Medical Research Centre Polish Academy of Sciences, Warsaw, Poland
jjaworska@imdik.pan.pl

Neonatal encephalopathy is the most important cause of severe neurological disability in children. There are currently no effective therapies to reduce brain damage and its long-term sequel in infants. Mounting evidence indicate that treatment of adult animals with histone deacetylase inhibitors (HDACis) administered after stroke provides neuroprotection and also promotes neurogenesis. Based on the above data it can be hypothesised that HDACis provide a suitable option for the treatment of neonatal HI injury. This prompted us to check whether the administration of Trichostatin A, one of the HDACi, stimulates neurogenesis after neonatal hypoxic-ischemia.

We utilized a model of hypoxia-ischemia induced in rats of postnatal day 7. TSA (0.2 mg/kg) was injected subcutaneously in one single dose for 5 consecutive days starting immediately after the insult. The proliferation profile was estimated by BrdU injection at specific time points after HI. BrdU positive cells were determined by immunohistochemistry method.

At 3-14 days after hypoxia-ischemia BrdU-positive cells were seen in both hemispheres, with the greatest number of dividing cells in ischemic side. The strongest proliferation level occurs within 3 and 6 days after the injury. The labelling pattern revealed structure-dependent differences. Three days after HI the highest density of BrdU-positive cells was seen in the hilus, whereas at longer survival time (9-14 days) labelled cells changed their localization towards the subgranular zone (SGZ) of DG.

To determine the phenotype of newborn cells, BrdU was administered twice daily, at 5 to 7 days after HI and the animals were sacrificed 14 days after the HI insult. To analyse if BrdU-positive cells represent newly generated neuroblasts and oligodendrocyte progenitors, we used double immunohistochemical staining BrdU/ DCX and NG2/BrdU, respectively. We found that administration of TSA stimulates the generation of neuroblasts and oligodendrocyte progenitors, restoring their reduced number after HI to control level.

Conclusion: Our preliminary results show that Histone deacetylase inhibitor Trichostatine A exerts beneficial

effects after neonatal HI by stimulating the proliferation of neural progenitors.

Supported by NSC grant no 2012/05/B/NZ3/00436 and POKL.04.03.00-00-060/12.

|B18|

Alteration of arginases and nitric oxide synthase in cells transfected with human wild-type beta amyloid precursor protein (βAPP)

Henryk Jęśko*[1], Anna Wilkaniec[1], Magdalena Cieślik[1], Wojciech Hilgier[2], Magdalena Gąssowska[1], Walter J. Lukiw[3], Agata Adamczyk[1]

[1]Department of Cellular Signalling
[2]Department of Neurotoxicology, Medical Research Centre, Polish Academy of Sciences, Warsaw, Poland
[3]Neuroscience Center of Excellence and Departments of Neurology and Ophthalmology, Louisiana State University Health Sciences Center, New Orleans, LA 70112, USA

Silgrin@interia.pl

L-arginine is a semi-essential amino acid with a number of bioactive metabolites. Accumulating evidence suggests the implication of altered arginine metabolism in the pathogenesis of Alzheimer's disease (AD). However, the impact of amyloid β (Aβ) peptides on arginine degradation and re-synthesis is unknown.

In the present study we investigated the activity and expression level of arginase I and II as well as neuronal, endothelial and inducible NO synthase isoforms (*NNOS, ENOS, INOS*), enzymes that metabolize arginine or resynthesize it from citrulline and the levels of corresponding amino acids in rat pheochromocytoma (PC12) cells overexpressing human Aβ precursor protein (APPwt cells). Moreover, we investigated the changes in miRNAs responsible for modulation of arginine metabolism in AD brains. Arginase activity was assessed spectrophotometrically, and mRNA levels of arginase I and II and other urea cycle enzymes were measured using real-time PCR. Our results showed that the expression of *ARG1* and *ARG2* genes was significantly lower in APPwt than in control PC12 cells: *ARG1* mRNA was reduced 3-fold whereas *ARG2* was down-regulated by 50%. Moreover, total activity of arginases was significantly reduced by 52% in APPwt cells. Concomitantly, *NNOS* and *ENOS* mRNAs were significantly elevated in APPwt cells while *iNOS* was undetectable in both cell lines. Other urea cycle enzymes were also altered in APPwt cells. The expression of argininosuccinate synthase (*ASS*) that metabolizes citrulline was down-regulated while argininosuccinate lyase (*ASL*) remained unchanged. Ornithine decarboxylase (*ODC*), which decarboxylates ornithine to form putrescine, a precursor of other polyamines was also reduced. Arginine, the substrate for both arginases and NOS, was unchanged in APPwt cells. However, NOS product citrulline was significantly elevated. Using miRNA arrays and cluster analysis we have investigated microRNAs (miRNAs) known to interact with 3'-UTRs of mRNAs linked to arginine metabolism and *NOS* mRNAs. We have found elevated hsa-miRNA-9 and hsa-miRNA-128a in AD patients' brains as compared to the same brain areas of age-matched controls. Their changes might modulate the expression of *ASS* and *NOS*, respectively. Our results suggest the significance of arginases for the promotion of NOS-dependent cellular stress by βAPP/Aβ in a system where up-regulated, potentially pathogenic miRNAs are involved.

Supported by Mossakowski Medical Research Centre statutory theme no. 8.

|B19|

Carbon monoxide-releasing molecule (CORM-2) deflates neuropathic pain symptoms and potentiates opioid effectiveness in rat CCI model

Agnieszka M. Jurga*, Anna Piotrowska, Joanna Starnowska, Ewelina Rojewska, Wioletta Makuch, Joanna Mika

Department of Pain Pharmacology, Institute of Pharmacology, Polish Academy of Sciences, Krakow, Poland

jurga@if-pan.krakow.pl

Chronic pain is one of the most urgent clinical problems for of poor understanding of its pathogenesis. It may appear as a consequence of nerve mechanical damage or as a co-symptom of many diseases, and may be divided into inflammatory and neuropathic pain. Due to P2X purinergic receptors, with the special focus on subtypes 4 and 7, are indicated to play a significant role in pain development, we decided to introduce a pharmacological antagonist of P2X4 receptor (P2X4R) and measure its analgesic potency - alone and together with opioid drugs. Experiments were performed to evaluate the contribution of P2X4R in modulation of neuropathic pain, and their ability to amplify the morphine and/or buprenorphine

effectiveness in Wistar rat chronic constriction injury (CCI) neuropathic pain model. Study consisted of behavioural tests (von Frey's and cold plate) and dorsal, lumbar (L4-L6) spinal cord biochemical analysis (Western blot) after CCI to the right sciatic nerve. We have demonstrated that single administration of CO donor: CORM-2, significantly reduced allodynia and hyperalgesia two hours after intraperitoneal injection as efficiently as morphine and buprenorphine. What is more, CORM-2 intensified the analgesic effect of both morphine and buprenorphine comparing to the effect of these drugs alone, completely revoking hypersensitivity. The analgesic potency of CORM-2 administered for 7 consecutive days was greater on day 7th than on day 2nd, suggests no tolerance development, accretion of anti-nociceptive effect over time. We are the first to demonstrate that even single intraperitoneal administration of CORM-2 potentiates the morphine and buprenorphine anti-hyperalgesic and anti-allodynic properties in rat CCI model. Our data complete those published so far in neuropathic pain field and are in agreement that P2X4R may indeed play significant role in neuropathic pain development.

This study is supported by grant OPUS NCN 2011/03/B/NZ4/00042 and Institute of Pharmacology statutory funds. Agnieszka M. Jurga and Joanna Starnowska are holders of KNOW scholarship sponsored by Ministry of Science and Higher Education, Republic of Poland

|B20|

The effect of designer drugs on neurotransmission in the rat brain

Katarzyna Kamińska*, Alexandra Jurczak, Krystyna Gołembiowska

Department of Pharmacology, Institute of Pharmacology of the Polish Academy of Science, Kraków, Poland
katkam@if-pan.krakow.pl

Designer drugs, also known as "legal highs" or "legal drugs", are synthetic compounds developed to provide similar effects to illicit drugs of abuse, which are not subjected to legal control. Legal highs are widely available online and in clubs. These drugs come in various forms. Some of these are herbal mixtures, others come as a white powder or as tablets or capsules. They can be taken orally, smoked, inhaled, added to drinks or injected.

Synthetic drugs are classified roughly, based on their chemical formula, into phenethylamines, tryptamines, and piperazines. Although designer drugs still have the reputation of being safe, several experimental studies in rats but also in humans indicated risks including life threatening serotonin syndrome, hyperthermia, heart disease, neurotoxicity, and abuse potential.

The least investigated and most dangerous synthetic components found in the designer mixtures are phenylalkylamines: para methoxyamphetamine (PMA), para-methoxymethamphetamine (PMMA) and synthetic cathinone: mephedrone. Our study is aimed on examining the effects of the above-mentioned on extracellular levels of dopamine, serotonin and their metabolites using microdialysis in freely moving rats. Dialysates are assayed using HPLC witch coulochemical detection, following i.p. administration of each drug at doses of 5 and 10 mg/kg.

PMA, PMMA and mephedrone given intrastriatally, have strong inhibitory effects on re-uptake of serotonin and to lesser extent dopamine, causing their extracellular increase and decrease in their metabolites.

Our results suggest that designer drugs have strong impact on the central nervous system causing profound alterations in neurotransmission, but the exact mechanism by which they act still needs to be clarified.

Acknowledgements: Supported by grant from National Centre of Science (NCN) no 2013/09/B/NZ7/04104.

|B21|

Alternative methods for staining and characterization of extracellular vesicles derived from human bone marrow mesenchymal stromal cells

Sylwia Koniusz[1]*, Andrea Del Fattore[2], Małgorzata Frontczak-Baniewicz[3], Maurizio Muraca[4], Barbara Lukomska[1]

[1]NeuroRepair Department, Mossakowski Medical Research Centre, PAS, Warsaw, Poland
[2]Bambino Gesú Children's Hospital, Regenerative Medicine Unit, IRCCS, Rome, Italy
[3]Electron Microscopy Platform, Mossakowski Medical Research Centre, PAS, Warsaw, Poland
[4]Department of Women's and Children's Health, University of Padua, Padua, Italy
s.koniusz@gmail.com

Introduction: Mesenchymal stromal cells (MSCs) are of great interest in regenerative medicine and clinical strategy because of their ability to migrate to injured sites, function in tissue repair and to modulate immune

response. The predominant mechanisms by which MSCs participate in tissue repair seem to be related to their paracrine activity. Besides the long-time notion of growth factors and cytokines it now appears that MSCs secrete large amounts of extracellular vesicles (EVs). Several studies have suggested that MSC-derived EVs have functions similar to their cellular counterparts. Thus, MSC-EVs represent a promising opportunity to develop novel cell-free therapy approaches.

The aim of the study was to optimize the method of staining for EVs derived from mesenchymal stromal cells in term of their visualization after transplantation.

Material and methods: The experiments were performed on human bone marrow mesenchymal stem cells (hBM-MSCs) (Lonza). hBM-MSCs were labelled with three different dyes: lipophilic stain (PKH26), iron nanoparticles conjugated with rhodamine (SPIO) and quantum dots (Qdots). Then immunocytochemical staining for tetraspanins (characteristic markers for EVs): CD9, CD63, CD81 was performed. EVs were isolated from the culture media of previously labelled hBM-MSCs by centrifugation at 1800 × g for 30 min at 4°C to remove debris, then followed by two times ultracentrifugation at 100 000 × g for 60 min at 4°C in order to isolate EVs. The results were analyzed in confocal microscopy and transmission electron microscopy.

Results: Our results depicted the presence of intracellular structures positively stained with PKH26, SPIO or Qdots visible inside hBM-MSCs. These structures co-express CD9, CD63 and CD81 markers specific for EVs. The isolated EVs represent heterogeneous population differed with size and content as confirmed by electron microscopy together with their positive staining with SPIO and Qdots. Conclusions. All three different dyes proved to be efficient stains for EVs although iron nanoparticles conjugated with rhodamine and quantum dots have wider application for EM and MRI and can be useful to monitor EVs in vivo after their transplantation.

|B22|

Genetic variants of SLC6A4, HCRTR1, KCNK18 genes in migraine patients

Marta Kowalska[1]*, Anna Oczkowska[1], Michał Prendecki[1], Magdalena Kapelusiak-Pielok[2], Wojciech Kozubski[2], Jolanta Dorszewska[1]

[1]Laboratory of Neurobiology, Department of Neurology
[2]Chair and Department of Neurology, Poznan University of Medical Sciences, Poznan, Poland

martak_89@o2.pl

Introduction: Migraine is one of the most common neurological disorder that affects 11% of adults. There are two main clinical subtypes of this disease: migraine with aura (MA) and without aura (MO). Migraine has a significant genetic basis. It is believed that polymorphisms in SLC6A4, HCRTR1, KCNK18 genes may be involved in its pathomechanism. No genetic studies of migraine have been performed on polish population so far.

Aims: The aim of the study was to analyze exon 7 of HCRTR1 gene, exons 1 and 2 of KCNK18 gene, 5-HTTLPR length polymorphism and the plasma level of serotonin.

Methods: The studies included 34 migraine patients (MA: 17, MO: 17) and 34 healthy controls. The mean age of participants was 40 years. Genotyping was performed using PCR, HRM, RFLP and sequencing while 5-HT levels were determined using HPLC/EC technique.

Results: The studies confirmed presence of two polymorphisms in HCRTR1 gene: G29A and G1222A. Genotype AA of HCRTR1 G1222A was observed only in migraine patients ($p<0.01$), both MA and MO. HCRTR1 G29A GA may be involved in MA or MO. Presence of another two variants: A28G and T328C was confirmed in KCNK18 gene. Long allele of 5-HTTLPR polymorphism occurred more frequently in migraine ($p < 0.05$) as compared to the controls. There have been no statistical evidence for association of analyzed polymorphisms with the plasma concentration of serotonin.

Conclusions: The AA genotype of G1222A HCRTR1 seems to be a risk factor for migraine in Polish population. The presence of long allele of 5-HTTLPR polymorphism is associated with a tendency for increased concentrations of plasma serotonin.

|B23|

Regulation of the membrane potential in the medial prefrontal cortex (mPFC) pyramidal neurons by muscarinic receptors

Przemyslaw N. Kurowski*, Maciej Gawlak, Pawel Szulczyk

Department of Physiology and Patophysiology, Centre for Preclinical Research and Technology (CePT), Medical University of Warsaw, Warsaw, Poland

przemyslaw.kurowski@wum.edu.pl

Damage to the cholinergic input to the prefrontal cortex has been implicated in neuropsychiatric disorders. Cholinergic endings release acetylcholine, which activates nicotinic and/or G-protein-coupled muscarinic receptors. Muscarinic receptors activate transduction system(s), which control cellular effectors which regulate the membrane potential in medial prefrontal cortex (mPFC) neurons. The mechanisms responsible for the cholinergic-dependent depolarization of mPFC layer V pyramidal neurons in slices obtained from young rats were elucidated in this study. Glutaminergic and GABAergic transmissions, tetrodotoxin (TTX)-sensitive Na^+ and voltage-dependent Ca^{2+} currents were eliminated. Cholinergic receptor stimulation by carbamoylcholine chloride (CCh; 100 μM) evoked depolarization (10.0 ± 1.3 mV), which was blocked by the M1/M4 (pirenzepine dihydrochloride, 2 μM) and M1 (VU 0255035, 5 μM) muscarinic receptor antagonists and was not affected by a nicotinic receptor antagonist (mecamylamine hydrochloride, 10 μM). CCh-dependent depolarization was temporarily diminished by current step (100 msec, 500 pA) and was attenuated by an inhibitor of the βγ-subunit-dependent transduction system (gallein) applied extra- (20 μM) or intracellularly (50 μM). It was also inhibited by intracellular application of the βγ-subunit binding peptide (GRK2i, 10 μM). mPFC pyramidal neurons express Nav1.9 channels. CCh-dependent depolarization was abolished in the presence of antibodies against Nav1.9 channels in the intracellular solution and augmented by ProTx-I toxin (100 nM) in the extracellular solution. CCh-induced depolarization was not affected by the following reagents: intracellular transduction system blockers, including U 73122 (10 μM), chelerythrine chloride (5 μM), SQ 22536 (100 μM) or H-89 (2 μM); channel blockers, including Ba^{2+} ions (200 μM), apamin (100 nM), flufenamic acid (200 μM), 2-APB (200 μM), SKF 96365 (50 μM), and ZD 7288 (50 μM); and a Na^+/Ca^{2+} exchanger blocker, benzamil (20 μM). We conclude that muscarinic M1 receptor-dependent depolarization in mPFC pyramidal neurons is evoked by activating Nav1.9 channels and that the signal transduction involves G protein βγ subunits.

|B24|

Influence of isolation and cultivation methods on stemness properties of human Wharton's Jelly-derived MSC population

Wioletta Lech[1]*, Katarzyna Drela[2], Anna Sarnowska[1], Krystyna Domanska-Janik[1]

[1]Stem Cell Bioengineering Unit, Mossakowski Medical Research Centre, Polish Academy of Sciences, Warsaw, Poland
[2]NeuroRepair Department, Mossakowski Medical Research Centre, Polish Academy of Sciences, Warsaw, Poland

lech.wioletta@gmail.com

Human umbilical cord Wharton's Jelly Mesenchymal Stem Cells (WJ-MSC) are of a great research and clinical interest since their first isolation in 1991.

The main purpose of this paper was to elaborate and optimize enzymatic method of cell isolation in comparison to the classical method of mechanical isolation used routinely in our laboratory. Enzymatic method of MSC isolation relays here on the limited proteolysis of the tissue by collagenase I using different durations of the digestion.

Mesenchymal character of the cells isolated by both methods was verified by mesodermal lineage differentiation ability into fat, bone and cartilage. We tested also specific markers expression with flow cytometry, immunocytochemistry and quantitative RT-PCR analysis. For comparison the proliferation rate, long-term culture (population doubling time), one-week curve and expression of proliferating cells marker Ki67 analysis was performed. In addition we analyzed ability to create CFU-F by both types WJ-MSC and calculated percentage of senescence cells at late passages.

The results allow to conclude that, though comparable expression of the classical mesenchymal markers, the cells isolated by quantitatively more efficient enzymatic method proliferate much slower in culture and differentiate scarcely into typical for MSC mesodermal lineages in comparison with mechanically isolated MSC.

Moreover, in WJ-MSC(M) a significantly higher expression of early neuroectodermal marker nestin and primitive cell marker α-SMA has been observed, suggesting their pluripotent differentiation ability allowing the cells to cross mesodermal lineage barriers.

In contrast, absence of the above properties in WJ-MSC(E), together with the lack of their ability to CFU-F

formation (a golden mark of the stem cells) and faster cell senescence with limitation of typical mesodermal differentiation lineages may question the stemness characteristic of the cells isolated by the described enzymatic method.

Key words: stem cells, Wharton's jelly, WJ-MSC, mechanical method, enzymatic method, differentiation, proliferation, CFU-F

The work was supported by National Science Centre grant No 6430/B/P01/2011/40 and The National Centre for Research and Development grant No STRATEGMED1/234261/2/NCBR/2014.

|B25|

Alkaloids from *Huperzia selago* protect dopaminergic PC12 cells against sodium nitroprusside-evoked oxidative stress, mitochondrial dysfunction and apoptosis

Anna M. Lenkiewicz*[1], Grzegorz A. Czapski[1], Anna Wilkaniec[1], Wojciech Szypuła[2], Agata Adamczyk[1]

[1]Department of Cellular Signalling, Mossakowski Medical Research Centre Polish Academy of Sciences, Warsaw, Poland
[2]Department of Pharmaceutical Biology and Medicinal Plant Biotechnology, Faculty of Pharmacy, Medical University of Warsaw, Warsaw, Poland

amlenkiewicz@gmail.com

Mitochondrial dysfunction and enhanced cellular oxidative stress have long been recognized to play a major role in the pathogenesis of several neurodegenerative disorders such as Alzheimer's and Parkinson's diseases. Energy depletion, reactive oxygen species (ROS) generation and increased oxidative damage to several macromolecules may result in loss of calcium homeostasis and in consequence neurodegeneration occurs. Under this perspective, compounds which acting as radical scavengers and protected against oxidative stress and mitochondrial damage might be considered as a potential cytoprotective agents. Our previous data indicated that alkaloids isolated from *Huperzia selago* exhibited antioxidant activity and effectively protected against lipid and protein oxidation in rat brain tissue homogenate. Therefore, the aim of the present study was to investigate the antioxidative and cytoprotective capabilities of alkaloid fractions from *Huperzia selago* to protect dopaminergic PC12 cell against oxidative stress evoked by sodium nitroprusside (SNP). These cells were exposed to 0.5 mM SNP and the effect of alkaloid-rich extract (ARE) was evaluated. The experiments were carried out using spectrophoto- and spectrofluorometrical analysis, fluorescent microscopy and real-time PCR. Our data indicated that 24 h exposure of PC12 cells to SNP leads to significant, about 4-fold increase in free radicals and nitric oxide (NO) generation. Treatment with ARE (2.5 µg/ml) prevented SNP-induced NO liberation. Moreover, alkaloid fractions significantly protected against DNA fragmentation and mitochondrial damage evoked by SNP treatment. We observed that ARE notably attenuated SNP-induced changes in mitochondrial membrane potential and decreased the elevated mitochondrial calcium levels. Furthermore, we have analysed the effect of ARE on SNP-induced modification of Parkin, which is responsible for removal of damaged mitochondria via its poly-ubiquitylation and promotion of mitophagy. SNP-evoked apoptotic processes lead to decrease in PC12 cells viability and ARE protected cells against SNP-induced cytotoxicity. In conclusion, these results suggest that the alkaloid extract from *Huperzia selago* show good effects against SNP-induced oxidative injury in PC12 cells by adjusting oxidative stress, and suppression of mitochondrial dysfunction, and could be developed as a potential candidate as a neuroprotective compound.

Supported by NCN grant 2012/05/B/NZ3/02047 and EU from ESF under the OPHC NCBIR grant POKL.04.03.00-00-060/12.

|B26|

Minocycline enhance botulinum neurotoxin a analgesia under neuropathic pain via glia modulation

Wioletta Makuch[1]*, Ewelina Rojewska[1], Magdalena Zychowska[1], Sara Marinelli[2], Siro Luvisetto[2], Flaminia Pavone[2], Barbara Przewlocka[1], Joanna Mika[1]

[1]Department of Pain Pharmacology, Institute of Pharmacology, Polish Academy of Sciences, Krakow, Poland
[2]CNR, Institute of Cell Biology and Neurobiology – IRCCS, Santa Lucia Foundation, Roma, Italy

makuch@if-pan.krakow.pl

Recent studies show a promising analgesic effect using botulinum neurotoxins (BoNTs) for chronic pain state. The present study was undertaken to determine the influence of minocycline on botulinum neurotoxin serotype A (BONT/A) analgesia under neuropathic pain. The objec-

tive of this studies was also to assess whether botulinum neurotoxin serotype A (BONT/A) affects the markers of microglial and astroglial activation in CCI-exposed rats.

The experiments were carried out according to IASP recommendations and local Bioethics Committee The chronic constriction injury (CCI) to the sciatic nerve was performed on male Wistar rats (Bennett and Xie, 1988) and all experiments were conducted 7 days after CCI. The effects of BoNT/A administered intraplantarly into the injured hindpaw were assessed by von Frey test. Biochemical studies comprised the RT-PCR and Western blot analysis in the spinal cords and DRGs.

A single intraplantar (i.pl.) injection of BONT/A (75pg) caused strong antiallodynic effect in CCI-exposed rats which was enhanced after chronic intraperitoneal minocycline (30 mg/kg) administration. BONT/A decreased the injury-induced ipsilateral upregulation of C1q and GFAP mRNA expression in the spinal cord and dorsal root ganglia (DRG) and diminished elevated IBA-1 protein level in the spinal cord in CCI-exposed rats. The ipsilateral DRG and dorsal spinal cord of CCI-exposed rats showed no changes in GFAP protein levels. Minocycline inhibited C1q mRNA expression at the level of the spinal cord and DRG in CCI-exposed rats. Moreover, minocycline decreased GFAP mRNA expression in the DRG in a neuropathic pain model in rats. Decreased protein level of C1q and IBA-1 after minocycline injection in the spinal cord was significantly upregulated after BONT/A. The changing the activity of glial processes may affect BoNT/A-induced analgesia and biochemical markers. The results of this research indicate the ability to the development of new pharmacotherapeutic approaches of neuropathic pain. Acknowledgments: This research was supported by statutory funds from the Department of Pain Pharmacology and by a grant Harmonia 5 2013/10/M/NZ4/00261, both from the Ministry of Science and Higher Education. The scientific collaboration between PAN and CNR (Italy) is greatly acknowledged. Rojewska have a scholarship from the START sponsored by the Foundation of Polish Science and Zychowska from the KNOW sponsored by Ministry of Science and Higher Education, Poland.

|B27|

Ammonia reduces intracellular ADMA concentration in cultured astrocytes and brain endothelial cells (RBE-4) via y+LAT2-mediated efflux

Krzysztof Milewski*, Jan Albrecht, Wojciech Hilgier, Magdalena Zielińska

Department of Neurotoxicology, Mossakowski Medical Research Center PAS, Warsaw, Poland

kmilewski@imdik.pan.pl

Toxic effects of ammonia in the brain are partly related to impaired NO production. Asymmetric dimethylarginine (ADMA), is an endogenous NOSs inhibitor and symmetric dimethylarginine (SDMA) is arginine (Arg) transport inhibitor. ADMA is synthesized by protein arginine methyl transferases (PRMTs), released during proteolysis and then degradated mainly by dimethylarginine-dimethylaminohydrolase (DDAH-1) (Teerlink *et al*., 2009). Previously we reported an increase of ADMA and SDMA concentration in brain of rats with acute liver failure (Milewski *et al*., 2014), but distribution of the ADMA/SDMA surplus between the particular intra and extracellular compartments has not been studied.

We hypothesize that ADMA/SDMA transport from astrocytes and brain endothelial cells in vitro, could be mediated by y+LAT2 carrier, belonging to y+L family of cationic amino acids transporters. Of note, y+LAT2 under hyperammonemic conditions is up-regulated both in astrocytes and RBE-4 cells (Skowrońska *et al*., 2012; Zielińska *et al*., 2012) and we speculated that this transporter may influence the concentration of both Arg derivatives.

The aim of this study was to evaluate the intracellular concentration of ADMA/SDMA/Arg in astrocytes and RBE-4 cells and the effect of ammonia treatment (48 h, 5 mM) on this issue.

In RBE-4 cells not treated with ammonia the ADMA concentration was twice higher and the Arg/ADMA ratio was much lower than in astrocytes, confirming well documented role of ADMA in endothelial NOS inhibition (Pope *et al*., 2009). Ammonia treatment led to an almost 50% reduction of ADMA and SDMA intracellular concentration in both cell type (measured by HPLC) with the accompanying ADMA/SDMA accumulation in the cultured medium (determined by mass spectroscopy). This phenomenon occurs without PRMT-1 and DDAH-1 gene expression changes or DDAH-1 protein level alteration. This observation suggests ammonia induced ADMA/SDMA transport changes. Indeed, silencing of the Slc7a6 (y+LAT2) gene

expression diminished the reduction of intracellular ADMA concentration caused by ammonia treatment in astrocytes and decrease NO production.

This results suggest that increased ADMA (and possibly SDMA) efflux mediated by upregulated y+LAT2 may be one of the ways in which ammonia interferes with intracellular ADMA content and, subsequently, NO synthesis.

Supported by NCN grant 2013/09/B/NZ4/00536.

|B28|

The effect of preconditioning with hyperbaric oxygen on brain tissue expression of proteasomal and apoptotic proteins after experimental global brain ischemia

Robert P. Ostrowski[1]*, Katarzyna Stępień[1], Emanuela Pucko[1], Renata Wojda[1], Marcin Gamdzyk[2], Wanda Chrzanowska[1], Ewa Matyja[1]

[1]Department of Experimental and Clinical Neuropathology
[2]Department of Neurochemistry, Mossakowski Medical Research Centre, Polish Academy of Sciences, Warsaw
rostrowski@imdik.pan.pl

Research hypothesis implies that hyperbaric oxygen preconditioning (HBO-PC) induces proteasome changes accompanied by a decrease in the level of apoptotic proteins, what may implicate participation of proteasome in the preconditioning mechanism.

The aim was to study whether HBO-PC has an impact on brain tissue expression of selected proteasome and apoptotic proteins after global brain ischemia.

The experiments were conducted under general anesthesia on male Wistar rats subjected to 5 min global brain ischemia obtained via bilateral common carotid artery ligation and a reduction of arterial blood pressure. Five sessions of HBO-PC, alone or combined with the inhibitor of proteasome MG132 were performed for 5 days preceding ischemia, 1 hr daily at 2.5 ATA. With immunohistochemistry techniques we investigated 20S proteasome β1 (catalytic) and proapoptotic proteins; p53 upregulated modulator of apoptosis (PUMA) and B cell lymphoma-2 interacting mediator of cell death (BIM) as well as neurofilaments (NF) and glial fibrillary acidic protein (GFAP). Klüver-Barrera stain was used to determine myelin and neuronal morphology.

At 7 days after ischemia partial sparing of the hippocampus CA1 zone neurons was noted with HBO-PC. As for the proteasomal 20S protein, perinuclear cytoplasmic stain was noted in neuronal cells of the hippocampus and cerebral cortex in the control. With HBO-PC, both cerebral cortex and the hippocampus exhibited the enhanced, predominately neuronal, 20S immunoreactivity.

PUMA showed a diffuse neuronal stain in the hippocampus and cerebral cortex in control. While after ischemia there was a strong PUMA reactivity in remaining pyramidal cells and dentate gyrus granule cells. Weak immunoexpression was found with the HBO-PC, especially in the CA1 zone, unless associated with focal cell loss. BIM exhibited cytoplasmic and perinuclear stain, enhanced after ischemia. A weak BIM expression was found after ischemia preceded with HBO-PC.

NF of the cytoskeleton showed postischemic depletion throughout the hippocampal pyramidal layers. Astroglial reaction to ischemia, as determined with GFAP stain, especially in the CA1 was reduced with HBO-PC. The HBO-PC combined with proteasome inhibitor exhibited changes of tissue expression within investigated characteristics similar to the ischemia alone.

These results seem to suggest the participation of proteasome and diverse alterations of apoptotic proteins within the postischemic brain after HBO-PC.

|B29|

Neuroprotective benefits of physical activity in a chronic mouse model of Parkinson's disease

Ewelina Palasz[1], Anna Gasiorowska[1,2], Wiktor Niewiadomski[2], Grazyna Niewiadomska[1]

[1]Nencki Institute of Experimental Biology, Warsaw, Poland
[2]Mossakowski Medical Research Centre, Warsaw, Poland
e.palasz@nencki.gov.pl

Parkinson's disease (PD) is neurodegenerative syndrome, where progressive degeneration of the nigro-striatal dopaminergic pathway leads to motor disturbances. The mechanisms underlying the pathological changes in PD are not clearly understood yet. The current pharmacological treatment is used mainly for symptomatic control and provide short-term benefits. Therefore, it is highly relevant to investigate the therapy, which prevents cell death. Accumulating clinical evidences suggest that physical activity and exercise can generally slow down aging, prevent chronic disease and promote health.

The aim of the study was to examine the protective effects of physical exercise and particularly the role of its

timing with respect to neurotoxin treatment, on motor, behavioral, and neurochemical characteristics in chronic 1-methyl-4-phenyl-1,2,3,6-tetrahydropyridine(MPTP)-induced mouse model of Parkinson's disease. Mice were subdivided into four groups: (i) control, (ii) sedentary (non-exercising, with induction of PD), (iii) early trained PD mice (exercising before during and after the induction of PD), and (iv) late trained PD mice (start of exercising after the induction of PD). Motor performance was tested before and after induction of PD on Rotarod. Brains were collected for immunohistochemistry of tyrosine hydroxylase (TH), vesicular monoamine transporter 2 (VMAT-2), brain-derived neurotrophic factor (BDNF) and glial cell-derived neurotrophic factor (GDNF) in substantia nigra pars compacta (SNpc) and for Western Blot analysis to determine dopamine transporter (DAT) level in the striatum and TH level in the midbrain.

Early training started before the induction of PD protects from massive degeneration of SNpc dopaminergic neurons and not only maintains but even improves motor performance. Late training started after the induction of PD has very limited protective effect. It is possible that the physical activity can prevent the degeneration of dopaminergic neurons in SNpc by the activation of signaling pathways of neurotrophic factors, however their effectiveness may be limited once the damage has been incurred.

Supported by NCN grant 2011/01/D/NZ7/04405.

|B30|

Participation of pro- and antinociceptive interleukins in maraviroc analgesia in rat neuropathic pain model

Anna Piotrowska*, Klaudia Kwiatkowski, Ewelina Rojewska, Wioletta Makuch, Joanna Mika

Department of Pain Pharmacology, Institute of Pharmacology, Polish Academy of Sciences, Krakow, Poland

ania.piotrowska@uj.edu.pl

Neuropathic pain is caused by the nervous system damage. Treatment of neuropathic pain remains a challenge and requires combination therapy, because of not fully understood pathomechanism as well as many components involved in nociceptive transmission. Targeting chemokine signaling pathways is crucial in neuropathy development. The study examined the influence of CCR5 antagonist (maraviroc) on neuropathy development after chronic constriction injury of sciatic nerve in rats, and changes in pro- and antinociceptive interleukins. Research was carried out on Wistar rats implanted with intrathecal (i.t.) catheters. Neuropathic pain was developed using Bennett's model (CCI; chronic constriction injury to the sciatic nerve). Maraviroc (20 µg/5 µl) was dissolved in 12% DMSO and preemptively administered i.t. 16 h and 1 h before CCI and then once daily for 7 days. Two behavioral tests were conducted to measure allodynia (von Frey test) and hyperalgesia (cold plate test). Experiments were carried out according to IASP recommendations and were approved by the local Bioethics Committee. Behavioral studies have shown that chronic i.t. administration of maraviroc attenuated the allodynia and hyperalgesia on days 7 after CCI. Western blot results demonstrated down-regulation of pronociceptive interleukins: IL-1beta, IL-18, parallel to up-regulation of antinociceptive interleukins: IL-1RA, IL-18BP as measured on day 7 after chronic maraviroc administration. In summary, these results suggest that maraviroc reduces neuropathic pain by restoring the balance between pro- and antinociceptive interleukins. Our work provides the first evidence for its effect on interleukins. Maraviroc is especially promising because it is already used in human therapy; our results suggest that CCR5 is a potential novel target for neuropathic pain drug development. Acknowledgements: This study is supported by Institute of Pharmacology PAS statutory funds.

|B31|

The influence of 3D microenvironment and oxygen tension on WJ-MSC and HUCB-NSC fate decisions

Martyna Podobińska[1], Michał Piątek[1], Krystyna Pietrucha[2], Ashok Kumar[3], Anna Sarnowska[1], Leonora Buzanska[1]

[1]Mossakowski Medical Research Centre, Polish Academy of Sciences, Warsaw, Poland
[2]Lodz University of Technology, Lodz, Poland
[3]Indian Institute of Technology, Kanpur, India

mpodobinska@imdik.pan.pl

In this study the effect of 3D microenvironment and the oxygen tension on the growth, proliferation and differentiation of stem cells was investigated. The response to changing microenvironment of two different types of cells was compared: freshly isolated mesenchymal stem cells from Wharton jelly (WJ-MSC) and neurally-committed progenitor cells derived from umbilical cord blood (HUCB-NSC). Different biological three-dimensional (3D) scaffolds

were applied: (1) keratin based scaffolds; (2) a new family of scaffold consisting of two components: collagen (Col) and chondroitin sulphate (CS) and (3) electroconductive chitosan scaffold.

The analysis of settlement performed with scanning electron microscope revealed that both WJ-MSC and HUCB-NSC weakly adhere to keratin small rectangular fibers, but remained seated on the long hair-like fibers. The HUCB-NSC poorly adhere chitosan-based scaffolds, while WJ-MSC are present on the scaffold, but remain undifferentiated. We demonstrated that both cell types highly adhered and grow on Col-CS scaffolds. Moreover, Col-SC scaffolds did not affect the proliferation of the cells.

Immunohistochemical analysis revealed that HUCB-NSC growing on the surface of the Col-SC scaffolds had branched phenotype and expressed neuronal markers (β-Tubulin III, MAP2), while the cells that penetrated inside the scaffold remained rounded. Under the same conditions WJ -MSC penetrated inside the scaffold and proliferated (Ki67 positive cells), with no signs of differentiation.

The response to different oxygen concentration was cell type and developmental stage specific. The 5% O_2 level and Col-SC scaffolds prevent HUCB-NSC from further neuronal differentiation (lack of MAP2 expression). Moreover, only HUCB-NSC cultured on Col-SC scaffolds in 21% oxygen level expressed OLIG1 and OLIG2 genes (oligodendroglial differentiation).

On the other hand we have not observed the influence of oxygen level or 3D microenvironment on neural differentiation of WJ-MSC. However, 3D microenvironment promote CD 105 expression in WJ-MSC cultured in both tested oxygen concentrations.

We have demonstrated that geometry, structure and composition of the scaffold have an impact on cells adhesion, proliferation and differentiation, but the cellular response varies with the oxygen concentration and the type of investigated cells.

The work was supported by National Science Centre via Grant No 05728/B/NZ4/2011/01, Grant No DEC-2011/03/B/ST8/05867 and MMRC statutory funds.

|B32|

Possible involvement of kinin B1 receptor in the development of experimental autoimmune encephalomyelitis in rats

Karolina Podsiadło, Beata Dąbrowska-Bouta, Tomasz Grygorowicz, Lidia Strużyńska

Laboratory of Pathoneurochemistry, Department of Neurochemistry, Mossakowski Medical Research Centre, Polish Academy of Sciences, Warsaw, Poland

podsiadlokarolina@wp.pl

Introduction: Experimental autoimmune encephalomyelitis (EAE) is the most commonly used animal model of multiple sclerosis (MS). According to the previous studies mammalian central nervous system presents all components of the kallikrein-kinin system. The biological activity of kinin is mediated by two types of G protein-bound receptors – B1 and B2. It is believed that activation of B1R leads to the induction of inflammation by the release of pro-inflammatory cytokines and increased vascular permeability.Therefore, there are reasons to investigate the role of B1 receptor in the enhancement of the BBB permeability during development of EAE.

Methods: One group of female Lewis rats was immunized by intradermal injection of 100 µl inoculum containing homogenate of guinea pig spinal cord. The second group was injected i.p. with DALBK (B1R antagonist) after immunization. Control group was not immunized. Rats were monitored daily for clinical signs and loss of weight. Animals were sacrificed in different stages of the disease. Parts of brains were used for Western blotting analysis and measurement of inflammatory cytokines using RayBio Rat Cytokine Antibody Array (RayBiotech, Inc.). Immunohistochemical study on isolated fraction of microvessels was also performed.

Results: We noticed the increased level of B1R protein in rat brain in the symptomatic phase of EAE. Animals treated with DALBK exhibited improvement of neurological symptoms and decreased level of B1R protein in most cases. Using a confocal microscope, we observed lowered immunoreactivity of thight jounctions proteins (ZO-1, Occludin, Claudin 5) in microvessels' fraction obtained from EAE rats which increased after DALBK treatment. We also noticed changes in the level of astroglial markers (GFAP and AQP4) in both experimental groups. Preliminary analysis showed increased protein level of cytokines: IFN-γ, IL-1β, IL-6, TNF-α, VEGF in EAE animals which tends to decrease in DALBK-treated EAE animals in syptomathic phase of the disease.

Conclusion: Administration of kinin B1 receptor antagonist (DALBK) significantly improved the condition of animals by reducing the intensity of neurological symptoms and delaying the onset of the disease. Results show that B1R-mediated proinflammatory effect of kinins may be involved in pathomechanisms operating during the pre-onset phase of EAE which lead to the changes in the blood-brain barrier.

This work was supported by funds from KNOW 2013-2017 project.

|B33|

Effects of microglial cell polarization on nociception and morphine-analgesia – *in vivo* and *in vitro* studies

Katarzyna Popiołek-Barczyk*, Anna Piotrowska, Natalia Kołosowska, Ewelina Rojewska, Wioletta Makuch, Dominika Piłat, Agnieszka Jurga, Joanna Mika

Department of Pain Pharmacology, Institute of Pharmacology, Polish Academy of Sciences, Krakow, Poland

popiolek@if-pan.krakow.pl

Neuropathic pain is clinically challenging because it is resistant to alleviation by morphine. Glial activation and increased spinal pronociceptive factors strongly influence on neuronal transmission, therefore they are crucial in the development and maintenance of neuropathic pain. Microglial activation is a polarized process divided into potentially neuroprotective phenotype M2 and neurotoxic phenotype M1. Recent studies suggest that the microenvironment of the spinal cord after injury favors M1 polarization with only a transient appearance of M2 microglia/macrophages. We investigated the effect of parthenolide (PTL), an inhibitor of NF-κB, on the chronic constriction injury to the sciatic nerve (CCI)-induced neuropathy in rat. PTL (5 µg; i.t.) was preemptively and then daily administered for 7 days after CCI. The administration of PTL decreased allodynia and hyperalgesia and significantly potentiated morphine effects. We analyzed spinal changes in glial markers and M1 and M2 polarization factors, as well as intracellular signaling pathways. PTL increased the protein level of IBA1 (a microglial/macrophage marker) but did not change GFAP (an astrocyte marker) on day 7 after CCI. PTL reduced the protein level of M1 (IL-1β, IL-18, and iNOS) and enhanced M2 (IL-10, TIMP1) factors. In addition, it downregulated the phosphorylated form of NF-κB, p38MAPK, and ERK1/2 protein level and upregulated STAT3. In primary microglial cell culture we have shown that IL-1β, IL-18, iNOS, IL-6, IL-10, and TIMP1 are of microglial origin. Summing up, PTL attenuates neuropathy symptoms and promotes M2 microglia/macrophages polarization. Our result suggest that microglia-derived pronociceptive factors may influence on nociceptive transmission and morphine analgesia, therefore neuropathic pain therapies should be shifted from neurotoxic phenotype M1 to neuroprotective phenotype M2.

Grants NCN 2012/07/N/NZ3/00379, KNOW and statutory funds.

|B34|

The study of influence of minocycline on Botulinum toxin A on pro- and antinociceptive interleukins under neuropathic pain

Ewelina Rojewska[1], Magdalena Zychowska[1], Wioletta Makuch[1], Sara Marinelli[2], Siro Luvisetto[2], Flaminia Pavone[2], Barbara Przewlocka[1], Joanna Mika[1]

[1]Department of Pain Pharmacology, Institute of Pharmacology, PAS, Krakow, Poland
[2]CNR, Institute of Cell Biology And Neurobiology- IRCCS, Santa Lucia Foundation, Roma, Italy

rojewska@if-pan.krakow.pl

Neuropathic pain are some of the pathological states that have been recently treated with BoNTs with beneficial effects. The main target of BoNT/A action induce SNAP-25 cleavage and prevention of neurotransmitter release. The main target of minocycline is p38MAPK and MMP-9. Both of substance shows antinociceptive effect in neuropathic pain, however their influence on some pro- and antinociceptive cytokines remain to be clarified. The aim of the present study was to demonstrate the effects of intraperitoneal chronic minocycline administration and at day 5 intraplantar (i.pl.; 75 pg/paw) BoNT/A administration on pain behavior and CCI-induced changes on cytokines protein level in the DRG and spinal cord. Chronic constriction injury (CCI) of the sciatic nerve was performed according to Bennett and Xie (1988) were conducted to measure hyperalgesia (cold plate test). The experiments were carried out according to IASP rules. To study a potential role of neuroimmunological factors under neuropathy we studied in the lumbar spinal cords and DRG the IL-6, IL-10, IL-1beta and

IL-1RA protein levels using Western blot method. A single intraplantar BoNT/A injection similar to minocycline chronic administration (30 mg/kg) induced antinociception. The analgesic effect of BoNT/A was potentiated by minocycline. Our results suggest that CCI-induced upregulated the protein level IL-6 and IL-1beta in ipsilateral spinal cord. In DRG we observed increase the protein level of IL-6 and IL-1beta. After BoNT/A injection in the ipsilateral spinal cords of CCI-exposed rats, the protein level of IL-6, IL-10, IL-1beta and IL-1RA were not changes, but in the DRG BoNT/A enhance the protein level of antinociceptive factors (IL-10 and IL-1RA).Interestingly, minocycline diminished the protein levels of pro-nociceptive factor (IL-1beta) in the spinal cord and/or DRG. Our results show that BoNT/A significantly attenuates pain-related behaviors and enhance the level of some antinociceptive factors. Moreover, the minocycline enhance BoNT/A analgesic effects. The modulation of neuroimmune interactions by BoNT/A and minocycline can have some clinical implication in future. Acknowledgments: This work was supported by the National Science Centre, Poland, Harmonia 5 2013/10/M/NZ4/00261. Rojewska have a scholarship from the START sponsored by the Foundation of Polish Science, Poland. Zychowska is scholarship holder from the KNOW sponsored by Ministry of Science and Higher Education, Poland.

|B35|

Neuroprotective action of 3,3'-diindolylmethane on hippocampal cells exposed to ischemia involves inhibition of caspases and p38 stress-activated protein kinase

Joanna Rzemieniec, Ewa Litwa, Agnieszka Wnuk, Małgorzata Kajta, Władysław Lasoń

Institute of Pharmacology Polish Academy of Sciences, Department of Experimental Neuroendocrinology, Krakow, Poland

rzemien@if-pan.krakow.pl

Stroke is the fourth-leading cause of death and the primary cause of long-term disability worldwide. Ischemic insult triggers apoptosis regulated by activation of caspase cascade, which depends either upon the interaction of a death receptor with its ligand and subsequent activation of procaspase-8 or on the participation of mitochondria and the activation of procaspase-9. Our previous study demonstrated that stimulation of aryl hydrocarbon receptor (AhR) leads to caspase-3-dependent apoptosis of neuronal cells [1]. Apart from caspases, important regulators of neuronal apoptosis are also MAP kinases, p38/MAPK and JNK. Selective AhR modulators (SAhRMs) are class of compounds that act as AhR agonist or antagonist in a tissue-specific manner. Among the ligands that exhibit properties of SAhRMs is 3,3'-diindolylmethane (DIM). Recent data have shown neuroprotective potential of DIM against brain inflammation and Parkinson's disease [2,3]. However, there are no data concerning the protective capacity and mechanisms of DIM action in neuronal cells exposed to ischemia. The aim of the present study was to investigate the neuroprotective potential of DIM against the ischemia-induced damage with a special focus on caspases and p38 stress-activated protein kinase. In our study ischemic conditions were evoked by exposure of primary hippocampal cell cultures to oxygen and glucose deprivation. DIM and specific inhibitors of caspases-8,-9 and p38/MAPK kinase were added to the medium just prior to ischemia. We have shown that ischemia increased the lactate dehydrogenase release (LDH) and caspase-3 activity, whereas DIM (0.1-10 μM) inhibited these parameters in tissue-dependent manner. Inhibition of p38/MAPK kinase and caspase-8, but not caspase-9, intensified the neuroprotective effect of DIM. These preliminary data indicate strong neuroprotective potential of DIM against ischemia. They also suggest that mechanism of its anti-ischemic action could be mediated not only by targeting caspases but also by inhibition of stress-activated protein kinases.

References

1. Kajta M, Litwa E, Rzemieniec J, Wnuk A et al. (2014) Mol Cell Endocrinol. 392: 90-105.
2. Carbone DL, Popichak KA, Moreno JA et.al (2009) Mol Pharmacol. 75: 35-43.
3. De Miranda BR, Popichak KA, Hammond SL et.al (2015) Toxicol Sci. 143:360-73.

Joanna Rzemieniec and Agnieszka Wnuk are holder of scholarship from the KNOW sponsored by Ministry of Science and Higher Education, Poland.

|B36|

Vasculoprotective effect of WJ-derived MSC and EPC-like culture on post-ischemic organotypic hippocampal slices

Patrycja Siedlecka*, Anna Sarnowska, Lukasz Strojek, Krystyna Domanska-Janik

Stem Cell Bioengineering Unit, Mossakowski Medical Research Centre, Polish Academy of Sciences, Warsaw, Poland

patrycja.siedlecka@gmail.com

The aim of study was to evaluate ability of mesenchymal stem cells derived from human Wharton jelly (WJ-MSC) to differentiate into endothelial progenitor cells (WJ-EPC) and then support vascular network and cell survival in rat hippocampal organotypic culture (OHC) model of ischemic injury.

WJ-MSC were cultured in growth medium (MSCGM) or in endothelial differentiating medium (EGM-2). Cells were characterized by flow cytometry, immunocytochemistry and molecular methods on the basis of expression of endothelial and mesenchymal markers. The functional behavior of WJ-EPC was tested by DiI-Ac-LDL-uptake and Matrigel assay. Priming of WJ-MSC/EPC was performed by incubation with LPS and/or poly(I:C) to stimulate TL ¾ receptors. After 5 div the hippocampal slices undergo oxygen-glucose deprivation (OGD). Next, WJ-MSC or WJ-EPC were co-cultured with intact or post-ischemic OHC. Supporting effect of WJ-MSC and WJ-EPC supplementation on vascular network was evaluated with rat EC-specific antibody (RECA-1). The cell survival was measured by propidium iodide (IP) staining. Concentration of secreted human MSC-derived cytokines into culture medium was estimated by the BD CBA assays system.

Our results showed that WJ-MSC after 7 days of differentiation acquired typical for EPC cobblestone morphology, were able to form capillary-like structures and to took up DiI-Ac-LDL. Both cell types were positive for MSC and EC markers CD73, CD90, CD105, VEGFR2, VEGF, but only EPC-like cells expressed vWF and CD31 antigens. Moreover, indirect co-culture of WJ-derived MSC or EPC with OGD-OHC inhibited cell death and blood vessel atrophy in hypoxia-sensitive CA1 hippocampal region. These results suggest involvement of paracrine-related mechanism of MSC/EPC vasculoprotection in post-ischemic OHC injury.

Looking for putative mechanism of the MSC/EPC protection, the concentration of several human cytokines like TGF-β1, IL-6 and IL-1β was estimated in OHC co-culture media. Their secretion were found significantly higher under WJ-EPC co-culture except of VEGF growth factor released equally high in both, WJ-MSC/EPC cases. However, release of these cytokines remained stable independently from Toll-like receptor stimulation by LPS or Poli(I:C) in all investigated agonists concentration. Thus, in the next step we will estimate expression level of TLR ¾ genes in the WJ-derived MSC/EPC cultures.

The work was supported by NCN grant 2011/01/B/NZ3/05401 and NCRD grant Strategmed 1/234261/2/NCBR/2014.

|B37|

The impact of di-(2-ethylhexyl) phthalate (DEHP) on PPAR-gamma, MMP-2 and MMP-9 expression in mouse astrocytes and cortical neurons *in vitro*

Agnieszka M. Sitarz[1]*, Konrad A. Szychowski[1,2], Anna K. Wójtowicz[1]

[1]Department of Animal Biotechnology, Animal Sciences Faculty, University of Agriculture, Kraków, Poland
[2]Department of Public Health, Dietetics and Lifestyle Disorders, Faculty of Medicine, University of Information Technology and Management in Rzeszów, Tyczyn, Poland

ag.sitarz@gmail.com

Di-(2-ethylhexyl) phthalate (DEHP) is the most frequently used plasticizer of polyvinyl chloride (PVC) products such as food packaging, cosmetics, building materials, clothing, toys and medical devices. DEHP is not chemically bound to plastic polymer, therefore it is continuously released into environment through manufacturing, processing and disposal. Epidemiologic data showing the impact of DEHP on the development of psychiatric disorders in children such as Attention Deficit Hyperactivity Disorder (ADHD) and autism have been published. Several phthalates, have been reported to cause their toxicity via peroxisome proliferator-activated receptor gamma (PPAR gamma) in liver and testis. PPAR gamma is widely expressed in brain, where it has a crucial role in the regulation of nervous cell proliferation, differentiation and apoptosis. Therefore, the elucidation of the involvement of this receptor in phthalates actions in neuronal cells is necessary. Matrix metalloproteinases-2 and -9 (MMP-2 and MMP-9) actions are important in developing and adult nervous system and their potential to improve repair or regeneration after nervous system injury is well known. It is, however, unclear how MMPs are involved in DEHP

action and whether PPARγ regulates the function of these enzymes in the brain.

The aim of this research was to investigated the impact of DEHP on expression of PPAR-gamma and MMP-2 and MMP-9 in mouse neocortical astrocytes and neurons in vitro. The primary cultures were prepared from Swiss mouse embryos on 15/16 days of gestation. Phenol red-free DMEM/F12 medium supplemented with glutamine and 10% FBS was used for astrocytes and phenol red-free Neurobasal medium supplemented with glutamine and B27 was used for neurons. The cells were cultured in the presence of 10 μM concentration of DEHP for 1, 3, 6, 24 and 48 h. Afterwards, the cells have been lysed and the protein concentration has been determined. The expression of PPAR-gamma, MMP-2 and MMP-9 has been assessed by Western blot analysis.

The results showed that the effect of DEHP was depend on cell type. In astrocytes, PPAR-gamma and MMP-2 expression was increased while MMP-9 expression was decreased. In neurons, PPAR-gamma and MMP-2 expression decreased with a simultaneous increase in MMP-9 expression.

To sum up, DEHP mechanism of action might involve the PPAR-gamma receptors and therefore modulate the expression of matrix metalloproteinases.

Support by NCN grant 2012/07/B/NZ4/00238.

|B38|

Changes of glutathione homoeostasis in rat brain during subchronic oral exposure to silver nanoparticles or silver ions

Joanna Skalska[1]*, Małgorzata Frontczak-Baniewicz[2], Aleksandra Lenkiewicz[1], Lidia Strużyńska[1]

[1]Laboratory of Pathoneurochemistry, Department of Neurochemistry
[2]Electron Microscopy Platform, Mossakowski Medical Research Centre Polish Academy of Sciences, Warsaw, Poland

jskalska@imdik.pan.pl

Despite the developmental potential of silver nanoparticles (AgNPs) in many fields of nanotechnology, there is a concern about possible negative influence of nanosilver on the environment, organisms and human health.

The selected studies on biodistribution show the accumulation of AgNPs in mammalian brain. Moreover, neurotoxic effects of silver nanoparticles has been confirmed in both in vitro and in vivo studies. There is also evidence that AgNPs can cause oxidative stress. However, the mechanisms of their toxicity have not been fully understood.

The aim of this study was to examine the effect of subchronic oral exposure of rats to citrate-stabilized AgNPs (10 ± 4 nm in diameter) or silver ions on glutathione homoeostasis.

Solutions of AgNPs or silver citrate were administered to male Wistar rats (180-210 g) via the gastric tube at a dose of 0.2 mg AgNPs or Ag(I)/kg b.w. per day for 14 days. The control group received the saline. Animals were sacrificed 24 h after last exposure and brain was collected for further studies. We confirmed the presence of silver nanoparticles in brains of exposed rats using TEM method.

The level of total glutathione did not change after exposure to both forms of silver, whereas the ratio of reduced to oxidized glutathione decreased in AgNPs- or silver ions-exposed rats in comparison to control group. Moreover, the statistically significant changes in glutathione peroxidase and glutathione reductase activities were observed.

The results of the present study showed that AgNPs and silver ions are able to induce a pro-oxidative environment inside the cells influencing the cellular glutathione system.

|B39|

The k-nn and roc estimation of significance of some matrix metalloproteinases as markers in als and edmd patients

Beata Sokołowska[1]*, Irena M. Niebroj-Dobosz[2], Marta Hallay-Suszek[3], Agnieszka Madej-Pilarczyk[2], Michał Marchel[4], Piotr Janik[5], Adam Jóźwik[6,7], Irena Hausmanowa-Petrusewicz[2†]

[1]Bioinformatics Laboratory, Mossakowski Medical Research Center, Polish Academy of Sciences, Warsaw, Poland
[2]Neuromuscular Unit, Mossakowski Medical Research Center, Polish Academy of Sciences, Warsaw, Poland
[3]Interdisciplinary Center for Mathematics and Computational Modelling, University of Warsaw, Poland
[4]Department of Cardiology, Medical University of Warsaw, Warsaw, Poland
[5]Department of Neurology, Medical University of Warsaw, Warsaw, Poland
[6]Institute of Biocybernetics and Biomedical Engineering, Polish Academy of Science, Warsaw, Poland
[7]Faculty of Physics and Applied Informatics, Łódź University, Łódź, Poland

beta.sokolowska@imdik.pan.pl

New statistical estimations of the significance of several matrix metalloproteinases (MMPs) in two neuromuscular diseases such as amyotrophic lateral sclerosis (ALS) and Emery-Dreifuss muscular dystrophy (EDMD) were used.

The ALS is a serious fatal progressive neurodegenerative disorder, the EDMD is a rare genetic disease manifested as skeletal muscle atrophy, dilated cardiomyopathy and often sudden death.

MMPs are recognized as taking part in many neurological diseases and may have diagnostic or prognostic significance. The altered levels of some MMPs are observed in ALS and EDMD patients [1,2]. Significance of serum MMPs such as membrane type matrix metalloproteinase-1 (MT1-MMP), gelatinases A (MMP-2) and B (MMP-9) are estimated as potential marker(s). The k-Nearest Neighbors (k-NN) classifier (the pattern recognition algorithm) with the ROC (Receiver-Operating Characteristic) curve analysis and the correlation matrixes was applied for differentiation between: (a) ALS patients with mild and severe symptoms and (b) AD- and X-EDMD patients based on set of the MMPs.

Our previous [3,4] and current results indicate that MMP-2 is effective as the biomarker in evaluation of ALS progression, MT1-MMP as the best of the MMPs as the biomarker in the recognition both AD- and X-EDMD forms.

In conclusion, a set of selected MMPs are helpful to recognize the ALS progression and the both EDMD forms in the proposed computer statistical-analytical approach.

References

1. Niebroj-Dobosz I, Madej-Pilarczyk A, Marchel M, Sokołowska B, Hausmanowa-Petrusewicz I: Matrix metalloproteinases in serum of Emery-Dreifuss muscular dystrophy patients. Acta Biochimica Polonica 2009, 56 (4): 717-722.
2. Niebroj-Dobosz I, Janik P, Sokołowska B, Kwieciński H: Matrix metalloproteinases and their tissue inhibitors in serum and cerebrospinal fluid of patients with amyotrophic lateral sclerosis. European Journal of Neurology 2010, 17; 226-231.
3. Sokołowska B, Jóźwik A, Niebroj-Dobosz I, Janik P, Kwieciński H: Evaluation of matrix metalloproteinases in serum of patients with amyotrophic lateral sclerosis with pattern recognition methods. Journal of Physiology and Pharmacology 2009, 60 (Suppl.5), 117-120.
4. Sokołowska B, Jóźwik A, Niebroj-Dobosz IM, Hausmanowa-Petrusewicz I: A pattern recognition approach to Emery-Dreifuss muscular dystrophy (EDMD) study. Journal of Medical Informatics & Technologies 2014, 23: 165-171.

|B40|

Opioid agonist-neurokinin 1 antagonist designed multiple ligands alleviate both acute and neuropathic pain in rats

Joanna Starnowska[1], Wioletta Makuch[1], Cecilia Betti[2], Lukasz Frankiewicz[2], Alexandre Novoa[2], Dirk Tourwé[2], Steven Ballet[2], Joanna Mika[1], Barbara Przewlocka[1]

[1]Department of Pain Pharmacology, Institute of Pharmacology, Krakow, Poland
[2]Department of Organic Chemistry, Vrije Universiteit Brussel, Brussels, Belgium

joanna.starnowska@gmail.com

Prolonged opioid administration (e.g. morphine) under neuropathic pain conditions (caused by nerve tissue damage) leads to changes in activity of endogenous nociceptive systems: increased release of pronociceptive substance P, together with up-regulation of its corresponding neurokinin 1 (NK-1) receptors, are associated with development of analgesic tolerance and opioid-induced hypersensitivity to painful stimuli. It is assumed that counteracting pronociceptive activity of this biochemical route with NK-1 receptor antagonists may improve opioids' effectiveness in neuropathic pain. In this study, the antinociceptive activity of novel hybrid opioid-NK1 peptidomimetics was evaluated in Wistar rats in acute pain (measured by tail-flick test) and neuropathic pain in chronic constriction injury (CCI) model on seventh day after injury. All results were compared to the analgesic potency of morphine and 'parent' compound containing only NK-1 pharmacophore. It was determined that hybrids provide dual alleviation of acute and neuropathic pain, providing the effect comparable to morphine, but in 3.5 to 4.5-fold lower doses, and are more efficient than morphine in attenuating hyperalgesia (measured by cold plate test) in CCI rats. NK-1 antagonist brought hardly any analgesic response in acute pain test, but proved to be very potent in diminishing allodynia and hyperalgesia in neuropathic rats. This may prove that NK-1 system is pivotal for pronociceptive signaling in neuropathy. Tolerance to analgesic effect of all compounds occurred at sixth day of daily intrathecal administration in CCI rats (the effect of hybrids was similar to the long-term profile of morphine administration), but there was no cross-tolerance between morphine and one of the hybrids. This proves that high antinociceptive effects of morphine and hybrid ligand may be reinstated during prolonged therapy. As a whole, these results give a promising outlook for using opioid-NK1 hybrids as a complementary treatment to pure opioid therapy in neuropathic pain states.

The work of JS, WM, JM and BP was supported by a MAESTRO NCN2012/06/A/NZ4/00028;statutory funds; J. Starnowska is a holder of KNOW scholarship sponsored by Ministry of Science and Higher Education, Poland. The work of CB, SB, DT was supported by a collaboration convention between the Ministère du Développement Economique, de l'Innovation et de l'Exportation du Québec and the Research Foundation – Flanders (FWO Vlaanderen).

|B41|

Impact of triclosan on cyp1a1 and cyp1b1 expression and activity in mouse neocortical neurons

Konrad A. Szychowski[1,2]*, Agnieszka Wnuk[3], Małgorzata Kajta[3], Anna K. Wójtowicz[1]

[1]Department of Animal Biotechnology, Agricultural University in Krakow, Krakow, Poland
[2]Department of Public Health, Dietetics and Lifestyle Disorders, Faculty of Medicine, University of Information Technology and Management in Rzeszow, Tyczyn, Poland
[3]Department of Experimental Neuroendocrinology, Institute of Pharmacology, Polish Academy of Sciences, Krakow, Poland
konrad.szychowski@gmail.com

Triclosan (TCS) is an antimicrobial agent used extensively in personal care and sanitizing products such as soaps, toothpastes, and hair products. TCS has been incorporated into growing number of medical products as well as in household items such as plastic cutting boards, sport equipment, textiles and furniture. A number of studies has shown presence of TCS in different human tissues such as blood, adipose tissue, liver, brain and in breast milk and urine. It is well known that TCS has a similar chemical structure to dioxin and in the presence of sunlight might be transformed to produce up to four dioxin compounds. Cytochromes CYP1A1 and CYP1B1 are involved in the metabolism of many endogenous compounds such as cholesterol, steroids hormones well as environmental xenobiotics especially dioxin. Interestingly, it has been well proven that some xenobiotics can inhibit activity of many metabolizing enzymes such as CYP1A1, CYP1B1 or UDP-glucuronosyltransferase.

The aim of the present study was to investigate the impact of TCS on the expression and activity of cytochrome CYP1A1 and CYP1B1 in mouse neocortical neurons.

The cultures of the neocortical neurons were prepared from Swiss mouse embryos on 15/16 day of gestation. The cells were cultured in phenol red-free Neurobasal medium with B27 and glutamine. After 7 days of culture in vitro, neurons were exposed to 10 μM of TCS. After 3 and 6 h, expression of mRNA CYP1A1 and CYP1B1 was measured. Additionally after 48 h of exposure protein expression of both enzymes and activity of CYP1A1 was measured.

Our preliminary data demonstrated that in the presence of 10 μM of TCS, mRNA expression of CYP1A1 and CYP1B1 was decreased. However, protein expression of CYP1A1 and CYP1B1 increased significantly. Moreover, TCS exhibited ability to inhibit activity of CYP1A1.

In summary, the presented study demonstrated that CYP1A1 and CYP1B1 are involved in TCS mechanism of action. Moreover, since the TCS inhibits activity of CYP1A1, it might also affect metabolism of other compounds.

Support by NCN grant 2014/13/N/NZ4/04809.

|B42|

Amyloid beta and its role in regulation of gene expression for APP cleaving enzymes. Implication in Alzheimer's pathology

Przemysław Wencel*, Robert P. Strosznajder

Laboratory of Preclinical Research and Environmental Agents, Department of Neurosurgery, Mossakowski Medical Research Centre, Polish Academy of Sciences, Warsaw, Poland
pwencel@imdik.pan.pl

Amyloid precursor protein (APP) is a membrane protein that plays an essential role in regulation of synapse formation, neuronal growth and repair. APP is metabolized by secretase β and secretase γ which lead to amyloid-β peptides (Aβ) release. Excessive Aβ production and oligomerization play a key role in oxidative stress and cells death in Alzheimer's disease (AD). Moreover, alteration of presynaptic protein alpha synuclein (ASN) is involved in the pathology of AD. Oxidative stress influences two NAD dependent enzymes families: sirtuins (SIRTs) and poly(ADP-ribose) polymerases (PARPs) which are involved in the regulation of energy metabolism, transcription, and DNA repair. SIRTs (3,4,5) located in mitochondria regulate antioxidative enzymes and electron transport proteins. SIRTs and PARPs are responsible for DNA repair, however, under massive stress PARP1 can be over activated and may lead to NAD+ depletion and cells death.

The aim of our study was to determine changes in gene expression profile of enzymes involved in non amyloidogenic and amyloidogenic pathways of APP metabo-

lism in PC12 cells after Aβ42 treatment. Moreover, transcription of mitochondria SIRTSs and DNA bound PARPs was determined and their functional role in cell death/survival was evaluated.

Rat pheochromocytoma (PC12) cells were treated for 24h with Aβ 1-42 in oligomeric/monomeric form at 1μM. Moreover, the effect of endogenously liberated Aβ in PC12 cells transfected with human gene for APP wild type (APPwt) and bearing Swedish mutation (APPsw) was investigated. Our results show that Aβ42 reduces viability of PC12 cells by 60% and inhibits gene expression of α-secretase responsible for nonamyloidogenic APP metabolism. Concomitantly Aβ peptide enhances expression for β and γ secretases, the enzymes which lead to Aβ release. Increased expression for β- and γ-secretase was also observed in the APP wt cells. ASN (0.5 μM) induces also similar effect on transcription of APP cleaving enzymes. Moreover, Aβ peptides modulate gene expression for PARPs (1,2,3) and mitochondria SIRTs.

These results indicate the crucial role of Aβ peptides and ASN in regulation of APP metabolizing enzymes and suggest that ASN through alterations of APP processing may enhance Aβ toxicity. Moreover, interactions between NAD dependent enzymes may play important role in regulation of metabolism and cell fate under Aβ toxicity.

Supported by NCN grant 2013/09/B/NZ3/01350.

|B43|

Pathomechanism of multiple sclerosis and polymorphism of osteopontin gene

Mieczyslaw Wender[2]*, Justyna Biernacka-Lukanty[1,3], Slawomir Michalak[2,3], Beata Raczak[3], Wojciech Kozubski[3], Dariusz Urbanski[4], Grazyna Michalowska-Wender[1,2,3]

[1]Laboratory of Neurogenetics, Department of Neurology, Medical University of Poznan, Poznan, Poland
[2]Neuroimmunological Unit, Mossakowski Medical Research Centre, Polish Academy of Sciences, Poznan, Poland
[3]Department of Neurology, Poznan University of Medical Sciences, Poznan, Poland
[4]Neuropsychiatric Hospital, Kościan, Poland
mwender@ump.edu.pl

Osteopontin (OPN) is one of the key cytokines involved in T-cell activation in multiple sclerosis (MS). The OPN gene is therefore recognized as an early T-cell activation gene, which underlies immunological events involved in the aetiopathogenesis of MS. In an earlier study, we found OPN to be a useful marker to differentiate between malignant and benign ovarian tumours. In patients with optic neuritis, cerebrospinal fluid (CSF) OPN levels have been shown to be correlated with CSF chitinase-3-like protein 1, myelin basic protein, and neurofilament, light polypeptide. OPN also enhances the production of interleukin 12 and interferon gamma, and reduce interleukin 10. Moreover, OPN is expressed in MS plaques in the central nervous system.

Disability in 100 MS patients was evaluated using the expanded disability status scale (EDSS). Genotype and allele frequencies at exons 6 and 7 were examined by PCR. Using appropriate statistical tests, the distribution of variables was tested and means ± SD compared.

Genotype distribution and allele frequency differences between patients and control individuals were not statistically significant. No association of OPN with susceptibility to MS was found in the Polish population. The EDSS score was higher in 8090 T/T + 9250 C/C patients than in 8090 C/C + 9250 C/C MS patients (p = 0.0120), and the disability in 8090 C/C + 9250 C/T MS patients was higher than in 8090 C/C + 9250 C/C MS patients (p = 0.0137). Logistic regression analysis revealed age to be an independent factor influencing disability.

The polymorphism of OPN gene in positions 8090 T/T + 9250 C/C, 8090 C/C + 9250 C/T, and 8090 C/T + 9250 C/T were linked with relatively higher levels of disability in MS patients.

|B44|

Apoptotic and toxic effects of benzophenone-3 (BP-3) in mouse embryonic neuronal cells

Agnieszka Wnuk*, Joanna Rzemieniec, Ewa Litwa, Małgorzata Kajta

Department of Experimental Neuroendocrinology, Institute of Pharmacology, Polish Academy of Sciences, Krakow, Poland
wnuk@if-pan.krakow.pl

Benzophenone-3 (BP-3) is a commonly used chemical sunscreen agent, absorbing radiation in the range of UVB and UVA. The industrial use of BP-3 has been increasing over the past decade. Since UV filters are photostable and often lipophilic, they are persistent in the environment. Humans can be exposed to UV screens by dermal absorption or through the food chain. The most disturbing seems to be the fact that breastfed babies are exposed to BP-3.

Certain UV-filters (e.g. BP-3, BP-2, 4-MBC) were present in 85% of Swiss human milk samples (Schlumpf *et al*., 2010). There is no data that BP-3 crosses blood-placenta barrier, but bisphenol A which has similar structure to BP-3 has been found to pass this barrier. One may assume that chemicals like BP-3 also are able to enter the embryo/fetus and cause deleterious effects on prenatal development. Insufficient data (*in vitro* or *in vivo*) related to the possible impact of BP-3 on the nervous system both in terms of neurodevelopment and neurodegeneration processes confirm the relevance of presented report.

Our study demonstrated that BP-3 activated caspase-3 in the mouse neuronal cell cultures, which was found within 6 hours after the treatment and accompanied by significant increase in lactate dehydrogenase-release (LDH) at 6 and 24 h of experiment. These effects were observed in neocortical and hippocampal cells, however, hippocampal cells were less vulnerable to BP-3 than neocortical. Therefore, the use of neocortical and hippocampal embryonic cells allowed us to demonstrate neurodevelopmental and brain tissue-specific patterns of response to BP-3. These biochemical data were supported by increased apoptotic body formation and impaired cell survival, evidenced by Hoechst 33342 and calcein AM staining.

These data point to apoptotic and neurotoxic capacity of BP-3 that position this UV filter as a compound that may increase risk of developmental abnormalities.

This study was supported by the Polish National Center of Science grant No. 2014/13/N/NZ4/04845 and the statutory fund of the Institute of Pharmacology Polish Academy of Sciences, Krakow, Poland.

Agnieszka Wnuk and Joanna Rzemieniec are holders of scholarship from the KNOW sponsored by Ministry of Science and Higher Education, Republic of Poland.

|B45|

Cardiorespiratory activity of PK20, a potent anti-inflammatory and antinociceptive hybrid peptide

Piotr Wojciechowski[1]*, Patrycja Kleczkowska[2], Katarzyna Kaczyńska[1]

[1]Laboratory of Respiration Physiology, Mossakowski Medical Research Centre, Polish Academy of Sciences, Warsaw, Poland
[2]Department of Pharmacodynamics, Centre for Preclinical Research and Technology, Medical University of Warsaw, Warsaw, Poland

pwojciechowski@imdik.pan.pl

Objectives: PK20, chimeric peptide characterized by having in its structure an opioid and neurotensin pharmacophores has been demonstrated to induce anti-inflammatory activity in our in vivo studies and dose-dependent prolonged analgesic response in animal pain model (Kleczkowska *et al*., 2010). We have shown that local application of the PK20 in cream in a dose dependent fashion reduced oedema in mice ears with induced contact sensitivity response. In the present study we would like to investigate whether our new promising compound – PK20 exerts any unfavourable cardiovascular and/or respiratory action in experimental animals after intravenous injection.

Methods and results: Anaesthetized, spontaneously breathing rats were used. Tidal volume was measured at tracheostomy. The timing components of the breathing pattern, arterial blood pressure, and heart rate were recorded. Intravenous administration of PK20 in the neurally intact rats evoked a dose-dependent apnoea followed by short-lived insignificant increase in tidal volume and breathing rate, which resulted in ephemeral increase in minute ventilation. The blood pressure changes were biphasic: transient increase was replaced by prolonged hypotension. Midcervical vagotomy did not influence blood pressure response but abrogated post-PK20 respiratory effects including an arrest of breathing. Respiratory changes were substantially reduced by blockade of both: NTS1 and mu-opioid receptors, while hypotension was eliminated after neurotensin NTS1 receptors.

Conclusions: The respiratory changes triggered by chimeric PK20 seem to be resultant of simultaneous excitation of both opioid and neurotensin receptors of the vagus nerve. Hypotension is mediated beyond the vagi via activation central and peripheral neurotensin NTS1 receptors. This chimeric peptide should be used with care via intravenous administration in anaesthetized animals since in high doses PK20 may evoke respiratory apnoea and hypo-

tension. Nevertheless, applied locally or intraperitoneally in conscious mice induced no adverse effects.

The study was supported by a grant from National Science Centre, Poland, 2014/13/B/NZ7/02247.

|B46|

Comparison between enzymatic and nephelometric serum ceruloplasmin assays in the diagnosis of Wilson's disease

Mariola Wolanin[1]*, Bożena Kłysz[1], Tomasz Litwin[1], Iwona Kurkowska-Jastrzębska[1], Grażyna Gromadzka[1], Grażyna Sygitowicz[3], Anna Członkowska[1,2]

[1]Institute of Psychiatry and Neurology, II Department of Neurology, Warsaw, Poland
[2]Medical University of Warsaw, Department of Experimental and Clinical Pharmacology, Warsaw, Poland
[3]Department of Biochemistry and Clinical Chemistry, Medical University of Warsaw, Warsaw, Poland
mariolawolanin@wp.pl

Wilson's disease (WD) is a rare autosomal recessive copper metabolism disorder due to inappropriate incorporation of copper into ceruloplasmin.

Ceruloplasmin binds about 90-95% of copper in the blood and protects cells against free radical injury. Many studies have shown that decreased levels (< 25 mg/dl) of ceruloplasmin besides WD occurs in Alzheimer's disease, Parkinson's disease and aceruloplasminemia. Assesement of activity of ceruloplasmin is a very important test in diagnosis of WD. The measurement of ceruloplasmin value is generally carried out by one of different analytical methods: manual - enzymatic and automated - nephelometric. The enzymatic assay measures active form of ceruloplasmin (Cu-containing). Nephelometric method measures non active ceruloplasmin and Cu-containing (active) form of ceruloplasmin. Nephelometric method is now widely used due to its simplicity.

In this study was tested discrepancy between the nephelometric and enzymatic measurements of ceruloplasmin concentration on four groups: non treatment WD (n = 38), treatment WD (n = 40), heterozygous carriers (n = 93) and healthy individuals (n = 183) (Wilcoxon's matched pairs test). Differences between groups on each methods was examined by Mann-Whitney U test. Based on the ROC curve (Receiver Operating Characteristics) was specified diagnostic accuracy (sensitivity, specificity, positive predictive value – PPV, negative predictive value – NPV) of the enzymatic and the nephelometric method.

Enzymatic measurements of ceruloplasmin was statistically significantly lower than nephelometric on three groups: non-treatment WD (14.9 mg/dl vs. 16.6 mg/dl), treatment WD (5.1 mg/dl vs. 7.1 mg/dl) and heterozygous carriers (30.6 mg/dl vs. 32.3 mg/dl). In healthy persons group enzymatic measurements was higher than nephelometric (33.4 mg/dl vs. 29.1 mg/dl). Statistically significant divergences was observed between groups by enzymatic and nephelometric assays. Interesting marked decrease of ceruloplasmin was observed in WD group treated by anti-copper drugs. Enzymatic method has better diagnostic accuracy in WD than nephelometric method – higher sensitivity (100% vs. 86.8%), PPV (1 vs. 0.86) and area under ROC curve (0.986 vs. 0.957) and should be recommended to diagnosis and monitoring WD.

|B47|

Effect of telmisartan on kynurenic acid production in rat brain cortex

Izabela Zakrocka*, Waldemar A. Turski, Tomasz Kocki

Department of Experimental and Clinical Pharmacology, Medical University of Lublin, Collegium Pathologicum, Lublin, Poland
izabela.zakrocka@umlub.pl

A renin-angiotensin-aldosterone system (RAAS) is one of the regulators of water – electrolyte metabolism. It is thought to control not only the thirst, blood vessels tone, vasopressin release, but it is responsible for thermoregulation, learning, memory, emotions, reproduction and sexual behaviors as well. Among angiotensin receptors, the most prominent role in pharmacotherapy possesses receptor type 1 (AT-1). It was reported that RAAS in the brain may have important role in animal seizure models or in the development of neurodegenerative disorders.

Kynurenic acid (KYNA) is an endogenous antagonist of glutamate receptors and of α7 nicotinic receptors.

The cerebral synthesis of KYNA from its precursor L-kynurenine (L-KYN) is catalyzed by kynurenine aminotransferases (KAT), from which the most important are KAT I and KAT II. The disturbances of KYNA production have been linked to the neurodegenerative diseases and epilepsy. Recent experimental data indicated that KYNA could play a role in the central blood pressure control.

In this study the influence of telmisartan, an AT1 – receptor antagonist, on brain KYNA production was investigated.

In cortical slices telmisartan at the concentration of 0.01; 0.1 and 0.5 mM decreased KYNA synthesis to 72% (p < 0.05); 65% (p < 0.05) and 54% (p < 0.05) of control,

respectively. The activity of KAT I was decreased by telmisartan at the concentration of 0.01; 0.05, 0.1 and 0.5 mM to 92%, 84%, 76% ($p < 0.05$) and 37% ($p < 0.001$) of control, respectively.

Similar inhibitory effect on KAT's II activity after telmisartan administration was observed.

Our data shows that telmisartan can modulate brain production of KYNA probably through the influence on KAT's activity.

Supported by the grant from National Science Centre (NCN) PRELUDIUM 4 No UMO-2012/07/N/NZ4/02088.

|B48|

Effect Of Zn On N-acetyl-L-aspartate Synthesis In SN56 Neuroblastoma Cells

Marlena Zyśk*, Sylwia Gul-Hinc, Beata Gapys, Andrzej Szutowicz, Hanna Bielarczyk

Chair of Clinical Biochemistry, Department of Laboratory Medicine, Medical University of Gdańsk, Gdansk, Poland

e-mail: marzysk@gumed.edu.pl

N-acetyl-L-aspartate (NAA) is one of most abundant amino acid derivative in the mammalian brain. NAA is synthesized exclusively in neurons from acetyl-CoA and L-aspartate in the presence of aspartate acetyltransferase (A-NAT). Acetyl-CoA production is catalyzed by pyruvate dehydrogenase complex (PDHC). In cholinergic neurons, acetyl-CoA is also used for energy production and acetylcholine synthesis. Considering the additional utilization of acetyl-CoA in cholinergic neurons, deficit of this metabolite can be the cause of particular cholinergic susceptibility to neurotoxic factors.

Therefore, the aim of our study was to investigated whether neurotoxic concentration of Zn might evoke NAA substrates shortages and changes of aspartate N-acetyltransferase activity.

SN56 neuroblastoma cells with high expression of cholinergic phenotype were used as experimental model of cholinergic neurons.

Chronic exposition of differentiated SN56 neuroblastoma cells to 0.15mM Zn increased the Zn level from 1.9 to 8.5 nmol/mg protein. In this experimental conditions the nonviable cells fraction increased for about 57%. The acetyl-CoA level in control condition was estimated for equal 24.0 pmol/mg protein. In 0.15 mM Zn-exposed SN56 assayed level of acetyl-CoA was decreased by over 50%. Furthermore, level of NAA was decreased by 74 %. Simultaneously, Zn caused 58% reduction of both PDHC and A-NAT activities.

Achieved results indicate that impairment of NAA level caused by cytotoxic agents in cholinergic neurons is due to both shortage of acetylo-CoA as well as inhibition of A-NAT activity.

Supported by MN0059/08 and ST-57 GUMed fund.

DOI: 10.5114/fn.2015.56555

Abstracts from the Conference of Polish Association of Neuropathologists

"Biopsy research-challenge of modern neuropathology"

October 16th, 2015

Warsaw, Poland

Primary intradural mesenchymal chondrosarcoma of the spinal canal: a case report and literature review

Marek Derenda[1], Damian Borof[1], Ireneusz Kowalina[1], Wojciech Wesołowski[2], Ewa Iżycka-Świeszewska[3]

[1]Department of Neurosurgery, Neurotraumatology and Spine Surgery, District Hospital, Elbląg, [2]Department of Pathomorphology ELPAT, Elbląg, [3]Department of Pathology and Neuropathology, Medical University of Gdansk, Poland

Mesenchymal chondrosarcomas are rare tumors of the bone and soft tissues. Extraskeletal tumors located in the spinal canal are very rare, and those located intradurally, have been described incidentally. The diagnosis of this tumor can create difficulties, because it is neoplasm with polyphenotypic differentiation and features that overlap those of other small cell malignances of bone and soft tissue. We report on a case of a 22-year-old woman with a primary intradural mesenchymal chondrosarcoma arisen from the arachnoidea at the T12-L1 level without dural attachment. At 13 years of follow-up, there have been three local recurrences in years 4, 6 and 10.6 after initial resection respectively. During the initial surgery procedure a mass was found intradurally with attachment to arachnoidea with normal dura mater. Tumor was resected totally via osteoplastic laminotomy T12-L1 with subsequent reconstruction of spinal canal roof. Microscopic examinations and immunohistochemical studies revealed mesenchymal chondrosarcoma at initial resection and at local recurrences. The tumor was composed of small, round or spindled cells, and scanty stroma with small hyaline cartilage islands. The mitotic index was low. Immunohistochemically expression of CD99, S100, NSE and desmin focally was found. Cytokeratins, myogenin, HMB45 and EMA were negative. Pathological picture of the neoplastic tissue was similar in the consecutive relapses. The patient received radiotherapy after the first resection, and chemotherapy after the first recurrence. All recurrences were treated surgically via osteoplastic re-laminotomies. Despite the four surgical resections of the spinal tumors, 19 months after the last surgery, neurological condition of the patient is still relatively good. Described protracted clinical course of disease is quite typical, making long-term follow up obligatory in mesenchymal chondrosarcoma cases.

Role of skin-muscle biopsy in diagnostics of cerebral small vessel diseases

Dorota Dziewulska

Department of Neurology, Medical University, Warsaw, Poland

Cerebral small vessel diseases (CSVD) consist a relatively new group of neurological disorders. Regardless of their significant clinical heterogeneity, CSVD commonly manifest as recurrent ischemic strokes, progressing dementia and migraine. These symptoms usually appear in patients below 45 y.o. without typical risk factors for vascular diseases. In neuroimages, diffused or disseminated changes in the cerebral white matter are characteristic. In spite of the name, majority of CSVD are generalized angiopathies with clinical predominance of neurologic symptoms. Therefore skin-muscle biopsy can be helpful in their diagnostics. Skin-muscle biopsy has been popularized with an increased interest of clinicians and scientists in CADASIL (Cerebral Autosomal-Dominant Arteriopathy with Subcortical Infarcts and Leukoencephalopathy), the best known and common cerebral microangiopathy. Its introduction into routine diagnostics of patients suspected for CADASIL has led to discovery of several new vascular disorders such as PADMAL, COL4A1, HERNS, CRV or HVR, and spectrum of the cerebral microangiopathies still broadens out. Histopathological, immunohistochemical and ultrastructural assessment of the biopsy material unable diagnosis of CSVD *in vivo* – in some cases even nosologic diagnosis. Currently, skin-muscle biopsy and genetic tests constitute "gold standard" procedure in diagnostics of cerebral small vessel diseases.

Effectiveness and safety of stereotactic biopsy of the brain lesions

Jacek Furtak[1], Tadeusz Szylberg[2], Marek Harat[1], Marzena Lewandowska[3]

[1]Department of Neurosurgery, 10-th Military Research Hospital, Bydgoszcz, [2]Department of Neurosurgery, 10-th Military Research Hospital, Bydgoszcz, [3]Department of Genetics, The Franciszek Lukaszczyk Oncology Centre in Bydgoszcz, Poland

Background: Obtaining tissue material from changes in the CNS allows them appropriate treatment. Objective: The purpose of this study was to evaluate effectiveness and safety of stereotactic biopsy of the brain tumors based on a large number of cases.

Methods: From October 1996 to September 2015 authors performed over than 2300 stereotactic biopsies of brain lesions. In each case the biopsy was performed under local anaesthesia, in a semi-sitting position, supported by MRI/CT fusion, using stereotactic system and software provided by Brainlab AG and Inomed.

Results: During the performed biopsies the following tumors were diagnosed: low-grade astrocytoma, anaplastic astrocytoma, lymphoma, glioblastoma multiforme, metastases, non-tumors lesion. Complications occurred in less than 1.5% of cases.

Conclusions: Stereotactic biopsy is a hardly invasive and effective method of tissue sampling from the brain tumors. It is a safe and reliable method, carrying low risk of complications.

Biopsy of paediatric brain tumours – usefulness and limitation

Wieslawa Grajkowska[1], Ewa Matyja[2]

[1]Department of Pathology, Children's Memorial Heath Institute, [2]Department of Experimental and Clinical Neuropathology, Mossakowski Medical Research Centre, Polish Academy of Sciences, Warsaw, Poland

Brain tumours are the second malignancy of childhood in order of frequency. Correct and precise pathologic classification is the most important prognostic indicator. Major differences in therapy result from different pathological diagnoses for tumours of similar location, identical clinical presentation, and the same radiological features.

The most common techniques for biopsy of paediatric brain tumours include stereotactic biopsy, neuroendoscopic biopsy and open biopsy.

The biopsy is very useful in the management of pineal region tumours. In these cases, the tissue taken via neurendoscopic biopsy allows for precise diagnosis of germinoma and pineoblastoma. However, the diagnosis of mixed germ cell tumours in material obtained by neuroendoscopic biopsy is difficult because of their heterogenic histopathologic pattern.

Diffuse intrinsic brain stem gliomas are the most common brain stem tumours in children. The differential diagnosis of lesions in brain stem include low-grade astrocytomas, gangliogliomas, as well as non-glial tumours, such as ependymoma and primitive neuroectodermal tumours, or even nonneplastic lesions such as inflammation. The majority of these tumours are benign and amenable to surgical resection. The biopsy is the only way to diagnose tumours in this location.

The biopsy is limited in diagnosis of desmoplastic infantile astrocytomas (DIAs) and desmoplastic infantile gangliogliomas (DIGs). The presence of primitive small-cell components within these tumours may be missdiagnosed as a high grade gliomas or PNET.

Conclusions: biopsy of paediatric brain tumours is useful diagnostic method for germinoma, pineoblastoma, brain stem tumours, and optic gliomas. In cases of DIA/DIG and mixed germ cell tumours the biopsy tissue material has a limited diagnostic value because of heterogenic histopathological patters of these tumours.

GLUT-1 and GLUT-3 in glioblastoma

Blanka Herman[1], Edyta Szwed[2], Karolina Gizelbach-Żochowska[1], Witold Libionka[3], Wojciech Kloc[4], Ewa Iżycka-Świeszewska[1]

[1]Department of Pathology and Neuropathology, Medical University of Gdansk, [2]Department of Pathomorphology Copernicus, Gdańsk, [3]Department of Neurosurgery Copernicus, Gdańsk, [4]Department of Neurology and Neurosurgery, Faculty of Medical Sciences University of Warmia and Mazury, Olsztyn, Poland

Altered metabolism in malignant tumors in hypoxic conditions, and especially the process of glycolysis, are the result of dysregulation of various metabolic pathways, including AKT/mTOR, Ras/MAPK and SHH pathway. One of observed phenomena is changed expression of glucose transporters GLUT. The aim of the study was to analyze the expression of Glut1 and Glut3 in glioblastoma. The study was conducted on 52 archival cases of glioblastoma. Representative sections from tumors were selected and microarrays were manually prepared from the paraffin-embedded tissue. Immunohistochemical staining for GLUT-1 and GLUT-3 was performed, and was microscopically evaluated qualitatively and semi-quantitatively. The semi-quantitative method was based on the percentage of cells with membranous immunopositivity and staining intensity. The scale used was SIS (staining intensity score), wherein the % of stained cells were assigned to the corresponding range of values (0, 1-33%, 34-66%, 67-100%), giving number of points (resp. 0 to 3). Staining intensity was defined as: 0-none, 1-low, 2-medium, 3-strong. Both values were multiplied and the number of possible points ranged from 0 to 9. The qualitative method analyzed the distribution of staining in tumor tissue based on microscopic image assessed under small and/or medium zoom. Tumors with intense membranous reaction located around necrosis and/or vascular thrombosis awarded 3 points. Points collected in both methods were summed, and

tumors that with <6 points were classified as low-GLUT, while those with a score ≥6 as a high-GLUT. It was revealed that tumors with high expression of GLUT-1 (high-GLUT-1) accounted for 76% of the cases, wherein the reaction with strong intensity and the location in perinecrotic areas and/or around thrombotic blood vessels affected 68% of gliomas. Tumors with high expression of GLUT-3 (high-GLUT-3) represented 71% of cases, and 53% had a distinct perinecrotic distribution. 27% of gliomas showed intense GLUT-3 membrane staining in areas with intense glomerular vascular proliferation. Furthermore, it was observed that in 19% of cases, relating glioblastoma with a significant proliferation of microvessels, MVP showed strong expression of GLUT3. The results revealed a frequent expression of GLUT in tumor cells of glioblastoma, indicating the dependence of expression of transporter Glut-1 and Glut-3 from an oxygen content in the tumor tissue and the potential association with angiogenesis.

Brain tissue in the gynecological biopsy material

Ewa Iżycka-Świeszewska[1], Jacek Gulczyński[1], Blanka Herman[1], Wojciech Wesołowski[2], Piotr Czauderna[3], Elżbieta Drożyńska[4]

[1]Department of Pathology and Neuropathology, Medical University of Gdansk, [2]Department of Pathomorphology ELPAT, Elbląg, [3]Chair & Clinic of Surgery and Urology for Children and Adolescents, Medical University of Gdansk, [4]Chair & Clinics of Paediatrics, Haemathology & Oncology, Medical University of Gdansk, Poland

We present two very rare situations when the nervous tissue of brain type was diagnosed in a gynecological biopsy material. The first case was an intrauterine 1,5 cm mass in a 22-years old woman with a history of uncomplicated delivery 13 months earlier and recent vaginal bleeding. The polyp was excised and histologically disclosed dense astroglial tissue with thick wall blood vessels, covered with a layer of a normotypic proliferative endometrium. Immunohistochemistry revealed GFAP, GLI1 and S100 expression, while SMA, desmin, CD10, CK AE1/3, CK, synaptophysin and CD34 negativity. The final diagnosis was glial endometrial polyp (focal gliomatosis). The second case concerns a 16-years-old girl with an abdominal discomfort due to a big ovarian tumor with dissemination within the peritoneal cavity, suspected of ovarian cancer. Macroscopically the tumor was multicystic, and histologically presented as mature teratoma. The samples taken from the peritoneal implants were made of mature neuro-glial tissue (GFAP+, NFP+, Synaptophysin +, GLI1+), covered by reactive mesothelium. The endometrial glial polyp can be explained as embryonal/fetal neural tissue graft or metaplasia/transformation of the pluripotent Mullerian tissue within the endometrium. The second case examplifies peritoneal gliomatosis originating from ruptured/ disseminated most probably initially immature ovarian teratoma.

Comparison of the effectiveness of stereotactic biopsy and open biopsy in the neurooncologic diagnosis

Bożena Jarosz, Mirosław Jarosz, Radosław Rola, Katarzyna Obszańska, Adrian Odrzywolski, Tomasz Trojanowski

Chair and Department of Neurosurgery and Paediatric Neurosurgery, Medical University of Lublin, Poland

Brain biopsy is an invasive procedure of obtaining material for histopathological examination, threatened by the risk of complications, especially intracranial bleeding and infection. Stereotactic biopsy is particularly useful in the case of inoperable tumors, since obtaining histopathologic diagnosis, allows the implementation of radio- or chemotherapy. Initially, in our clinic, a biopsy of the brain using stereotactic frame was performed. Since 2008, this procedure is assisted by a neuronavigation system "Brainlab".

The aim of the study was to compare the effectiveness of stereotactic biopsy and open biopsy in the neuro-oncologic diagnosis.

In 10 years (2005-2015) at our center 276 biopsies were performed (160 stereotactic and 116 open biopsy) in cases of 123 female and 153 male patients. Histopathological diagnoses were divided into following categories: 1) full diagnosis, 2) partial diagnosis and 3) lack of diagnosis (non-diagnostic material). The t-Student test was performed for testing significance of difference of two mean values. Significance of the relationships and differences in distribution was investigated using the Chi-square test. The significance level was set at $p = 0.05$.

The female patients ranged in age from 14 to 80 years (Mean = 56.3, SD = 15.13), and male patients aged 17 to 83 years old (Mean = 52.3, SD = 15.55). The difference in age between female and male patients was 3.8 years and was statistically significant ($p = 0.045$). Stereotactic biopsy in 97 (60.6%) cases, allowed for a full diagnosis, in 30 (18.8%) cases allowed for a partial diagnosis, and in 33 (20.6%) cases the material was non-diagnostic. In contrast, open biopsy in 71 (61.2%) cases allowed for full diagnosis, in 9 (7.8%) cases allowed partial diagnosis and in 36 (31.0%)

the material was non-diagnostic. The differences in these proportions were statistically significant ($p = 0.013$).

On the basis of presented analysis, a full histopathological diagnosis is possible as often in the case of stereotactic biopsy (60.6%) as in the case of open biopsy (61.2%). However, the partial diagnosis in the case of stereotactic biopsy is possible more than twice as frequently (18.8%) than in the case of open biopsy (7.8%). In contrast, in case of stereotactic biopsy a non-diagnostic material appears much less common (20.6%) than in the case of open biopsy (31.0%). The results confirm the higher diagnostic efficacy of stereotactic biopsy.

CADASIL-syndrome: difficulty in the ultrastructural diagnosis

Eliza Lewandowska[1], Paulina Felczak[1], Tomasz Stępień[1], Julia Buczek[2], Teresa Wierzba-Bobrowicz[1]

[1]Department of Neuropathology, Institute of Psychiatry and Neurology, [2]2nd Department of Neurology, Institute of Psychiatry and Neurology, Warsaw, Poland

Introduction: Skin and skeletal muscle biopsies are routinely processed in the diagnosis of CADASIL syndrome using electron microscopy (EM). EM examination shows deposits of granular osmiophilic material (GOM) in small vessels, specific and pathognomonic features of CADASIL. We report the case of an 84-year-old male patient afflicted by CADASIL. He showed minimal symptoms of the disease diagnosed on the basis of genetic and ultrastructural examinations.

Material and methods: Biopsy samples were fixed in 2.5% glutaraldehyde and post-fixed in 2% osmium tetroxide and routinely processed to Spurr resin. Ultrathin sections were contrasted with uranyl acetate and lead citrate, and examined with a transmission microscope Opton DPS 109.

Results: On ultrastructural examination of muscle and skin vessels, typical vascular pathologies, such as destruction and loss of pericytes and vascular smooth muscle cells (VSMCs) as well as thickening of the membrane basement were revealed. In abnormal capillary vessel walls no GOM deposits were found, while single arterioles in GOM deposits were identifiable. The deposits were located typically in indentations of VSMCs or in close vicinity to VSMC and they showed various structures of which only some resembled the structure characteristic of GOM.

Conclusions: Our experience, as well as that of other authors indicate that effective EM detection of GOM depends not only on the ability of EM operator and examination of an adequate number of small blood vessels but also on the patient's age. It should be emphasized that in our study case a successful EM examination required much time due to the fact that the patient's family history and positive result of genetic-testing only prompted us to search for GOM deposits.

Diagnostic yield and accuracy in frame-based stereotactic needle biopsy without intraoperative neuropathological verification

Witold Libionka[1], Stanisław Adamski[1], Michał Woźnica[1], Ewa Iżycka-Świeszewska[1,2], Blanka Herman[1], Karolina Gizelbach-Żochowska[1,2], Wojciech Kloc[1,3]

[1]Department of Neurosurgery Copernicus, Gdańsk, Gdansk University of Physical Education and Sport, [2]Department of Pathology and Neuropathology, Medical University of Gdansk, [3]Department of Neurology and Neurosurgery, Faculty of Medical Sciences University of Warmia and Mazury, Olsztyn, Poland

Background and aim: Stereotactic biopsy is an established method of the diagnosis of brain tumors. Recently, with the advance in neuroimaging, use of intraoperative histological verification has been questioned. The aim of the study is to assess diagnostic yield and accuracy of stereotactic needle biopsy without intraoperative neuropathological examination, as verified with histological study after tumor resection.

Material and methods: We prospectively collected patients who underwent frame-based stereotactic biopsy between 2013 and 2015. Of 93 biopsied patients, 22, who later underwent open tumor resection, and in whom final histological diagnosis was obtained, were included in the study. Biopsies were performed under local anesthesia, using Inomed ZD system and PraezisPlus planning software. Multiple biopsy samples were taken from 2-4 sites within the tumor with side-cutting biopsy cannula. Tissue was inspected macroscopically by the surgeon and no neuropathological assessment was done intraoperatively.

Results: A positive diagnosis was established in 20 cases (90.9%). One biopsy revealed no neoplastic but necrotic tissue related to the central tumor necrosis on MRI, and another one revealed gliosis. There were no hemorrhagic or infective complications and none of the studied patients developed new neurological deficits after the operation. Histological diagnosis showed GBM in 6 cases, grade III glioma in 3, grade II in 10, DNET in 1, necrosis in 1, and gliosis in 1. Final histological diagnoses in these patients, based on openly resected tumor tissue, confirmed GBM diagnosis in all 6 cases, grade III glioma

in 2 of 3, grade II in 4 of 9, and DNET in 1 case. GBM was diagnosed in 1 case, previously assessed as grade III, grade III in 3 cases, previously diagnosed as grade II and GBM in 3 cases diagnosed as grade II. In 2 patients with necrosis/gliosis, final diagnosis was GBM. Majority of patients were discharged on the first postoperative day.

Conclusions: The described biopsy technique proved to have high diagnostic yield with excellent safety profile. Lack of intraoperative neuropathological examination did not negatively influence diagnostic accuracy of stereotactic biopsy.

Histopathological diagnosis of brain biopsy specimens – the risk of diagnostic pitfall

Ewa Matyja[1], Wiesława Grajkowska[2]

[1]Department of Experimental and Clinical Neuropathology, Mossakowski Medical Research Centre, Polish Academy of Sciences, [2]Department of Pathology, Children's Memorial Heath Institute, Warsaw, Poland

The stereotactic biopsy of intracranial lesions is considered as a method with high diagnostic validity. Nevertheless, the histopathological diagnosis of brain tumours based on small tissue samples is associated with the risk of incorrect assessment of pathological changes. We would like to present the histopathological dilemmas associated with surgical stereotactic biopsy specimens.

The material from stereotactic biopsies obtained for the pathologic studies does not always allow for proper interpretation of morphological changes. In some cases, the biopsy specimen appears to be not representative for the whole tumour or contains only the margins of neoplastic infiltration with unspecific glial or mesodermal reaction. Moreover, the patient's follow-up is not always compatible with the defined grade of tumour malignancy. This especially refers to the tumours of astroglial origin, mainly glioblastomas, which exhibit significant histologic heterogeneity and variable degrees of differentiation in subsequent sections. It is possible to determine varying histological grades of malignancy in certain areas of the same tumour. Moreover, the identical cellular components and similar histopathologic patterns are common for tumours of different origin. The low grade astrocytomas, especially pilocytic astrocytomas with oligo-like component, might be upgraded but more often malignant gliomas are underestimated. Focal necrosis or accompanying glial reactive tissue may lead to a false diagnosis. Nonspecific reactive changes may occur in both non-neoplastic as well as neoplastic lesions. Serious diagnostic error may occur in patients with postradiation necrosis. The identification of the nature of brain lesions is typically confirmed by immunohistochemical studies but the expression of tumour markers are not always conclusive.

Conclusions: Our experience in surgical pathology indicates that histopathological diagnosis of stereotactic biopsies does not always allow to established the correct diagnosis. There is need to correlate the clinical data with findings obtained at biopsy material. It could be postulated that in the cases when the presumptive diagnosis of brain lesion is not conclusive, the clinical and neuroimaging findings should be the basis for appropriate therapeutic treatment.

Brain biopsy in the diagnosis of non cancerous lesions – cerebral amyloid angiopathy

Tomasz Mendel[1], Teresa Wierzba-Bobrowicz[2], Tomasz Stępień[2], Sławomir Barszcz[3], Tomasz Mandat[3], Paweł Nauman[3]

[1]2nd Department of Neurology, Institute of Psychiatry and Neurology, Warsaw, [2]Department of Neuropathology, Institute of Psychiatry and Neurology, Warsaw, [3]Department of Neurosurgery, Institute of Psychiatry and Neurology, Warsaw, Poland

General clinical indications, contraindications and diagnostic approach to brain biopsy in non cancerous lesions are presented. A detailed description of cerebral amyloid angiopathy (CAA) cases diagnosed by biopsy are analyzed. CAA is a progressive degenerative disease characterised by the deposition of β-amyloid aggregates in the wall of the brain vessels. Of all brain stereotaxic and open neurosurgical biopsy performed in the years 2011–2015, 5 biopsies confirmed CAA. The study group consisted of 5 patients (3 women and 2 men), aged between 67 and 78 years, mean 74.4 ± 4.83. Neuroimaging done before brain biopsy suggests cerebral tumor in one case and in 4 cases intracerebral hemorrhage was suspected. Amyloid lesions were mostly found in cerebral vessels in moderate to severe grades of CAA according to Vonsattel's scale under an optical microscope. Older age of patients and characteristic MRI findings with T2* weighted gradient echo and SWI (susceptibility weighted imaging) can help to establish the correct clinical diagnosis of CAA.

Conclusions: 1. Brain biopsy is frequently a very useful tool to establish the final diagnosis. 2. Brain biopsy done to diagnose CAA is contraindicated. 3. Due to the risk during and after brain biopsy this procedure should be indicated after very careful analysis and multidisciplinary team consultation.

Comparison between Laitinen System and Vario-guide Brain-Lab System in obtaining diagnostic brain tumor tissue

Katarzyna Obszańska[1], Piotr Obszański[2], Bożena Jarosz[1], Tomasz Trojanowski[1]

[1]Chair and Department of Neurosurgery and Paediatric Neurosurgery, Medical University of Lublin, [2]Medical University, Lublin, Poland

Introduction: Contemporary neurosurgery has benefited greatly from introduction of CT and MRI – compatible image-based stereotactic instrumentations. In image-based stereotaxy mechanical device is attached rigidly to the patients head and MRI or CT scan is obtained. The computer in the scanner determinates the three-dimensional coordinates of any point inside the brain in relation to the stereotactic space of the frame. Therefore tissue can be obtained safely from the deep structures of the brain with low mortality and morbidity rate.

Aim: Evaluation of Laitinen and Vario-guide Brain-Lab Systems in brain tumor biopsies.

Material and methods: Patients treated in the Neurosurgical Departament of University Hospital of Lublin from 2000 to 2008 underwent stereotactic biopsy using Laitinen Stereotactic System on the basis of CT scans under local anaesthesia. From 2008 biopsies are performed on the basis of MRI-scans for neuronavigation examination (thickness of slices – 1 mm) under general anaesthesia using Vario-guide Brain-Lab Stereotactic System. Data obtained from 30 patients who underwent biopsy using Laitinen System were compared with data collected form 30 patients who underwent biopsy using Brain-Lab System. Efficacy in obtaining a representative sample of tumor tissue, duration of the surgery, hospitalization time, complications rate and procedure costs were evaluated.

Results: Efficacy in obtaining a representative sample of tumor tissue is higher in the group operated using Brain-Lab System. Hospitalization time of these patients was also shorter. Hospitalization costs differed between the two groups while the number of complications in both groups was comparable.

Conclusions: Stereotactic biopsy is a safe procedure, effective in the diagnosis of intracranial neoplasmatic pathologies.

Biopsy diagnosis of neuromuscular diseases in children

Maciej Pronicki

Department of Pathology, Children's Memorial Heath Institute, Warsaw, Poland

Skeletal muscle biopsy is a well recognized method in diagnosis of neuromuscular disorders, being in practical use for over 100 years. Tissue sampling include open surgical biopsy and needle biopsy, both having their followers and opponents. Muscle most often biopsied is quadriceps femoris due to its relatively large mass and accessibility. It is mandatory to process muscle sample to frozen sections with snap-freezing technique, and perform a panel of histochemical/immunohistochemical reactions concordant with the clinical suspicion. Most often performed panel includes: hematoxylin and eosin, modified Gomori trichrome stain, oil red O, succinate dehydrogenase (SDH), NADH dehydrogenase (NADH-D), cytochrome c oxidase (COX), acid phosphatase, myosin ATP-ase at pH 4.3; 4.6; and 9.4, periodic acid Shiff (PAS), picrosirius, etc. Immunohistochemical assessment in children usually include dystrophin and merosin among other selected antibodies. It is to be empasized that fixation in formalin and paraffin embedding is definitely improper processing in muscle biopsy material for histopathological assessment. Tissue blocks should be also submitted for transmission electron microscopy, at least to the stage of semi-thin epon section for initial assessment. Lesions that may be observed in skeletal muscle biopsy are traditionally divided into myopathic and neurogenic. Several disorders display the diagnostic or nearly diagnostic pattern. Approximately 30-50% of biopsies demonstrate non-specific lesions, or even no detectable pathology at all. In such cases further diagnostic approach should include multidisciplinary workout employing clinicians, biochemists, and molecular geneticists.

Biopsy-based assessment of mitochondrial ultrastuctural changes in patients with suspected mitochondrial disease

Tomasz Stępień[1], Paulina Felczak[1], Eliza Lewandowska[1], Iwona Stępniak[2], Teresa Wierzba-Bobrowicz[1]

[1]Department of Neuropathology, Institute of Psychiatry and Neurology, [2]Department of Genetics, Institute of Psychiatry and Neurology, Warsaw, Poland

Mitochondria are the powerhouses of cells. They generate chemical energy in ATP. They are also involved in the apoptosis signaling pathway. Mitochondrial disease represents a group of metabolic disorders commonly defined by a lack of or decrease in cellular energy due to oxidative phosphorylation (OXPHOS) defects. Mitochondrial disorders are a genetically heterogeneous group of different diseases caused by mutations in mitochondrial and/or nuclear DNA. These mutations may affect different ultrastructural changes of the mitochondria. We report on two patients with suspected mitochondrial disease. The clinical symptoms of the first patient (23-year-old woman) included myoclonic epilepsy, a mild form of the Fahr disease, bilateral sensorineural hearing loss and kidney stones. The patient was provided with cochlear implant HiRes 90K to the right ear. The diagnostic tests demonstrated elevated levels of lactate and creatine kinase (CK). Magnetic resonance imaging (MRI) scan of the brain showed focal changes in the basal ganglia. The other patient (38-year-old man) was admitted to the hospital with cognitive changes, extrapyramida-cerebellar syndrome, impaired hearing both sides and binocular cataracts. Magnetic resonance imaging scan T2 of the brain showed diffuse white matter changes and atrophy of cerebellum. Laboratory tests showed the increased levels of long-chain fatty acids and lactic acidosis. Ultrastructural studies were carried out by performing the biopsy of the biceps muscle derived from two patients with suspected mitochondrial disease. Tissue samples were fixed in 2.5% glutaraldehyde, post-fixed in 2% osmium tetroxide, and embedded in epoxy resin after dehydration. Ultrathin sections were counterstained with uranyl acetate and lead citrate and examined with a transmission electron microscope Opton DPS 109. On the biopsy examination proliferation and ultrastructural changes in the mitochondria in skeletal muscle fibres impaired were found in both patients. We also observed mitochondria showing altered shape, swelling, particularly in giant mitochondria, loss and/or altered configurations of cristea (concentric or irregular cristae), paracrystalic inclusions, vacuoles and lipid droplets. The presented ultrastructural changes in mitochondria are characteristic of a large group of mitochondrial diseases. The diagnosis of mitochondrial specific disease requires a complex synthesis of clinical, morphological, biochemical and genetic investigations.

Granular cell astrocytoma with features of high-grade glioma (WHO G IV). Case report

Anna Taraszewska[1,3], Waldemar Koszewski[2], Jolanta Opertowska[1], Elżbieta Grzywaczewska[1], Maria Zielińska[1]

[1]Department of Clinical and Experimental Neuropathology, Mossakowski Medical Research Centre, Polish Academy of Sciences, [2]Department of Neurosurgery, Medical University of Warsaw, [3]Department of Pathomorphology, Bielanski Hospital, Warsaw, Poland

Granular cell astrocytoma (GCA) is an uncommon brain tumor composed of granule cells of astrocytic lineage. GCA distinguishes from the others, usually benign granular cell tumors, seen elsewhere in the body, by its highly aggressive biological behavior. We report on the case of GCA in a 74-year man, with radiological and histological features corresponding to WHO G IV glioma (according to proposed grading system for GCAs by Brat *et al*. 2002). Radiologically, the right parietal tumor was contrast-enhancing and partially cystic, with prominent perifocal edema. Surgical subtotal resection of the tumor was performed. Histological examination of the surgical biopsy showed granular cell astrocytoma with malignant features. This tumor was composed of cells, filled with PAS-positive granules and immunoreactive for GFAP and CD-68. Furthermore, it demonstrated cellular pleomorphism, frequent mitoses and pseudopalisading necroses. Tumor cells expressed strong reactivity for EGFR and focal nuclear expression of p53. Proliferative MIB-1 labeling index was about 20%.

The presented case illustrates the potential malignancy of GCA showing some morphological and cytogenetic features of glioblastoma in primary tumor. In literature, GCA with transformation to glioblastoma were mainly observed in cases with progression and recurrence of the tumor.

The role of the biopsy in the diagnosis of vascular malformation of the central nervous system – clinical, radiological and neuropathological features

Sylwia Tarka[1], Tomasz Stępień[2], Emilia Sołtan[3], Teresa Wierzba-Bobrowicz[2]

[1]Departament of Forensic Medicine, Medical University of Warsaw, [2]Department of Neuropathology, Institute of Psychiatry and Neurology, Warsaw, [3]Department of Neurosurgery, Institute of Psychiatry and Neurology, Warsaw, Poland

The diagnosis of vascular malformation of the central nervous system (CNS) is usually based on characteristic radiological features. Biopsy is performed only in a few cases of vascular malformation with nonspecific clinical symptoms and nondiagnostic radiological images. In this study seven cases of vascular malformation of the brain and frontal squama with neuroimaging findings representative of vascular malformations, were verified histologically. Radical surgical removal was performed in all of lesions. Biopsy was performed in only one case: a 46-year-old women who suffered from low back pain with lesion in spinal canal described in magnetic resonance imaging (MRI) as probable benign extradural tumor at the L1-L2 level, compressing dural sac and spinal cord (imaging study suggested meningioma or neurofibroma). Surgical specimen and biopsy material were embedded in paraffin, then histological and immunohistochemical methods assays were performed. In all lesions removed from the brain and frontal squama the neuropathological study confirmed radiological diagnosis. All cases exhibited microscopic findings characteristic of vascular malformations: collections on nonneoplasmic blood vessels, abnormal in the structure or the number, composed of normal and malformed arteries, veins or their mixture. Neuropathological examination of biopsy specimen revealed lesions consisting of numerous pathological blood vessels, mostly thin-walled with one layer of endothelium. Among them a few vessels with thicken wall and amorphous eosinophilic material in the lumen of vessels were seen. Vascular malformation of different structure was recognized. Neurosurgeons face much difficulty in evaluating patients for biopsy. In patients with progressive symptomatic lesions with diagnostically inconclusive laboratory and imaging studies biopsy is sometimes necessary. It is important that the neuropathological diagnosis of biopsy specimen give an opportunity to provide the specific and lesion-directed treatment.

Cerebral toxoplasmosis mimicking a brain tumour

Teresa Wierzba-Bobrowicz[1], Anna Taraszewska[2], Tomasz Tykocki[3], Emilia Sołtan[3], Tomasz Stępień[1]

[1]Department of Neuropathology, Institute of Psychiatry and Neurology, [2]Department of Clinical and Experimental Neuropathology, Mossakowski Medical Research Centre, Polish Academy of Science, [3]Department of Neurosurgery, Institute of Psychiatry and Neurology, Warsaw, Poland

In HIV-infected patients toxoplasmosis is a frequent cause of mass lesions in the central nervous system (CNS). We analysed two HIV positive cases of cerebral toxoplasmosis, diagnosed as a result of neurosurgical intervention and neuropathological examination. The clinical symptoms of the first patient (a 40-year-old man) were manifested by cognitive changes with disorders of consciousness, leukopenia and oral candidiasis. Magnetic resonance imaging (MRI) scan of the brain showed a compact-cystic lesion with surrounding edema in the left cerebral peduncle and temporal lobe. The other patient (a 58-year-old man) was brought to the Department of Neurology because of seizure, head trauma and left hemiparesis. A cranial MRI revealed homogeneously enhancing lesion located at the parietal lobe with surrounding edema. Based on the MRI findings, possible primary brain tumours were diagnosed in these two cases. Neuropathological examination of biopsy specimens showed areas of necrosis walled by a broad band of macrophages, occlusive hypertrophic vessels and perivascular micronodules composed of histiocytic/lymphocytic and microglial cells. Microglial nodules were also frequently seen, while astroglial reaction was relatively rare. Single toxoplasmic cysts and trophozoides positive for anti-*Toxoplasma gondii* (clone TP3) antibody spread freely in the brain specimens. In the first patient serological tests confirmed the sero-positive reaction for IgG antibody responses to *Toxoplasma gondii*. The non-invasive diagnosis of cerebral toxoplasmosis is very important. Serologic assays and imaging can be used to diagnose toxoplasmosis. Unfortunately, up to 20% patients with CNS toxoplasmosis are sero-negative for *Toxoplasma gondii*. On neuroimaging examination a specific T2W/ Flair "concentric target" sign (concentrically hypo- and hyperintense zones) are not always visible. Therefore, the distinction between cerebral toxoplasmosis and CNS lymphoma and tuberculosis is a challenging task. In our opinion the brain biopsy proves to be an important diagnostic method, since the identification of toxoplasmic cysts and trophozoides (tachyzoides) provides a reliable diagnosis of cerebral toxoplasmosis.

This instruction is based upon *Uniform Requirements for Manuscripts Submitted to Biomedical Reviews* (the complete document appears in N Engl J Med 1997; 336, 309-315).

Aims and scope

Folia Neuropathologica is an official journal of the Mossakowski Medical Research Centre Polish Academy of Sciences and the Polish Association of Neuropathologists. The journal publishes original articles and reviews that deal with all aspects of clinical and experimental neuropathology and related fields of neuroscience research. The scope of journal includes surgical and experimental pathomorphology, ultrastructure, immunohistochemistry, biochemistry and molecular biology of the nervous tissue. Papers on surgical neuropathology and neuroimaging are also welcome. The reports in other fields relevant to the understanding of human neuropathology might be considered.

Ethical consideration

Papers describing animal experiments can be accepted for publication only if the experiment conforms to the legal requirements in Poland as well as with the European Communities Council Directive of November 24, 1986 or the National Institute of Health Guide (National Institute of Health Publications No. 80-23, Revised 1978) for the care and use of Laboratory Animals for experimental procedure. Authors must provide a full description of their anesthetics and surgical procedures. Papers describing experiments on human subjects must include a statement that experiments were performed with the understanding and consent of each subject, with the approval of the appropriate local ethics committee.

Submission of manuscripts

Articles should be written in English. All new manuscripts should be submitted through the online submission at http://panel2.termedia.pl/fn
For authors unable to submit their manuscript online, please contact with Prof. E. Matyja, Editor-in-Chief of *Folia Neuropathologica*, ematyja@imdik.pan.pl
The Editorial Board reserves the right to reject a paper without reviewers' opinion if the content or the form of the paper does not meet minimum acceptance criteria or if the subject of the paper is beyond the aims and scope of the journal.

Legal aspects

In sending the manuscript the author(s) confirm(s) that (s)he has (they have) not previously submitted it to another journal (except for abstracts of no more than 400 words) or published it elsewhere. The author(s) also agree(s), if and when the manuscript is accepted for publication, to automatic and free transfer of copyright to the Publisher allowing for the publication and distribution of the material submitted in all available forms and fields of exploitation. The author(s) accept(s) that the manuscript will not be published elsewhere in any language without the written consent of the copyright holder, i.e. the Publisher.
All manuscripts submitted should be accompanied by an authors' statement including signed confirmation of the above and confirming that this publication has been approved by all co-authors (if any), as well as by the responsible authorities at the institution where the work has been carried out. The authors' statement should be signed by ALL co-authors. Additionally, the author(s) confirm(s) that (s)he is (they are) familiar with and will observe the "Instruction to Authors" included in *Folia Neuropathologica* and also that all sources of financial support have been fully disclosed. Materials previously published should be accompanied by written consent for reprinting from the relevant Publishers. In the case of photographs of identifiable persons, their written consent should also be provided. Any potential conflict of interest will be dealt with by the local court specific to the Publisher. Legal relations between the Publisher and the author(s) are in accordance with Polish law and with international conventions binding on Poland.
Authors agree to waive their royalties.

Anonymous review

All manuscripts will be subject to a process of anonymous editorial review.

Preparation of manuscripts

Articles must be written in English, with British spelling used consistently throughout. Authors not entirely familiar with English are advised to correct the style by professional language editors or native English speakers.

- The length of original article should not exceed 20 printed pages including text, illustrations, tables, and references.
- Manuscripts should be typed using 12pts.font, double-spaced, and fully corrected. Allow a margin at least 2.5 cm at the top, bottom and left side of the page. Text should not be justified.

- The title page should contain: the author's full names, title of the paper, all authors' affiliations, full name and address of the communicating author (including e-mail address and fax number), running title (not exceed 40 characters including spaces).
- The abstract should not exceed 350 words. A list of 3–10 key words is recommended below the abstract.
- The manuscript body should be organized in a standard form with separate sections: Introduction, Material and Methods, Results, Discussion, and References. Review articles should be divided into sections and subsections as appropriate without numbering.
- Do not underline in the text. Avoid footnotes.
- All dimensions and measurements must be specified in the metric system.
- The source of any drug and special reagent should be identified.
- Particular attention needs to be paid to the selection of appropriate analysis of data and the results of statistical test should be incorporated in the results section.
- The nomenclature used should conform to the current edition of the Nomina Anatomica or Nomina Anatomica Veterinaria.
- Acknowledgements should be made in a separate sheet following Discussion and before References. These should contain a list of dedications, acknowledgements, and funding sources.
- Legends of figures and tables should be typed on separate pages.
- The editor reserves the right to make corrections.

Tables

- Tables numbered in Roman numerals require a brief but descriptive heading.
- The major divisions of the table should be indicated by horizontal rules.
- Explanatory matter should be included in footnotes, indicated in the body of the table in order of their appearance.
- Tables must not duplicate material in the text or in illustration.

Illustrations

All figures should be supplied electronically at resolution 300dpi in all standard formats (tiff, jpg, Adobe Photoshop, Corel Draw, and EPS). Name your figure files with "Fig" and the figure number, e.g., Fig1.tif

- The maximum figure size is 84 mm or 174 mm for use in a single or double column width, respectively.
- When possible, group several illustrations on one block for reproduction. Like all other figures, block should be prepared within a rectangular frame to fit within a single or double column width of 84 and 174 mm, respectively, and a maximum page height of 226 mm.
- Each figure should include scale magnification bar; do not use magnification factors in the figure legends.
- All figures, whether photographs, graphs or diagrams, should be numbered using Arabic numerals and cited in the text in consecutive numerical order
- **Immunohistochemical study requires color illustrations of very good quality. The papers with white and black immunohistochemistry will not be accepted.**
- **The expense of color illustrations must be borne by the authors.** The cost of color print for every successive 8 pages is 200 euro irrespective of the number of color pages, i.e., the price remains the same whether there is one or eight pages.

The Publisher makes out the bill to the communicating Author.

References

The list of references (written on a separate page) should include only those publications that are cited in the text. Avoid citation of academic books, manuals and atlases. References may be arranged alphabetically and numbered consecutively. References should be given in square brackets with no space between the comma and the consecutive number, e.g. [3,4,6-12].

References should be written as follows:

Journal papers: initials and names of all authors, full title of paper, journal abbreviation (according to Index Medicus), year of publication, volume (in Arabic numerals), first and last page (example below):

1. Valverde F. The organization of area 18 in the monkey. Anat Embryol 1978; 154: 305-334.
2. Uray NJ, Gona AG. Calbindin immunoreactivity in the auricular lobe and interauricular granular band of the cerebellum in bullfrogs. Brain Behav Evol 1999; 53: 10-19.

Book and monographs: initials and names of all authors, full title, edition, publisher, place, year (examples below):

1. Pollack RS. Tumor surgery of the head and neck. Karger, Basel 1975.
2. Amaral DG, Price JL, Pitkanen A, Carmichael ST. Anatomical organization of the primate amygdaloid complex. In: Aggleton JP (ed.). The amygdala. Wiley-Liss, New York 1992; pp. 1-66.

Reference to articles that are accepted for publication may be cited as „in press" or Epub.

Proofs

Corrections to the proofs should be restricted to printer's errors only; other alterations will be charged to the authors. In order to maintain rapid publication, proofs should be returned within 48 hours, preferably by e-mail, fax or courier mail. If the Publisher receives no response from the authors after 10 days, it will be assumed that there are no errors to correct and the article will be published.

Subscription information

The journal is published in one volume per year consisting of four numbers. The annual subscription price is 160 PLN for Institutions from Poland and 80 PLN for individual subscribers from Poland and 140 Euro for foreign Institutions and 70 Euro for foreign individual subscribers.
Payment should be made to:
Termedia sp. z o.o., ul. Kleeberga 8, 61-615 Poznan
BZ WBK III O/Poznan PL 61 1090 1359 0000 0000 3505 2645
SWIFT: WBKPPLPP

The publisher must be notified of a cancellation of a subscription not later than two months before the end of the calendar year. After that date the subscription is automatically prolonged for another year.
Publishing, Subscription and Advertising Office:
TERMEDIA Publishing House
ul. Kleeberga 2
61-615 Poznan, Poland
phone/fax +48 61 822 77 81
e-mail: termedia@termedia.pl
http://www.folianeuro.termedia.pl

Folia Neuropathologica

AUTHOR'S STATEMENT

Title of the article

.....

.....

.....

The author(s) hereby confirm(s) that:

☐ The above-mentioned work has not previously been published and that it has not been submitted to the Publishers of any other journal (with the exception of abstracts not exceeding 400 words).

☐ All co-authors named and the relevant authorities of the scientific institutions at which the work has been carried out are familiar with the contents of this work and have agreed to its publication.

☐ In sending the manuscript together with illustrations and tables agree(s) to automatic and free transfer of copyright to the Publisher allowing for the publication and distribution of the material submitted in all available forms and fields of exploitation, without limits of territory or language, provided that the material is accepted for publication. At the same time the author(s) accept(s) that the submitted work will not be published elsewhere and in whatever language without the earlier written permission of the copyright holder, i.e. the Publisher.

☐ (S)he (they) agree to waive his(her)(their) royalties (fees).

☐ (S)he (they) empower(s) the Publisher to make any necessary editorial changes to the submitted manuscript.

☐ All sources of funding of the work have been fully disclosed.

☐ The manuscript has been prepared in accordance with the Publisher's requirements.

☐ (S)he (they) is (are) familiar with the regulations governing the acceptance of works as published in *Folia Neuropathologica* and agree(s) to follow them.

☐ (S)he (they) agree to accept appropriate invoice from the Publisher in case colour illustrations are implemented.

Date *Signatures of **all authors***

The covering letter formula can be found at: www.folianeuro.termedia.pl
-The covering letter should be sent to Associate Editor:

Milena Laure-Kamionowska
-Editorial Office of Folia Neuropathologica
Mossakowski Medical Research Centre, Polish Academy of Sciences
Poland Medical Research Centre
ul. Pawinskiego 5
02-106 Warszawa, Poland

CONTENTS

Toxic effects of silver nanoparticles in mammals – does a risk of neurotoxicity exist?_281
Joanna Skalska, Lidia Strużyńska

Effects of mGluR5 positive and negative allosteric modulators on brain damage evoked by hypoxia-ischemia in neonatal rats_301
Dorota Makarewicz, Marta Słomka, Wojciech Danysz, Jerzy W. Łazarewicz

Protective effect of valproic acid on cultured motor neurons under glutamate excitotoxic conditions. Ultrastructural study_309
Ewa Nagańska, Ewa Matyja, Anna Taraszewska, Janina Rafałowska

The influence of glutamatergic receptor antagonists on biochemical and ultrastructural changes in myelin membranes of rats subjected to experimental autoimmune encephalomyelitis_317
Beata Dąbrowska-Bouta, Lidia Strużyńska, Małgorzata Chalimoniuk, Małgorzata Frontczak-Baniewicz, Grzegorz Sulkowski

Collateral sprouting axons of end-to-side nerve coaptation in the avulsion of ventral branches of the C5-C6 spinal nerves in the brachial plexus_327
Paweł Reichert, Zdzisław Kiełbowicz, Piotr Dzięgiel, Bartosz Puła, Jan Kuryszko, Marcin Wrzosek, Maciej Kiełbowicz, Jerzy Gosk

Polymorphism of the osteopontin gene and clinical course of multiple sclerosis in the Polish population_343
Justyna Biernacka-Lukanty, Grazyna Michałowska-Wender, Slawomir Michalak, Beata Raczak, Wojciech Kozubski, Dariusz Urbanski, Mieczyslaw Wender

Toll-like receptor 2 (TLR2) is a marker of angiogenesis in the necrotic area of human medulloblastoma_347
Danuta Maslinska, Milena Laure-Kamionowska, Sławomir Maslinski, Dariusz Szukiewicz

Sporadic inclusion body myositis: clinical, pathological, and genetic analysis of eight Polish patients_355
Biruta Kierdaszuk, Mariusz Berdynski, Piotr Palczewski, Marek Golebiowski, Cezary Zekanowski, Anna Maria Kaminska

NF-κB deficit in spinal motoneurons in patients with sporadic amyotrophic lateral sclerosis – a pilot study_367
Dorota Sulejczak, Stanisław J. Chrapusta, Dorota Dziewulska, Janina Rafałowska

Effects of supplementation with branched chain amino acids and ornithine aspartate on plasma ammonia and central fatigue during exercise in healthy men_377
Tomasz Mikulski, Jan Dabrowski, Wojciech Hilgier, Andrzej Ziemba, Krzysztof Krzeminski

Holoprosencephaly with agenesia of the prosencephalic ventricle_387
Milena Laure-Kamionowska, Krystyna Szymanska, Teresa Klepacka

Abstracts from the Neurochemical Conference 2015; The Days of Neurochemistry; "Neuropsychoimmunological mechanisms in the pathology of neurodegenerative diseases: From biomarkers to therapeutics"_395

Abstracts from the Conference of Polish Association of Neuropathologists; "Biopsy research-challenge of modern neuropathology"_439